Managing the transportation of hazardous materials with time windows and uncertainties

by

© *Saeed Tasouji Hassanpour*

A thesis submitted to the
School of Graduate Studies
in partial fulfilment of the
requirements for the degree of
Doctor of Philosophy

Department of *Business*
Memorial University of Newfoundland

October 2022

St. John's Newfoundland

Abstract

The dependence of modern life on numerous hazardous products is an undeniable matter. Considering the dangerous nature of these materials, providing versatile means of transportation is critical and essential. The flexibility and applicability of the mode of truck transportation have made it the most favorable method for conveying hazardous materials (hazmats), yet the shipping performance can be largely susceptible to ever-changing traffic and weather conditions. Inspired by the importance as well as lack of joint considerations of uncertainties, random disruptions, and time-relevant issues, this research plans to examine the location-routing decisions in hazmat transportation by applying stochastic and robust programming models to vehicle routing problems with time windows, so to ensure the corresponding efficiency, efficacy, and equity. Providing effective solutions to the hazmat location-routing problems is of significant importance for both logistics companies and the government. Exact and heuristic algorithms will be explored for timely and accurate solutions. To assess the practicability and validity of the proposed approaches, real-world case studies will be investigated from the optimization perspective, from which we derive managerial insights that enhance decision-making for system stakeholders. In this regard, this thesis contributes to the current literature in the following three ways. First, we develop a scenario-based robust location-routing model for hazmat transportation with joint consideration of time windows, time-dependency, multiple existing paths between nodes, and disruptions. Second, a stochastic location-routing problem of infectious waste during a pandemic is discussed in a 3-tier network. Em-

bedding temporary facilities, uncertainty, and chance-constrained time windows into the model, a brach-and-price algorithm is developed to solve the model to optimality. Finally, the stochastic location-routing problem of the hazardous waste network is addressed using a three-stage decision framework. The critical features involved in this model are stochastic waste release dates, the risk-aversion parameter, and the proposed decision framework of the model. The framework is built upon a cost-clustering approach, risk-oriented a priori plan, and recourse actions respectively for location-allocation, routing, and adaption decisions. We summarize the contributions of this thesis, discuss the overall results obtained, and present the potential future research directions.

Acknowledgements

I would like to convey my sincere gratitude to my supervisor Dr. Ginger Y. Ke for her continuous support and for offering priceless advice and encouragement during my Ph.D. career. I have immensely benefited from her wealth of knowledge. Besides my supervisor, I would like to thank my co-authors, Dr. David M. Tulett and Dr. Jiahong Zhao, for their invaluable feedback and contributions to the available research pieces of this project. An immense thank you to all the committee members for their insightful comments and encouragement. I am also thankful to the graduate program directors of the Business Faculty, Dr. Joerg Evermann, Dr. Rachelle Shannahan, and Dr. Travor Brown. Research funding from Mitacs and BMO Financial Group is sincerely acknowledged.

My foremost acknowledgment goes to my wife, Nava, who has stood by me through all my travails, unceasingly motivated me, and endured my absences and my fits of impatience. Acknowledgment is also due to my parents and brother, for without their encouragement and support, none of this may have been possible.

Contents

List of Tables

List of Figures

Chapter 1

Introduction

1.1 Introduction

Since logistics advanced in the 1950s, numerous researchers have concentrated on its various applications, leading to significant improvements in this field (Chira, 2014). Logistics now encompass a broader impact on business and economic prosperity due to the existing nationalization and globalization trend in recent decades. Companies are aware that utilizing proper logistic management techniques contributes to optimal assignment and use of resources and consequently optimizing the existing production and distribution processes. One of the key elements in logistics management is the transportation system accounting for one-third of the logistics costs (Zunic et al., 2020). Transportation systems hugely influence logistics systems' performance as they are required in the whole production procedures, from manufacturing to delivery to the final consumers and returns. Only a well-established transportation network between each component would maximize the benefits. A poorly functioning

transportation system can lead to a shortage of products and burden additional costs on the organization. In contrast, a well-functioning transportation system can help an organization cut off significant expenses and increase customer satisfaction.

The primary modes of transportation in logistics are shipments by truck (road), ship (marine), train (rail), and plane (air). In some cases, the pipeline mode is also used for shipping specific materials such as crude oil. In this thesis, we are interested in road transportation mode as one of the most popular shipment methods in logistics. For example, in January 2020, truck freight accounted for more than 54% (26.1 billion dollars) of all northern border freight between Canada and the United States. Also, routes constituted 71.1% (35 billion dollars) of all southern border freight (Bureau of Transportation Statistics, 2020). Road freight offers many advantages, such as more affordable shipments, highly accessible nature, flexibility in scheduling deliveries, easier freight tracking, and fewer restrictions.

In addition to the regular shipment, large volumes of hazardous materials (hazmat) are transported daily through the transportation networks. Since the late 1980s, the transportation of hazardous materials has been the subject of interest by researchers, and much research has been done so far addressing different aspects of it. A hazardous material is a substance that, despite being widely used in industry, can cause damage to a vulnerable element due to its physical or chemical properties. Vulnerable features include humans, animals, the environment, properties, and buildings. Hazardous materials are classified into nine categories by the United Nations based on their physical, chemical, and nuclear properties: 1) explosives and pyrotechnics, 2) gasses, 3) flammable and combustible liquids, 4) flammable, combustible, and dangerous-when-wet solids, 5) oxidizers and organic peroxides, 6) poisonous and

infectious materials, 7) radioactive materials 8) corrosive materials (acidic or basic), 9) miscellaneous dangerous goods, such as hazardous wastes (Erkut et al., 2007).

Modern industrialized societies are dependent on applications of chemicals and hazardous materials as inevitable elements of their process. The industry and the residents' lives rely on numerous hazardous products such as petroleum derivatives and a variety of detergents. In addition, residues and the relevant generated waste from these activities might contain hazmat. To highlight the importance of the matter, it is noteworthy to mention that even handling municipal household waste is associated with elements threatening individuals and the environment. According to (U.S. Department of Energy, 2019), there is an increasing trend of hazmat shipments between the U.S. Petroleum Administration for Defense Districts. The crude oil and petroleum shipments were estimated to be around 167, 186, and 205 thousand barrels in 2016, 2017, and 2018, respectively. Besides the general benefits of road transportation, the truck mode for hazmat shipments faces fewer restrictions than other modes of transportation. Also, many specialized trucking companies are available to accommodate hazardous goods. As a result, this method is a favorable means of dangerous cargo conveyance worldwide, especially for short to medium distances.

Confronting the public's concerns and government restrictions, urban hazmat transportation's primary challenges are determining the vehicle courses that minimize the associated network cost and risk while handling the existing disruptions and meeting the time windows. Therefore, optimizing the location-routing choices by addressing the available realistic assumptions is an important area for research to improve knowledge of this class of hazmat transport management. In this research, we formulate this problem and examine a new algorithm to solve the model. This

procedure can also provide several recommendations and managerial insights serving as the ground for managing the corresponding risks in this area by manufacturing companies, logistic corporations, and management enterprises. The proposed framework in the research can guarantee the safety of the hazmat transportation process while saving the financial resources of the stakeholders.

This thesis includes five chapters. The introduction to the thesis, chapter 3.1, includes six main sections. Sections 1.2 and 1.3 portray a big picture of this research. The research statement and objectives are highlighted in section 1.2, where expected outcomes and deliverables of this project are discussed in section 1.3. Methodologies applied in this project are explained in section 1.4, focusing on different aspects of the model, from risk assessment to solution algorithms. Finally, the co-authorship statement has been provided in section 1.5.

1.2 Research statement and research objectives

This thesis explores the location-routing problem in the hazmat transportation field in an uncertain environment. Stochastic programming techniques and scenario-based robust optimization methods are applied in the corresponding models to encompass the uncertain nature of several parameters. The uncertainty might arise from link disruptions, generated waste amount, or generation waste speeds. The logistic company (distributor or collector) handles the routing problem in several tours by adhering to the available time windows. Both cost and risk objectives are addressed to satisfy different stakeholders of the process, underlining the importance of discussing the trade-offs between these objectives. Moreover, we introduce several helpful indicators

to facilitate the carrier in making appropriate decisions. The developed models can be applied to a real-world hazmat transportation network, from which practical insights are derived. Finally, the bi-objective nature of the model is handled using an ε-constraint method, and a branch-and-price exact method is developed to overcome the complexity of the resulting mathematical models.

Building the model based on the most recent literature gaps, this research not only fulfills its mission in academia but also, using realistic assumptions, offers a practical solution to assist associated authorities. Also, more contributions can be added to these models in the future based on the authorities' point of view. As a result, by providing a better understanding of current hazmat transportation networks, this thesis aims to generate more reliable and robust systems with realistic features as its general objective. Different shareholders can benefit from the outcomes and the suggested managerial insights of this project, with the government establishing more risk-efficient decisions and the hazmat carriers employing more economical and environment-friendly transportation plans.

More particularly, we seek to answer the following questions:

- Where is the optimal location for the candidate facilities considering the trade-offs between the cost and risk objectives?
- What is the proper capacity for these facilities and the vehicles?
- What is the optimal customer allocation decision for the activated facilities employing a finite number of vehicles?
- What is the optimal customer service sequence according to the derived vehicle routing decisions?

- What are the implications of time windows, potential network disruptions, and uncertainties?
- What additional measures may be taken to mitigate those influences?

Within the general objective, the following activities are carried out:

1. *Investigating the trade-offs in a bi-objective hazmat planning model.* A significant challenge that needs to be addressed in the hazmat transportation concept is the bi-objective nature of the network. Cost and risk objectives are crucial in this type of network, as they need to be balanced to keep the network functioning effectively. Failure to do so can lead to inefficient use of resources and increased risk, both of which are detrimental to the network's overall goal. The developed location-routing models help logistic planners to achieve a balanced decision based on both hazmat-planning objectives. The model also allows planners to account for each objective's impact on the other objectives and to make informed decisions about the best way to achieve the desired results by assessing the available trade-offs.

2. *Embedding realistic assumptions as time considerations and possible disruptions into the model.* In order to create a realistic hazmat transportation model that can be used for risk assessment and management purposes, it is necessary to have realistic assumptions embedded into the model. In this regard, inspired by real-life networks, several factors have been added to this project. First, we have assumed time considerations through time windows and time-dependent parameters. Second, disruptions or deviations from the original plan are involved as a basis of uncertainty in reacting against unplanned situations. Also,

the model incorporates other uncertainty sources through stochastic and robust programs. Finally, the decision-maker's perspective impacts have been studied in the model through the risk-aversion concept.

3. *Incorporating uncertainties in the model.* In order to incorporate different existing uncertainties into the hazmat model, it is necessary for researchers to develop proper methods for parameter estimation as well as improved knowledge about how these uncertainties interact with other elements of the model. Therefore, selecting the most influential components as uncertain parameters and addressing them with suitable techniques is challenging for researchers. There should be a supporting logic for the application of specific methods. For example, access to sufficient historical records of an attribute leads to the application of stochastic programming or scenario-based robust optimization technique. However, when dealing with a deep uncertainty with insufficient supporting data, some robust optimization or fuzzy logic approaches have priority over stochastic programming. This research examines the efficiency of both stochastic and robust programs by considering different uncertain parameters and demonstrates how they affect the solutions of the model.

4. *Applying efficient exact algorithms to achieve the optimal solution of the hazmat transportation model.* Today, there is a great need for efficient algorithms that can be used to solve problems in the hazmat transportation domain, especially considering the lack of such algorithms in the hazmat location-routing problem (HLRP) literature. Hazmat transportation is one of the industries where accurate and timely decisions are essential for averting potential disasters. This

thesis presents an algorithm that has been explicitly employed to optimize the hazmat transport planning process. The proposed algorithm uses a branch-and-price methodology to derive the optimal solution, while the bi-objectiveness is tackled with the ϵ-constraint technique.

5. *Exploring the model's validity and applicability by adopting a real case of hazmat logistics network.* This project's proposed hazmat logistics networks are validated and proven to apply to different industries and case studies. The developed models are demonstrated to be effective in helping businesses transport hazmat-sensitive materials and products safely and efficiently. The network has also been shown to be reliable in helping businesses to comply with different hazmat transportation attributes affecting the network. The finding of this research can be utilized for most types of hazmats, including flammable liquids and gases, corrosive agents, toxic chemicals, explosive devices, household waste, medical waste, and hazardous waste, as their relevant networks share significant similarities.

1.3 Expected outcomes and deliverables

In this thesis, we explore hazardous materials, infectious waste, and hazardous waste in separate chapters. We develop redundant and robust location-routing models for both ordinary days and unpredicted situations such as pandemics. Also, more realistic assumptions are included in the model, such as time windows, time-dependency, disruptions, multi-period problems, uncertainty, and decision-maker's risk adversity. Providing a comprehensive analysis of hazmat transportation with different variants

and features, the findings of this research would be an asset to the stakeholders and relevant authorities in hazmat logistics. Less risky and more cost-efficient solutions are derived by deriving practical and realistic decisions, from which both the government and the logistic company may benefit. Finally, optimal locations for establishing or activating facilities, assignment of customers to the chosen facilities, routing and scheduling decisions, inventory management of the network, and obtaining the optimal number of required vehicles are arranged.

Considering the aforementioned points, studying the location-routing problem of hazardous materials and providing improved hazmat logistic plans is inevitable. Hazmat planners must find ways to optimize routes while minimizing environmental impact, ensuring safe transport, and reducing the associated network expenses. This project applies to different parts of the world, including Newfoundland and Labrador. In Newfoundland and Labrador, the harsh weather might cause disruptions in the road due to edge unavailabilities. We assess disruptions and deviations in optimistic, normal, and pessimistic situations, covering the majority of possible scenarios. Therefore, the outcomes of this project are economically and environmentally practical worldwide. The associated economic orientation of this project is as follows.

1. **Providing cost-effective plans for carrier companies.** Providing cost-effective plans for carrier companies is a common and constant endeavor in today's competitive business environment. With so many carriers vying for customers, it is essential that providers create strategies to maintain and grow their customer base while saving their financial resources as much as possible. The financial savings can be related to selecting the most economical location

for establishing the facilities like depots, following routing plans requiring a low budget for transportation and handling the hazmat, optimizing the inventory management, and utilizing a reasonable number of trucks in the vehicle fleet. Carrier planning should concentrate on both short-term and long-term goals, taking into account the current economic climate and future trends. For this purpose, we assess different uncertain scenarios, from optimistic to pessimistic, to make the system applicable and effective in the short and long run. Also, in the case of unpredicted circumstances like the COVID-19 pandemic, the authorities want to adapt to the realized situation at a low cost. Therefore, optimizing the location-routing decisions of hazmat transportation networks, this project aims to propose sustainable plans and ameliorate the financial status of carriers.

2. **Providing risk-effective plans for the government.** The associated statistics we mentioned earlier highlighted the importance of risk consideration and mitigation in hazmat logistics. Apart from the potential adverse impacts on people, properties, and the environment, reckless and unwise location-routing decisions might lead to social unrest. People oppose their government when they believe it is not acting in the best interests of its citizens. As a result, when dangerous cargo is transported in highly populated areas, hauled without inequity considerations, or hazmat processing facilities are established in crowded locations, the governments are more likely to be questioned by individuals. Therefore, to improve the safety of hazmat transportation, the government should focus on creating risk-effective plans and improving the hazmat transportation

planning process. The other challenge for logistic companies and the regulating authorities is that not every safe path is also a cost-efficient plan. The collector or distributor is looking to minimize the logistic expenses while the government favors routes that impose low risks to the vulnerable elements. Therefore, an optimal plan should incorporate both risk and cost reductions. Exploring the trade-off between different objectives, this research can be utilized to assess the trade-off between the risk and cost to derive acceptable solutions for both the government and carriers.

3. **Applicability to real-life systems.** The proposed models in this thesis are applicable to many real-life hazmat transportation systems. From petroleum shipments to handling medical waste can be addressed using these models. In fact, each model is tested and verified using a real-life case study. Each model has unique features embedded in the problem to yield more practical solutions. For example, customer time window consideration is a vital component for maintaining customer satisfaction while adhering to some particular roles, such as an infectious generated waste that should be handled in a permissible time interval. Ignoring such crucial criteria can result in irreversible losses. This project's other outstanding realistic feature is the inclusion of disruptions and deviations from the original plan. Regions such as Newfoundland and labrador have harsh weather with significant precipitation and snowfall rates. As a result, disruptions are inevitable due to road closures, traffic congestion, or other accidents. Therefore, to be prepared for deviations from the initial scheduled plans, the corresponding agencies should organize alternative and adjustable plans that re-

main close to the optimum path. Also, the proposed model can highly simulate the real-case transportation systems by embedding many time restrictions and assumptions such as decision-maker risk-aversion and time-dependent parameters. The former incorporates the mentality of the decision-maker in the model through a subjective risk-aversion parameter, while the latter applies variations of specific parameters as a function of time.

1.4 Methodologies

Generally belonging to the mathematical optimization field, this study plans to construct a mixed-integer programming model with multiple objectives. Various methodologies are applied in this research for a comprehensive formulation of the HLRP problem that can be effectively solved.

1.4.1 Risk assessment

Accidents associated with hazardous substances in the literature are known as low-probability, high-consequence events. Therefore, despite the relatively low probability of such incidents, the consequences can be catastrophic and sometimes irrecoverable. The recent report by Canadian Transport Emergency Center (2021), operated by the Transport of Dangerous Good Directorate of Transport Canada, stated that from 2017 to 2021, Petroleum Crude Oil, diesel, and liquefied petroleum gases accounted for the most hazmat incidents. This department was respectively involved in 2850, 2950, 2320, and 2021 emergencies from 2017 to 2021. Here, we review several disastrous incidents in the hazmat field. On July 11, 1978, a propane tanker blast killed more

than 200 people and led to more than 120 individuals in Spain. The other associated incident was the evacuation of more than 200,000 people in Ontario due to chlorine gas leakage in 1979. The gasoline tanker explosion (1982) in Afghanistan that killed 2,700 people and the Neyshabur 2003 train derailment accident that left 295 dead and 460 injured are other examples of historical tragedies in hazardous materials accidents that demonstrate the necessity of exploring this field. The tragic event in Lac–Mégantic (Québec) in July 2013 is a more recent accident where a runaway train hauling 72 tankers filled with crude oil derailed as it approached the center of the town of Lac-Mégantic.

Generally, highways are the primary source of hazmat transportation with more associated incidents. In the U.S. between 2011 and 2015, as announced by the U.S. Department of Transportation Pipeline and Hazardous Materials Safety Administration (PHMSA, 2015), highways accounted for around 87% of all hazmat-related accidents. In another report by the U.S. Department of Transportation it was indicated that from 2004 to 2013, highways with 140,742 incidents out of 163,469 in total have the most significant portion of fatalities, injuries, and damage among all modes of transportation. Also, this report emphasizes the importance of focusing on risk mitigation on hazmat road networks and explaining the motivations of researchers from OR/MS fields of studies to explore hazmat transportation scope. In Germany, road hazmat transportation was the most favorable mode, responsible for over 46% of the transported hazmat in 2015, which was a total of 141.48 million tonnes (Holeczek, 2019).

Risk is the most crucial factor separating hazardous transportation problems from other transportation subjects. In this concept, the risk is defined by calculating the

probability and severity of harm to the exposed recipient through unintentional accidents caused by the transportation of hazardous materials. The exposed recipient of the risk can be a person, environment, or environmental attributes of the proximity of the accident, and the unintended incident is the distribution of hazardous material because of the occurrence of the accident. Dissemination of hazmat has consequences, including the effects on the health of individuals (death, injury, or long-term effects due to exposure to hazardous substances) or the loss of property, environmental impacts such as soil contamination or effects on plant health and animals, or evacuation nearby populations because of anticipation of imminent danger and traffic congestion along the evacuation route.

Different considerations must be taken into account in estimating the risk of leakage because of accidents during the transportation of hazardous materials. The consequences regarding the cost can be categorized as follows (Erkut et al., 2007):

- Injuries and deaths
- Property damage
- Evacuation of residents
- Traffic delays
- Cleaning costs
- Loss of hazardous substances
- Environmental damage

Generally, two types of risks exist, including individual and societal risks. An individual's risk is when a person is at risk in a particular situation, the risk is measured at a particular point and only for him. This risk generally depends on the source of risk, while societal risk indicates the relationship between the frequency of an accident and the number of people injured; in other words, the risk is measured for a group of individuals. Based on previous studies, risk calculation and evaluation are classified into three groups: qualitative, quantitative, and hybrid (quantitative-qualitative) (Yacob and Hassim, 2017).

Qualitative risk assessment uses judgment and sometimes expert opinions about probability and consequences. In other words, qualitative risk assessment deals with identifying possible accident situations and trying to estimate adverse outcomes and is often used when there is little reliable information to accurately estimate the probability and severity of an accident. In fact, the only purpose is to identify probable and/or very traumatic events and focus on them. In this method, keywords or descriptive terms are used to indicate the magnitude of a possible outcome and the probability of its occurrence. Qualitative risk assessment is based on the personal experience and skills of experts and engineers in this field. Depending on the appropriateness of the resources available, this approach can produce acceptable results. The "What-If Analysis" analytical method and the "Safety audits" are examples of qualitative risk methods. The basis of these methods is the first attempt to identify potential problems by using general questions about a system and determining what causes the problem. Then, their possible consequences are also considered qualitatively. The output of this approach, given its thorough knowledge of the system and its risk points, is used in various decisions for that system and in providing appropri-

ate suggestions for maintaining its safety. Examples of qualitative work can be found in Ikeagwuani and John (2013).

1.4.1.1 Quantitative risk assessment

Quantitative risk assessment is a numerical risk assessment. The language of quantitative risk assessment is the language of frequency analysis and results and, unlike qualitative risk analysis, leads to numerical risk assessment. A comprehensive explanation for the risk models was provided in Erkut et al. (2007). They focused on Quantitative Risk Assessment (QRA) with three fundamental steps: hazard and exposed receptor identification, frequency analysis, and Consequence modeling and risk calculation. The consequences of an incident are a function of the exposure zone, population, property, and environmental assets within this area. Several factors affect the shape and size of an impact area, such as the material being transported, topology, weather, and wind speed and direction Erkut et al. (2007).

Hazard identification is the identification of potential sources of pollutant release into the environment, type (for example, heat radiation, explosion, metals, or other objects thrust due to explosion wave and toxic cloud) and amount of compounds emitted, and potential effects of each substance on health and safety matters. In some cases, such as the release of carcinogens due to an accident while transporting hazardous substances, we need to consider the long-term effects on human health and the environment. It is also necessary to examine the risks associated with different types of exposure recipients. Quantitative risk assessment is based on statistical and probabilistic methods that require numerical data, which represents the numerical value of the probability of occurrence and consequences, to calculate risk.

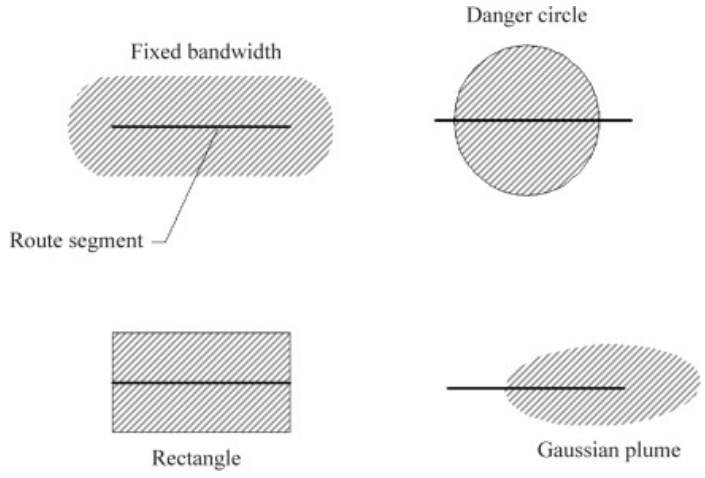

Figure 1.1: Possible shapes of impact area around the route segment (Erkut et al., 2007)

Hazmat transportation accidents have many undesirable consequences, such as economic losses, injuries, environmental pollution, and fatalities. These consequences are a function of the impact area (or exposure zone) and population, property, and environmental assets within the impact area. In this regard, the traditional risk model, based on the product of the consequence and the probability of an unwanted incident, is the most frequent definition approach in hazmat networks (Holeczek, 2019; Erkut et al., 2007). Even if the number of hazmat incidents with the release seems insignificant compared to the number of hazmat-carrying shipments, the consequences can still be catastrophic. Apart from the destructive nature of the associated incidents, they can lead to social and media attention and consequently act as pressure leverage from these groups on the authorities. Different geometric shapes have been utilized to represent the exposure area. Figure 1.1 displays four commonly applied shapes for the impact area.

The shape and size of an impact area depend on several factors, such as the

substance being transported, topology, and wind speed and direction. In the danger circle case, the impact area can be defined as the associated area of the danger zone with the radius of λ as $\pi \times \lambda^2$. The radius of the danger zone depends on the class and the amount of hazmat loaded on the vehicle. Usually, due to the hazardous nature of the material, the worst-case situation is applied by assuming that the radius represents the danger zone of a fully-loaded vehicle for one given hazmat class. Subsequently, the consequence of the incident can be achieved by multiplying the impact area by a measure such as the average population density along the arcs. Similarly, we can define the impact area in a rectangle danger zone by $2 \times l_{i,j} \times \lambda$ as we have two rectangles above and below the arc $l_{i,j}$. In the fixed bandwidth approach, if $l_{i,j}$ stands for the length of an arc (i, j), the impacted area of a hazmat incident using the bandwidth method is calculated by $2 \times l_{i,j} \times \lambda + \pi \times \lambda^2$ (Holeczek, 2019).

The Gaussian plume model is more complicated than the three other methods. The concentration of the airborne contaminant depends on the distance from the source of the accident in an airborne hazmat. Here the impact of wind and the distance from the source leads to lower concentration. Therefore, the Gaussian plume model is applied to achieve more realistic approximations of the impact area. The following is the associated formulation from Erkut et al. (2007):

$$C(x, y, z, h_e) = \frac{Q}{2\pi\mu\sigma_y\sigma_z} exp\left(-\frac{1}{2}\left(\frac{y}{\sigma_y}\right)^2\right) \times \left[exp\left(-\frac{1}{2}\left(\frac{z-h_e}{\sigma_z}\right)^2\right) + exp\left(-\frac{1}{2}\left(\frac{z+h_e}{\sigma_z}\right)^2\right)\right] \tag{1.1}$$

In the above formulation C is the concentration level (mass per unit volume

$-\mu g/m^3$ or parts per million –ppm), x is the distance downwind from the source (m), y is the distance crosswind (perpendicular) from the source (m), z is the elevation of the destination point (m), h_e is the elevation of the source (m), Q is the release rate of pollutant (mass emission rate $-g/s$ or volumetric volume rate $-m^3/s$), μ is the average wind speed (m/s), σ_y and σ_z are the dispersion parameters in the y and z directions (m).

Gaining more knowledge about the potential adverse impacts of these materials, people from industries, government, and academia have concentrated on the hazmat field of study. This covers from providing training for personnel and utilizing more hazmat-resistant vehicles to the development of safer and more economical transportation networks. In academia, the researchers have tried to alter the traditional perspective, which only takes into account cost or profits when establishing the system. For this purpose, many studies have involved risk mitigation in their decision-making process, mainly employing risk as an indicator of the probability and severity of loss to an exposed receptor due to potential unwanted events regarding a hazmat (Alp, 1995).

1.4.2 Facility location problem

The facility location decisions have drawn considerable attention due to their impact on strategic and operational policies in mid-term and long-term horizons. This issue in determining the locations of hazmat-related facilities is highlighted more due to the dangerous nature of the products. There are many hazmat incidents that occur in the facilities; some have irreversible consequences. Take the Tianjin port incident

that happened on August 12, 2015, for example. In this catastrophe, 165 people were killed, and almost 7 billion RMB of economic losses were caused by an explosion at hazmat depots. There were many casualties and property losses due to improper selection of the hazmat depot, located only 600 meters from a large community that accommodates 5600 people.

The location and allocation of hazmat logistics systems play a crucial role in mitigating network risk to a great extent. This is because both storage and transportation risks are closely connected to facility location and customer allocation decisions. As the facility location process determines the best location for establishing a site from the set of candidate spots, it directly impacts storage risk while affecting transportation risk indirectly. Furthermore, based on the located stations, customer allocation makes the optimal allocation plans and determines the amount of hazmat to be stored in each facility, which directly impacts transportation risks and indirectly impacts storage risks (Fan et al., 2019).

In this section, we go through the capacitated facility location problem (CFLP), which is one of the bases for the optimization problems explored in this thesis. Each facility in CFLP has a limited capacity that cannot be violated. Hence, both demand satisfaction and capacity constraints should be considered when modeling such a problem setting.

Here, a mathematical model for CFLP is introduced. We represent the set of facilities and customers respectively by $\mathcal{F}$ and $\mathcal{V}$. Let us assume that we have a network with n customers ($i = \{1, ..., n\}$) with associated demand of d_i and m facilities or sites ($j = \{1, ..., m\}$). Also, assume that x_{ij} is a continuous variable defining the amount serviced from facility j to demand point i, and y_j is a binary variable where $y_j = 1$

indicating if a facility is established at location j. Each facility has a fixed opening/activating cost of f_j and an associated transportation cost to customer j equal to c_{ij}. Finally, Cap_j stands for the capacity of site j or the maximum service volume that can be handled by facility j. Based on the notation, the relevant optimization model for the CFLP can be specified as follows:

$$\min \sum_{j=1}^{m} f_i y_i + \sum_{i=1}^{n} \sum_{j=1}^{m} c_{ij} x_{ij} \tag{1.2}$$

$$\sum_{j=1}^{m} x_{ij} = d_i \qquad \forall i \in \mathcal{V} \tag{1.3}$$

$$\sum_{i=1}^{n} x_{ij} \leq Cap_j y_j \qquad \forall j \in \mathcal{F} \tag{1.4}$$

$$x_{ij} \leq d_i y_j \qquad \forall i \in \mathcal{V}, \forall j \in \mathcal{F} \tag{1.5}$$

$$x_{ij} \geq 0 \qquad \forall i \in \mathcal{V}, \forall j \in \mathcal{F} \tag{1.6}$$

$$y_j \in \{0, 1\} \qquad \forall j \in \mathcal{F} \tag{1.7}$$

The objective function addresses the minimization of facility activation costs and transportation expenses. Constraint (1.3) ensures that each customer's demand is satisfied. Constraint (1.4) indicates that if a facility is activated, the total demand satisfied by this site cannot exceed its capacity. An upper bound for variable x_{ij} has been provided in (1.5). Although this constraint might seem redundant, it can lead to tighter linear programs with better performance. It implies that if a facility is established, the maximum amount of satisfied demand for customer i from site j cannot exceed d_i. Finally, (1.6) and (1.7) specify the nature of the decision variables in the problem.

1.4.3 Vehicle routing problem

The initial work in the Vehicle Routing Problem area was presented in an article by Dantzig and Ramser (1959). Entitled "Truck Dispatching Problem," their model consisted of a fleet of homogeneous trucks originating from a central hub and responsible for satisfying the oil demands of several gas stations. Later on, a more generalized form of this model was developed by Clarke and Wright (1964) as a linear optimization problem. In their logistics-oriented model, a set of geographically dispersed customers around the central depot were served using a fleet of capacitated vehicles. These two studies were the pillars for developing the well-known vehicle routing problem as one of the most widely examined subjects in the operations research scope.

There has been an exponential growth in the number of publications in this scope after the introduction of VRP by citedantzig1959truck and Clarke and Wright (1964). In this regard, Eksioglu et al. (2009) stated that the VRP literature has been expanding at a rate of 6% each year. Moreover, different variants of VRP have been developed, incorporating real-life complexities, such as time window considerations, time-dependent parameters, and multi-period planning horizons.

The VRP models explicitly specify a set of routes utilized by a vehicle starting from and ending in the same depot or warehouse so that all customer needs are met, all operational constraints are satisfied, and transportation costs are minimized. Embedding more features into the original VRP drags more complexity into the model. It was proven by Lenstra and Kan (1981) that the VRP is an NP-hard problem. Therefore, only the small-scale problems can be solved by the exact algorithms optimally in a reasonable computational time, leaving the large-scale ones as a challenge for the

researchers. Considering that large-size problems are an inevitable part of modern life, just imagine the available interactions in a company like Amazon, many authors have tried to handle them by employing more efficient exact algorithms, heuristics, and metaheuristics. Now, determining the daily routes of vehicles is not the only application for the VRP algorithms. These algorithms and models also handle other strategic and tactical decisions such as facility location, inventory management, fleet sizing, scheduling, and production problems (Andersson et al., 2010; Vidal et al., 2020).

The proposed models in this thesis determine optimal facility locations and transportation routes for the available fleet of vehicles, raising the necessity of applying VRP-based formulations. We explore location-routing with time windows (LRPTW) with time-dependent parameters in chapter 3. Chapter 4 deals with an LRPTW in a waste collection network, while a multi-period LRP with permissible service intervals is investigated in chapter 5. The time window limitations are one of the most important features of the model. The quality of customer service plays a vital role in the stability and growth of corporations. As a requirement of establishing a customer-oriented business, organizations strive to satisfy their customers' needs to retain them as long as possible. An essential element of customer satisfaction is adhering to their service time windows, especially in the logistics and transportation area, where VRP plays a significant role. Apart from customer satisfaction, neglecting time windows in the strategic planning phase, if there are any, can lead to infeasible routing decisions in the operative planning or other stages. Having tighter time windows puts more pressure on the logistics company's resources and may lead to higher investments to compensate for the hectic service time windows. When the time windows

are wider, it is easier for the decision-maker to determine optimal routing decisions. This is because of the higher degrees of freedom of shifting customers in a wider time interval. In this section, we review three important variants of VRP, including capacitated vehicle routing problem (CVRP), vehicle routing problem with time windows (VRPTW), and multi-period vehicle routing problem (MPVRP).

1.4.3.1 Capacitated vehicle routing problem

In this problem, we are given a network of $\mathcal{G} = (\mathcal{V}, \mathcal{A})$ which represents the network graph of the transportation system, in which $\mathcal{V}$ is equal to the set of vertices (nodes) and A is equal to the set of arcs. $\mathcal{V}$ consists of a depot and multiple customers where the distances between each pair of nodes are known. A number of vehicles are available to serve the customers defined by $\mathcal{K} = \{1, ..., K\}$. All customers have a specific demand, and the vehicles have the same maximum capacity. Therefore, conveying shipments beyond the capacity of the vehicles is not allowed. CVRP tries to find the shortest route for the vehicles while satisfying all customers' demands. In this model, the vehicles all start and end their route at the depot.

In this section, a linear integer programming model of a CVRP is presented. The objective function for this model is minimizing the total cost of the system, which in this particular case is the total distance of the route, where all customers' demands are satisfied. Let x_{ijk} be a binary variable with a value of 1 if the arc from node i to node j using vehicle k exists in the optimal routing decision, whereby there is no travel from a node to itself. Also, c_{ij} indicates the cost of traveling from node i to node j. Here, dem_i represents each customer's demand, and $VCap$ is the maximum capacity of each vehicle. Here, the cumulative sum of the satisfied demands by vehicle

k in a route should not violate its capacity. Based on the explanations mentioned above, and assuming node 1 as the depot, the related mathematical model of a CVRP can be formulated as follows:

$$\min \sum_{i=1}^{n} \sum_{j=1}^{n} \sum_{k=1}^{K} c_{ijk} x_{ijk} \tag{1.8}$$

$$\sum_{i=1}^{n} x_{ijk} = \sum_{i=1}^{n} x_{jik} \qquad \forall j \in \mathcal{V}, k \in \mathcal{K} \tag{1.9}$$

$$\sum_{i=1}^{n} \sum_{k=1}^{K} x_{ijk} = 1 \qquad \forall j \in \{2, ..., n\} \tag{1.10}$$

$$\sum_{j=2}^{n} x_{1jk} = 1 \qquad \forall k \in \mathcal{K} \tag{1.11}$$

$$\sum_{i=1}^{n} \sum_{j=2}^{n} dem_j x_{ijk} \leq VCap \qquad \forall k \in \mathcal{K} \tag{1.12}$$

$$\sum_{i \in S} \sum_{j \in S} \sum_{k=1}^{K} x_{ijk} \leq |\mathcal{S}| - 1 \qquad \forall \mathcal{S}, |\mathcal{S}| \in \{2, ..., n\} \tag{1.13}$$

$$x_{ijk} \in \{0, 1\} \qquad \forall i, j \in \mathcal{V}, k \in \mathcal{K} \tag{1.14}$$

The cost objective is presented by (1.8). Constraint (1.9) guarantees that the number of times a vehicle enters a node equals the number of times it leaves that node. Constraint sets (1.9) and (1.10) together ensure that each node is visited only once using the same vehicle. Constraint (1.11) makes sure that each vehicle ends its route at the depot. The capacity limitation is applied in constraint (1.12). Finally, the sub-tour elimination is handled utilizing constraint (1.13). It is noteworthy to mention that there are different methods to handle the sub-tours, such as Dantzig-Fulkerson-Johnson formulation and Miller-Tucker-Zemlin formulation. Here, we have applied the former in the model, which indicates that the number of arcs that can be packed in the clique defined by the set of nodes $\mathcal{S}$ cannot exceed $|\mathcal{S}| - 1$. Finally,

(1.14) determines the nature of the decision variables in the problem.

1.4.3.2 Vehicle routing problem with time windows

The VRPTW is an extension of the CVRP in which the service time of each customer should adhere to a specified time interval or window, and vehicles arrive at the customer station at that specified time window. The assumptions are similar to the ones addressed in the CVRP model. In addition to the previous notation, some extra variables are required. Let $[\alpha_i, \beta_i]$ be the time window of costumer i. Therefore, a vehicle must arrive at costumer i not earlier than α_i and not later than β_i. Here, t_{ij} denotes the required time to arrive at costumer i from costumer j, which includes the service time at costumer i as well. The arriving time of the vehicle to customer i is denoted by s_i. Now, the associated model of VRPTW can be formulated as follows:

$$\min \sum_{i=1}^{n} \sum_{j=1}^{n} \sum_{k=1}^{K} c_{ijk} x_{ijk} \tag{1.15}$$

$$\sum_{i=1}^{n} x_{ijk} = \sum_{i=1}^{n} x_{jik} \qquad \forall \mathcal{V}, k \in \mathcal{K} \tag{1.16}$$

$$\sum_{i=1}^{n} \sum_{k=1}^{K} x_{ijk} = 1 \qquad \forall j \in \{2, ..., n\} \tag{1.17}$$

$$\sum_{j=2}^{n} x_{1jk} = 1 \qquad \forall k \in \mathcal{K} \tag{1.18}$$

$$s_i + t_{ij} + M(1 - x_{ijk}) \leq s_j \qquad \forall i \in \mathcal{V}, j \in \mathcal{V} \backslash \{1\}, k \in \mathcal{K} \tag{1.19}$$

$$\alpha_i \leq s_i \leq \beta_i \qquad \forall i \in \mathcal{V} \tag{1.20}$$

$$x_{ijk} \in \{0, 1\} \qquad \forall i, j \in \mathcal{V}, k \in \mathcal{K} \tag{1.21}$$

$$s_i \geq 0 \qquad \forall i, \in \mathcal{V}, k \in \mathcal{K} \tag{1.22}$$

Constraint (1.16) to (1.18) is the same as the CVRP. Constraint (1.19) ensures

that the hard time window limitations are established when developing the optimal routing plans. Considering a soft time windows necessitates a penalty function in the objective function for potential violations of the time windows. Constraint (1.20) is utilized to keep track of the duration of the routes. If there is a route from i to j, servicing node j can be initiated at least t_{ij} later than the start of the service time at costumer i. It is noteworthy to mention that when applying time windows, it is not necessary to incorporate sub-tour elimination constraints because the time window constraints automatically exclude sub-tours. Also, (1.21) and (1.22) define the nature of the decision variables. It is noteworthy to mention that Big-M constraints are a common source of instability for optimization problems. Generally, they include a large coefficient determined to be larger than any reasonable value assigned to a continuous variable or expression. The big M impacts the constraint based on the binary variable getting a value of zero or one.

1.4.3.3 Multi-period vehicle routing problem

First introduced by Beltrami and Bodin (1974), MPVRP is a variant of the capacitated VRP, in which serving the customers is handled during a multi-period planning horizon. The real-life applications of MPVRP are available in many topics such as green VRP, VRP in reverse logistics, and waste collection problems. In MPVRP, the decision-maker is interested in assigning the customers to the available days of the planning horizon, clustering customers to tours, and defining the sequence of customers in each tour.

To develop the MPVRP, we need to adjust the variables to encompass the time concept and also introduce a new variable to identify the scheduling of customers over

the planning horizon $\mathcal{T} = \{1, ..., T\}$. Therefore, we adopt x_{ijk}^t as the binary variable indicating the movement from node i to node j using vehicle k in day t. Also, define the binary variable $z_{ik}^t = 1$ if node i is assigned to day t using vehicle k. Then, we can formulate MPVRP as follows:

$$\min \sum_{t=1}^{T} \sum_{i=1}^{n} \sum_{j=1}^{n} \sum_{k=1}^{K} c_{ijk} x_{ijk}^t \tag{1.23}$$

$$\sum_{i=1}^{n} x_{ijk} = \sum_{i=1}^{n} x_{ijk}^t \qquad \forall j \in \mathcal{V}, k \in \mathcal{K}, t \in \mathcal{T} \tag{1.24}$$

$$\sum_{t=1}^{T} \sum_{i=1}^{n} \sum_{k=1}^{K} x_{ijk}^t = 1 \qquad \forall j \in \{2, ..., n\} \tag{1.25}$$

$$\sum_{j=2}^{n} x_{1jk}^t \leq 1 \qquad \forall k \in \mathcal{K}, t \in \mathcal{T} \tag{1.26}$$

$$\sum_{j=2}^{n} x_{j1k}^t \leq 1 \qquad \forall k \in \mathcal{K}, t \in \mathcal{T} \tag{1.27}$$

$$\sum_{i=1}^{n} \sum_{j=2}^{n} dem_j x_{ijk}^t \leq VCap \qquad \forall k \in \mathcal{K}, t \in \mathcal{T} \tag{1.28}$$

$$z_{ik}^t = \sum_{j=1}^{n} x_{ijk}^t \qquad \forall i \in \mathcal{V}, k \in \mathcal{K}, t \in \mathcal{T} \tag{1.29}$$

$$\sum_{i \in S} \sum_{j \in S} \sum_{k=1}^{K} x_{ijk}^t \leq |\mathcal{S}| - 1 \qquad \forall \mathcal{S} \in \{2, ..., n\}, t \in \mathcal{T} \tag{1.30}$$

$$x_{ijk}^t, z_{ik}^t \in \{0, 1\} \qquad \forall i, j \in \mathcal{V}, k \in \mathcal{K}, t \in \mathcal{T} \tag{1.31}$$

The cost objective is presented by (1.23). Constraint (1.24) is the flow balance constraint. Constraint sets (1.25) to (1.27) together ensure that each node is visited only once in just one period and using the same vehicle. Constraint (1.28) ensure the solution adheres to the capacity limitations. The connection between the assignment and routing variables is established in 1.29. Also, sub-tour elimination is addressed

by constraint (1.30). Finally, (1.31) determines the nature of the decision variables in the problem.

1.4.4 Optimization with uncertain data

Unknown data and the lack of perfect information abound in decision-making problems in the real world. However, actions still need to be taken, and decisions must be made, even without perfect access to information. This has motivated the application of different methods for decision-making under uncertainty. We are not exactly looking to measure the uncertainty. In fact, these models seek a proper way to provide a measure to estimate the uncertainty and adequately formulate it as in an optimization problem. Considering well-defined and deterministic input data for a model, the associated optimal solution is derivable. However, with uncertain but describable (using some measures such as probability function) data, a desirable solution can be achieved, although not globally optimal. Therefore, here, the decision-maker is trying to describe the uncertain data through some measures, such as probability functions.

Assuming that the uncertainty has been described using probability functions, the decision-maker can formulate the problem in different ways. Maybe the easiest method is using corresponding expected values of uncertain data, from which the deterministic optimization problem is achievable. The drawback of this approach is that the outcome might not be satisfactory as the data variance might be significant. Alternatively, different scenarios (plausible input data sets) can be assumed with their associated probability of occurrence. This approach belongs to the stochastic optimization category. A single solution can be achieved by formulating the prob-

lem implicitly by weighting the individual solutions associated with each input data set. In other words. the obtained solution is sufficiently pre-positioned concerning all the scenarios but not particularly to any of them. How to formulate uncertain data meaningfully in optimization problems is the main topic of optimization with uncertain data approaches.

Although different studies have provided interpretations of uncertainty, they share similarities, and three main groups can be developed based on them. The uncertainty was defined as the difference between available information and the amount of demanded information when performing a specific task by Galbraith (1973). Two types of uncertainty were introduced in Mula et al. (2007) based on flexibility in the constraints, aspiration levels of goals, and uncertainty in input data: randomness and epistemic uncertainty. The main difference between these two classes is that randomness originates from the random nature of the parameters, whereas epistemic uncertainty suffers from a lack of knowledge of data. The epistemic uncertainty can originate from insufficient data or unavailability of reliable data about input parameters.

Bairamzadeh et al. (2018) proposed three types of uncertainties: randomness, epistemic, and deep uncertainty based on the amount of available information. The randomness can be tackled using stochastic programming methods or the scenario-based robust optimization technique. Epistemic uncertainty can be addressed by possibilistic programming (fuzzy logic) or a robust optimization approach. Finally, deep uncertainties are handled by convex robust optimization and with fuzzy logic techniques. According to Bairamzadeh et al. (2018) deep uncertainty can be characterized by lack of information to estimate objective or subjective probability/possibility of

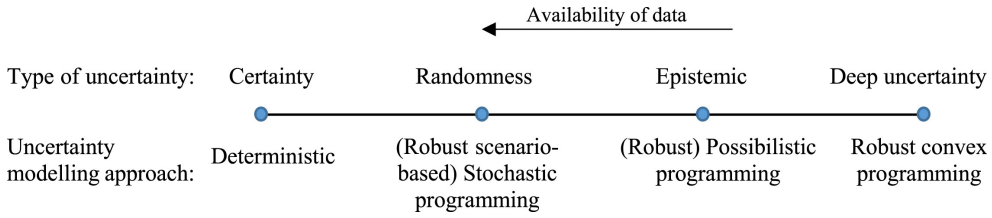

Figure 1.2: Uncertainty types and modelling approaches (Bairamzadeh et al., 2018)

plausible future situations. In other words, deep uncertainty is a condition in which the decision-maker does not know either the suitable models to characterize interactions among a system's variables or the probability/possibility measures to describe uncertainty about critical parameters in the models. A similar category has been provided by Bairamzadeh et al. (2018) in Figure 1.2. It is noteworthy to mention that epistemic uncertainty is presented in linguistic form or judgmental data, and they are associated with the lack of knowledge about input data. In this type of uncertainty, experts' opinion is a primary component.

The fuzzy set and possibility theories are pertinent to decision-making among the complementary techniques developed for an uncertain environment. In both theories, imprecision is represented and manipulated mathematically through separate but related mathematical frameworks (Julien, 1994). There may also be cases in which some of the parameters of a decision model are not precisely known, and thus their probability distributions cannot be determined. Using the fuzzy set theory, it may be possible to represent the uncertainty resulting from this lack of knowledge. Fuzzy sets can also often be expressed in terms of possibility theory, where the membership functions represent possibility distributions describing fuzzy restrictions on the allowable values of the parameters.

In possibility theory, uncertainty is characterized by employing a possibility function $\pi_Y(y)$. The degree of possibility of each y in a set S is represented by $\pi_Y(y)$. A situation is considered impossible when $\pi_Y(y) = 0$ for some y. When $\pi_Y(y) = 1$ for some y, the outcome y is deemed to be possible, i.e., just unsurprising, normal, usual. Compared to a probability of 1, this is a much weaker statement. Based on the possibility function $\pi_Y(y)$ necessity and possibility measures, (N_Y, Π_Y), can be described as probability bounds (upper and lower probabilities) (Zio and Pedroni, 2014). In this regard. the possibility of a set $\mathcal{A}$, $\Pi_(\mathcal{A})$, is defined by:

$$\Pi_Y(\mathcal{A}) = \sup_{y \in \mathcal{A}} \{\pi_Y(y)\} \tag{1.32}$$

Also, the necessity measure is obtained using (1.33):

$$N_Y(\mathcal{A}) = 1 - \Pi_Y(\overline{\mathcal{A}}) = 1 - \sup_{y \notin \mathcal{A}} \{\pi_Y(y)\} \tag{1.33}$$

In the above formulation, $\overline{A}$ stands for the complement of $\mathcal{A}$. Considering $\mathcal{P}(\pi_Y)$ as a family of probability distributions such that for all sets $\mathcal{A}$, we have $N_Y(\mathcal{A}) \leq P(A) \leq \Pi_Y(\mathcal{A})$. Then

$$N_Y(\mathcal{A}) = \inf P(\mathcal{A}) \tag{1.34}$$

$$\Pi_Y(\mathcal{A}) = \sup P(\mathcal{A}) \tag{1.35}$$

where inf and sup are concerning all probability measures in $\mathcal{P}$. As a result, the necessity level is regarded as a lower probability level, while the possibility level represents an upper limit of probability.

On the other hand, when estimating the probability or possibility of parameters is not an option, deep uncertainty can be utilized to involve uncertainty in the model.

Also, each of these categories is comprised of several sub-classes, and even there are hybrid methods, such as fuzzy robust optimization. In this thesis, we utilize different approaches to reflect the existing uncertainties: stochastic programming, scenario-based robust optimization, and chance-constrained programming. Here, we review the basics of these methods.

Finally, it is noteworthy to highlight the difference between a dynamic program and a stochastic one. The first issue differentiating a stochastic program from a dynamic one is uncertainty. In stochastic programming, there is uncertainty, and the decision results in a distribution of changes. However, dynamic programming, does not necessarily involve uncertainty. For example, in two-stage stochastic programming, the model simultaneously decides the solutions for design and control variables, not in sequence. In dynamic programming, a complex problem is divided into more manageable subproblems, which are solved recursively to find the optimal solution to the complex problem. Here using Bellman's principle of optimality, it is assumed that whatever the initial state is, the remaining decisions must form an optimal policy concerning the state resulting from the first decision. However, applications for integrating two techniques as a stochastic dynamic program are available in the literature, such as Han et al. (2018).

1.4.4.1 Stochastic programming

In this section, a standard formulation of the two-stage linear program introduced by Birge (1997) has been provided. The model can be equivalently formulated as a large-scale linear program that can be solved employing standard linear programming techniques. In this model, X and Y are two polyhedral sets, the uncertain parameter

$\omega \in \Omega$ is a random variable from a probability space. The first stage is built upon the first-stage variable x in problem $(SP1)$, which is decided before the realization of the uncertain parameter ω. The second stage, problem $(SP2)$, involves corrective actions that can be taken after the realizations of the random variables. In other words, problem $(SP1)$ seeks a first-stage decision that minimizes the first-stage objective and the expected cost of second-stage decisions (recourse decisions). It is noteworthy to mention that a single-stage stochastic program only optimizes the expected value with no subsequent recourse.

$$(SP1)\ \min c^t x + E_\omega[Q(x,\omega)]$$
$$x \in X \tag{1.36}$$

$$(SP2) Q(x,\omega) = \min f(\omega)^t y \tag{1.37}$$
$$D(\omega)y \geq h(\omega) + P(\omega)x \tag{1.38}$$
$$y \in Y \tag{1.39}$$

1.4.4.2 Scenario-based robust optimization

Robust optimization is applied in this study to handle the uncertainty of parameters. This method can be extremely useful especially in the case with limited information about the distribution of data. Based on partial details of the uncertain parameters' distribution, a proper design of uncertainty sets can ensure the consistency between the robust counterpart and the primary problem. Mulvey et al. (1995) extended the objective function of problem $(SP1)$ and introduced the scenario-based robust optimization approach. They discussed the robust optimization of mathematical pro-

gramming problems with noisy, erroneous, or incomplete data where the optimization process is related to problems that the data type is of scenario type. That research raised two issues, including model robustness and solution robustness, and presented a robust optimization model by considering the cost-benefit analysis between these two concepts. The optimal solution of mathematical programming regarding optimality is still robust if it remains close to the optimal for each realization of a particular scenario, called solution robustness. On the other hand, the solution is robust if it remains almost feasible for any realization of a specific scenario, named model robustness. The penalty function measures the infeasibility of the model. In their robust optimization model, there are two types of variables: design variables and control variables. For design variables, possible parameters are decided before the realization of the uncertain parameters, and they cannot be altered after the realization. Control variables are adjusted after a certain realization of the uncertain parameters. Therefore, they depend both on the realization of uncertain parameters as well as the optimal vector of the design variables.

In this formulation, the objective function is (1.40). Here, $f(y)$ is a variability measure of the second-stage objective. The variance is a widely used measure for this purpose. Also, λ is a non-negative scalar that stands for the risk tolerance of the modeler. The first element of the objective function stands for the design variables. The second component incorporates the expected value of the objective function for different scenarios with regard to control variables. Finally, the last part is utilized as a penalty term to maintain the stability of controls over all scenarios.

$$\min c^t x + E_\omega[Q(x,\omega)] + \lambda f(y) \tag{1.40}$$

1.4.4.3 Chance-constrained programming

First introduced by Charnes and Cooper (1959) and Miller and Wagner (1965), chance-constrained programming (CCP) is a competitive tool for solving optimization problems under uncertainty. This method guarantees that the model's constraints are satisfied with a specific confidence level. In fact, quantifying the relationship between profitability and reliability, CCP guarantees a certain performance level.

We assume that $X \in \mathcal{R}^n$, and the uncertain parameter $\omega \in \Omega$ is a random variable with a probability distribution of P. Also, α is the confidence level that belongs to interval $(0, 1)$. We define the original model as:

$$\min c^t x$$

$$G(x, \omega) \leq 0 \tag{1.41}$$

$$x \in X \tag{1.42}$$

Then, we can develop the associated CCP of the model as:

$$\min c^t x$$

$$P\left(G(x, \omega) \leq 0\right) \geq (1 - \alpha) \tag{1.43}$$

$$x \in X \tag{1.44}$$

1.4.5 Solution algorithms

There are mainly two points to be considered in the developed solutions algorithms for this research: managing the bi-objective nature of the problem, deriving efficient solutions and handling large-scale problems. The former matter is addressed in the associated models using an augmented ε-constraint method from which global Pareto

front points are achieved. Also, this technique is an effective way to explore the existing trade-offs between the objective functions. The second question is handled by applying branch-and-cut (available in the programming software) and developed branch-and-price techniques.

1.4.5.1 ε-constraint method

The augmented ε-constraint method was proposed by Mavrotas (2009) and then improved by Mavrotas and Florios (2013). We select this method due to its advantages in effectively and efficiently generating the Pareto optimal set for the decision-maker. Belonging to the category of generation methods for multiple objective problems, the ε-constraint method outshines the most commonly applied weighting approach (Mavrotas, 2009) in the following aspects: 1) capability of producing non-extreme efficient solutions and hence providing a richer representation of the solution set, 2) being able to handle integer and mixed-integer models, 3) indifference in the scale of multiple objectives (as only one objective remains as the main objective, and the rest are treated as constraints), and 4) the easiness in adjusting the number of solutions. In addition to the benefits of the standard ε-constraint method, the augmented ε-constraint method is further enhanced by incorporating acceleration issues to ensure the solution efficiency while keeping reasonable solution times. Moreover, according to a numerical test conducted by Zhao et al. (2021), it is demonstrated that the augmented ε-constraint approach delivers better performance (i.e., average gap and computational time) over the weighted goal programming and the lexicographic approach in a waste management network. Furthermore, unlike many other popular multi-objective approaches, such as goal programming and weighted sum meth-

ods, the augmented ϵ-constraint approach exempts the decision-maker from agitating about the weights of objective functions, which in turn omits the need for scaling them over each other. Given the above features, the augmented ε-constraint method is applied in this research to derive a global Pareto set of solutions effectively with both continuous and discrete variables. This method can be formulated as follows:

$$\begin{aligned} \min\ & f_1(x) - eps \times (^{\delta}/_{\Delta}) \\ & f_2(x) + \delta = \varepsilon \\ & B(x, b) = 0 \\ & \delta \geq 0 \end{aligned}$$

The symbol ε represents the upper bound of the second objective, and δ is the corresponding slack variable for the constraint. Given the range of the second objective function, parameter Δ is included to avoid scaling issues. Furthermore, parameter *eps* is an adequately small number that usually takes a value in the interval $[10^{-6}, 10^{-3}]$ (Mavrotas, 2009).

1.4.5.2 Branch-and-price algorithm

Obtained by combining branch-and-bound (BB) with column generation (CG) methods, branch-and-price (BP) is a combinatorial optimization technique for solving integer linear programming and mixed-integer linear programming problems with many variables. This method takes advantage of CG as a pricing scheme to deal with large-scale problems. CG avoids unnecessary enumerations by considering the most negative (or positive) reduced cost. However, when an LP relaxation is solved by

column generation, the solution is not necessarily integral, and it is not clear how to obtain an optimal or even feasible integer solution to the IP since standard branch-and-bound techniques can interfere with the column generation algorithm.

The procedure in BP starts with reformulating the model using the Dantzig-Wolfe formulation technique to generate the master problem (MP). The challenge in solving the master problem lies in a large number of generated columns. To deal with this issue, BP considers a restricted master problem (RMP) in which only a subset of columns has been considered. Then, a relaxed form of the RMP is solved, and the achieved solution's optimality is examined using a sub-problem named pricing-problem. The pricing problem determines if any new columns exist to be added to the basis in RMP. The algorithm terminates whenever no columns are available to be added to the RMP. Also, the branching takes place when no columns price out to enter the basis, meaning that the LP solution does not satisfy integrality conditions. In other words, if the optimal solution set of the linear master problem contains fractional values, then two new complementary subproblems are generated using the branching rules.

1.5 Co-authorship Statement

I, Saeed Tasouji Hassanpour, hold a principal author status for all the manuscript chapters (Chapters 2-4) in my thesis. However, each of the manuscripts is supervised by Dr. Ginger Y. Ke and co-authored by Dr. David M. Tulett and/or Dr. Jiahong Zhao, whose contributions have considerably facilitated the development of the ideas in the associated project, enhanced the quality of outputs, provided better practical

aspects of the computational experiments, and improved the manuscript writing. The contributions for each manuscript are listed in the followings.

Chapter 3 Tasouji Hassanpour, S., Ke, G. Y., & Tulett, D. M. (2021). A time-dependent location-routing problem of hazardous material transportation with edge unavailability and time window. *Journal of Cleaner Production*, 128951.

- Presented in *CORS 2021*
- Presented in *Brown Bag seminar at MUN, 2021*

Chapter 4 Tasouji Hassanpour, S., Ke, G. Y., Zhao, J., & Tulett, D. M. (October, 2022). A Stochastic Location-Routing Problem for Infectious Waste Management During a Pandemic with Application of Chance Constrained Time Windows. Submitted to *Computers & Industrial Engineering*, **2nd Review**.

- Presented in *INFORMS 2021*
- Presented in *POMS 2022*

Chapter 5 Tasouji Hassanpour, S., Ke, G. Y., Zhao, J., & Tulett, D. M. (September, 2022). A multi-stage decision framework for managing hazardous waste logistics with random release dates. Submitted to *Expert Systems with Applications*.

- Presented in *INFORMS International/CORS 2022*
- Presented in *Brown Bag seminar at MUN, 2022*
- Presented in *INFORMS Annual Meeting 2022*

Chapter 2

Literature Review

This chapter explores the relevant literature in several pathways, including time considerations, uncertainty issues, disruption management, solution methods, and hazardous waste management, from which literature gaps are identified.

In academia, different classification exists for the studies in the hazmat field. The first classification was introduced by Erkut et al. (2007) dividing the existing works into four categories: risk assessment, routing, combined facility location and routing, and network design. Later, Bianco et al. (2013) added another group as toll setting to the above classification. Recently, Mohri et al. (2021) considered six classes for the related problems: Hazmat Risk Assessment/Analysis, hazmat routing, hazmat routing-scheduling, hazmat facility location, hazmat location-routing, and hazmat transportation network design. Regardless of their category, all the papers in these classifications have contributed a lot to developing efficient networks. Focusing on single or multi objectives, a significant number of operational research and mathematical optimization techniques have been applied to solve hazmat transportation problems considering particular objectives. The primary difference between a haz-

mat transportation model with other transportation models originates from the term risk. Risk is an inevitable element of any hazmat-related network due to the potential threats to human beings, the environment, and properties. In the literature, there is almost a consensus over the definition of the term hazardous material, and different references share similarities in explaining it. On the contrary, the definition of risk alters widely, and many distinct methods have been presented and discussed in the last decades.

In Figure 2.1a, we can see that since 2019 the road transportation mode accounted for more than 72% of the articles, highlighting the importance of exploring such a common and vital shipping mode for hazardous materials. Also, as illustrated in Figure 2.1b, risk assessment and routing problems constitute the most investigated classes of hazmat transportation.

This project aims to develop a mathematical model that is able to determine the simultaneous options for the locations of hazmat facilities and the routing plans by minimizing both cost and risk objectives. For identifying the available gaps in the relevant literature, the review focus has been on the location-routing problems in the hazardous material area, including non-medical and medical networks. The taxonomy of the relevant literature has been provided in Table 2.1. For this purpose, several features of the related publications such as model decisions (location, routing, and inventory), uncertainty considerations, disruptions, time-dependent nature, time windows application, and solution methods have been explored.

The first part of the literature review section focuses on the four most relevant areas in hazmat transportation: 1) time considerations, 2) uncertainty issues, 3) disruption management, and 4) solution methods. According to different model features,

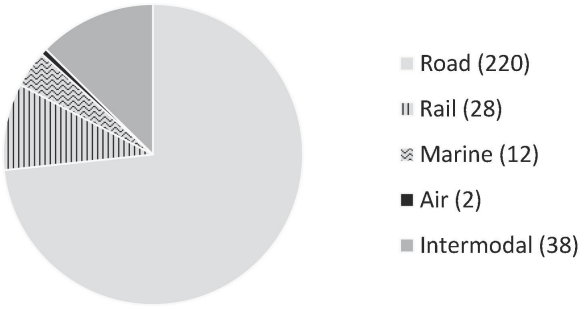

(a) Number of articles divided by transportation mode

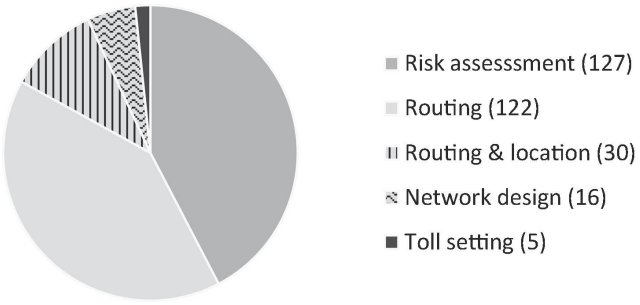

(b) Number of articles divided by problem category

Figure 2.1: Number of contributions by transportation mode and problem category (Holeczek, 2019)

the second part investigates an important branch of hazardous location-routing problems (HLRP), which is medical waste management. Then, based on the review, the literature gap identification is presented at the end of this section.

2.1 Time considerations

The applications of time-related attributes in the transportation networks generally appear in the form of time windows and time-dependent characteristics. The former employs restrictions on the arrival and departure times of specific locations in a dynamic road network. The latter, apart from the spatial considerations, incorporates time-varying parameters in the model. Although involving time attributes seems to be a realistic and vital component of any road network setting, they have been addressed only in a small number of articles in the hazmat location-routing literature.

As one of the pioneers in applying time windows in the vehicle routing problem of hazardous materials, Tarantilis and Kiranoudis (2001) considered hard time windows at the depot. Later on, Zografos and Androutsopoulos (2004) studied the vehicle routing problem with time windows (VRPTW) by assuming permissible service time intervals. Adopting a weighted sum approach, they converted the bi-objective model into a single objective one and solved it using an insertion heuristic. Moreover, they examined the proposed model based on tight and loose time windows in four different scenarios. Another application of hard time windows can be found in the work of Zhang et al. (2005a). They implemented hard time windows on the delivery time of vehicles. Employing load upper bounds on the road segments, a load limitation was imposed on the various edges of the road, based on the nature of the pathway.

Table 2.1: A comparison of relevant literature

#	Reference	Decision		Uncertainty				Time Windows	Time-dependent	Solution		
		LR	I	Deterministic	Stochastic	Robust	Fuzzy			Approach	Exact	Approximate
1	Zografros and Samara (1989)	✓		✓						GP	✓	
2	ReVelle et al. (1991)	✓		✓						MIP	✓	
3	List and Mirchandani (1991)	✓		✓						WS	✓	
4	Alidi (1992)	✓		✓						GP	✓	
5	Stowers and Palekar (1993)	✓		✓						MIP	✓	
6	Warmerdam and Jacobs (1994)	✓					✓			B&B, Pivot&Complement	✓	
7	Jacobs and Warmerdam (1994)	✓		✓						CA	✓	
8	Current and Ratick (1995)	✓		✓						WS	✓	
9	Wyman and Kuby (1995)	✓		✓						WS+CA	✓	
10	Giannikos (1998)	✓		✓						GP	✓	
11	Nema and Gupta (1999)	✓		✓						WS	✓	
12	Nema and Gupta (2003)	✓		✓						GP	✓	
13	Cappanera et al. (2003)	✓		✓						Lagrangian heuristic, B&B	✓	
14	Zhang et al. (2005b)	✓		✓						A greedy procedure		✓
15	Alumur and Kara (2007)	✓		✓						WS	✓	
16	Emek and Kara (2007)	✓		✓						MIP	✓	
17	Zhao and Zhao (2010)	✓		✓						GP	✓	
18	Shuai and Zhao (2011)	✓		✓						TOPSIS-based	✓	
19	Aboutahoun (2012)	✓		✓						Floyd Warshall's Algorithm	✓	
20	Boyer et al. (2013)	✓		✓						WS	✓	
21	Samanlioglu (2013)	✓		✓						LWT	✓	
22	Berglund and Kwon (2014)	✓				✓				Full enumeration, GA	✓	✓
23	Ardjmand et al. (2015)	✓		✓						GA		✓
24	Wei et al. (2015)	✓					✓			A fuzzy simulation–based GA	✓	✓
25	Zhao and Verter (2015)	✓	✓	✓						GP	✓	

ALNS: Adaptive Large Neighborhood Search, *B&B*: Branch and Bound, *BD*: Benders Decomposition, *CA*: Constraint Approach, *CPA*: Cutting Plane Algorithm , *EC*: ϵ-constraint, *GA*: Genetic Algorithm, *GP*: Goal Programming, *I*: Inventory decision, *LR*: Location-routing decision, *LWT*: Lexicographical Weighted Tchebychef, *MC*: Monte Carlo Simulation, *MIP*: Mixed Integer Programming, *MOHCGA*: Multi-Objective Hybrid Cultural and Genetic Algorithm, *MOPSO*: Multi-Objective Particle Swarm Optimization, *MOSA*: Multi-Objective Simulated Annealing, *NSGA-II*: Non-dominated Sorting Genetic Algorithm II, *PESA-II*: Pareto Envelope-based Selection Algorithm II, *SAA*: Sample Average Approximation, *SPEA-II*: Strength Pareto Evolutionary Algorithm II, *TS*: Tabu Search, *VNS*: Variable Neighborhood Search, *WS*: Weighted Sum

Table 2.1 (continue) : A comparison of relevant literature

#	Reference	Decision		Uncertainty				Time Windows	Time-dependent	Solution		
		LR	I	Deterministic	Stochastic	Robust	Fuzzy			Approach	Exact	Approximate
26	Ghezavati and Beigi (2016)	✓					✓	✓		WS	✓	
27	Ardjmand et al. (2016)	✓			✓					GA		✓
28	Farrokhi-Asl et al. (2017)	✓		✓						NSGA-II, MOPSO		✓
29	Zhao and Zhu (2016)	✓	✓	✓						LWT	✓	
30	Zhao et al. (2016)	✓		✓						LWT, EC, WS	✓	
31	Tunahoğlu et al. (2016)	✓		✓						ALNS		✓
32	Yu and Solvang (2016)	✓		✓						EC	✓	
33	Asgari et al. (2017)	✓		✓						MIP, Memetic algorithm + TS	✓	✓
34	Mantzaras and Voudrias (2017)	✓		✓						GA, MC		✓
35	Yılmaz (2017)	✓		✓						MIP, EC	✓	
36	Zhao and Ke (2017)	✓		✓						TOPSIS-based	✓	
37	Aydemir-Karadag (2018)	✓		✓						MIP	✓	
38	Farrokhi-Asl et al. (2018)	✓		✓						NSGA-II, SPEA-II, MOPSO, MOSA, MOHCGA		✓
39	Rabbani et al. (2018)	✓		✓						NSGA-II, MOPSO, MIP	✓	✓
40	Asefi et al. (2019)	✓		✓						MIP,VNS,VNS+SA	✓	✓
41	Hu et al. (2019)	✓		✓				✓	✓	A single GA and an adaptive weight GA	✓	✓
42	Rabbani et al. (2019b)	✓			✓					NSGA-II, MC, MIP	✓	✓
43	Delfani et al. (2020)	✓				✓	✓	✓		MIP, EC	✓	
44	Liu and Kwon (2020)	✓				✓				CPA+ BD	✓	
45	Saeidi-Mobarakeh et al. (2020)	✓				✓				Three-part MIP-based	✓	
46	Rabbani et al. (2021)	✓		✓				✓		NSGA-II, PESA-II, SPEA-II, MIP	✓	✓
47	Tirkolaee et al. (2020)	✓					✓	✓		GP	✓	
48	Yu et al. (2020c)	✓			✓					MC, SAA-GP		✓
49	Zhao et al. (2021)	✓	✓			✓				EC, LWT, GP	✓	

ALNS: Adaptive Large Neighborhood Search, *B&B*: Branch and Bound, *BD*: Benders Decomposition, *CA*: Constraint Approach, *CPA*: Cutting Plane Algorithm , *EC*: ϵ-constraint, *GA*: Genetic Algorithm, *GP*: Goal Programming, *I*: Inventory decision, *LR*: Location-routing decision, *LWT*: Lexicographical Weighted Tchebychef, *MC*: Monte Carlo Simulation, *MIP*: Mixed Integer Programming, *MOHCGA*: Multi-Objective Hybrid Cultural and Genetic Algorithm, *MOPSO*: Multi-Objective Particle Swarm Optimization, *MOSA*: Multi-Objective Simulated Annealing, *NSGA-II*: Non-dominated Sorting Genetic Algorithm II, *PESA-II*: Pareto Envelope-based Selection Algorithm II, *SAA*: Sample Average Approximation, *SPEA-II*: Strength Pareto Evolutionary Algorithm II, *TS*: Tabu Search, *VNS*: Variable Neighborhood Search, *WS*: Weighted Sum

Ma et al. (2012) examined the VRPTW and link capacity constraints in a hazmat network. In this study, the arrival time of vehicles to customer nodes should adhere to the hard time window of the associated customer. Moreover, the vehicles were obliged to provide a complete service to each location before leaving the spot. Also, the link capacity feature for the road segments was affected by the weight of the shipment. Restricting the accessing times of customers and depots, Pradhananga et al. (2014) and Pradhananga et al. (2016) took advantage of similar time window settings in formulating the vehicle routing problem. In these studies, the time of starting and ending the operations of the vehicles in depots as well as the service time of customers was controlled by predefined time intervals. The former research developed a bi-objective optimization model for a routing and scheduling problem of a hazmat network and minimized the total scheduled travel time and transportation risk. The latter extended the previous work by considering the impacts of significant traffic delays associated with hazmat incidents, in addition to the risk to the exposed population. This was performed by utilizing a measure based on the probable loss due to congestion created by the probable incident.

Imposing time intervals in the models is not limited to the time window concept. There are occasions where a link is not accessible for the routing decisions as a result of traffic control, inappropriate weather conditions, or construction activities, which is called road closure. Unlike the time window, which outlines accessible intervals during a specific period, road closure restricts the use of a link within a period. In this regard, the road closure considerations were included in the routing problem of hazmat shipments by Fan et al. (2015) through assuming no parking or waiting for the closed road to open. The authors presented a bi-objective nonlinear programming

model and a heuristic algorithm to optimize the hazmat risk and transportation cost subject to road closure constraints.

The associated literature is still in its infancy regarding the utilization of time-dependent attributes. Toumazis and Kwon (2013) included the time-dependent accident probabilities and consequences depending on the shipment's entrance time in the arc and employed the conditional value-at-risk (CVaR) method to measure the hazmat transportation risks. Zhou et al. (2014) examined the time-dependent lane reservation problem for hazmat shipment with time-varying transportation risk throughout the day. They proposed a mixed integer model minimizing the impact on the normal traffic from lane reservation and the time-dependent transportation risk. In their work, a cut-and-solve-based ε-constraint method was developed to solve the model. Incorporating road conditions and time-dependent fuzzy transportation risk, Meiyi et al. (2015) formulated a location-scheduling model. They designed a greedy method-based adaptive hybrid particle swarm optimization algorithm to find the optimal facility locations and the scheduling of vehicles. The research by Hu et al. (2017) concentrated on a time-dependent hazardous materials vehicle routing problem in a two-echelon supply chain system. Their mixed-integer model determined the departure time and the routing arrangement that minimizes the expected risk using a five-level risk function. This function depended on the different population densities caused by traffic congestion and was introduced to reflect the peak and off-peak hours during the day.

There are some articles in the literature that involve both time considerations. Time-dependent risks taking into account accident probabilities and load-dependent population exposure were addressed in Androutsopoulos and Zografos (2012). They

applied a multi-objective integer network flow model to the hazmat distribution problem with hard customer time windows. For solving the problem with intermediate stops, a label-setting algorithm was integrated into a route-building heuristic algorithm. Esfandeh et al. (2018) proposed a bi-level time-dependent hazmat logistics network with road closures as a policy to control the hazmat transportation risk. Providing a set of alternatives for each shipment in their model, they suggested a column generation-based heuristic by generating the set of alternatives for each shipment. In a more recent study, the location-routing problem of hazmat shipments was investigated in Hu et al. (2019). Their model comprised time-dependent features on edge and customer soft time windows while considering alternative routes between each origin-destination pair. However, other practical factors such as possible uncertainties and disruptions were entirely ignored in that study.

2.2 Uncertainty issues

Considering the sensitivity of hazmat transportation, embedding uncertainties in the model, and being prepared for different plausible scenarios in the future is a vital matter. In this regard, optimization with uncertain data can be categorized into three main branches: stochastic, epistemic, and deep uncertainties (Bairamzadeh et al., 2018). While the first two groups (stochastic programming and fuzzy logic) are mainly measure-based approaches, the last one generally belongs to the robust optimization concept. It should be noted that by being measure-based, we mean they can be estimated using proper measures, such as probability and possibility. The stochastic division requires at least one variable with a volatile or random nature to

fit density probabilities based on the historical data. Sometimes, logical assumptions might be replaced with data records as well. On the other hand, when there is no access to sufficient data records or there is inadequate cognition of the investigated case, applying fuzzy logic and expert opinions would be a suitable alternative. Finally, if we face deep uncertainty regarding the required information or want to explore the worst-case results of the model, the robust optimization approach can be beneficial. Besides, the application of scenario-based approaches exists in all three categories.

It is almost implausible to perceive that the actual process of a problem would strictly adhere to the determined plan. Each project is exposed to sudden and unpredicted situations, which can lead to disruptions during the process. In reality, severe weather conditions, natural or man-made disasters, and traffic congestion are some examples that might disrupt the facilities or the transportation routes. The organization should be prepared for managing the situation when facing disruptions in the system with contingency plans. In this case, by enhancing the practicality of the transportation framework, deviating from the original plans will be controlled with a minimum amount of risk and expenses. Motivated by the importance of incorporating customer-related services in hazmat transportation, this research particularly will examine the possibility of random edge disruptions. Since edge-disruption is one common type of resource unavailability in the real-world, this project will support the hazmat carrier in making proactive location-allocation-routing decisions. As a result, decision-makers will benefit from cost-effective and environmentally friendly networks with or without disruptions.

Furthermore, the recent COVID-19 pandemic has been a serious matter for hazmat transportation. Healthcare waste is known as the second most hazardous waste after

radiation waste. Processing the tremendous amount of medical waste during the pandemic has become a considerable burden for the authorities, especially during the pandemic (Das et al., 2021). The global economy still suffers the loss and irreversible damages due to the ongoing COVID-19 pandemic. The significant number of infected people with a high mortality rate due to COVID-19 demonstrates the pandemic's pressure on the associated organizations. According to WHO (2021)'s dashboard, the number of reported COVID-19 cases worldwide has passed 530 million by June 2022, claiming around five million lives. The high amount of generated waste during the outbreak is also a potential threat to the environment due, considering both medical (Ding et al., 2021; Abu-Qdais et al., 2020) and plastic (Nowakowski et al., 2020; Prata et al., 2020) wastes. As stated by State Council's joint prevention and control mechanism in China, although a 30% cut in the amount of municipal solid waste was observed during the pandemic in Hubei Province, the generated medical waste experienced a surge of 370% (Klemeš et al., 2020).

A significant effort has been undertaken by many authors to deal with deterministic location-routing problems (LRPs). However, in reality, assuming fixed values for many parameters will lead to impractical solutions due to the impacts of factors such as traffic jams, weather conditions, or road construction imposing uncertainty on their associated values. Lately, being recognized as a vital component to generate practical solutions, the necessity of embedding uncertainties in LRPs has been further highlighted. As mentioned earlier, three main optimization under uncertainty approaches have been employed, including robust optimization, stochastic programming, and fuzzy logic.

Stochastic programming. Several studies have explored the stochastic programming applications in the HLRP literature. The work by Ardjmand et al. (2016) assumed stochastic transportation costs for hazardous materials and applied a genetic algorithm to develop a bi-objective stochastic HLRP. Moreover, the role of customers was also involved in their model as an influential parameter. Their model sought to determine the locations of customer serving facilities and the disposal sites while making the optimal routing choices considering both risk and cost objectives. Rabbani et al. (2019a) proposed a stochastic multi-period model with an uncertain amount of generated waste and the number of people at risk. Aiming for three model decisions as facility location, inventory, and routing, their model introduced a simulation-optimization approach based on a multi-objective evolutionary algorithm through combining NSGA-II and Monte Carlo simulation. Finally, Yu et al. (2020a) incorporated uncertainty considerations using stochastic cost, demand, and affected population in the network design of hazardous waste management. The authors formulated a two-stage stochastic multi-objective model for the network planning of this system and implemented a sample average approximation-based goal programming to solve the mathematical model.

Robust optimization. Berglund and Kwon (2014) investigated the joint hazardous waste facility location and vehicle routing problems under demand and risk uncertainty utilizing a budgeted robust optimization methodology. Their research consisted of an independent route-choice behavior of hazmat carriers, which was reformulated as a single-level mixed-integer program. Focusing on a multi-objective multi-product hazardous waste LRP, Delfani et al. (2020) developed a basic pos-

sibilistic chance-constrained programming approach and compared its results with a robust possibilistic programming model of the proposed problem. Liu and Kwon (2020) considered a bi-level robust mixed-integer optimization problem for addressing a combined facility location and hazmat network design. In this study, the upper-level problem handled the facility location and risk mitigation decisions using a min-max structure while the routing decisions were made at the lower level. Finally, a cutting plane algorithm combined with Benders decomposition was designed to solve the developed model. Another bi-level LRP of hazardous waste management network was examined in Saeidi-Mobarakeh et al. (2020). The uncertainty considerations were embedded in the model through a scenario-based robust technique to tackle the highly fluctuating nature of hazardous waste generation rates. An exact multi-part solution method was presented as a solution method to deal with the bi-level and robust nature of the problem. Finally, the application of temporary facilities in a 4-tiered infectious waste management network during a pandemic was explored in Zhao et al. (2021). They Developed a bi-objective scenario-based robust model for the system and employed a two-commodity flow formulation assuming a set of scenarios for the generated waste in hospitals and clinics.

Fuzzy logic. The first research incorporating fuzzy numbers in HLRP scope is Warmerdam and Jacobs (1994). As the pioneers in applying fuzzy sets in this area, they introduced fuzzy sets standing for the public's degree of acceptance and implemented linear and non-linear fuzzy membership functions. The very first attempt to utilize credibilistic chance-constrained programming in the hazardous materials transportation literature was made in Wei et al. (2015). The authors adopted fuzzy

variables for the transportation cost and the number of affected people. Considering fuzzy customer satisfaction level, Ghezavati and Beigi (2016) suggested a multi-waste HWLRP with multiple treatment technologies. As mentioned earlier, Delfani et al. (2020) formulated a hybrid robust-fuzzy method by taking advantage of a robust possibilistic and a basic possibilistic chance-constrained programming approaches. Implementing fuzzy chance-constrained programming technique to address the uncertain demand parameters Tirkolaee et al. (2020) explored the sustainable location-routing problem under the pandemic setting with time windows for medical waste management. The weighted goal programming method was employed to deal with the multi-objective nature of the model.

2.3 Disruption management

Considering disruptions in the hazardous products network can play a crucial role in planning the transportation of the shipments. Failing to make the appropriate decisions in this section might impose high expenses and risks on the system. Moreover, route and facility disruptions for various reasons make them inaccessible, probably for an unknown period. This issue will harm the performance of the system with likely severe consequences. Despite the importance of this subject, only a few studies have incorporated disruptions in the hazmat literature, with no publication exploring disruptions in the HLRP field of study.

In this regard, Mohammadi et al. (2017) proposed a mathematical model for hazmat transportation network by embedding hub node disruptions through external events as well as hazmat incidents. Also, integration of the chance-constrained pro-

gramming with a possibilistic programming framework was developed to handle the uncertainties. A bi-modal hazmat transportation network with transfer yard disruptions was presented by Ghaderi and Burdett (2019). For this purpose, a two-stage stochastic HLRP was developed and solved using three heuristic methods based on statistical sampling. Jabbarzadeh et al. (2020) proposed a bi-objective two-stage stochastic program for rail shipment planning in the presence of random disruptions. Their results suggested that the implementation of disruption contingency plans can significantly mitigate hazmat risks. A mathematical model addressing the rail-truck intermodal transportation for hazmat under random yard disruptions was presented in Ke (2020a). In this article, a scenario-based robust optimization model with several recovery mechanisms at both the operational and strategic levels was proposed.

2.4 Solution methods

Reviewing the LRP literature reveals that the research on the applications of exact algorithms has attracted relatively less attention compared to other types of solutions methods. This issue is even worse regarding the HLRP publications, with only a few studies adopting exact algorithms. The classical branch-and-bound algorithms were the most popular approaches in the early publications in the LRP scope, such as Laporte and Nobert (1981) and Laporte et al. (1989). Later, more complicated approaches were developed employing branch-and-price (Berger et al., 2007; Akca et al., 2009; Ponboon et al., 2016; Yu et al., 2019) and branch-and-cut (Belenguer et al., 2011; Karaoglan et al., 2011; Contardo et al., 2013,0) algorithms for the LRP. Talking about LRPTW, Ponboon et al. (2016) was the first work applying an exact

solution approach by developing a branch-and-price approach. This method consisted of a column generation and the elementary shortest path problem with resource constraint as the pricing problem. It is noteworthy to mention that the branch-and-price algorithm has been shown to be a practical method in solving complicated and time-consuming problems in the field of transportation and logistics (Li et al., 2012; Xue et al., 2016; Qiu et al., 2017; Gao et al., 2020; Li et al., 2021b).

In LRP of hazardous materials or waste management networks, a few publications have applied exact algorithms. Focusing on obnoxious LRP, Cappanera et al. (2003) applied a Lagrangean heuristic approach, decomposing the model into location and routing subproblems, followed by a branch-and-bound algorithm. Xie et al. (2016) presented a Lagrangian relaxation with embedded column generation and local search for handling the LRP assuming probabilistic facility disruptions. In this research, the Lagrangian relaxation decomposes the problem into location and routing subproblems, while the column generation algorithm is responsible for solving the subproblems. A hybrid exact algorithm integrating branch-and-bound with several local search structures was developed in Alvarez et al. (2020) to explore the HLRP with split deliveries in a two-echelon network. The only publication addressing decomposition methods for hazardous waste location-routing problems was Wang et al. (2021). The authors employed the ε-constraint method to deal with the multi-objectiveness and utilized Benders decomposition for solving the two-stage stochastic household hazardous waste network.

2.5 Hazardous waste management

Waste management is one of the most important concerns of human societies. On the one hand, the increasing volume of waste with its various available types, and on the other hand, finding proper waste-handling methods adds to the complexity of the available conditions. Moreover, hazardous waste forms a considerable portion of the whole hazmat network. Examples of this hazmat type are solvent wastes, detergents and cleaning chemicals, pesticides and garden chemicals, and petroleum refinery wastewater treatment sludges. Therefore, it is worth reviewing their network structure.

Generally, each hazardous waste management network is built upon a combination of several operation sequences to fulfill the system's requirements. These activities include the collection, storage, treatment, recycling, and disposal of wastes. Therefore, a suitable way to differentiate the associated network of hazardous waste is to categorize them based on their system framework or hierarchy levels. According to this classification logic, there are 2-tiered networks that involve two operation levels, 3-tiered networks with three operation levels, and so forth. In the 2-tiered networks, the waste generation locations (generation nodes) are mainly the first level, where the second tier encompasses the treatment or disposal facilities. Here, the generated waste is collected from the first-tier locations and conveyed to the related operational facilities in the second tier of the network. Consideration of disposal facilities in a 2-tiered waste logistics system can be found in the works of Zografros and Samara (1989), ReVelle et al. (1991), Warmerdam and Jacobs (1994), Current and Ratick (1995), Cappanera et al. (2003), Aboutahoun (2012), Farrokhi-Asl et al. (2018), Liu

and Kwon (2020), and Tirkolaee et al. (2020). On the other hand, there are several studies (List and Mirchandani, 1991; Stowers and Palekar, 1993; Wyman and Kuby, 1995; Giannikos, 1998; Zhang et al., 2005b; Berglund and Kwon, 2014; Tunalıoğlu et al., 2016) with treatment facilities as the destination for the collected waste. Most publications with a 3-tiered waste management network investigate the interactions between generation nodes, treatment, and disposal facilities. However, there are cases addressing storage and disposal activities (Jacobs and Warmerdam, 1994), or storage and recycling centers (Zhao and Zhu, 2016; Zhao and Ke, 2017).

The most popular approach in the literature is the 4-tiered network. The authors in this type of waste management system mainly explore the interactions between the generation nodes, treatment centers, recycling facilities, and disposal locations. In this scope, the application of storage activities alongside the treatment and disposal locations exists only in Zhao and Verter (2015) and Mantzaras and Voudrias (2017). Finally, Asefi et al. (2019) and Aydemir-Karadag (2018) are the only works that developed 5-tiered networks by incorporating all the available operation options to manage the system waste.

Apart from the hierarchy categorization of the waste management systems, it is noteworthy to mention that recently mobile facilities and temporary stations have attracted the attention of researchers for effective waste management. Especially considering that establishing temporary storage or treatment stations can be a cost-effective choice when dealing with high demands. In this regard, except for Zhao et al. (2021) no papers have studied the temporary facilities in the associated literature so far.

2.6 Literature gap

In summary, Table 5.1 provides a comparison of the relevant hazmat literature regarding road transportation. For this purpose, several criteria consisting of decisions, uncertainty involvement, time considerations, and solution methods have been presented. As shown in the table, so far, no joint consideration of robust optimization, disruptions, time windows, and time-dependency issues exist in the hazmat location-routing field of study. To that end, our work will attempt to fill the gap in the road transportation of hazmat literature in several pathways. First, both the time window and time-dependent parameters will be embedded into the hazmat carrier's decisions to achieve cost-efficient location and routing decisions while mitigating the associated risk of the whole system. Second, random edge unavailabilities will be addressed as one of the uncertain factors affecting the system performance, and a proper optimization under the uncertainty technique will be applied to deal with them. Moreover, multiple connecting edges will are assumed in the model to add extra flexibility to the hazmat transportation network. The importance of this assumption is highlighted when a balanced trade-off between the risk and cost needs to be achieved in hazmat logistics.

Considering the medical waste literature in the LRP scope, we plan to formulate a stochastic LRP for infectious waste management during a pandemic with the application of chance-constrained time windows. Except for Tirkolaee et al. (2020) and Zhao et al. (2021), no publications in the medical waste field determine joint facility location and vehicle routing decisions under the pandemic setting. Also, Tirkolaee et al. (2020) and Delfani et al. (2020) are the only publications in the relevant litera-

ture that have utilized chance-constraint programming in their mathematical model. Moreover, the time window is a critical issue that is overlooked in most publications. Especially assuming a dynamic road network setting for a model necessitates the application of this feature. Only three studies have incorporated time windows in their models in the HWLRP scope. Ghezavati and Beigi (2016) considered vehicle routing with fuzzy time windows. Determining a service level function to measure satisfaction levels, they compared service level functions of fuzzy time windows with hard time windows. Rabbani et al. (2021) embedded customer satisfaction in HWLRP by meeting customers' time window. Time windows were defined for each demand node in Tirkolaee et al. (2020), and minimizing the total violation from time windows was included in the objective function.

Chapter 3

A Time-Dependant Location-Routing Problem of Hazardous Material Transportation with Edge Unavailability and Time Window

Abstract The transportation of hazardous materials (hazmat) is an inseparable component of any industrial society, where truck transportation is the most applied transportation solution for hazmat due to its versatility and flexibility, especially for short-distance and direct shipments. This paper explores the application of robust optimization in hazmat location-routing problems with edge unavailability, time-dependent parameters, and delivery time window. To be specific, random disruptions are formulated as a scenario-based robust optimization model, which is integrated with a vehicle routing problem with time windows, and then solved by an augmented epsilon constraint method. In applying the robust optimization, variabilities in cost and risk functions are introduced as critical indicators for designing robust and reliable transportation plans. In the end, the model is applied to a real-world hazmat transportation network, from which practical insights are derived. The resulting assessments shed light on the trade-off between hazmat risk versus cost, and introduce several useful indicators to facilitate the carrier in making appropriate decisions.

Keyword Hazardous Materials, Location-Routing Problem, Time Window, Time-Dependent, Uncertainty, Disruption

3.1 Introduction

The transportation of hazardous materials (hazmat), such as petroleum products, receives a great deal of attention, both in academia and industry, due to the potential catastrophic impacts on people, property, and the environment. The statistics of hazmat transportation indicate an increasing trend regarding the number of hazmat shipments in the world. As shown by the U.S. Department of Energy (2019), the amount of crude oil and petroleum shipments among the US Petroleum Administration for Defense Districts was approximated to be around 3,741, 3,943, 4,258, and 4,545 thousand barrels in the years of 2016, 2017, 2018, and 2019, respectively. Another reason for the importance of studying hazmat transportation is that the amount of hazmat shipments in the US account for about 15% of the total cargoes, and almost 60% of this amount is conveyed using road transportation in the US (Bureau of Transportation Statistics, 2017). A report published by the U.S. Department of Transportation Pipeline and Hazardous Materials Safety Administration (PHMSA, 2015) pointed out that, between 2011-2015, around 87% of all hazmat incidents in the US have occurred on the highways, and in the 2019 report, PHMSA (2019) indicated that the number of hazmat incidents on US highways in the year 2017, 2018, and 2019 was 15,746, 17,928, and 20,657, respectively.

The aforementioned statistics are only one aspect of the significance of this issue. The other challenging factor is that hazmat transportation can jeopardize the lives of people residing near the roads, as the trucks usually have to pass through human settlements, as well as its potential negative effects on the environment. Apart from the risks alongside the roads, the depots containing such materials are a potential

hazard for the residents as well as the flora and fauna in proximity. According to the Statistics Canada website, in 2018 road-related accidents accounted for 56.5% of the hazmat incidents, while 36.6% occurred at terminals and warehouses. This highlights the importance of both the routes utilized to carry hazmat and the depots that stock such materials. In August 2020, approximately 2,750 tons of ammonium nitrate exploded at a port warehouse in Beirut, Lebanon. Leading to at least 204 deaths, 6,500 injuries, and US$15 billion property damage (BBC News, 2020), the incident is a recent example of a location-related disaster which further accentuates the need for hazmat management.

In addition to the issues of incident rates and consequences, there are occasions where the shipping destination requires a specific interval of delivery, called a *time window*, which the carrier should adhere to. If the truck arrives at the destination out of this interval, it has to wait until the next permissible time window. This situation adds an extra amount of risk to the whole system. Most existing studies in hazmat transportation assumed time-invariant networks. However, the network parameters may vary dramatically throughout the day. For example, based on multiple data sources, Frank et al. (2000) stated that the accident rate varies in terms of both times of the day and weekday/weekend (Figure 3.1). Different traffic densities on the roads at specific times of the day can also directly affect the routing and scheduling problems in many ways. Nonetheless, very few studies have explored the above time attributes and corresponding influences to the hazmat carrier's routing decisions.

Furthermore, it is very unlikely that the real process of a problem would exactly follow the planned solution. Disruptions may happen when there are sudden and unpredicted situations, such as severe weather conditions, natural or man-made dis-

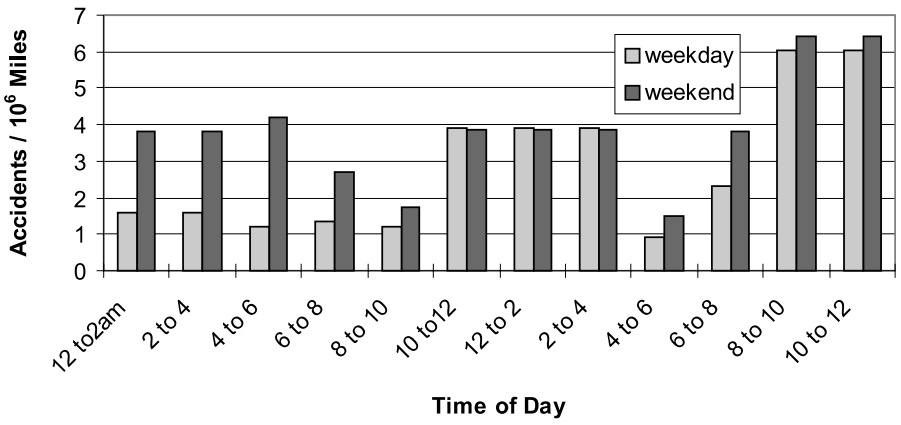

Figure 3.1: Truck accident rates (Frank et al., 2000)

asters, and traffic congestions. When these occur, there should be plans on how to return operations to normal. Being prepared for reducing the negative impacts of disruptions and optimizing the relationship between planned and real processes surely enhances the practicality of the transportation plan. Motivated by the importance of incorporating customer-related services in hazmat transportation, this research specifically considers the possibility of random edge disruptions, one common type of resource unavailability in the real-world. Through examining disruption scenarios with probabilities derived from historical data, we aim to assist the hazmat carrier in making proactive location-allocation-routing decisions, such that the total cost and risk associated with the transportation routes and warehouse sites are minimized simultaneously, both with or without disruptions.

To be specific, the contribution of this work is threefold. *First*, a scenario-based robust optimization model is integrated with the vehicle routing problem with time windows, considering possible edge disruptions. To the best of our knowledge, this is the very first attempt to construct such an integrative approach to address together

the time windows, time-dependent issues, and uncertainties. *Second*, also for the first time, the optimization model is applied to the location-routing problem of hazmat transportation. Both the system costs and risks for routing and storing hazmats are minimized and investigated through a trade-off analysis based on the ε-constrained method. *Third*, a real-world hazmat transportation network is used to illustrate the benefit of comprehensively addressing various issues in determining the facility locations and delivery routes. The numerical experiments reveal managerial insights that can enable the hazmat carrier to maintain cost efficiency and mitigate associated risks.

The remainder of this paper is organized as follows. Section 3.2 surveys the relevant literature in location-routing problems and hazmat transportation. Based on the problem description in section 3.3, section 3.4 presents the mathematical formulation with details. Section 3.5 performs a series of numerical experiments and elaborates on the findings of the model. Finally, managerial insights are summarized in section 3.6 followed by conclusions and possible future research directions in section 3.7.

3.2 Literature Review

The present research constructs a mathematical model jointly determining hazmat facility locations and travel route choices that minimize time-dependent cost and risk simultaneously. The location-routing problem for hazardous materials (HLRP) has been actively examined, especially in the area of hazardous waste management. A thorough survey of this group of literature can be found in Zhao and Ke (2017). We next focus our review on the three most relevant areas in hazmat transportation: 1)

time considerations, 2) uncertainty issues, and 3) disruption management.

3.2.1 Time considerations

The consideration of time attributes in transportation usually includes two aspects, namely the time windows and time-dependent parameters.

The time window is a critical issue frequently surfacing when planning and routing distributions under a dynamic road network setting. However, only very limited publications can be found which address this issue in the hazmat location-routing problem. The work by Tarantilis and Kiranoudis (2001) was one of the pioneers in presenting time windows in the routing problem of hazmat, where the hard time window was considered at the depot. A bi-objective vehicle routing problem with time windows (VRPTW) was presented by Zografos and Androutsopoulos (2004). Focusing on time windows for service time, they converted the problem into a single objective model using a weighted sum approach and solved it through an insertion heuristic. Their algorithm was tested under four scenarios based on both tight and loose time windows. Zhang et al. (2005a) applied hard time windows on the delivery time of vehicles and employed load upper bounds on the road segments. In that research, depending on the nature of the pathway, a load restriction was enforced on the various edges of the road. Ma et al. (2012) studied the VRPTW of the hazardous materials considering the link capacity feature for the road segments, which was affected by the weight of dangerous goods. Their model considered a hard time window for delivery at the customer that has to be adapted with the arrival time. Restricting the accessing times of customers and depots, Pradhananga et al. (2014) formulated

a bi-objective optimization model for routing and scheduling hazmat transportation, such that the total scheduled travel time and transportation risk are minimized. That study was later extended by Pradhananga et al. (2016) with similar time window settings. They considered the significant traffic delays associated with hazmat incidents, in addition to the risk to exposed population. Differing from the time window, which allows access during a certain period, road closure restricts the use of a link within a time period due to traffic control, weather conditions, or construction activities. Fan et al. (2015) presented a bi-objective nonlinear programming model to optimize the routing of hazmat shipments with the road closure. That paper assumed no parking or waiting for the closed road to open.

Concerning time-dependent accident probabilities and consequences, Toumazis and Kwon (2013) employed the conditional value-at-risk (CVaR) method to measure the hazmat transportation risks. Zhou et al. (2014) proposed a mixed integer model minimizing the impact on the normal traffic from lane reservation and the time-dependent transportation risk. A cut-and-solve-based ε-constraint method was designed to solve the model. Assuming the risks are time-dependent fuzzy random variables, Meiyi et al. (2015) formulated a location-scheduling model to find the optimal locations of depots and the scheduling of vehicles. Hu et al. (2017) developed a mixed-integer model to determine the departure time and optimal route that minimizes the expected risk. Considering the different population densities caused by traffic congestion situations, a five-level risk function was presented to reflect the peak and off-peak hours during the day. Hu et al. (2019) investigated the location-routing decisions in delivering hazmat products to customers with time-dependent characteristics on edges as well as time windows, such as intervals for delivering service to

customers. However, possible uncertainties and disruptions were entirely ignored in that study.

Addressing time-dependent times and risks as well as time windows, Androutsopoulos and Zografos (2012) applied an integer network flow model with multiple objectives to the hazmat distribution problem. A label-setting algorithm is integrated in a route-building heuristic algorithm for solving the problem with intermediate stops. More recently, Esfandeh et al. (2018) suggested time-dependent road closures as a policy to control the hazmat transportation risk. That research provided an alternative-based formulation, which was claimed to be simpler and more effective than the link-based model.

3.2.2 Uncertainty issues

The classical location-routing problems (LRPs) assume fixed and deterministic values for the data. However, in reality, the existence of situations such as traffic jams, weather conditions, or road construction, leads to uncertainty of those values. The application of uncertainty in LRPs is receiving more attention lately, where, mainly, uncertainty sets (robust optimization), probability distributions (stochastic programming), or fuzzy numbers are utilized to represent the uncertain parameters.

Stochastic programming. Ardjmand et al. (2016) applied a genetic algorithm to the bi-objective stochastic HLRP, where the transportation cost of hazardous materials was considered to be stochastic. In this research, the objective function aims to minimize the related cost and risk of locating and transporting hazmat. A multi-objective simheuristic approach through combining NSGA-II and Monte Carlo simu-

lation was applied to solve a stochastic multi-period industrial hazardous waste LRP in Rabbani et al. (2019a). Inventory control considerations, as well as the uncertainty in the waste quantity and number of people at risk, were embedded in the model. Their model focuses on minimizing the total cost, transportation risk, and site risk. The cost, demand, and affected population were structured as stochastic parameters to model the LRP in the network design of hazardous waste in Yu et al. (2020a). The authors implemented a sample average approximation-based goal programming to handle the associated two-stage stochastic bi-objective mathematical model.

Robust optimization. Berglund and Kwon (2014) studied the budgeted robust LRP for hazardous waste management by considering the number of trucks and the exposure risk as the uncertain parameters. Delfani et al. (2020) compared the results of a basic possibilistic chance-constraint model with the findings of a robust possibilistic program developed for hazardous waste LRP. A multi-objective function with consideration of multi-product transportation was considered in the model. In the study by Liu and Kwon (2020), a leader-follower game was adopted as a bi-level problem, where the facility location and risk mitigation decisions were made at the upper level, and the lower level dealt with the routing decisions. Saeidi-Mobarakeh et al. (2020) presented a bi-level scenario-based robust formulation for hazardous waste LRP and solved it by an exact three-part solution method. At the upper level, the facility location and risk mitigation decisions were made. However, the lower level concentrated on the associated costs with the collection and transportation of hazardous waste. Finally, considering temporary facilities in a 4-tiered network, Zhao et al. (2021) developed a bi-objective scenario-based robust model for the manage-

ment of infectious wastes during a pandemic. They developed the model with a two-commodity flow formulation and assuming a set of scenarios for the generated waste in hospitals and clinics.

Fuzzy logic. Wei et al. (2015) considered fuzzy variables for the transportation cost and the number of affected people in HLRP. Considering the time windows as a critical factor in determining the priority of services for hospitals, Tirkolaee et al. (2020) formulated the sustainable multi-trip LRP with time windows for medical waste management in the COVID-19 pandemic situation.

3.2.3 Disruption management

Many internal or external factors may cause resource unavailability, and therefore the consideration of system disruption is a necessary addition to transportation planning. However, only a few studies have considered disruptions in the hazmat literature. Note that the stochastic and robust methodologies can also be employed when system disruptions are considered random.

A mixed-integer nonlinear model was developed by Mohammadi et al. (2017) for hazmat transportation networks hub disruptions due to hazmat incidents or some external events. Ghaderi and Burdett (2019) presented a two-stage stochastic programming model for the location-routing problem of a bi-modal hazmat transportation network, considering possible disruptions at transfer yard facilities. Jabbarzadeh et al. (2020) developed a bi-objective two-stage stochastic program for rail shipment with the implementation of disruption contingency plans. Exploring the yard disruptions in rail-truck hazmat networks, Ke (2020a) proposed a scenario-based robust

optimization model with several recovery mechanisms at both the operational and strategic level.

3.2.4 Literature gap and our contribution

In summary, Table 3.1 provides a comparison of relevant literature (road transportation only), containing decisions, methodologies, and the above issues that were implemented in the existing studies and our proposed work. As shown in the table, so far no work has addressed all four issues jointly in the hazmat location-routing problem. To that end, our work endeavors to fill the gap in the hazmat-transportation literature in the following ways. First, both the time window and time-dependent parameters (namely the transportation risk and traveling speed in this paper) are embedded into the hazmat carrier's decisions on properly locating facilities and efficiently routing the shipments to customers. Second, random edge unavailabilities are considered as system uncertainties, which are hence formulated by a robust optimization model given various disruption scenarios. Moreover, the existence of multiple connections between the network nodes adds extra flexibility to the hazmat transportation network, especially when a balanced trade-off between the risk and cost needs to be achieved.

3.3 Problem Description

Consider a network of $G = (N, E)$ with N nodes and E edges. There are two types of nodes in the network, namely warehouse nodes (N_w) and customer nodes (N_c). The warehouses have to satisfy customers' demands across the network. A

Table 3.1: A comparison of relevant literature

#	Reference	Decision		Methodology			Uncertainty	Time Windows	Time-dependent	Disruption
		Location	Routing	Stochastic	Robust	Fuzzy				
1	Tarantilis and Kiranoudis (2001)		✓					✓		
2	Zografos and Androutsopoulos (2004)		✓					✓		
3	Zhang et al. (2005a)		✓					✓		
4	Androutsopoulos and Zografos (2012)		✓					✓	✓	
5	Ma et al. (2012)		✓					✓		
6	Toumazis and Kwon (2013)		✓						✓	
7	Berglund and Kwon (2014)	✓	✓		✓		✓			
8	Pradhananga et al. (2014)		✓					✓		
9	Zhou et al. (2014)		✓						✓	
10	Fan et al. (2015)		✓					✓		
11	Meiyi et al. (2015)	✓				✓	✓		✓	
12	Wei et al. (2015)	✓	✓			✓	✓			
13	Ardjmand et al. (2016)	✓	✓		✓			✓		
14	Pradhananga et al. (2016)		✓					✓		
15	Hu et al. (2017)		✓			✓	✓		✓	
16	Mohammadi et al. (2017)	✓		✓			✓			✓
17	Zhao and Ke (2017)	✓	✓							
18	Esfandeh et al. (2018)		✓						✓	
19	Ghaderi and Burdett (2019)	✓	✓	✓			✓			✓
20	Hu et al. (2019)	✓	✓					✓	✓	
21	Rabbani et al. (2019a)	✓	✓	✓			✓			
22	Delfani et al. (2020)	✓	✓	✓	✓		✓			
23	Liu and Kwon (2020)	✓	✓		✓		✓			
24	Saeidi-Mobarakeh et al. (2020)	✓	✓		✓		✓			
25	Tirkolaee et al. (2020)	✓	✓			✓	✓	✓		
26	Yu et al. (2020a)	✓	✓	✓			✓			
27	Zhao et al. (2021)	✓	✓		✓		✓			
	This study	✓	✓		✓		✓	✓	✓	✓

decision must be made on each warehouse, whether to be opened or not. Also, the total customers' demands must not exceed the maximum capacity of the related warehouse. A customer's demand must be satisfied by only one warehouse center. Therefore, in each scenario, there are at maximum N_w tours starting from warehouses, then traveling toward their assigned points of demand, and finally returning to the warehouses. For each edge $(i, j) \in E$, where $i \neq j$, there are alternative paths indexed by k with different cost and risk factors. This assumption makes it more realistic considering that there are usually different types of roads such as highways, main roads, and back roads between cities in most countries. Note that when an edge is unavailable due to disruptions, the truck is not allowed to take any of the paths of the proposed edge.

3.3.1 Disruption scenarios

Entwined with uncertainty, edge disruption is one of the main considerations in this research. To better manage the impact of disruptions on the routing plans, this study considers multiple disruption scenarios, each containing a set of unavailable edges. These disruption scenarios are generated based on the magnitude and range of disasters. To that end, one of the scenarios is the normal case, in which none of the edges is affected. Then, according to the appropriate scaling, other scenarios can be determined based on a measure of magnitude ranging from low to high impacts. More specifically, three scenarios, encompassing the uncertainty as the normal, optimistic, and pessimistic cases, are defined and incorporated in our analyses. This type of setting can also be seen in the literature on logistics (De Sensi et al., 2008; Piecyk

and McKinnon, 2010; Azadeh et al., 2014; Aalaei and Davoudpour, 2017; Lagarda-Leyva et al., 2019), while there are also studies focusing only on the optimistic and pessimistic scenarios (Klibi and Martel, 2012; Pavlov et al., 2019).

We further assume that all scenarios are independent of each other. Thus the formula by Snyder and Daskin (2007) can be exploited to calculate the incident probability of each disruption scenario:

$$p''_s = \prod_{e \in A_s} \omega_e \times \prod_{e \notin A_s} (1 - \omega_e), \tag{3.1}$$

where ω_e represents a probability by which an edge is disrupted. The first element of the formula accounts for all the disrupted edges by multiplying their associated incident probabilities, while the second part incorporates the undisrupted edges' probabilities. Historical data can be used to estimate these probability values. As a rule of thumb, the number of days that an out-of-service event is observed based on a particular period of time in the past can be used to estimate the probability (Ke, 2020a). For example, if an edge was disrupted for 20 days during the past year, its probability of unavailability can be computed as roughly 0.055. More sophisticated probabilistic models like Poisson distribution functions can be used in better shaping the behavior of the disruption.

3.3.2 Cost and risk functions

Cost and risk functions are defined for warehouses and tours separately. The warehouse cost is determined by such things as the rental cost of the property and other maintenance expenses. Every edge is assigned a transportation cost, which is a measure for calculating the transportation cost of tours by the truck. This research

calculates the transportation cost as a function of distance traveled on the kth path linking i and j (d_{ijk}), fuel price per unit (FP), and fuel consumption rate of truck type (FC), i.e., $c_{ijk} = d_{ijk} \times FP \times FC$. For more complicated situations, an extra cost of a toll can be included as well. Applications of toll systems in hazmat transportation can be found in Bianco et al. (2009); Ke et al. (2020).

For the risk assessment, we adopt the traditional risk assessment approach, where the transportation risk of a specific path is calculated by multiplying the incident rate along the path and the population exposure. The en-route population exposure can be estimated as either the population residing alongside a path within a radius from the path (Verma and Verter, 2007) or the traffic density on the path (Hu et al., 2019). The risk of installing a warehouse is similarly defined simply by the multiplication of the residing population around the site by the incident probability of that site.

3.3.3 Delivery time window and time-dependent parameters

The time-related assumption in this research encompasses three aspects: customer service periods; population exposures; and vehicle velocities. All parameters depend on the time of the day.

The first parameter, the customer service period, refers to the time period that the corresponding customer plans to receive the delivery. Mathematically, it can be expressed as a time window $[ot_c, ct_c]$ every day for customer c. Here, ot_c and ct_c respectively indicate the opening and closure time of customer c. For example, if an ordered package can be delivered to a customer only from 9 in the morning to 9 in the evening, the truck must visit the customer in that interval or it has to wait

until 9 a.m. the next day. In this case, the time window of this customer becomes $[9, 21]$. It is important to note that the planning horizon may cover more than a day, which can cause problems when determining if the arrival time is permitted at the customer node. Say in scenario s, the truck arrives at customer c at time 40, i.e., $a_c^s = 40$. This value is clearly on the second planning day, which is not compatible with the 24-hour-based time window of $[9, 21]$. Hence, we employ l to denote the day within the planning horizon, and convert the time window to a cumulative format. Accordingly, we have the following constraints:

$$24(l-1) + ot_c - M(1 - q_{cl}^s) \leq a_c^s \leq 24(l-1) + ct_c + M(1 - q_{cl}^s) \quad \forall c, s, l, \quad (3.2)$$

$$\sum_l q_{cl}^s = 1 \quad \forall c, s, \quad (3.3)$$

where q_{cl}^s is a binary variable that indicates if customer c is to be served in the lth day in the planning horizon in scenario s. Also, M is a big number that should be larger than any reasonable value that can be assigned to decision variables. Constraint (3.2) ensures that the arrival time of a truck for a particular customer happens between the opening and closure times of the customer within the planned day. In our above example, we have $l = 2$ and $q_{c2}^s = 1$, and so the cumulative time window becomes $[33, 45]$. Constraint (3.3) forces the truck to travel on only one day for the delivery to customer c among all days in the planning horizon.

Secondly, it is assumed that the population exposures vary in different time horizons (TH) during the day, and consequently, the corresponding hazmat transportation risks change at different times of the day. Letting uu_i^s be the departure time from node i in a 24-hour format in scenario s, the proposed time-dependent transportation

risk can then be formulated as

$$R^s_{ijk} = p_{ijk}P^h_{ijk}, \quad \text{if } uu^s_i \in TH_h,\ h = 1, 2, ..., H, \tag{3.4}$$

where p_{ijk} stands for the incident probability of traveling from node i to j through path k, and P^h_{ijk} indicates the population exposure along the kth path of edge linking nodes i and j in time horizon h. Note that the incident probabilities is normally derived using historical data on each link. To that end, the accident rate can be calculated using the number of hazmat transport accidents in a given time period divided by the total distance that hazmat trucks traveled in the same time interval. Multiplying the accident rate by the length of road segment yields the hazmat accident probability. As can be seen, the population exposure of path k between nodes i and j is determined by the time horizon of a day that a truck departs from node i.

Also, the vehicles' average traveling speeds on different paths are assumed to vary in different time horizons throughout the day. As a result, the travel time between nodes i and j by path k in scenario s (t^s_{ijk}) is calculated based on the relevant distance factor (d_{ijk}) and the average traveling speed within that path in the proposed time horizon as:

$$t^s_{ijk} = \frac{d_{ijk}}{v^h_{ijk}}, \quad \text{if } uu^s_i \in TH_h,\ h = 1, 2, ..., H \tag{3.5}$$

where v^h_{ijk} is the average velocity of trucks traveling from node i to j within time horizon h.

Similar to the arrival time in the time window consideration, the departure time from node i in scenario s, u^s_i, is also in the cumulative format. This cumulative value needs to be converted into the 24-hour format, uu^s_i, such that the corresponding time horizon of the day i.e., TH_h, can be found to determine the population exposure and

travel time. To assure this transformation, we present the following constraints.

$$uu_i^s \geq u_i^s - 24(l-1) - (1-q_{il}^s)M, \qquad \forall i, l, s \tag{3.6}$$

$$uu_i^s \leq u_i^s - 24(l-1) + (1-q_{il}^s)M, \qquad \forall i, l, s \tag{3.7}$$

$$uu_i^s \geq TH_{h-1} - (1-p_{ih}^s)M, \qquad \forall i, h, s \tag{3.8}$$

$$uu_i^s \leq TH_h + (1-p_{ih}^s)M, \qquad \forall i, h, s \tag{3.9}$$

Constraints (3.6) and (3.7) jointly play the role of a linear formulation to calculate the remainder of the variable u_i^s over 24, and calculating the variable uu_i^s. For instance, if $u_i^s = 42$, uu_i^s can be computed as $42 - 24 = 18$. As in Constraint sets (3.2), q_{il}^s shows on which day node i is served. Because a customer in a particular scenario is only served on a specific day due to Constraint (3.3), the big number M inactivates Constraints (3.6) and (3.7) for other days. Also, let variable p_{ih}^s determine which time horizon is to be chosen when a truck wants to travel from node i to j. Constraints (3.8) and (3.9) jointly guarantee that if a departure is going to happen in a particular time horizon h, variable uu_i^s must remain in the corresponding time range of the day. TH_0 is considered zero when $h = 1$. In addition, to guarantee that the departure time of the customer occurs in only one of the available time horizons, the following constraint is required:

$$\sum_h p_{ih}^s = 1, \quad \forall i, s. \tag{3.10}$$

Then, we have the following constraints to decide the values from time horizons to be chosen for parameters R_{ijk}^s and t_{ijk}^s in the model.

$$R_{ijk}^s \geq p_{ijk}P_{ijk}^h - (1-p_{ih}^s)M, \qquad \forall i, h, s \tag{3.11}$$

$$R_{ijk}^s \leq p_{ijk}P_{ijk}^h + (1-p_{ih}^s)M, \qquad \forall i, h, s \tag{3.12}$$

$$t^s_{ijk} \geq \frac{d_{ijk}}{v^h_{ijk}} - (1 - p^s_{ih})M, \qquad \forall i, h, s \tag{3.13}$$

$$t^s_{ijk} \leq \frac{d_{ijk}}{v^h_{ijk}} + (1 - p^s_{ih})M, \qquad \forall i, h, s \tag{3.14}$$

Constraints (3.11) and (3.12) are used to assign the related risk values regarding the time horizon in which the truck departs from node i to node j through path k. In the same manner, Constraints (3.13) and (3.14) assign the related travel time in regard to the time horizon in which the truck departs from node i to node j through path k. In all of the inequalities from (3.6) to (3.14), the big number M eliminates the inequalities for other unrelated time horizons.

3.4 Mathematical Formulation

In this section, we present a scenario-based robust optimization approach, proposed by Mulvey et al. (1995), to deal with the uncertainty. First, the mathematical notation is given in Figure 3.2. It can be seen that decision variables are categorized into two different groups as design variables and control variables. Design variables are independent of the unavailability scenarios, while the control variables are dependent upon those scenarios and hence are adjusted as they unfold.

Based on these two types of variables, the objective evaluation can be divided into two parts accordingly. As demonstrated by model (3.15), the design part is $f(x)$, where x denotes the set of design variables; and the control part is assessed by a combination of the expectation (μ) and variability (σ) of the control variable set y.

$$\min Z = \alpha_1 f(x) + \alpha_2 \mu_{g(y)} + \alpha_3 \sigma_{g(y)} \tag{3.15}$$

$$\text{s.t.} \quad B(x, y, b) = 0$$

Sets
N : Set of nodes regardless of their nature (warehouses and customers), indexed by i and j
N_c : Set of customer nodes, indexed by c
N_w : Set of warehouse nodes, indexed by w
E : Set of edges, indexed by e
K : Set of paths, indexed by k
S : Set of disruption scenarios, indexed by s
A_s : Set of edges affected by disruption scenario s
L : Set of days during the planning horizon, indexed by l
H : Set of time horizons during the day, indexed by h
Parameters
M: a big number
FC: Fuel consumption of each truck
FP: Unit price of fuel
ot_c: Opening time of customer c
ct_c: Closure time of customer c
sv_c : Service time on customer c
D_c: Demand of customer c
d_{ijk} : Distance of the kth path of the edge linking nodes i and j
v^h_{ijk}: Average speed of trucks in the kth path of the edge linking nodes i and j in time horizon h
t^s_{ijk} : travel time of a truck from node i to j under path k in scenario s
c_{ijk}: Cost of traveling from node i to j through path k
$c^{'}_w$: Cost of installing warehouse w
R^s_{ijk} : Risk of traveling from node i to j through path k in scenario s
$R^{'}_w$: Risk of installing warehouse w
P^h_{ijk} : Population exposure (road traffic) along the kth path of edge linking nodes i and j in time horizon h
$P^{'}_w$: Population exposure around warehouse site w
p_{ijk} : Incident probability of traveling from node i to j through path k
$p^{'}_w$: Incident probability regarding warehouse w
$p^{''}_s$: Incident probability of scenario s
Cap_w : Capacity of warehouse w
$\lambda^s_{ij} = 1$, if the edge connecting node i and j is available in scenario s; 0 otherwise
ω_e: Probability of edge e being out of service
Design decision variables
$y_w = 1$, if warehouse w is installed; 0 otherwise
$z_{cw} = 1$, if customer c is assigned to warehouse w; 0 otherwise
Control decision variables
$x^s_{ijk} = 1$ if a truck travels from node i to j under path k in scenario s; 0 otherwise
a^s_c : Arrival time of a truck to customer node c
u^s_i: Departure time of a truck from node i in a cumulative format
uu^s_i: Departure time of a truck from node i in a 24-hour format
r^s_i: Rank of node i in scenario s
q^s_{cl}= 1 if customer c is going to be served in lth day in the planning horizon in scenario s; 0, otherwise
$p^s_{ch} = 1$ if the truck is going to depart customer c in hth time horizon in scenario s; 0, otherwise

Figure 3.2: Notation

Coefficients α_1, α_2, and α_3 are applied for balancing the importance of each segment of the objective function. The first element of the objective function is composed of the design variables. The expected value of the objective function for different scenarios regarding control variables is addressed in the second component. Finally, the last element is the robustness guarantee component, which controls the variability. Note that $\sigma_{g(y)}$ is used as a penalty term to maintain the stability of controls over all scenarios. This is one of the major advantages of applying a robust approach in hazmat transportation. What follows presents the mathematical formulation of the proposed problem in the form of a scenario-based robust optimization program.

3.4.1 Objective functions

The cost objective can be formulated by

$$\begin{aligned} \min Z_1 = \ & \alpha_1 \sum_w c'_w y_w + \alpha_2 \sum_s p''_s \sum_i \sum_j \sum_k c_{ijk} x^s_{ijk} \\ & + \alpha_3 \sum_s p''_s \left| \sum_i \sum_j \sum_k c_{ijk} x^s_{ijk} - \sum_{s'} p''_{s'} \sum_i \sum_j \sum_k c_{ijk} x^{s'}_{ijk} \right| . \end{aligned} \tag{3.16}$$

As can be seen, following the structure given by (3.15), three segments are included here: the total installation cost of warehouses, as well as the expected routing (i.e., transportation) cost and the variability of cost (shown as an absolute value) over all scenarios.

The risk objective function is comprised of three parts as well. The first term is about the risk of installing warehouse sites, while the second and third terms are the expected transportation risk and the related variability, respectively.

$$\min Z_2 = \ \beta_1 \sum_w R'_w y_w + \beta_2 \sum_s p''_s \sum_i \sum_j \sum_k R_{ijk} x^s_{ijk} \tag{3.17}$$

$$+ \beta_3 \sum_s p''_s \left| \sum_i \sum_j \sum_k R_{ijk} x^s_{ijk} - \sum_{s'} p''_{s'} \sum_i \sum_j \sum_k R_{ijk} x^{s'}_{ijk} \right|.$$

3.4.2 Problem constraints

In this subsection, we present and then describe all constraints that shape the proposed problem.

$$\sum_w z_{cw} = 1 \qquad \forall c \quad (3.18)$$

$$z_{cw} \leq y_w \qquad \forall c, w \quad (3.19)$$

$$\sum_{j \neq c} \sum_k x^s_{cjk} = 1 \qquad \forall c, s \quad (3.20)$$

$$\sum_j \sum_k x^s_{ijk} = \sum_j \sum_k x^s_{jik} \qquad \forall i, j \notin N_w (i \neq j), s \quad (3.21)$$

$$\sum_k x^s_{cwk} \leq z_{cw} \qquad \forall c, w, s \quad (3.22)$$

$$\sum_k x^s_{wck} \leq z_{cw} \qquad \forall c, w, s \quad (3.23)$$

$$\sum_c \sum_k x^s_{cwk} \leq 1 \qquad \forall w, s \quad (3.24)$$

$$\sum_k x^s_{ijk} \leq z_{iw} z_{jw} \qquad \forall i, j \in N_c (i \neq j), s \quad (3.25)$$

$$r^s_i - r^s_j \geq -1 - M\Big(1 - \sum_k x^s_{ijk}\Big) \qquad \forall i, j \in N_c (i \neq j), s \quad (3.26)$$

$$r^s_i - r^s_j \leq -1 + M\Big(1 - \sum_k x^s_{ijk}\Big) \qquad \forall i, j \in N_c (i \neq j), s \quad (3.27)$$

$$\sum_c D_c z_{cw} \leq Cap_w y_w \qquad \forall w, s \quad (3.28)$$

$$a^s_j \geq u^s_i + \sum_k t_{ijk} x^s_{ijk} - M\Big(1 - \sum_k x^s_{ijk}\Big) \quad \forall i, j (j \neq i \cap i \notin N_w \cap j \notin N_w), s \quad (3.29)$$

$$a_j^s \leq u_i^s + \sum_k t_{ijk} x_{ijk}^s + M\Big(1 - \sum_k x_{ijk}^s\Big) \quad \forall i, j(j \neq i \cap i \notin N_w \cap j \notin N_w), s \quad (3.30)$$

$$u_c^s \geq a_c^s + s v_c \quad \forall c, s \quad (3.31)$$

$$x_{ijk}^s \leq \lambda_{ij}^s \quad \forall i, j(j \neq i \cap i \notin N_w \cap j \notin N_w), s \quad (3.32)$$

$$x_{ijk}^s, y_w, z_{cw}, p_{ch}^s, q_{cl}^s \in \{0, 1\} \quad \forall i, j, k, s, c, w, l, h \quad (3.33)$$

$$a_c^s, u_i^s, uu_i^s \geq 0 \quad \forall i, s \quad (3.34)$$

$$r_i^s \in Z^+ \quad \forall i, s \quad (3.35)$$

Constraint sets (3.18)-(3.19) are concerned with location-allocation decisions. Constraint set (3.18) assigns every customer to a warehouse. Not every warehouse needs to be activated, but every customer must be assigned to those active ones. Constraint (3.19) makes sure that if a warehouse is not activated, no customers are assigned to it. Constraint sets (3.20)-(3.27) are relevant to the routing decisions. Constraint (3.20) guarantees there is always a move from a customer node to a neighboring node, whether it is a warehouse or customer. This setting ensures every customer node is eventually met by a truck. Constraint set (3.21) indicates that if a truck enters a node, it must exit from it. Constraint sets (3.22) and (3.23) together ascertain that a truck never enters the warehouse from a customer if this customer is not assigned to that warehouse, and vice versa. Constraint set (3.24) guarantees that, on the one hand, the truck is allowed to enter a warehouse from at most one customer node if the warehouse is active; and on the other hand, no travel to this warehouse is made if it is not active. Constraint set (3.25) shows that a truck is allowed to travel between two customer nodes only if these customers belong to the same tour/warehouse. Constraints (3.26) and (3.27) eliminate possible sub-tour con-

structions, which is typical of the Traveling Salesman Problems (TSP). Accordingly, if there is a consecutive move from node i to j (i.e., $\sum_k x^s_{ijk} = 1$), the subtraction of the rank of the nodes ($r^s_i - r^s_j$) equals -1, which means their ranks are only different up to one degree. In this formulation, there are only moves from nodes with lower ranks to nodes with higher ones. Constraint set (3.28) is about capacity restrictions. It states that the total demand of customers assigned to a particular warehouse must not exceed its capacity. Constraint sets (3.29)-(3.31) are time window restrictions. These constraints guarantee that, if there is a move from i to j, the arrival time in the destination (j) should adhere to the prespecified time windows. Constraint sets (3.29) and (3.30) together calculate the time that a truck arrives at node j after departuring from node i. Based on these formulations, if there is a consecutive move from node i to j, the arrival time to node j equals the departure time from node i plus the travel time of the path between the two nodes. Complementary to Constraint sets (3.29) and (3.30), Constraint (3.31) computes the departure time from a node as the arrival time plus the service time. Constraint set (3.32) guarantees that there is no trip over an edge if this edge is not available in a disruption scenario. Finally, Constraint sets (3.33)–(3.35) determine the nature of the decision variables in the problem. It is important to mention that the summation $\sum_k$ embedded in most of the constraints above ensures that only one path is chosen when traveling between two neighboring nodes.

3.4.3 Linearization of the model

Note that Objectives (3.16) and (3.17) are nonlinear in nature due to the absolute value term. By applying the linearization method proposed by Yu and Li (2000), we rewrite Objective (3.16) as (3.36) accompanied by an auxiliary coefficient θ_s^1 and add a new Constraint set (3.37) as the following.

$$\begin{aligned}\min Z_1 = \ & \alpha_1 \sum_w c'_w y_w + \alpha_2 \sum_s p''_s \sum_i \sum_j \sum_k c_{ijk} x_{ijk}^s \\ & + \alpha_3 \sum_s p''_s \left(\sum_i \sum_j \sum_k c_{ijk} x_{ijk}^s - \sum_{s'} p''_{s'} \sum_i \sum_j \sum_k c_{ijk} x_{ijk}^{s'} + 2\theta_s^1 \right)\end{aligned} \tag{3.36}$$

s.t.

$$\sum_i \sum_j \sum_k c_{ijk} x_{ijk}^s - \sum_{s'} p''_{s'} \sum_i \sum_j \sum_k c_{ijk} x_{ijk}^{s'} + \theta_s^1 \geq 0 \tag{3.37}$$

According to this modification, we present the two following counteracting cases, both of which help the absolute value sign act in a linearized format.

$\sum_i \sum_j \sum_k c_{ijk} x_{ijk}^s > \sum_{s'} p''_{s'} \sum_i \sum_j \sum_k c_{ijk} x_{ijk}^{s'}$: In this case, the content inside the absolute value term is positive, and hence Constraint set (3.37) is met no matter what value θ_s^1 takes. As θ_s^1 is placed in the minimization objective function in (3.36), it must take the lowest possible value, i.e., zero.

$\sum_i \sum_j \sum_k c_{ijk} x_{ijk}^s < \sum_{s'} p''_{s'} \sum_i \sum_j \sum_k c_{ijk} x_{ijk}^{s'}$: In this case, the content inside the absolute value term is negative, and thus Constraint (3.37) is met only when θ_s^1 takes a value greater than zero. Due to the minimization function in (3.36), $\theta_s^1 = \sum_{s'} p''_{s'} \sum_i \sum_j \sum_k c_{ijk} x_{ijk}^{s'} - \sum_i \sum_j \sum_k c_{ijk} x_{ijk}^s$, is certainly a positive value. Here $2\theta_s^1$ in the objective function (3.36) ensures that we still have an extra $\sum_{s'} p''_{s'} \sum_i \sum_j \sum_k c_{ijk} x_{ijk}^{s'} - \sum_i \sum_j \sum_k c_{ijk} x_{ijk}^s$ term in the objective function.

Following the same linearization approach, objective (3.17) can be linearized by (3.38) and (3.39) where θ_s^2 is an auxiliary coefficient.

$$\min Z_2 = \beta_1 \sum_w R'_w y_w + \beta_2 \sum_s p''_s \sum_i \sum_j \sum_k R_{ijk} x^s_{ijk} + \beta_3 \sum_s p''_s \left(\sum_i \sum_j \sum_k R_{ijk} x^s_{ijk} - \sum_{s'} p''_{s'} \sum_i \sum_j \sum_k R_{ijk} x^{s'}_{ijk} + 2\theta_s^2 \right) \tag{3.38}$$

s.t.

$$\sum_i \sum_j \sum_k R_{ijk} x^s_{ijk} - \sum_{s'} p''_{s'} \sum_i \sum_j \sum_k R_{ijk} x^{s'}_{ijk} + \theta_s^2 \geq 0 \tag{3.39}$$

Moreover, constraint (3.25) is also nonlinear. To linearize the multiplication of two binary variables, an auxiliary binary variable $g_{ijw} = z_{iw} z_{jw}$ is added to the model, and constraint (3.25) can be replaced with the following additional constraints.

$$\sum_k x^s_{ijk} \leq \sum_w g_{ijw} \qquad \forall i, j \in N_c (i \neq j), s \tag{3.40}$$

$$g_{ijw} \leq z_{iw} \qquad \forall i, j \in N_c (i \neq j) \tag{3.41}$$

$$g_{ijw} \leq z_{jw} \qquad \forall i, j \in N_c (i \neq j) \tag{3.42}$$

$$g_{ijw} \geq z_{iw} + z_{jw} - 1 \qquad \forall i, j \in N_c (i \neq j) \tag{3.43}$$

$$g_{ijw} \in \{0, 1\} \qquad \forall i, j, w \tag{3.44}$$

3.4.4 Augmented ε-constraint method for obtaining the bi-objective solution

To handle the two objectives in our model, we employ the augmented ε-constraint method (AECM) proposed by Mavrotas and Florios (2013). Regarded as an exact approach, AECM is able to produce a global set of Pareto frontier solutions, where the

density of solutions can be easily adjusted. This is because the augmented version has embedded the optimization process within the other objective functions, which are transferred to the problem constraints (Mavrotas and Florios, 2013). Furthermore, unlike many other popular multi-objective methods, the AECM frees the decision-maker from needing to determine about the weights of the objective functions, which eliminates the need to scale them over each other. Application of the AECM results in the following new terms in which one of the objective functions, here $f_1(x)$, remains as the primary objective function of the problem. However, the other objective function $f_2(x)$ is transferred into the problem constraints section as a new constraint with an enforcing upper bound as follows:

$$\min\ f_1(x) - eps \times (\delta/\Delta)$$

s.t:

$$f_2(x) + \delta = \varepsilon$$

$$B(x, b) = 0$$

$$\delta \geq 0$$

The symbol ε represents the upper bound of the second objective, and δ is the corresponding slack variable for the constraint. Given the range of the second objective function, parameter Δ is included to avoid scaling issues. Furthermore, parameter *eps* is an adequately small number that usually takes a value in the interval $[10^{-6}, 10^{-3}]$ (Mavrotas, 2009). Applying the AECM to the final model while ensuring that the cost function is the primary objective function, we obtain the formulation below:

$$\min Z_1 = \alpha_1 \sum_w c'_w y_w + \alpha_2 \sum_s p''_s \sum_i \sum_j \sum_k c_{ijk} x^s_{ijk} + \tag{3.45}$$

$$\alpha_3 \sum_s p''_s \left(\sum_i \sum_j \sum_k c_{ijk} x^s_{ijk} - \sum_{s'} p''_{s'} \sum_i \sum_j \sum_k c_{ijk} x^{s'}_{ijk} + 2\theta^1_s \right) - eps \times (\delta/\Delta)$$

s.t. constraints (3.18)- (3.24), (3.26)-(3.35), (3.37), (3.39), (3.40)-(3.44), and

$$\beta_1 \sum_w R'_w y_w + \beta_2 \sum_s p''_s \sum_i \sum_j \sum_k R_{ijk} x^s_{ijk} + \tag{3.46}$$
$$\beta_3 \sum_s p''_s \left(\sum_i \sum_j \sum_k R_{ijk} x^s_{ijk} - \sum_{s'} p''_{s'} \sum_i \sum_j \sum_k R_{ijk} x^{s'}_{ijk} + 2\theta^2_s \right) + \delta = \varepsilon.$$

3.5 Numerical Experiments

In this section, we evaluate different aspects of our model in terms of validity and applicability. For this purpose, a real-world hazmat transportation network in the province of Shandong, China, is employed for numerical experiments. As shown in Figure 3.3 (Hu et al., 2019), this network contains 3 warehouses and 9 customers (varying from industrial parks to cities), which are numbered Nodes #1-#12. There are two types of road types, "expressways" and "ordinary roads," represented in the model by indices 1 and 2, respectively. Relevant data of the warehouse sites and customers are given in Tables 3.2 and 3.3. Details of other data, such as edges with their transportation risks and costs can be found in Hu et al. (2019). The average fuel consumption rate for the truck type is set as 0.302 liter per kilometer, and it is assumed that the average diesel costs 5.3 RMB/Liter (RMB is the official currency of China). The time windows for service delivery to customers is considered to be a 12-hour interval starting from 8:00 a.m. The time horizons throughout the day are 6:00–10:59, 11:00–13:59, 14:00–18:59, 19:00–22:59, and 23:00–5:59, denoted as TH_1 to TH_5, respectively.

In addition to the network data from Hu et al. (2019), we further consider disrup-

Figure 3.3: A road network for numerical experiments (Hu et al., 2019)

Table 3.2: Data on the warehouse sites (Hu et al., 2019)

Warehouse	Capacity	Unit rent (RMB)	Incident probability	Population (persons)	Site risk
1	50	300	0.0001	800	0.08
2	50	500	0.0001	700	0.07
3	40	450	0.00012	600	0.072

Table 3.3: Data on the customers (Hu et al., 2019)

Customer	4	5	6	7	8	9	10	11	12
Demand (units)	1	1.5	2.5	3	3	3.5	2.5	1	1
Service time (hrs)	0.16	0.25	0.42	0.5	0.5	0.58	0.42	0.16	0.16

tion scenarios to handle uncertainty in the availability of edges during the planning horizon. To be specific, three scenarios are studied, where the first one represents the normal situation in which all the edges are available, and the other two scenarios are designated for handling a minor disastrous situation and a major disastrous situation. When the magnitude of disruption is minor, it is assumed that only edge (5, 6) is

affected. As to the major scenario, we consider that the magnitude of the disaster is high, and the set of edges, {(4, 5), (5, 6), (7, 8), (8, 9)}, is out of service when disruption happens. To summarize, Scenario #1 represents the normal situation, Scenario #2 is the minor disastrous scenario, and Scenario #3 serves as the major disastrous scenario. Moreover, the incident probabilities of Scenarios #1 to #3 are estimated as 0.7, 0.2, and 0.1. For optimization, the model is coded in LINGO 18, and the experiments are preformed on an Intel® Core ™i5 with 2 GB RAM.

3.5.1 Extreme Pareto solutions

We first minimize the two objectives individually for the two extreme Pareto solutions. Without loss of generality, all coefficients, α_1 to α_3 and β_1 to β_3, in the objective functions are considered to be equal to one for now. Additional experiments regarding the impacts of these coefficients are conducted and discussed in Section 3.5.4. Solving the proposed problem, we present the obtained pay-offs with the two extreme Pareto points in Table 3.4. Throughout this paper, a total of six indicators are used to illustrate the solution details. Specifically for the cost objective (Eq. (3.16)), the first term gives Site Cost (SC); the term multiplied by α_2 is named Transportation Cost Mean (TCM), which shows the average transportation cost for all three scenarios; and Transportation Cost Variability (TCV), the term multiplied by α_3, shows how much variability exists in the transportation cost function. As to the risk objective (Eq. (3.17)), following the same logic, Site Risk(SR), Transportation Risk Mean (TRM), and Transportation Risk Variability (TRV) are the terms multiplied by β_1, β_2, and β_3.

Table 3.4: Extreme Pareto solutions

Extreme Pareto points	**Z_1: Cost (RMB)**	**Z_2: Risk (persons)**	**Design variables**		**Best tours**		**Elapsed time (hh:mm:ss)**
			Ware-house	**Customers assignment**	**Scenario**	**Tours**	
Z_1^*	Total=1943	Total=26.80	#1	All	#1	$1^{(1)}10^{(2)}12^{(2)}11^{(2)}9^{(2)}8^{(1)}7^{(2)}6^{(2)}5^{(2)}4^{(2)}1$	00:19:07
Min	SC=300	SR=0.08			#2	$1^{(2)}4^{(2)}5^{(1)}7^{(1)}6^{(1)}8^{(2)}9^{(1)}11^{(2)}12^{(2)}10^{(2)}1$	
Cost	TCM=1490	TRM=23.79			#3	$1^{(2)}4^{(2)}8^{(2)}6^{(2)}7^{(2)}5^{(2)}9^{(2)}11^{(2)}12^{(2)}10^{(1)}1$	
	TCV=153	TRV=2.92					
Z_2^*	Total=3420	Total=13.80	#2	All	#1	$2^{(1)}11^{(1)}12^{(2)}10^{(1)}4^{(1)}5^{(1)}6^{(1)}7^{(1)}8^{(1)}9^{(1)}2$	00:31:23
Min	SC=500	SR=0.07			#2	$2^{(1)}4^{(1)}5^{(1)}7^{(2)}6^{(1)}8^{(2)}9^{(1)}12^{(2)}11^{(2)}10^{(2)}2$	
Risk	TCM=2708	TRM=12.84			#3	$2^{(1)}4^{(1)}7^{(1)}6^{(1)}8^{(1)}5^{(1)}9^{(1)}11^{(1)}12^{(2)}10^{(1)}2$	
	TCV=212	TRV=0.89					

SC: Site Cost; TCM: Transportation Cost Mean; TCV: Transportation Cost Variability; SR: Site Risk; TR: Transportation Risk; TRM: Transportation Risk Mean; TRV: Transportation Risk Variability

As shown in Table 3.4, when only the cost objective function is minimized, the priority is given to establishing the sites with lower installation costs and selecting edges with lower transportation costs. In this case, the total cost becomes 1,943 RMB, from which 300 RMB is the cost of installing Site #1 and 1,490 RMB is the average traveling cost. The customer nodes from Node #4 to Node #12 are all assigned to Warehouse #1. The corresponding risk objective function has a value of 26.80 persons, from which 0.08 is for the site risk and 23.79 for the transportation risk. The cost and risk variability values become 153 RMB and 2.92 persons, respectively. The optimal tour includes the sequence of cities as $1 \rightarrow 10 \rightarrow 12 \rightarrow 11 \rightarrow 9 \rightarrow 8 \rightarrow 7 \rightarrow 6 \rightarrow 5 \rightarrow 4 \rightarrow 1$; while in Scenario #2, as edge (5, 6) is disrupted, the optimal tour includes the sequence of cities as $1 \rightarrow 4 \rightarrow 5 \rightarrow 7 \rightarrow 6 \rightarrow 8 \rightarrow 9 \rightarrow 11 \rightarrow 12 \rightarrow 10 \rightarrow 1$, and in Scenario #3, as most of the key edges are affected the resulting longer route includes the sequence of cities as $1 \rightarrow 4 \rightarrow 8 \rightarrow 6 \rightarrow 7 \rightarrow 5 \rightarrow 9 \rightarrow 11 \rightarrow 12 \rightarrow 10 \rightarrow 1$. These tours are depicted in Figure 3.4. Also, the numbers in parentheses in the tours indicate which path is chosen for traveling between two consecutive nodes. For example, in solution point Z_1^*, in Scenario #3, the truck goes from Node #1 to Node #4 by path 2, then goes to Node #8 by path 2, and so forth.

In the second case where the focus is only on the risk reduction, the model aims to find a solution with the least possible risk. Here, warehouse #2 is the only active site, and the total risk becomes 13.80 persons with a risk variability of 0.89. Therefore, all the customers are assigned to Warehouse #2. The corresponding cost becomes 3,420 RMB, of which 500 RMB is for the site installation, and 2,708 RMB is for the transportation cost, and also, the cost variability is 212. The point is that while in Z_2^* the focus is on the minimization of risk, the cost variability increases by 39%

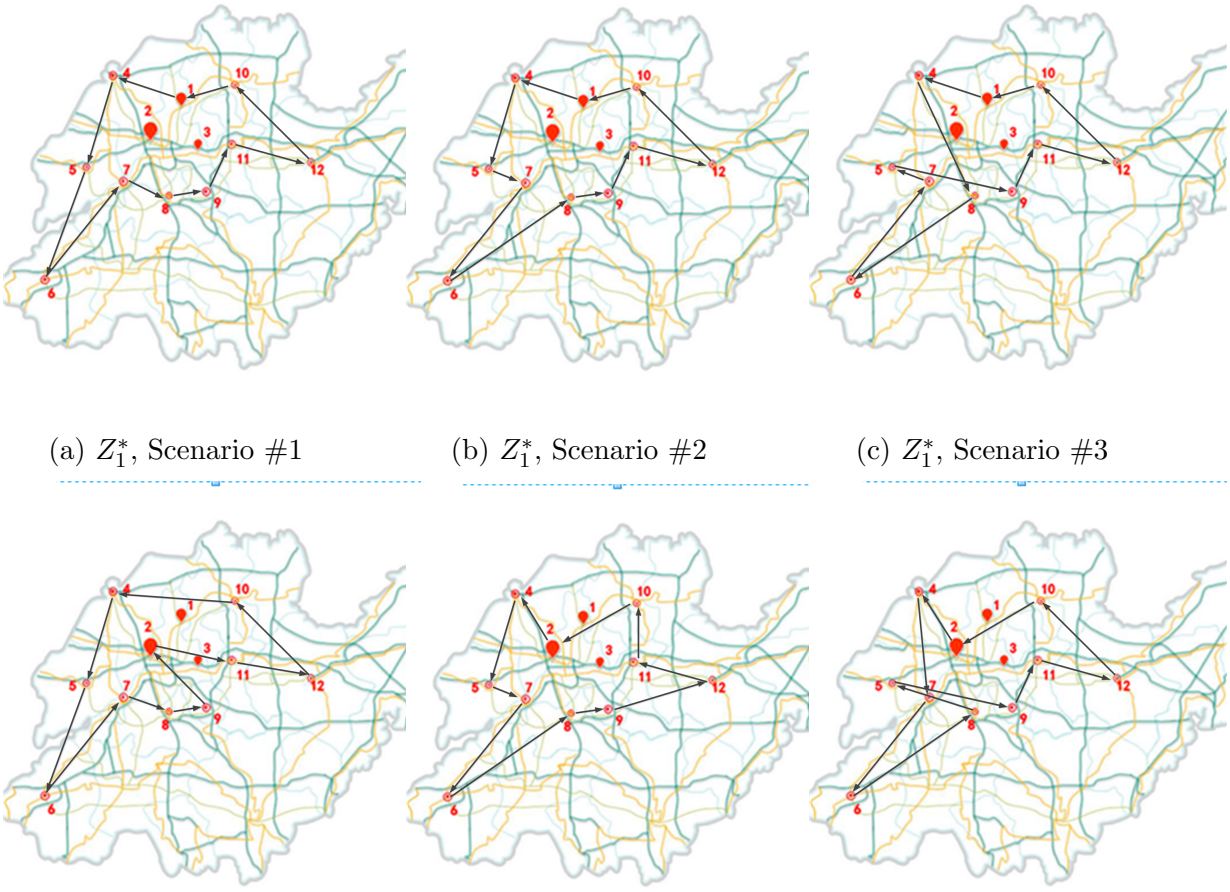

(a) Z_1^*, Scenario #1 (b) Z_1^*, Scenario #2 (c) Z_1^*, Scenario #3

(d) Z_2^*, Scenario #1 (e) Z_2^*, Scenario #2 (f) Z_2^*, Scenario #3

Figure 3.4: The optimal tours for the two extreme Pareto solution points

compared to the cost variability in solution point Z_1^* as well as a reduction of 70% in the risk objective function value.

Tables 3.5 and 3.6 are presented for more details about the scheduling of the truck's trip in completing its tours. Due to the huge amount of data, we restrict our investigations only to Scenario #1 in the two extreme Pareto solutions. In these tables, the "Edge" column shows which edges are chosen for the trip. The "Path" column determines which of the two possible paths are selected. The departure,

travel, and arrival time columns provide the times when the truck leaves a departing node, travels along the path, and arrives at the destination node. Note that the travel time values are dependent on the horizon time throughout the day in which the truck is leaving the departing node. For example, according to the first row of Table 3.5, the truck leaves Node #1 heading for Node #10 at time point 6.22 (i.e., 6:13 p.m. in the conventional representation). Because the departure time is within the first time horizon (6:00 p.m. to 10:59 p.m.), the travel time under TH_1 is extracted from the input data. Moreover, the horizon time in which the truck departs a node heading for its destination node has been determined in the column "Travel horizon." The truck then arrives at Node #10 at 8:00 p.m., and the service is delivered to the customer immediately. Then the vehicle departs to Node #12 once its service finishes at 8.42 (8:25 p.m.). The special case of this research is that the customers are only available in certain time intervals during the day. Thus, if the truck arrives at a customer node out of this interval, it must wait until the next day. This occasion happens a few times in the proposed example. One of them is when the truck departs Node #8 at time 19.89 (7:53 p.m.) and arrives at Node #7 at time 20.99 (9:00 p.m.). Because this arrival time at the customer happens after 8:00 p.m., the truck has to wait until the next day at 8:00 a.m. Similar information for Z_2^* is given in Table 3.6.

As tracking the tour is clear, we prefer to proceed to the next important information that can be perceived from these two tables. The "Cost" and "Risk" columns on Tables 3.5 and 3.6 present the costs and risks of alternative paths over the edges on the tour. Some figures in the two columns are in italics to easily see the values of cost and risk of the chosen paths along with the tours. As said before, in solution Z_1^*, attention is only given to the cost criterion, meaning that warehouses and paths with

Table 3.5: Details of the chosen paths along the tours in Scenario #1 of Z_1^*

Edge	**Path**	**Departure time**	**Travel time**	**Arrival time**	**Service start**	**Service time**	**Service finish**	**Travel horizon**	**Cost (RMB)**		**Lesser cost chosen?**	**Risk (Persons)**		**Lesser risk chosen?**
									Path 1	**Path 2**		**Path 1**	**Path 2**	
1-10	1	6.22	1.78	8	8	0.42	8.42	1	*78.57*	79.39	YES	*1.5*	2.84	YES
10-12	2	8.42	3.7	12.12	12.1	0.16	12.28	1	327.71	*147.38*	YES	3.29	*2.13*	YES
12-11	2	12.28	2.55	14.83	14.8	0.16	14.99	2	201.39	*109.47*	YES	1.85	*2.82*	NO
11-9	2	14.99	2.41	17.4	17.4	0.58	17.98	3	145.73	*90.54*	YES	1.32	*4.21*	NO
9-8	2	17.98	1.41	19.39	19.4	0.5	19.89	3	99.67	*57.05*	YES	0.77	*1.41*	NO
8-7	1	19.89	1.1	20.99	8	0.5	8.5	4	*52.51*	84.76	YES	*0.57*	0.87	YES
7-6	2	8.5	4.57	13.07	13.1	0.42	13.49	1	384.24	*198.95*	YES	3.14	*4.92*	NO
6-5	2	13.49	3.92	17.41	17.4	0.25	17.66	2	269.95	*165.6*	YES	1.84	*2.41*	NO
5-4	2	17.66	2.58	20.24	8	0.16	8.16	3	316.52	*121.05*	YES	2.34	*3.07*	NO
4-1	2	8.16	1.72	9.88	9.88		9.88	1	269.69	*79.44*	YES	3.08	*2.99*	YES
								Total:	1100.56		10	26.03		4

Table 3.6: Details of the chosen paths along the tours in Scenario #1 of Z_2^*

Edge	**Path**	**Departure time**	**Travel time**	**Arrival time**	**Service start**	**Service time**	**Service finish**	**Travel horizon**	**Cost (RMB) Path 1**	**Cost (RMB) Path 2**	**Lesser cost chosen?**	**Risk (Persons) Path 1**	**Risk (Persons) Path 2**	**Lesser risk chosen?**
2-11	1	6.71	1.29	8	8	0.16	8.16	1	*121.68*	67.95	NO	*1.32*	2.02	YES
11-12	1	8.16	1.96	10.12	10.1	0.16	10.28	1	*200.94*	114.43	NO	*2.11*	5.74	YES
12-10	2	10.28	3.7	13.98	14	0.42	14.4	1	327.71	*147.38*	YES	3.29	*2.13*	YES
10-4	1	14.4	2.33	16.73	16.7	0.16	16.89	3	*361.29*	164.14	NO	*3.96*	6.82	YES
4-5	1	16.89	2.2	19.09	19.1	0.25	19.34	3	*316.52*	121.05	NO	*2.34*	3.07	YES
5-6	1	19.34	2.18	21.52	8	0.42	8.42	4	*269.95*	165.6	NO	*1.84*	3.41	YES
6-7	1	8.42	2.58	11	11	0.5	11.5	1	*384.24*	198.95	NO	*3.14*	4.92	YES
7-8	1	11.5	1.1	12.6	12.6	0.5	13.1	2	*52.51*	84.76	YES	*0.57*	0.87	YES
8-9	1	13.1	1.12	14.22	14.2	0.58	14.8	2	*97.84*	54.75	NO	*0.57*	1.28	YES
9-2	1	14.8	1.61	16.41	16.4		16.41	3	*125.39*	83.81	NO	*1.47*	2.3	YES
								Total:	2077.74		2	19.45		10

lesser installation and transportation costs should be selected. Based on Table 3.3, Warehouse #1, with an installation cost of 300, has been installed in Z_1^*; while Warehouse #2, with an installation cost of 500, is chosen in Z_2^*. We witness the same trend when we take a closer look at the behavior of these two Pareto solutions in choosing the alternative paths in their tours. As for Scenario #1, the best tour in Z_1^* mostly selects the paths with lesser traveling costs rather than paths with lesser risks. To make this comparison more accurate, consider the times in which a path with lesser cost and risk has been selected among the possible two alternative paths over each edge. Based on Table 3.5, for Pareto solution Z_1^*, in 100% of the times (10 cases out of 10), a path with lesser cost is chosen between the two possible alternatives, while this percentage is only 40% (4 cases out of 10) for the risk criterion. On the other hand, Z_2^* pays more emphasis on solutions with lesser risk values, both on-site and on the transportation network. According to Table 3.6, paths with lesser risk values are selected among the possible alternative paths in 100% of the times; however, this figure drops to only 20% for the cost criterion. Moreover, the total cost and risk of the traversed tour by the truck through selected paths for Z_1^* and Z_2^* are also presented in the last row of these two tables.

3.5.2 Trade-off analysis

Based on the two extreme solutions, we apply AECM to facilitate risk-cost trade-off analysis. Figure 3.5 illustrates the plot of the proposed Pareto frontier containing a total of 11 non-dominated solutions. The detailed information about the nine additional Pareto solutions is explained in Table 3.7. Next, AECM is used to generate

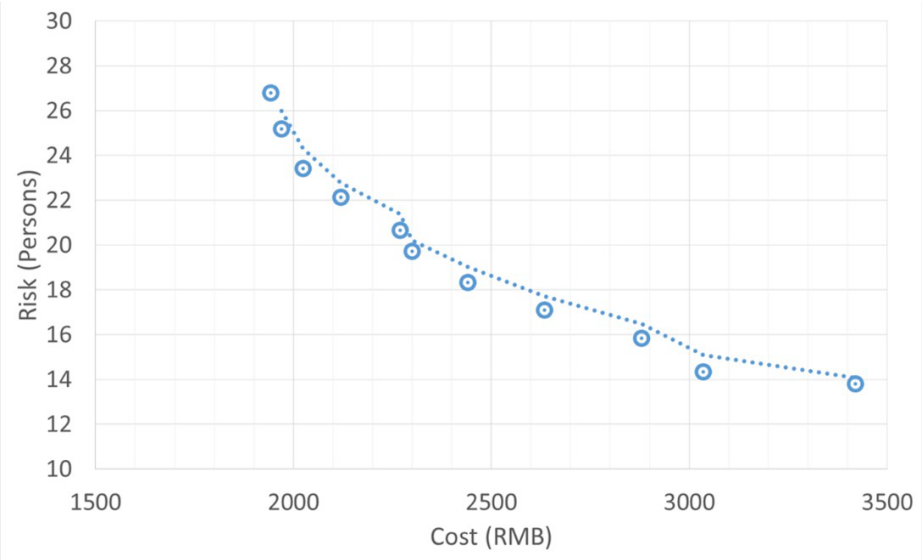

Figure 3.5: The Pareto front of the proposed problem

the intervening points in the Pareto set.

As can be seen from Tables 3.4 and 3.7, we obtain 11 Pareto points: (1,943, 26.8), (1,970, 25.19), (2,025, 23.42), (2,120, 22.12), (2,270, 20.67), (2,300, 19.73), (2,440, 18.33), (2,635, 17.10), (2,880, 15.85), (3,035, 14.35), and (3,420, 13.8). As for all of the intervening Pareto points from 1 to 9, Warehouse #1 has been activated. So the only different case belongs to Pareto solution Z_2^* in which Warehouse #2 is activated. For each scenario, the optimal tour for the majority of the Pareto solutions includes the same sequence of cities, and the only difference is in the paths chosen for travelling between nodes. For example, the optimal tour in Scenario #1 for most of the Pareto solutions includes the nodes in $1 \rightarrow 4 \rightarrow 5 \rightarrow 6 \rightarrow 7 \rightarrow 8 \rightarrow 9 \rightarrow 11 \rightarrow 12 \rightarrow 10 \rightarrow 1$; the optimal tour in Scenario #2 for all Pareto solutions includes the nodes in $1 \rightarrow 4 \rightarrow 5 \rightarrow 7 \rightarrow 6 \rightarrow 8 \rightarrow 9 \rightarrow 11 \rightarrow 12 \rightarrow 10 \rightarrow 1$, and the optimal tour in Scenario #3 for the majority of the Pareto solutions includes the nodes in

Table 3.7: Details of intervening Pareto points

Pareto	Z_1:	Z_2:	**Design variables**			**Best tours**	**Elapsed**
	Cost	**Risk**	**Ware-**	**Customers**			**time**
points	**(RMB)**	**(persons)**	**house**	**assignment**	**Scenario**	**Tours**	**(hh:mm:ss)**
1	Total=1970	Total=25.19	#1	All	#1	$1^{(1)}10^{(2)}12^{(2)}11^{(2)}9^{(2)}8^{(1)}7^{(2)}6^{(2)}5^{(2)}4^{(2)}1$	00:15:20
	SC=300	SR=0.08			#2	$1^{(1)}4^{(2)}5^{(1)}7^{(1)}6^{(1)}8^{(2)}9^{(1)}11^{(2)}12^{(2)}10^{(2)}1$	
	TCM=1546	TRM=23.59			#3	$1^{(2)}4^{(2)}7^{(2)}6^{(2)}8^{(2)}5^{(2)}9^{(2)}11^{(2)}12^{(2)}10^{(1)}1$	
	TCV=124	TRV=1.52					
2	Total=2025	Total=23.42	#1	All	#1	$1^{(2)}4^{(2)}5^{(2)}6^{(2)}7^{(1)}8^{(2)}9^{(1)}11^{(2)}12^{(2)}10^{(1)}1$	00:24:13
	SC=300	SR=0.08			#2	$1^{(1)}4^{(1)}5^{(1)}7^{(1)}6^{(1)}8^{(2)}9^{(1)}11^{(2)}12^{(2)}10^{(2)}1$	
	TCM=1591	TRM=22			#3	$1^{(2)}4^{(2)}7^{(2)}6^{(2)}8^{(2)}5^{(2)}9^{(2)}11^{(2)}12^{(2)}10^{(1)}1$	
	TCV=134	TRV=1.34					
3	Total=2120	Total=22.12	#1	All	#1	$1^{(2)}4^{(2)}5^{(2)}6^{(2)}7^{(2)}8^{(2)}9^{(2)}11^{(1)}12^{(2)}10^{(1)}1$	00:35:43
	SC=300	SR=0.08			#2	$1^{(1)}4^{(1)}5^{(1)}7^{(1)}6^{(1)}8^{(2)}9^{(1)}11^{(2)}12^{(2)}10^{(2)}1$	
	TCM=1683	TRM=20.75			#3	$1^{(2)}4^{(2)}7^{(2)}6^{(2)}8^{(2)}5^{(2)}9^{(1)}11^{(2)}12^{(2)}10^{(1)}1$	
	TCV=137	TRV=1.29					
4	Total=2270	Total=20.67	#1	All	#1	$1^{(2)}4^{(2)}5^{(1)}6^{(2)}7^{(1)}8^{(2)}9^{(2)}11^{(1)}12^{(2)}10^{(1)}1$	00:35:40
	SC=300	SR=0.08			#2	$1^{(1)}4^{(2)}5^{(1)}7^{(1)}6^{(1)}8^{(2)}9^{(1)}11^{(2)}12^{(1)}10^{(2)}1$	
	TCM=1825	TRM=19.27			#3	$1^{(2)}4^{(2)}7^{(2)}6^{(2)}8^{(2)}5^{(2)}9^{(2)}11^{(1)}12^{(2)}10^{(1)}1$	
	TCV=145	TRV=1.32					
5	Total=2300	Total=19.73	#1	All	#1	$1^{(2)}4^{(2)}5^{(2)}6^{(2)}7^{(1)}8^{(1)}9^{(1)}11^{(1)}12^{(2)}10^{(1)}1$	00:12:23
	SC=300	SR=0.08			#2	$1^{(2)}4^{(2)}5^{(1)}7^{(1)}6^{(1)}8^{(2)}9^{(1)}11^{(2)}12^{(1)}10^{(2)}1$	
	TCM=1805	TRM=18.47			#3	$1^{(2)}4^{(2)}7^{(2)}6^{(2)}8^{(1)}5^{(2)}9^{(1)}11^{(1)}12^{(2)}10^{(1)}1$	
	TCV=195	TRV=1.18					

SC: Site Cost; Transportation Cost; TCM: Transportation Cost Mean; TCV: Transportation Cost Variability; SR: Site Risk; TR: Transportation Risk; TRM: Transportation Risk Mean; TRV: Transportation Risk Variability

Table 3.7 (continue) : Details of intervening Pareto points

Pareto points	**Z_1: Cost (RMB)**	**Z_2: Risk (persons)**	**Design variables**		**Best tours**		**Elapsed time (hh:mm:ss)**
			Ware-house	**Customers assignment**	**Scenario**	**Tours**	
6	Total=2440	Total=18.33	#1	All	#1	$1^{(1)}10^{(1)}12^{(1)}11^{(1)}9^{(1)}8^{(1)}7^{(2)}6^{(1)}5^{(2)}4^{(2)}1$	00:14:45
	SC=300	SR=0.08			#2	$1^{(1)}4^{(1)}5^{(1)}7^{(2)}6^{(1)}8^{(1)}9^{(1)}11^{(2)}12^{(2)}10^{(2)}1$	
	TCM=1908	TRM=17.01			#3	$1^{(1)}10^{(2)}12^{(1)}11^{(1)}9^{(2)}5^{(1)}8^{(2)}6^{(2)}7^{(1)}4^{(2)}1$	
	TCV=232	TRV=1.24					
7	Total=2635	Total=17.10	#1	All	#1	$1^{(1)}10^{(2)}12^{(1)}11^{(1)}9^{(1)}8^{(1)}7^{(2)}6^{(1)}5^{(2)}4^{(2)}1$	00:14:45
	SC=300	SR=0.08			#2	$1^{(1)}4^{(1)}5^{(1)}7^{(1)}6^{(1)}8^{(2)}9^{(1)}11^{(1)}12^{(2)}10^{(1)}1$	
	TCM=2090	TRM=15.95			#3	$1^{(2)}4^{(1)}7^{(1)}6^{(2)}8^{(1)}5^{(2)}9^{(1)}11^{(1)}12^{(2)}10^{(1)}1$	
	TCV=245	TRV=1.07					
8	Total=2880	Total=15.85	#1	All	#1	$1^{(2)}4^{(2)}5^{(2)}6^{(1)}7^{(1)}8^{(1)}9^{(1)}11^{(1)}12^{(2)}10^{(1)}1$	00:17:01
	SC=300	SR=0.08			#2	$1^{(1)}4^{(2)}5^{(1)}7^{(1)}6^{(1)}8^{(1)}9^{(2)}11^{(2)}12^{(2)}10^{(1)}1$	
	TCM=2318	TRM=14.8			#3	$1^{(1)}10^{(2)}12^{(1)}11^{(1)}9^{(2)}5^{(1)}8^{(1)}6^{(1)}7^{(1)}4^{(2)}1$	
	TCV=262	TRV=0.97					
9	Total=3035	Total=14.35	#1	All	#1	$1^{(1)}10^{(2)}12^{(1)}11^{(1)}9^{(1)}8^{(1)}7^{(1)}6^{(1)}5^{(1)}4^{(2)}1$	00:15:20
	SC=300	SR=0.08			#2	$1^{(1)}4^{(1)}5^{(2)}7^{(1)}6^{(1)}8^{(2)}9^{(1)}11^{(2)}12^{(2)}10^{(1)}1$	
	TCM=2640	TRM=13.39			#3	$1^{(1)}10^{(2)}12^{(1)}11^{(1)}9^{(2)}5^{(1)}8^{(1)}6^{(1)}7^{(1)}4^{(2)}1$	
	TCV=295	TRV=0.88					

SC: Site Cost; Transportation Cost; TCM: Transportation Cost Mean; TCV: Transportation Cost Variability; SR: Site Risk; TR: Transportation Risk; TRM: Transportation Risk Mean; TRV: Transportation Risk Variability

$1 \rightarrow 4 \rightarrow 7 \rightarrow 6 \rightarrow 8 \rightarrow 5 \rightarrow 9 \rightarrow 11 \rightarrow 12 \rightarrow 10 \rightarrow 1$.

3.5.3 Analyzing the risk improvement over cost increment

In this section, to obtain more insight into the relationship between risk and cost objective functions, we define two indicators including Cost Increment Rate (CIR) and Risk Improvement Rate (RIR), which respectively show the incremental changes of the cost and risk. Given all 11 Pareto solution points starting with Pareto Point Z_1^* in Figure 3.5, we can compute ten different values for CIR's and RIR's for Pareto point #1 to Z_2^*. These values are shown in Table 3.8, with an additional column showing the RIR/CIR ratio. Starting from the minimum cost extreme point, the cost objective follows an increasing trend when moving from a Pareto solution to the subsequent one, leading to positive values of CIR. However, the RIR values are negative as the risk objective declines while moving toward the minimum risk extreme Pareto point. Without loss of generality, we neglect the negative sign in the RIR by applying the absolute value of RIR. Therefore, whenever we mention RIR in this manuscript, we mean the absolute value of it. This table gives details about the relationship between the RIR index and its relevant impact on the CIR index over different Pareto points. For instance, moving from Z_1^* to Pareto point #1 leads to an increase of 1.39% in the cost and a reduction in the risk (reducing the number of hazmat casualties) of 6.01%.

Given the RIR/CIR indicator, it can be inferred that on average, there is a relationship between risk and cost objective functions with a slope of 1.72, i.e., every unit of increment in the cost function leads to an average 1.72 units of improvement

Table 3.8: Details about the risk improvement over cost increment

Pareto point	Z_1**: Cost (RMB)**	Z_2**: Risk (persons)**	**CIR (%)**	**RIR (%)**	**|RIR| (%)**	**|RIR| /CIR**
Z_1^*	1943	26.8	-	-	-	-
1	1970	25.19	1.39	-6.01	6.01	4.32
2	2025	23.42	2.79	-7.03	7.03	2.52
3	2120	22.12	4.69	-5.55	5.55	1.18
4	2270	20.67	7.08	-6.56	6.56	0.93
5	2300	19.73	1.32	-4.55	4.55	3.44
6	2440	18.33	6.09	-7.1	7.1	1.17
7	2635	17.1	7.99	-6.71	6.71	0.84
8	2880	15.85	9.3	-7.31	7.31	0.79
9	3035	14.35	5.38	-9.46	9.46	1.76
Z_2^*	3420	13.8	12.69	-3.83	3.83	0.3
		Average	5.87	-6.41	6.41	1.72

in the risk function. In other words, if a reduction of 1% in people at risk is sought, the carrier has to invest 0.58% more on the current costs. However, there is a large gap between Pareto points 9 and Z_2^*, meaning that improving the risk factor by 1% requires the cost to be increased by 3.33%, which is four and a half times more than that of Pareto points Z_1^* to #9. Although it seems humane to reduce the number of casualties even by one person, the carrier may hesitate to do so given the significant increase in the cost (indicated by an RIR/CIR ration of 0.3).

3.5.4 Analyzing the weights of variability functions

In this section, we are interested in investigating how the results of the problem would change when we manipulate the weights of the variability functions, and then try to present guidelines on how to set these weights at different levels of risk thresholds

by the carrier. The reason why we do a separate analysis for variability functions is that the variability is a determining factor in uncertainty management and plays an important role in the success of the projects in unreliable environments (Jabbarzadeh et al., 2020; Ke, 2020a).

To analyze the weights of variability functions, we first define new indicators to evaluate the ratio of variability in results. TCV divided by TCM, or TCV/TCM for short, is an indicator that calculates the ratio at which variability in cost fluctuates over the average cost of the transportation plan. A similar TRV/TRM indicator can also be defined for the risk of the transportation plan. The higher this risk indicator is, the more the decisions made are unreliable. With that said, the carriers themselves may have a preset level of tolerance in accepting the variability in the results for the risk and cost functions. Herein, we call this subjective concept the "level of satisfaction" in the variability of the cost or risk, namely SLC or SLR, respectively. For example, if both SLC and SLR are set at 5%, any transportation plans with TCV/TCM and TRV/TRM of less than 0.05 are considered reliable by the carrier. Table 3.9 shows the TCV/TCM and TRV/TRM ratios for the Pareto solution points in Figure 3.5. Based on the results, on average, TCV ranges around 10% of TCM. The ratio is less for TRV/TRM, with an average of around 7%.

As discussed before, how much variability is tolerable in making transportation decisions is subjective, and it depends upon the carrier's attitude towards risk-taking. For example, the carrier may require to keep a level of satisfaction of 1% for both cost and risk variability functions. To obtain this, the variability weights in the model (here α_3 and β_3) must be adjusted by giving them increased values until the carrier obtains the intended results; or, the following two constraints can be added to the

mathematical model.

$$TCV/TCM \leq SLC \tag{3.47}$$

$$TRV/TRM \leq SLR \tag{3.48}$$

It is important to note that, depending upon the nature of the input data, adding these constraints may lead to infeasibility while solving. To handle this, another pay-off table can be developed to ensure the compatibility of weights. Table 3.9 lists the ratios of the above two indexes for all non-dominant solutions. The values for SLC and SLR can be determined accordingly.

Table 3.9: The ratio of cost and risk variability indexes to the problem of total cost and risk

Pareto points	Z_1^*	**1**	**2**	**3**	**4**	**5**	**6**	**7**	**8**	**9**	Z_2^*	**Min**	**Max**	**Ave**
TCV/TCM (%)	10	8	8	8	8	11	12	12	11	11	8	8	12	10
TRV/TRM (%)	12	6	6	6	7	6	7	7	7	7	7	6	12	7

TCM: Transportation Cost Mean; TCV: Transportation Cost Variability; TRM: Transportation Risk Mean; TRV: Transportation Risk Variability

Following the analysis on the importance of cost and risk variability functions, we know that the greater the weights α_3 and β_3 are, the smaller the ratios TCV/TCM and TRV/TRM become. Figure 3.6 shows the trend of how the ratios of TCV/TCM and TRV/TRM change over different values for α_3 and β_3. The numbers 1 to 5 for the horizontal axes in Figure 3.6 represent the weight combinations of (1, 5), (2, 4), (3, 3), (4, 2), (5, 1) for the pair of (α_3, β_3), respectively.

In particular, in Figure 3.6, we consider three solutions from the Pareto set representing high, medium, and low-risk situations. As discussed previously, the range of

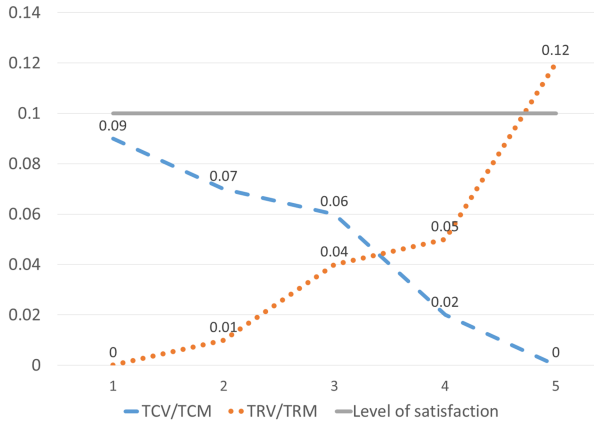

(a) Ratios of TCV/TCM and TRV/TRM for a different combination of weights for (α_3, β_3) with a level of satisfaction of 10% for both variabilities when a high-risk situation is pursued ($\varepsilon = 25$)

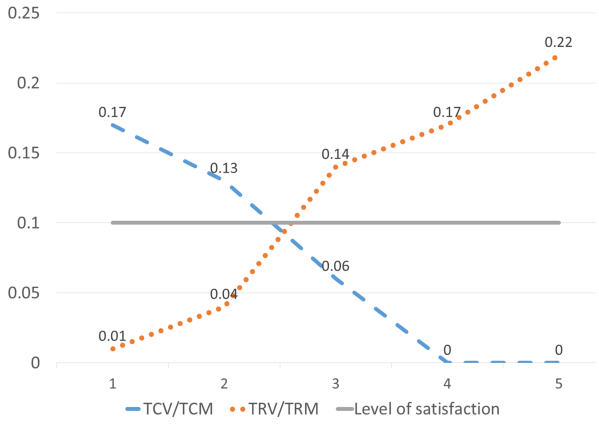

(b) Ratios of TCV/TCM and TRV/TRM for a different combination of weights for (α_3, β_3) with a level of satisfaction of 10% for both variabilities when a medium-risk situation is pursued ($\varepsilon = 20$)

Figure 3.6: The behavior of variability per average indicators with changes in variability weights

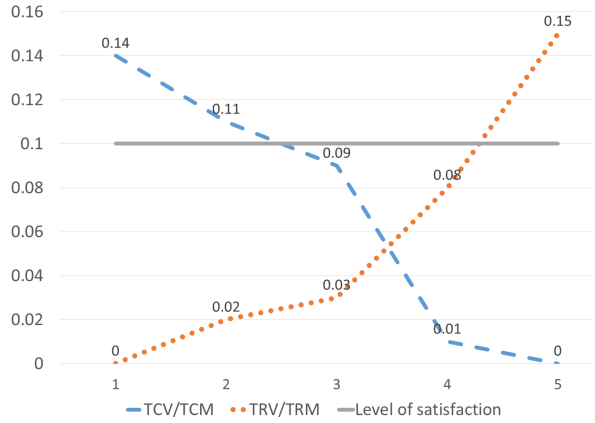

(c) Ratios of TCV/TCM and TRV/TRM for a different combination of weights for (α_3, β_3) with a level of satisfaction of 10% for both variabilities when a low-risk situation is pursued ($\varepsilon = 15$)

Figure 3.6 (continue) : The behavior of variability per average indicators with changes in variability weights

the risk objective function for this example ranges from 13.80 to 26.80. Therefore, we change the upper bound of the risk function or parameter ε in constraint (3.46). For the first solution, we set $\varepsilon = 25$ which is regarded as a high-risk situation. The other two upper bounds are set as $\varepsilon = 20$ and $\varepsilon = 15$ which are regarded as medium-risk and low-risk situations, respectively. Based on the plots in Figure 3.6, if we consider a level of satisfaction of 10% for variability in both cost and risk functions, we conclude that, as for the medium-risk situation (Figure 3.6b) the weights associated with the variability functions must be higher to make sure that the variability both in cost and risk functions are below the level of satisfaction and vice versa. For more details, the reader can refer to Figure 3.6a to see how in a high-risk situation, the lower weights for α_3 and β_3 can still remain with the variability of results below the level of satisfaction.

The low-risk situation places somewhere between the high and medium cases. To be more accurate, the cost variability is more sensitive in the low-risk situation so that it requires larger weights to be kept under a satisfaction level of 10%. However, the risk variability is more sensitive in the medium-risk situation. As can be seen as the red line in Figure 3.6b, more values of TRV/TRM are above the level of satisfaction compared to the other two risk situations.

3.5.5 A sensitivity analysis over warehouse capacity

In this section, we conduct a sensitivity analysis on the warehouse capacity. The reason for selecting this parameter is that warehouses themselves may be affected by disruptions which consequently reduce a share of their maximum capacity, and any loss of capacity in warehouses may highly influence the overall location-routing plan. In our original analysis, each warehouse's capacity was selected large enough to handle the demands of all customers in one single tour. This is why we witness only one warehouse that needs to be activated in all Pareto solutions. For investigation purposes, we restrict the capacities of all warehouses to 12, which can force the model to locate at least two facilities for demand fulfillment. Table 3.10 shows the details of the two extreme Pareto points Z_1^* and Z_2^*, and Figure 3.7 illustrates the best tours (regardless of paths) for Pareto points Z_1^* and Z_2^* to have a glimpse of how the location-routing plans change after capacity reductions.

As expected, the customers are served from more than one warehouse because of the reduction in the capacities. In Pareto solution Z_1^*, customers are supported by warehouses #1 and #3, while in Z_2^* with warehouses #2 and #3. This reduction

Table 3.10: Solution details for Pareto points Z_1^* and Z_2^* with new warehouse capacities

Extreme Pareto points	**Z_1: Cost (RMB)**	**Z_2: Risk (persons)**	**Design variables**		**Best tours**		**Elapsed time (hh:mm:ss)**
			Ware-house	**Customers assignment**	**Scenario**	**Tours**	
Z_1^*	Total=2150	Total=27.54	#1	4-7	#1	$1^{(2)}4^{(1)}5^{(2)}7^{(1)}1$	00:24:17
	SC=750	SR=0.15	#3	8-12		$3^{(1)}8^{(1)}6^{(2)}9^{(2)}11^{(1)}12^{(2)}10^{(1)}3$	
	TCM=1277	TRM=25.27			#2	$1^{(1)}4^{(2)}5^{(2)}7^{(2)}1$	
	TCV=123	TRV=2.12				$3^{(1)}8^{(1)}6^{(1)}9^{(2)}11^{(2)}12^{(1)}10^{(2)}3$	
					#3	$1^{(1)}4^{(1)}5^{(2)}7^{(2)}1$	
						$3^{(2)}8^{(2)}6^{(1)}9^{(1)}11^{(2)}12^{(1)}10^{(2)}3$	
Z_2^*	Total=3955	Total=14.35	#2	4-7	#1	$2^{(2)}4^{(1)}5^{(2)}7^{(2)}2$	00:41:02
	SC=950	SR=0.14	#3	8-12		$3^{(2)}8^{(2)}6^{(1)}9^{(1)}11^{(1)}12^{(1)}10^{(1)}3$	
	TCM=2739	TRM=13.26			#2	$2^{(1)}4^{(1)}5^{(1)}7^{(2)}2$	
	TCV=246	TRV=0.95				$3^{(1)}8^{(1)}6^{(1)}9^{(2)}11^{(2)}12^{(1)}10^{(2)}3$	
					#3	$2^{(2)}4^{(1)}5^{(2)}7^{(1)}2$	
						$3^{(1)}8^{(1)}6^{(1)}9^{(2)}11^{(2)}12^{(1)}10^{(2)}3$	

SC: Site Cost; TCM: Transportation Cost Mean; TCV: Transportation Cost Variability; SR: Site Risk; TR: Transportation Risk; TRM: Transportation Risk Mean; TRV: Transportation Risk Variability

(a) Pareto point Z_1^* (b) Pareto point Z_2^*

Figure 3.7: An illustration of how best tours change after imposing capacity restrictions to the model

in the capacity of the warehouses has burdened the system with extra cost and risk, as indicated by the fact that the total cost and risk of Z_1^* increase by 11% and 3%, respectively, while the total cost and risk of Z_2^* increase by 15% and 4%, respectively. The increase in total cost is more than that of the total risk because the warehouse installation costs comprise a more significant share of the total cost than the risk. Therefore, in the case of a possible reduction in the capacity of warehouses due to possible disruptions, we may face more tours with even more costs and risks to the transportation system.

3.5.6 A Comparison with the non-disruption case

This section studies the impact of considering edge disruptions on an optimal logistics network, and demonstrates why it is necessary to take into account possible random

system disruption when making location-routing decisions. In doing so, we compare our model (named as Case I, the disruption case) with a deterministic model with no disruption consideration (named as Case II, the non-disruption case). It is noteworthy to mention that the no disruption case is similar to the network presented in Hu et al. (2019) with a few modification of time window restrictions. In Case II, the objective functions are transformed to the deterministic format as follows:

$$\min Z_1 = \sum_w c'_w y_w + \sum_i \sum_j \sum_k c_{ijk} x_{ijk}, \tag{3.49}$$

$$\min Z_2 = \sum_w R'_w y_w + \sum_i \sum_j \sum_k R_{ijk} x_{ijk}. \tag{3.50}$$

Note that here the index s is removed because only one scenario (the normal one) is considered. Setting all coefficients in Objectives (3.49) and (3.50) (i.e., α_1 to α_3 and β_1 to β_3) to one and dividing the range of the risk function into ten segments, the obtained Pareto solutions are shown in Table 3.11, and Figure 3.8 plots the Pareto frontier of our model with disruptions against that of the non-disruption case.

The result shows that considering disruptions in making location-routing decisions creates both higher cost and risk, respectively 14% and 5% on average. This outcome is rather intuitive, as additional resources are required to overcome the impact of unavailable edges and recover from the disruption scenarios. This system redundancy also leads to difference between the results of Case II and the normal scenario in Case I, as indicated by comparing Tables 3.7 and 3.11.

For more details, consider Pareto point #8 in both cases. The risk value function for both cases is below 16 persons; however, Warehouse #1 is activated in Case I and Warehouse #3 in Case II. To mathematically prove how applying scenario-based robust optimization leads to solutions with a lesser cost, we solve the following

Table 3.11: Pareto solution points in case of no disruptions

Pareto points	Z_1: **Cost (RMB)**	Z_2: **Risk (persons)**	**Design variables**		**Best tours**	**Elapsed time (hh:mm:ss)**
			Ware-house	**Customers assignment**		
Z_1^*	Total=1612 SC=300 TC=1312	Total=25.23 SR=0.08 TR=24.15	#1	All	$1^{(1)}10^{(1)}12^{(2)}11^{(2)}9^{(2)}8^{(1)}7^{(2)}6^{(2)}5^{(2)}4^{(1)}1$	00:15:47
1	Total=1650 SC=300 TC=1350	Total=23.91 SR=0.08 TR=23.83	#1	All	$1^{(1)}10^{(1)}12^{(2)}11^{(2)}9^{(2)}8^{(1)}7^{(2)}6^{(2)}5^{(2)}4^{(2)}1$	00:10:43
2	Total=1794 SC=300 TC=1494	Total=22.02 SR=0.08 TR=21.94	#1	All	$1^{(1)}4^{(2)}5^{(2)}6^{(2)}7^{(1)}8^{(2)}9^{(1)}11^{(2)}12^{(2)}10^{(1)}1$	00:15:12
3	Total=1820 SC=300 TC=1520	Total=21.78 SR=0.08 TR=21.7	#1	All	$1^{(2)}4^{(2)}5^{(2)}6^{(2)}7^{(2)}8^{(2)}9^{(2)}11^{(2)}12^{(2)}10^{(1)}1$	00:20:21
4	Total=2010 SC=300 TC=1710	Total=20.33 SR=0.08 TR=20.25	#1	All	$1^{(1)}4^{(2)}5^{(2)}6^{(2)}7^{(1)}8^{(2)}9^{(2)}11^{(1)}12^{(2)}10^{(1)}1$	00:33:24

SC: Site Cost; TC: Transportation Cost; SR: Site Risk; TR: Transportation Risk;

Table 3.11 (continue) : Pareto solution points in case of no disruptions

Pareto points	Z_1: **Cost (RMB)**	Z_2: **Risk (persons)**	**Design variables**		**Best tours**	**Elapsed time (hh:mm:ss)**
			Ware-house	**Customers assignment**		
5	Total=2090 SC=300 TC=1790	Total=19.13 SR=0.08 TR=19.05	#1	All	$1^{(1)}4^{(1)}5^{(2)}6^{(2)}7^{(1)}8^{(1)}9^{(1)}11^{(1)}12^{(2)}10^{(2)}1$	00:10:34
6	Total=2120 SC=300 TC=1820	Total=17.95 SR=0.08 TR=17.78	#1	All	$1^{(2)}10^{(1)}12^{(1)}11^{(1)}9^{(1)}8^{(1)}7^{(2)}6^{(1)}5^{(2)}4^{(2)}1$	00:12:53
7	Total=2250 SC=300 TC=1950	Total=16.43 SR=0.08 TR=16.35	#1	All	$1^{(1)}10^{(2)}12^{(1)}11^{(2)}9^{(2)}8^{(1)}7^{(2)}6^{(1)}5^{(2)}4^{(2)}1$	00:11:14
8	Total=2415 SC=450 TC=2035	Total=15.11 SR=0.072 TR=14.44	#3	All	$3^{(2)}10^{(2)}4^{(2)}5^{(2)}6^{(1)}7^{(1)}8^{(1)}9^{(1)}12^{(1)}11^{(2)}3$	00:13:27
9	Total=2532 SC=450 TC=2082	Total=13.15 SR=0.072 TR=13.08	#3	All	$3^{(1)}10^{(2)}4^{(2)}5^{(1)}6^{(1)}7^{(1)}8^{(1)}9^{(1)}12^{(1)}11^{(2)}3$	00:09:19
Z_2^*	Total=2855 SC=500 TC=2355	Total=12.50 SR=0.07 TR=12.43	#2	All	$2^{(1)}12^{(2)}10^{(1)}4^{(2)}5^{(2)}6^{(1)}7^{(1)}8^{(1)}9^{(1)}11^{(1)}2$	00:24:17

SC: Site Cost; TC: Transportation Cost; SR: Site Risk; TR: Transportation Risk;

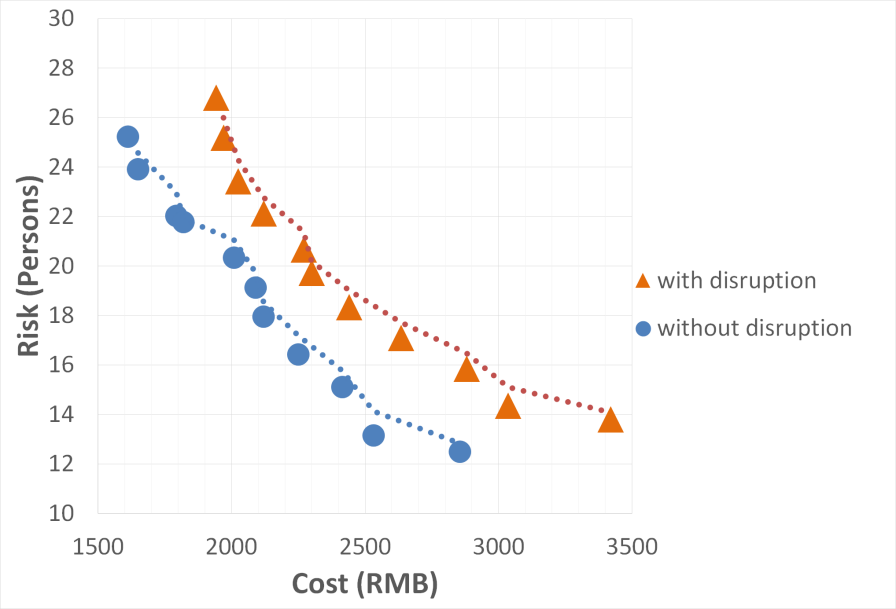

Figure 3.8: Difference between the proposed location-routing problem with and without disruption

optimization model. In this model, we keep the prior values for optimal values of design variables for both cases. The objective function is to minimize the expected cost of the carrier based on the proposed disruption scenarios while keeping the risk values function to no more than 16 persons.

$$\min Z_1 = \sum_w c'_w y_w + \sum_s p''_s \sum_i \sum_j \sum_k c_{ijk} x^s_{ijk} - eps \times (\delta/\Delta) \tag{3.51}$$

s.t.

$$\sum_w R'_w y_w + \sum_s p''_s \sum_i \sum_j \sum_k R_{ijk} x^s_{ijk} + \delta = 16 \tag{3.52}$$

Solving this model by keeping $y_3, z_{4,3}, ..., z_{12,3} = 1$, we obtain the expected cost of 3,010 RMB. Again, by inserting the design variables $y_q, z_{4,1}, ..., z_{12,1} = 1$ into the model, we obtain the expected cost of 2,618 RMB. Based on these results, there is a 15% increase in the expected cost of Case II over Case I. In other words, the design variables

derived from a no-disruption approach creates more cost to the carrier if there is a possibility for edge unavailability, and applying a scenario-based robust optimization model obtains the best possible solutions to the proposed location-routing problem.

3.5.7 Random instances

In this section, we check the validity of the proposed mathematical model for different sizes of problem instances. A series of random problem instances are generated with specific ranges for their parameters. The input parameters are considered to be uniformly distributed with lower and upper bounds specified in Table 3.12. Values of α and β parameters are all considered to be one.

Table 3.12: Distribution functions for generating random input parameters

Parameter	**Data**
Transportation cost over edge	$U \sim [50, 500]$
Travel time over edge (hour)	$U \sim [0.1, 10]$
Risk over edge	$U \sim [0.5, 30]$
Warehouse capacity	$U \sim [20, 100]$
Warehouse cost	$U \sim [200, 1000]$
Site risk	$U \sim [0.05, 0.1]$
Customer demand	$U \sim [0.5, 5]$
Service time (hour)	$U \sim [0.1, 1]$

For all problem instances, we record the three salient points of the Pareto frontier: two extreme points of "Min Cost" and "Min Risk" and an "Intermediate" point where the risk value is no more than 10% of Z_2^* from the "Min Risk" solution, that is $Z_2 + \delta = \varepsilon = 1.1 Z_2^*$. The instances in Table (3.13) are built upon four main elements,

including $|W|$, $|C|$, $|K|$, $|S|$ respectively as the numbers of warehouses, customers, paths between the nodes, and scenarios. The maximum time allowed for calculations is set to 3 hours. In this table, the gap is defined as the difference between the best-known solution (the best feasible objective value found so far) and the value that bounds the best possible solution. The bound can be explained as a limit indicating how far the solver will be able to improve the objective. Considering that the best objective value can never go beyond the bound, the closer these two values are, the better the solution will be.

Apart from the randomly generated values, instances #1 and #2 consider different numbers of scenarios. Compared to instance #1, the minimum cost value of #2 is slightly declined, while the minimum risk objective value gains an extra 50%. Moving from instance #2 to #3, the additional warehouses in the model reduce both minimum cost and risk values by approximately 32% and 48%, respectively. Here, the intermediate point experiences a drop regarding both of the objectives as well. From instance #4 on, the results show that increasing the number of customers causes the computation time to grow exponentially. The model reaches the optimum value in all the cases except for the minimum cost boundary point of instance #6 and all the cases in #7. The gap for #6 reaches almost 9%, and doubles in the corresponding point of #7, as a result of increasing the number of customers from 15 to 20. Therefore, while changes in the number of pathways between nodes have a trivial effect on the results, the model is very sensitive to increasing the number of customers. However, what is evident and definite is the exponential behavior of the computation time as the scale gets larger. This highlights the importance of considering algorithms such as branch-and-cut-and-price for shorter run times.

Table 3.13: Results of problem instances for the proposed mathematical model

#	Problem size	Min Cost				Min Risk				Intermediate Point			
	$[W-C-K-S]$	Cost (RMB)	Risk (persons)	Time	Gap	Cost (RMB)	Risk (persons)	Risk	Time	Cost (RMB)	Risk (persons)	Risk	Time
1	$3-10-2-2$	$Z_1^* = 2408.36$ $SC = 816$ $TCM = 1506.60$ $TCV = 85.76$	$Z_2 = 50.24$ $SR = 0.09$ $TRM = 37.98$ $TRV = 12.17$	00 : 30 : 26	0.00%	$Z_1 = 14095.48$ $SC = 816$ $TCM = 2842.20$ $TCV = 10437.28$	$Z_2^* = 27.17$ $SR = 0.09$ $TRM = 23.64$ $TRV = 3.44$	00 : 24 : 52	0.00%	$Z_1 = 3270.48$ $SC = 816$ $TCM = 2350.8$ $TCV = 103.68$	$Z_2 = 28.45$ $SR = 0.09$ $TRM = 24.49$ $TRV = 3.87$	00 : 17 : 50	0.00%
2	$3-10-2-3$	$Z_1^* = 2481.1$ $SC = 372$ $TCM = 1992.90$ $TCV = 116.20$	$Z_2 = 65.87$ $SR = 0.09$ $TRM = 40.01$ $TRV = 25.77$	00 : 45 : 52	0.00%	$Z_1 = 10450.3$ $SC = 727$ $TCM = 2715.50$ $TCV = 7007.80$	$Z_2^* = 40.76$ $SR = 0.19$ $TRM = 39.53$ $TRV = 1.04$	00 : 29 : 40	0.00%	$Z_1 = 2700.66$ $SC = 372$ $TCM = 0.09$ $TCV = 106.26$	$Z_2 = 44.21$ $SR = 0.09$ $TRM = 38.82$ $TRV = 5.30$	00 : 46 : 21	0.00%
3	$5-10-2-3$	$Z_1^* = 1693.40$ $SC = 210$ $TCM = 1373$ $TCV = 109.90$	$Z_2 = 98$ $SR = 0.07$ $TRM = 63.47$ $TRV = 34.46$	01 : 11 : 03	0.00%	$Z_1 = 3978.64$ $SC = 210$ $TCM = 3241.40$ $TCV = 527.24$	$Z_2^* = 21.24$ $SR = 0.07$ $TRM = 18.33$ $TRV = 2.84$	00 : 37 : 50	0.00%	$Z_1 = 2549.90$ $SC = 210$ $TCM = 2261.5$ $TCV = 78.4$	$Z_2 = 22.91$ $SR = 0.07$ $TRM = 20.82$ $TRV = 2.02$	00 : 28 : 51	0.00%
4	$5-10-3-3$	$Z_1^* = 2051.88$ $SC = 230$ $TCM = 1707.60$ $TCV = 114.23$	$Z_2 = 51.42$ $SR = 0.09$ $TRM = 23.44$ $TRV = 21.30$	01 : 20 : 54	0.00%	$Z_1 = 3533.80$ $SC = 230$ $TCM = 3098$ $TCV = 205.80$	$Z_2^* = 17.92$ $SR = 0.09$ $TRM = 17.29$ $TRV = 0.54$	00 : 48 : 15	0.00%	$Z_1 = 2799.3$ $SC = 230$ $TCM = 2266.9$ $TCV = 302.4$	$Z_2 = 19.55$ $SR = 0.09$ $TRM = 18.74$ $TRV = 0.67$	00 : 51 : 37	0.00%
5	$3-15-3-3$	$Z_1^* = 3104.21$ $SC = 540$ $TCM = 2350.70$ $TCV = 213.43$	$Z_2 = 76.32$ $SR = 0.08$ $TRM = 43.71$ $TRV = 32.53$	02 : 24 : 04	0.00%	$Z_1 = 6401.21$ $SC = 712$ $TCM = 4267.98$ $TCV = 1421.23$	$Z_2^* = 21.48$ $SR = 0.03$ $TRM = 18.72$ $TRV = 2.73$	01 : 55 : 16	0.00%	$Z_1 = 4520.50$ $SC = 712$ $TCM = 3596.10$ $TCV = 212.43$	$Z_2 = 23.10$ $SR = 0.03$ $TRM = 21.06$ $TRV = 2.01$	01 : 32 : 28	0.00%
6	$5-15-3-3$	$Z_1^* = 4782.2$ $SC = 892$ $TCM = 3440.10$ $TCV = 450.12$	$Z_2 = 123.13$ $SR = 0.21$ $TRM = 77.03$ $TRV = 45.89$	03 : 00 : 00	9.12%	$Z_1 = 10932.80$ $SC = 1150$ $TCM = 5110.80$ $TCV = 4672$	$Z_2^* = 29.4$ $SR = 0.08$ $TRM = 25.62$ $TRV = 3.70$	02 : 19 : 39	0.00%	$Z_1 = 8700.19$ $SC = 892$ $TCM = 7495.10$ $TCV = 313.10$	$Z_2 = 56.21$ $SR = 0.21$ $TRM = 51.68$ $TRV = 4.32$	02 : 14 : 04	0.00%
7	$5-20-3-3$	$Z_1^* = 13274.38$ $SC = 1442$ $TCM = 10887.26$ $TCV = 945.12$	$Z_2 = 407.10$ $SR = 0.21$ $TRM = 322.28$ $TRV = 184.61$	03 : 00 : 00	18.51%	$Z_1 = 19466.26$ $SC = 2145$ $TCM = 11520.67$ $TCV = 5800.59$	$Z_2^* = 101.77$ $SR = 0.18$ $TRM = 78.20$ $TRV = 23.4$	03 : 00 : 00	17.33%	$Z_1 = 16275.26$ $SC = 1754$ $TCM = 13276.87$ $TCV = 1244.39$	$Z_2 = 108.86$ $SR = 0.21$ $TRM = 79.45$ $TRV = 29.20$	03 : 00 : 00	14.48%

SC: Site Cost; TCM: Transportation Cost Mean; TCV: Transportation Cost Variability; SR: Site Risk; TR: Transportation Risk; TRM: Transportation Risk Mean; TRV: Transportation Risk Variability

3.6 Managerial Insights

This section highlights the managerial insights that are derived from previous discussions and can be used to help the carrier in constructing a robust hazmat logistic system for satisfying customer demands.

First of all, it is critical to maintain a certain level of system redundancy such that the transportation network is robust over time yet flexible enough to handle random variations, especially disruptions that may be caused by weather, traffic, or any other unforeseen events. This redundancy may be reflected in either a higher number of warehouses, or extra capacities at warehouses, or both. Note that it may seem costly to keep the redundancy when building up the network, but there will certainly be benefits during disruptions, as shown in Section 3.5.6. Moreover, an improvement of the geographical distribution of the warehouses may also help, not only in cost reduction but also in risk reduction. This is because, when warehouses are spread relatively evenly in the network, the system risk (including both en-route and on-site risks) would also be more equitably distributed.

Secondly, in searching for an effective and efficient solution, the scenario-based robust model presented in this research can be implemented as a useful facilitation tool. To enhance the practicality, those scenarios can be generated based on a detailed and comprehensive investigation of historical situations. Applying AECM provides the carrier with more details about the possible alternative solutions to the problem. None of the Pareto solutions have any priority over each other and the carrier can choose among them in accordance with other managerial priorities such as budget restrictions and/or the maximum tolerable risk. To assist in making a balanced

decision, the RIR/CIR indicator can be used to provide guidance, which indicates the appropriate range of increment in cost in return for an improvement in risk, as discussed in Section 3.5.3.

Thirdly, indicators TCV/TCM and TRV/TRM are considered as ways to show how much variability exists in the output (Section 3.5.4). A pre-defined level of satisfaction can be applied to ensure the robustness of the system both with or without disruptions. More importantly, in regard to adjusting the weights of variability terms in both cost and risk functions, the carrier's preference on the two objectives, i.e., the risk-taking situation, should be highly respected.

3.7 Conclusion

In this research, we address a new type of hazmat transportation problem with edge unavailability scenarios and time window assumptions. Edge unavailability is a practical aspect of transportation systems, but little attention has been given when hazmat shipments are involved. Other realistic considerations in making delivery plans are the time-dependent issues. Among these issues are the customer service time restrictions and the varying traffic density and speed over different times of the day, causing divergent transportation risks and costs associated with various departure times of the truck from a node. To handle the complicated situations with both disruptions and time constraints, a vehicle routing problem is embedded into a scenario-based robust optimization model, which is then solved by adopting an ε-constrained approach to examine the relationship of the two objectives. In applying the scenario-based robust optimization model, variability in cost and risk functions has been introduced as a

critical indicator for designing reliable transportation plans. By keeping variability functions within a threshold, it is guaranteed that the optimal solution covers all disastrous scenarios within an acceptable range. We also conduct a comprehensive analysis of the impact of the weights of variability functions on how the variability of results changes with different risk situations from the carrier. Moreover, a sensitivity analysis about the impact of warehouse capacity restriction on the final location-routing tours has been applied. Based on this analysis, the decrease in the warehouse capacity may burden the system with more transportation costs and risks.

For future research, the two-stage robust optimization technique developed by Ben-Tal et al. (2009) will be used. Integrating the ideas of a two-stage stochastic model and robust optimization, this technique can more practically reflect the real-world situations in developing a solution in two stages. A comparison of the result with our present work would provide additional interesting and informative insights for the carrier or other stakeholders. Other assumptions, such as vehicle capacities, emergency response networks to reduce transportation risk, and more sophisticated formulations for hazmat risk could also be applied to make the proposed model more realistic. The involvement of the salaries and wages in the transportation model would be another pathway for future studies. Time-dependent service time and hourly paid wages can be regarded in the model. The situation can become more realistic by incorporating the skill levels of the employees. In this regard, salary inclusion might necessitate a punishment or incentive motivator to be included in the model, especially when discussing time-dependent payments.

Chapter 4

Infectious Waste Management During a Pandemic: A Stochastic Location-Routing Problem with Chance-Constrained Time Windows

Abstract The COVID-19 pandemic has presented tremendous challenges to the world, one of which is the management of infectious waste generated by healthcare activities. Finding cost-efficient services with minimum threats to public health has become a top priority. The pandemic has induced extreme uncertainties, not only in the amount of generated waste, but also in the associated service times. With this in mind, the present study develops a mixed-integer linear programming (MILP) model for the location-routing problem with time windows (LRPTW). To handle the uncertainty in the amount of generated waste, three scenarios are defined respectively reflecting different severity levels of a pandemic. Furthermore, chance constraints are applied to deal with the variation of the service times at small generation nodes, and time windows at the transfer facilities. The complexity of the resulting mathematical model motivated the application of a branch-and-price (B&P) algorithm along with an ε-constraint technique. A case study of the situation of Wuhan, China, during the initial COVID-19 outbreak is employed to examine the performance and applicability of the proposed model. Our numerical tests indicate that the B&P algorithm outperforms CPLEX in the computational times by more than 83% in small-sized problem

instances and reduces the gaps by at least 70% in large-scale ones. Through a comparison with the current and deterministic systems, our proposed stochastic system can timely adjust itself to fulfill nearly four times the demand of other systems in an extreme pandemic scenario, while maintaining a cost-efficient operation with no outbreak.

Keyword Infectious Waste, Location-Routing Problem, Time Windows, Stochastic Programming, Chance Constrained Programming, Branch-and-Price Algorithm

4.1 Introduction

The ongoing COVID-19 pandemic has led to millions of deaths and irreversible damage to the economy and industry worldwide. According to WHO (2022), by May 3, 2022, the virus widespread has claimed more than 6.2 million lives out of approximately 512 million infected individuals. The outbreak is a potential menace to the environment due to the high amount of associated healthcare waste, both medical (Ding et al., 2021; Abu-Qdais et al., 2020) and plastic (Nowakowski et al., 2020; Prata et al., 2020). As stated by the State Council's joint prevention and control mechanism in China, despite a reduction of 30% in the amount of municipal solid waste, the generated medical waste experienced a surge of 370% during the virus epidemic in Hubei Province (Klemeš et al., 2020).

Healthcare waste is defined as the total waste generated at healthcare facilities. Infectious waste, particularly, contains infectious sharps (including needles, blades, or other items that can lead to direct injury) and infectious non-sharps (including materials that have been in contact with human blood or its derivatives, isolation waste from highly infectious patients, and other contaminated substances infected

with human pathogens) (WHO, 2005). On many occasions, the entire mixed volume of healthcare waste should be considered infectious as no proper categorization of waste takes place, despite the fact that infectious waste only counts for approximately 18% of the total healthcare waste.

The United Nations Conference on Environment and Development reported that medical waste related diseases cause the death of at least 5.2 million people (including 4 million children) each year (Das et al., 2021). During the COVID-19 pandemic, the large number of infected patients has led to the exponential growth of medical waste in healthcare facilities (Liu et al., 2022; Peng et al., 2020). This substantial amount of waste has become a new source of infection as it is an important transmission medium for the virus (Chen et al., 2021; Ranjbari et al., 2022). The highly contagious virus contained in the resulting infectious waste has been posing harmful impacts on the environment and human well-being (Homayouni and Pishvaee, 2020). The United Nations Environmental Programme (UNEP) recommended that authorities should follow the UN Basel convention's technical guidelines on the environmentally sound management of biomedical and healthcare waste, which distinctively stated that "exposure to hazardous or potentially hazardous biomedical and health-care waste can induce disease or injury" (Secretariat of the Basel Convention, 2003). The European Commission has also issued special guidelines on waste management in the context of the coronavirus crisis to prevent distortions in waste management and ensure the health and safety of citizens, along with a high standard of environmental security (European Commission, 2020).

The unpredictable behavior and mutations of the coronavirus impose a great deal of uncertainties, the most critical one being the variations in the number of active

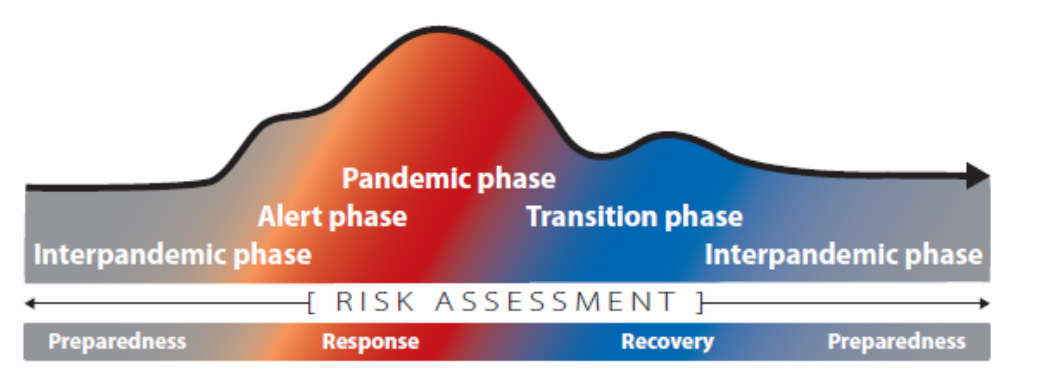

Figure 4.1: The continuum of pandemic phases CDC (2016)

pandemic cases over time, which leads to consequential unpredictability of the amount of waste generated from healthcare activities, and hence imposes tremendous pressure on the existing waste management system. Figure 4.1 displays the distribution curve of case averages during a pandemic summarized by CDC (2016), which also resembles WHO's influenza pandemic alert system (WHO, 2022). Being more contagious and faster spreading compared to regular influenza, COVID-19 has been demonstrating not only the increase and decrease of pandemic cases, but more critically, the incalculable scale of fluctuations and span of duration.

These notable characteristics of uncertainty in an unconventional pandemic emergency necessitate a resilient waste management system that can promptly and continuously adapt to the demand changes and recover from various contingencies. One additional feature that differentiates a sudden pandemic from other healthcare circumstances is the important role played by small medical clinics and offices. These locations generate relatively a small amount of waste and so require specially designed collection tours, different from the direct routes from large hospitals or medical centers to treatment facilities. As mentioned by Srivastava (1993), when dealing with

less than truckload status, serving multiple customers in a single tour is a more cost-effective approach than the straight-to-and-back manner. Also, Rathore and Sarmah (2020) highlighted that a shorter time for collection and disposal of waste is more desirable because of basic environmental principles. Applying tours instead of direct routes reduces waste management process time by omitting the unnecessary commuting between storage stations and generation nodes. An effective collection service is capable of mitigating the associated negative impacts on public health and the ecosystem (Eren and Tuzkaya, 2021). As a result, to improve the system's preparedness for such an unexpected event, different countries have applied diversified approaches. For example, in Wuhan, the authorities decided to construct a new medical waste disposal center and benefit from 46 mobile waste treatment facilities as well (Calma, Justine, 2020). When dealing with elevating demands in particular regions, establishing mobile faculties, such as temporary storage (used for collection among small) and treatment facilities, can be a wise and worthwhile option. Taking this idea, we propose a stochastic model to determine the existing waste-handling facilities that can be temporally converted to infectious-compatible ones during a pandemic. The scenario approach imitating the disparity of the number of active cases in different pandemic phases is employed to handle the exceedingly unpredictable demand variations and make use of the available data derived since the beginning of the pandemic.

Another aspect refers to the inconsistent service time at each generation node as it is mainly related to the amount of waste. This uncertainty in turn directly links to any possible time windows that may exist. Such a time-related uncertainty, nevertheless, so far has been overlooked in most literature. According to the "Management and Technical Guidelines for Emergency Disposal of Medical Waste in the Pneumonia

Pandemic of COVID-19" presented by the Ministry of Ecology and Environment of the People's Republic of China, COVID-related waste should be handled separately from any other types of waste, and the temporary storage time should not exceed 24 hours. The same time frame was also recommended by Peng et al. (2020). Explicitly for those temporary facilities, normally only limited hours of a day can be used for infectious materials, as a certain amount of time also needs to be guaranteed for the daily regular waste. In this work, we embed the uncertainty of the service time into our consideration, as well as the resulting possibility of violating the time window restrictions, and therefore introduce a set of chance constraints for facility time windows in accordance with stochastic service times at each small generation node.

In summary, the contribution of this paper is fourfold. *First*, we develop a bi-objective location-routing model for hazardous waste management considering time windows and uncertainties in demand and service time. More specifically, a well-organized approach is proposed to convert existing facilities into temporary ones when facing a pandemic, where the corresponding infectious waste can be processed separately. The designed network is based on a cost-efficient model addressing locations of temporary facilities, tour planning, direct routes, and the optimum vehicle acquisition simultaneously. *Second*, a two-commodity flow formulation with time windows is utilized for tour planning. The uncertainty in the amount of generated waste is described by three scenarios respectively reflecting different severity levels (i.e., phases as in Figure 4.1) of a pandemic. The chance constraint is implemented to ensure that, with stochastic service time, the pre-defined time windows of temporary facilities can be satisfied at a certain confidence level. *Third*, the augmented ε-constraint solution

technique and a branch-and-price algorithm are developed and integrated to solve the proposed bi-objective stochastic problem with chance constraint. *Fourth*, a case study of Wuhan in China during the coronavirus pandemic is studied. Practical indications and managerial insights are derived to facilitate real-world infectious waste management, especially during an unforeseen pandemic.

The rest of this paper is structured as follows. Section 4.2 reviews relevant literature on the management of medical waste. Section 4.3 presents the detailed network description and model formulation. Based on the solution methods discussed in section 4.4, the proposed model is applied to a case study in section 4.5 for validation and evaluation purpose. Beneficial managerial insights are derived from numerical experiments and summarized in section 4.6. Finally, section 4.7 concludes this work and suggests future research directions.

4.2 Related work

The most relevant research area is the management of medical waste. So far, much effort has been made to investigate different aspects of the medical waste being generated at hospitals and medical centers regarding the COVID-19 outbreak. Statistical analysis was conducted by Abu-Qdais et al. (2020) to evaluate the generation rates and the composition of the medical waste generated during the treatment of the coronavirus pandemic Yu et al. (2020c) suggested the application of temporary facilities in medical waste management during epidemic outbreaks. Yazdani et al. (2020) studied healthcare waste disposal location decisions using the best-worst method with interval rough numbers. They positioned the model in an uncertain environment using a

hybrid methodology and proposed a new rough-based framework of the best worst method and the Bonferroni aggregators model for processing imprecise (rough) information in multi-criteria decision making problems. Kulkarni and Anantharama (2020) explored different features of solid waste management during the COVID-19 pandemic focusing on waste treatment and disposal facilities. A study carried out by Nghiem et al. (2020) assessed the consequences of the COVID-19 outbreak on waste and wastewater service sectors. An effort to establishing efficient guidelines for collecting, transporting, treating, and disposing of the household waste or areas different from medical centers treating COVID-19 patients was made by Di Maria et al. (2020). Haque et al. (2020) discussed a future scenario of waste generation throughout the pandemic period. Eren and Tuzkaya (2021) developed an integer programming model to determine the safest and shortest transportation route for medical waste. In their work, the associated safety scores of medical centers are obtained using an AHP method.

Although the above studies have contributed to the literature in various aspects, only a few authors have employed analytical models or quantitative technologies for the logistic network of the medical waste, especially from a location and routing viewpoint. Table 4.1 lists the taxonomy of relevant works based on model decisions, optimization objectives, uncertainty techniques, time windows, and solution algorithms. A detailed survey is presented next.

The routing and scheduling problem for collection system planning of infectious medical waste was studied in Shih and Lin (2003). The application of RFID technology in the collection-managed inventory routing problem of infectious medical waste was examined in Nolz et al. (2014). Considering a sustainable logistic network, they

Table 4.1: A comparison of relevant literature

Reference	**Objectives**		**Decision**			**Uncertainty**	**Time Windows**	**Model**	**Solution Algorithm**	
	Cost	Risk (measure)	L	R	A				Exact	Approximate
Shih and Lin (2003)	✓			✓				ILP	DP	
Nolz et al. (2014)	✓			✓		Stochastic		MILP		ANLS, SM
Budak and Ustundag (2017)	✓		✓					MILP		
Alshraideh and Qdais (2017)	✓			✓		Stochastic	✓	MILP		
Mantzaras and Voudrias (2017)	✓		✓	✓						GA, MC
Gergin et al. (2019)	✓		✓					MILP		ABC
Osaba et al. (2019)	✓			✓			✓	MILP		DaIBA
Markov et al. (2020)	✓			✓		Stochastic	✓	MINLP		ALNS
Yao et al. (2020)	✓	✓(POP, ENV)	✓			Fuzzy		MINLP		GA
Kargar et al. (2020)	✓	✓(POP)	✓					MILP	GP	
Taslimi et al. (2020)	✓	✓(POP)		✓				MINLP		CG heuristic
Tirkolaee et al. (2020)	✓	✓(POP)	✓	✓		Fuzzy, CCP	✓	MILP	GP	
Govindan et al. (2021)	✓	✓(POP)	✓	✓		Fuzzy	✓	MILP	GP	
Zhao et al. (2021)	✓	✓(POP)	✓	✓	✓	Robust		MILP	EC, LWT, GP	
This study	✓	✓(POP)	✓	✓	✓	Stochastic, CCP	✓	MILP	EC, B&P	

L: Facility Location, *R*: Routing Plan, *A*: Vehicle Acquisition, *CCP*: Chance-constrained Problem, *DP*: Dynamic Programming, *ILP*: Integer Linear Programming, *MILP*: Mixed Integer Linear Programming, *MINLP*: Mixed Integer Non-linear Programming, *ALNS*: Adaptive Large Neighborhood Search, *SM*: Sampling Method, *GA*: Genetic Algorithm, *MC*: Monte Carlo Simulation, *ABC*: Ant Bee Colony, *DaIBA*: Discrete and Improved Bat Algorithm, *EC*: ϵ-constraint Method, *GP*: Goal Programming, *CG*: Column Generation, *LWT*: Lexicographical Weighted Tchebychef, *WS*: Weighted Sum, *B&P*: Branch and Price, *POP*: Population Exposure, *ENV*: Environmental Risk

used an adaptive large neighborhood search method to solve their two-stage stochastic model with uncertain demands. Budak and Ustundag (2017) studied the location-allocation problem for waste collection and disposal in Turkey. Alshraideh and Qdais (2017) developed a stochastic route scheduling model of medical waste collection in Northern Jordan, and showed how the stochasticity of collected waste can be applied in the model as a probability constraint representing the service level provided by the waste collector. Mantzaras and Voudrias (2017) introduced an optimization model to determine the locations and capacities of treatment plants and transfer stations. The continuous facility location problem of waste disposal sites was modeled in Gergin et al. (2019) using an artificial bee colony based on a clustering algorithm. Osaba et al. (2019) presented a multi-attribute clustered VRP addressing a real-world drug distribution problem with pharmacological waste collection processes. Markov et al. (2020) formulated the waste collection problem as a non-linear stochastic inventory routing model in terms of uncertain container overflows and route failures.

More recently, especially after COVID hit, many publications have taken into consideration the potential risk of infection when constructing decision models. Yao et al. (2020) explored the risk and cost mitigation in the location-allocation problem of medical waste disposal centers through a soft-path solution. A multi-trip medical waste reverse supply chain was investigated by Kargar et al. (2020) considering two types of hazardous wastes as well as the general medical waste. Taslimi et al. (2020) applied a periodic load-dependent capacitated vehicle routing problem to plan the inventory routing schedule for each week. Govindan et al. (2021) focused on the location-routing problem of medical waste management during the COVID-19 outbreak. They developed a bi-objective MILP model and solved it using a fuzzy goal

programming approach. Their model incorporated time window-based green vehicle routing problem and load-dependent fuel consumption to manage medical waste.

Tirkolaee et al. (2020) and Zhao et al. (2021) are two studies that are more related to this article. Focusing only on the infectious wastes related to the coronavirus, Tirkolaee et al. (2020) studied a sustainable multi-trip LRPTW. Their model was developed based on the two levels of a waste management system, including 1) hospitals and infirmaries 2) disposal sites. They applied a fuzzy chance programming approach by considering the demand as the uncertain parameter. Also, a weighted goal programming approach method was utilized to handle the multi-objective nature of the model. Zhao et al. (2021) proposed a bi-objective scenario-based robust model for the management of infectious wastes with a special focus on a pandemic. Considering temporary facilities in a 4-tiered network, they developed the model assuming a set of scenarios for the generated waste in hospitals and clinics.

Despite the aforementioned effort, the medical waste literature in the LRP scope is still in its infancy. Except for Tirkolaee et al. (2020) and Zhao et al. (2021), no publications in the medical waste field determine joint location-routing decisions under a pandemic setting. Even these two works did not integratively address uncertainties existing in multiple parameters, which may greatly influence the system performance, especially under sudden changes. To fill this gap in the literature, we apply different approaches according to the specific uncertain natures for different parameters. In more detail, the change in the amount of medical waste stemming from the severity levels of a pandemic can be substantial, but has to be controlled properly for public safety considerations. We therefore define several scenarios in this work to model the interpandemic, alter/transition, and widespread pandemic phases, which respectively

describe different severity levels of a pandemic. Taking into account these scenarios under various probabilities, our model can properly resemble real-world situations and provide effective decision support accordingly. On the other hand, the uncertainty in the service time, partially resulting from demand variability, is formulated as a set of chance constraints associated with each individual scenario, which takes extra precautions for the variations existing in the time of handling each unit of waste. To the best of our knowledge, this is the very first attempt to embed these uncertainties into a multi-tiered waste management system for location-routing decisions with time window considerations.

4.3 Model Development

We consider a three-tiered waste management system, as illustrated in Figure 4.2. There are five types of nodes in the network, separately located at different tiers. The small generation nodes (i.e., medical clinics and laboratories) constitute the first tier. The second tier includes large generation nodes (i.e., hospitals and medical centers) and temporary transfer stations. Finally, existing and temporary treatment centers form the last tier of this network. These treatment centers are considered to be integrated facilities, meaning that both the treatment and disposal of the infectious waste processes are done in a single facility. Taking well-planned collection tours, vehicles pick up the infectious waste from small generation nodes and deliver it to temporary transfer stations. Then, the accumulated waste is conveyed from those stations to treatment centers (existing or temporary) through direct routes. All large generation nodes are directly routed to treatment centers.

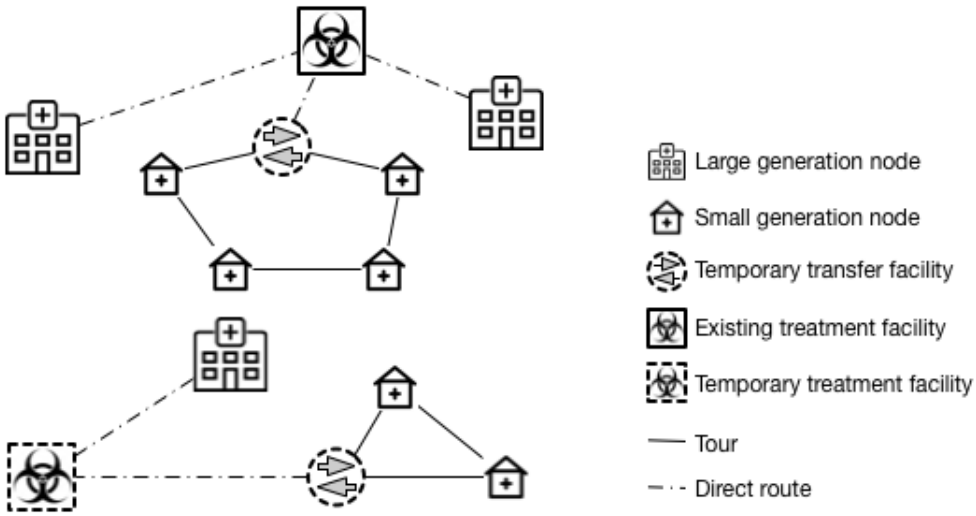

Figure 4.2: Network for the infectious waste management

Decisions needed to be made for this waste system include: location decisions focused on temporary transfer stations and treatment centers, acquisition decisions about how many vehicles are required for collections, and routing decisions for the collection tours from small generation nodes to temporary transfer stations, as well as direct routes between transfer stations/large generation nodes and treatment centers.

4.3.1 Assumptions and notation

In this model, the planning horizon is set as one day, since the infectious wastes are usually required to be shipped and handled within 24 hours for the purpose of infection prevention and control (Peng et al., 2020). Our model is built upon an existing system, aiming to improve the preparedness and responsiveness when a pandemic hits. We hence assume that the vehicles for direct routes have already been purchased, and only the number of vehicles for collection tours needs to be determined. It is also assumed that all vehicles and facilities meet the required security and safety standards

for infectious waste handling and treatment.

The amount of waste generated at each node (i.e., demand) is assumed to have an uncertain nature. Three scenarios are defined covering different pandemic phases, respectively addressing low, medium, and high demands. When historical data are available and reliable, the demand and probability for each scenario can be determined accordingly. However, in reality, existing data may not be enough to predict the highly unforeseeable pandemic severity level, like what we have experienced during the ongoing COVID-19 pandemic. In this regard, the decision maker's perception and attitude toward the possible degree of impacts that the pandemic may have on the system can be used to derive the parameters. Then the three scenarios indicate the decision maker's estimate of the outbreak severity, respectively optimistic, most likely, and pessimistic cases; in the meantime, the probabilities quantify the extent of concerns over those cases. A similar type of scenario setting can also be seen in the literature on logistics (Tasouji Hassanpour et al., 2021; Zhao et al., 2021).

Tables 4.2 and list the notation used in this work, based on which a detailed discussion of the mathematical model is then presented.

4.3.2 A two-commodity formulation

The two-commodity formulation (Baldacci et al., 2004) is utilized to examine the collection tours among temporary transfer stations and small generation nodes. By excluding the application of traditional sub-tour elimination constraints, this type of formulation results in a higher convergence rate. To that end, the original road network is extended by introducing nodes that present copies of temporary transfer

Table 4.2: Notation - sets & parameters

Sets	
N	set of nodes regardless of their nature, indexed by i and j
E	set of edges, indexed by (i, j)
G	set of small infectious generation nodes, indexed by g
L	set of large infectious generation nodes, indexed by l
T	set of candidate temporary transfer stations,indexed by t
$\bar{T}$	set of copies of candidate temporary transfer stations, indexed by τ
C	set of candidates for temporary treatment centers, indexed by c
C'	set of existing treatment centers, indexed by c'
S	set of uncertain scenarios, indexed by s
Parameters	
w_i^s	amount of waste generated at node $i \in G \cup L$ at scenario s
FCT_t	fixed cost of opening temporary transfer station t
FCC_c	fixed cost of opening temporary treatment center c
$FCA_{c'}$	fixed cost of activating the existing treatment center c'
VCT_t	variable cost of operating one unit of waste at temporary transfer station t
VCC_c	variable cost of operating one unit of waste at temporary treatment center c
$VCC_{c'}$	variable cost of operating one unit of waste at existing treatment center c'
TCT	transportation cost per kilometer in the tour
TCD	transportation cost for one unit of waste per kilometer in the direct route to the treatment center
CS_t	capacity of temporary transfer station t
CC_c	capacity of temporary treatment center c
$CC_{c'}$	capacity of existing treatment center c'
VCT	vehicle capacity for collection tours
VCD	vehicle capacity of the trucks for direct routes
VFC	Vehicle cost for tours
d_{ij}	length of edge $(i, j) \in E$
ot_t	opening time of transfer station $t \in T$
ct_t	closure time of transfer station $t \in T$
st_g	service time on node $g \in G$
tt_t^s	total traveling time of a truck in a tour, departing from a transfer station $t \in T$ and ending at its associated copy, in scenario s
M	a big number
t_{ij}	travel time of a truck from node i to j
R_{ij}	risk of traveling from node i to j
R_i	risk around facility $i \in T \cup C \cup C'$
Decision variables	
λ_t	1, if temporary transfer station is located at node t; 0, otherwise
γ_c	1, if treatment center is located at node c; 0, otherwise
$\gamma_{c'}$	1, if existing treatment center is located at node c'; 0, otherwise
$x_{ij\tau}^s$	amount of waste loaded in the vehicle on edge $(i, j) \in E$, where this vehicle is ended at copy station $\tau \in \bar{T}$ in scenario s
$x_{ji\tau}^s$	amount of empty space in the vehicle on edge $(i, j) \in E$, where this vehicle is ended at copy station $\tau \in \bar{T}$ in scenario s

Table 4.2 (continue) : Notation - decision variables

Decision variables	
y_{ij}^s	number of times for transporting infectious waste to treatment centers on edge $(i,j) \in E$ in scenario s
η_{ij}^s	amount of infectious waste transported to treatment centers on edge $(i,j) \in E$ in scenario s
ζ_t^s	amount of infectious waste collected at temporary transfer station t in scenario s
ϖ_j^s	amount of infectious waste collected at temporary treatment center ($j \in C$) or existing treatment center ($j \in C'$) in scenario s
n^s	number of vehicles required for collecting the infectious waste in scenario $s \in S$
a_τ^s	arrival time of a truck to the copy node $\tau \in \bar{T}$ in scenario s
u_t^s	departure time of a truck from transfer station $t \in T$ in scenario s
$r_{ij\tau}^s$	1, if edge $(i,j) \in E$ appears in the vehicle route where this vehicle is ended at copy station $\tau \in \bar{T}$ in scenario s; 0, otherwise
$o_{g\tau}^s$	1, if the produced waste of the small generation node $g \in G$ is collected at copy of the temporary station $\tau \in \bar{T}$ in scenario s; 0, otherwise.

facilities. Hence, a collection tour is defined as a route starting from a transfer station and finishing at the station's associated copy after visiting at least one small generation node, under the condition that the capacities of the vehicles and temporary transfer stations cannot be violated. The application of this type of formulation in the field of hazardous material transportation can be found in Zhao and Verter (2015) and Zhao and Ke (2017).

Fig. 4.3 depicts two types of flows that exist in each tour: a forward flow (solid arrow) from the original temporary transfer station (t) to its copy (τ), and a backward flow (dashed arrow) moving in the opposite direction from the copy to the original facility. While the flow in the former type indicates the vehicle's actual load, the backward flow represents the remaining empty space on the same vehicle. In this regard, the vehicle capacity equals the sum of the two flows, i.e., $VCT = x_{ij\tau}^s + x_{ji\tau}^s$ when the vehicle is ended at station τ in scenario s.

In addition, the net flow in each scenario equals twice the amount of generated

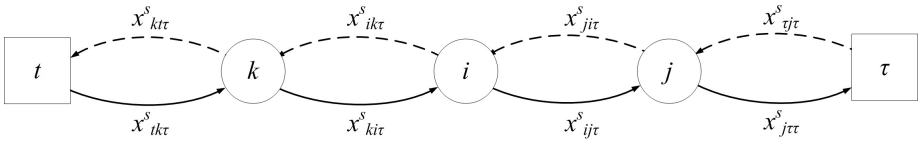

Figure 4.3: Two-commodity formulation's basic relationships in the network

waste at this specific node, because the waste amount is counted in both the forward and backward flows. Take node i in Figure 4.3 for example. In scenario s, the net flow can be calculated by the inflow ($x^s_{ki\tau}+x^s_{ji\tau}$) minus the outflow ($x^s_{ik\tau}+x^s_{ij\tau}$), which should equal to double amount of the waste generated at i ($2w^s_i$).

4.3.3 Objective functions

In this problem, we deal with two objectives, cost and risk. Both are computed separately for the system-level facility location decisions in the first stage, and the scenario-level vehicle and routing decisions in the second stage.

Let CF and RF respectively be the fixed components for the cost and risk objectives. We have

$$CF = \sum_{t\in T} \lambda_t FCT_t + \sum_{c\in C} \gamma_c FCC_c + \sum_{c'\in C'} \gamma_{c'} FCA_{c'} \tag{4.1}$$

$$RF = \sum_{t\in T} \lambda_t R_t + \sum_{c\in C} \gamma_c R_c + \sum_{c'\in C'} \gamma_{c'} R_{c'} \tag{4.2}$$

In Eq. (4.1), the fixed cost of establishing temporary facilities, such as the rental cost of the property and other maintenance expenses, for both transfer stations and treatment centers is calculated. In Eq. (4.2), the potential risk of opening or activating the facilities is computed by applying the exposed population in the proximity of the facility. Note that we estimate the risk as the population exposure within a certain

radius, which can be calculated by multiplying the size of the exposure area and the population density of the area. Concerning the worst-case scenario of a possible incident, this approach has been broadly applied to low-probability-high-consequence events, such as hazmat-related incidents (examples include Batta and Chiu (1988); Ke (2020b); Zhao et al. (2021), among others).

On the other hand, each objective also contains a variable portion in each scenario. The associated values, denoted respectively as CV^s and RV^s for scenario s, can be obtained as:

$$CV^s = n^s VFC + \sum_{t\in T} \zeta_t^s VCT_t + \sum_{c\in C} \varpi_c^s VCC_c + \sum_{c'\in C'} \varpi_{c'}^s VCC_{c'} + \sum_{i,j\in G\cup T\cup T'} \sum_{\tau\in\bar{T}} \frac{r_{ij\tau}^s d_{ij} TCT}{2} + \sum_{i\in L\cup T} \sum_{j\in C\cup C'} y_{ij}^s d_{ij} TCD \tag{4.3}$$

$$RV^s = \sum_{i,j\in G\cup T\cup T'} \sum_{\tau\in\bar{T}} \frac{r_{ij\tau}^s R_{ij}}{2} + \sum_{i\in L\cup T} \sum_{j\in C\cup C'} y_{ij}^s R_{ij} \tag{4.4}$$

Eq. (4.3) adds up the vehicle purchase cost, operation costs at the temporary and existing facilities, and transportation costs for collection tours and direct routes. Eq. (4.4) includes the en-route risks for the tours and routes. It is important to note that the tour-related computations are divided by 2. This is because variable $r_{ij\tau}^s = 1$ in both forward and backward flows in the two-commodity flow formulation, while only the forward flow contains actual waste, and the backward flow shows the vehicle's empty space and hence should not be counted.

Now, let π^s be the probability of scenario s, the mean cost and mean risk can be respectively calculated as:

$$\mu_{Cost} = \sum_{s\in S} \pi^s CV^s \tag{4.5}$$

$$\mu_{Risk} = \sum_{s \in S} \pi^s RV^s \tag{4.6}$$

Consequently, the objective functions, consisting of the fixed and variable elements, can be expressed as:

$$\min Z_{Cost} = CF + \mu_{Cost} \tag{4.7}$$

$$\min Z_{Risk} = RF + \mu_{Risk} \tag{4.8}$$

4.3.4 Chance-constrained time window

The time-related assumptions in this research are considered through the time window concept as permissible facility service periods. In more detail, we propose to use temporary transfer stations, which are regularly occupied for non-infectious waste. Without influencing the normal operations and avoiding transmission at those stations, it is reasonable to assign a specified service interval only for handling infectious waste. Such service intervals imply the corresponding facility's regulated time windows to start servicing the small generation nodes and receiving the collected waste from them. In this interval, ot_t and ct_t are respectively the earliest and latest times that the vehicle can depart from and arrive at the transfer station $t \in T$. Assuming hard time windows, the following set of constraints are applied:

$$tt_t^s = \sum_{i,j \in G \cup T \cup \bar{T}} \frac{r_{ij\tau}^s t_{ij}}{2} + \sum_{g \in G} st_g o_{g\tau}^s \qquad \forall t \in T, \forall \tau \in \bar{T}, \tau - t = |T|, \forall s \in S; \tag{4.9}$$

$$a_\tau^s + M(1 - \lambda_t) \geq u_t^s + tt_t^s \qquad \forall t \in T, \forall \tau \in \bar{T}, \tau - t = |T|, \forall s \in S; \tag{4.10}$$

$$ot_t \leq u_t^s \qquad \forall t \in T, \forall s \in S; \tag{4.11}$$

$$a_\tau^s \leq ct_t \qquad \forall \tau \in \bar{T}, \forall s \in S. \tag{4.12}$$

Constraint (4.9) calculates the traveling time of a truck in a tour by incorporating the related traveling times on the selected edges and the associated customer service times in that tour. Constraint (4.10) guarantees that the difference between the arrival time of a truck to the assumed copy of the transfer station node and its departure time from the associated facility at least equals the total traveling time of the related tour. Finally, Constraints (4.11) and (4.12) ensure that the arrival and departure times adhere to the associated service interval.

In relation to the time window constraints, the stochastic service time is modeled by Chance Constrained Programming (CCP), which seeks to ensure a certain service confidence level. In other words, this method formulates a problem in such a way as to guarantee that the probability of meeting a particular constraint is higher than a certain threshold. The vehicle's service times at small generation nodes are relatively dependent on the amount of generated waste at those nodes. The collection process becomes more sensitive to variations in the amount of load when dealing with hazardous materials and infectious waste. We assume here the service time is normally distributed with a known mean and standard deviation. This assumption is made on the basis of the central limit theorem, which leads to the fact that the normal distribution can often be applied to represent real-valued random variables when the distribution is hard to achieve (Casella and Berger, 2001). Practically, empirical studies can be conducted to find the best distribution that shows a good fit of the service time.

Applying CCP to Constraint (4.10) guarantees that the probability of meeting the time window at each transfer station is above a pre-determined confidence level

θ, that is

$$P(a^s_\tau + M(1-\lambda_t) \geq u^s_t + tt^s_t) \geq \theta \qquad \forall t \in T, \forall \tau \in \bar{T}, \tau - t = |T|, \forall s \in S. \quad (4.13)$$

Now, by moving u^s_t to the left-hand side of the inner inequality, we obtain $P(a^s_\tau + M(1-\lambda_t) - u^s_t \geq tt^s_t) \geq \theta$, which can be easily converted into the standard normal distribution, where we can utilize the cumulative distribution function properties of the normal standard distribution using the following steps:

$$\begin{aligned} P(\frac{tt^s_t - \mu_{tt^s_t}}{\sigma_{tt^s_t}} \leq \frac{a^s_\tau - u^s_t + M(1-\lambda_t) - \mu_{tt^s_t}}{\sigma_{tt^s_t}}) \geq \theta; \\ P(Z \leq \frac{a^s_\tau - u^s_t + M(1-\lambda_t) - \mu_{tt^s_t}}{\sigma_{tt^s_t}}) \geq \theta; \\ \varphi(\frac{a^s_\tau - u^s_t + M(1-\lambda_t) - \mu_{tt^s_t}}{\sigma_{tt^s_t}}) \geq \theta; \\ \frac{a^s_\tau - u^s_t + M(1-\lambda_t) - \mu_{tt^s_t}}{\sigma_{tt^s_t}} \geq Z_\theta. \end{aligned}$$

The final CCP deterministic equivalent of the associated constraint will be as follows:

$$a^s_\tau - u^s_t + M(1-\lambda_t) \geq \mu_{tt^s_t} + Z_\theta \sigma_{tt^s_t}, \qquad \forall t \in T, \forall \tau \in \bar{T}, \tau - t = |T|, \forall s \in S. \quad (4.14)$$

4.3.5 Mathematical formulation

Based on the two-commodity flow formulation, we present the complete mathematical model in the following.

$$\min Z_{Cost}$$

$$\min Z_{Risk}$$

subject to: (4.9),(4.11),(4.12),(4.14), and

$$\sum_{j\in G\cup T\cup\bar{T},j\neq i}(x^s_{ij\tau}-x^s_{ji\tau})=2w^s_i o^s_{i\tau} \qquad \forall i\in G\cup T,\forall\tau\in\bar{T},\forall s\in S; \tag{4.15}$$

$$\sum_{g\in G}\sum_{\tau\in\bar{T}}x^s_{\tau g\tau}=n^sVCT-\sum_{g\in G}\sum_{\tau\in\bar{T}}w^s_g o^s_{g\tau} \qquad \forall s\in S; \tag{4.16}$$

$$\sum_{g\in G}x^s_{g\tau\tau}=\sum_{g\in G}w^s_g o^s_{g\tau} \qquad \forall\tau\in\bar{T},\forall s\in S; \tag{4.17}$$

$$\sum_{g\in G}\sum_{m\in\bar{T}}\sum_{\tau\in\bar{T}}x^s_{gm\tau}\leq n^sVCT \qquad \forall s\in S; \tag{4.18}$$

$$x^s_{ij\tau}+x^s_{ji\tau}=VCTr^s_{ij\tau} \qquad \forall i,j\in G\cup T\cup\bar{T},i\neq j, \quad \forall\tau\in\bar{T},\forall s\in S; \tag{4.19}$$

$$\sum_{g\in G}x^s_{tg\tau}=0 \qquad \forall t\in T,\forall\tau\in\bar{T},\tau-t=|T|,\forall s\in S; \tag{4.20}$$

$$\sum_{i\in G\cup T\cup\bar{T},i\neq g}(r^s_{gi\tau}+r^s_{ig\tau})=2o^s_{g\tau} \qquad \forall g\in G,\forall\tau\in\bar{T},\forall s\in S; \tag{4.21}$$

$$\sum_{i\in G\cup T\cup\bar{T},i\neq\tau}(r^s_{ti\tau}+r^s_{it\tau})=0 \qquad \forall t\in T,\forall\tau\in\bar{T},\tau-t\neq|T|,\forall s\in S; \tag{4.22}$$

$$\sum_{j\in G\cup T\cup\bar{T},j\neq\tau}(r^s_{mj\tau}+r^s_{jm\tau})=0 \qquad \forall m,\tau\in\bar{T},m\neq\tau,\forall s\in S; \tag{4.23}$$

$$r^s_{tg\tau}\leq\lambda_t \qquad \forall g\in G,\forall t\in T,\forall\tau\in\bar{T},\tau-t=|T|,\forall s\in S; \tag{4.24}$$

$$\sum_{\tau\in\bar{T}}o^s_{g\tau}=1 \qquad \forall g\in G,\forall s\in S; \tag{4.25}$$

$$\zeta^s_t=\zeta^s_\tau \qquad \forall t\in T,\forall\tau\in\bar{T},\tau-t=|T|,\forall s\in S; \tag{4.26}$$

$$\zeta^s_t=\sum_{g\in G}w^s_g o^s_{g\tau} \qquad \forall t\in T,\forall\tau\in\bar{T},\tau-t=|T|,\forall s\in S; \tag{4.27}$$

$$\zeta^s_t=\sum_{j\in C\cup C'}\eta^s_{tj} \qquad \forall t\in T,\forall s\in S; \tag{4.28}$$

$$w^s_l=\sum_{j\in C\cup C'}\eta^s_{lj} \qquad \forall l\in L,\forall s\in S; \tag{4.29}$$

$$\varpi^s_j=\sum_{i\in L\cup T}\eta^s_{ij} \qquad \forall j\in C\cup C',\forall s\in S; \tag{4.30}$$

$$\zeta^s_t\leq CS_t\lambda_t \qquad \forall t\in T,\forall s\in S; \tag{4.31}$$

$$\sum_{j \in L \cup T} \eta_{jc}^{s} \leq CC_c \gamma_c \qquad \forall c \in C, \forall s \in S; \tag{4.32}$$

$$\sum_{j \in L \cup T} \eta_{jc'}^{s} \leq CC_{c'} \gamma_{c'} \qquad \forall c' \in C', \forall s \in S; \tag{4.33}$$

$$\frac{\eta_{ij}^{s}}{VCD} \leq y_{ij}^{s} \qquad \forall i \in L \cup T, \forall j \in C \cup C', \forall s \in S; \tag{4.34}$$

$$\sum_{i \in L \cup T} \eta_{ij}^{s} \leq M(\gamma_c + \gamma_{c'}) \qquad \forall j \in C \cup C', \forall s \in S; \tag{4.35}$$

$$\lambda_t, \gamma_c, \gamma_{c'}, r_{ij\tau}^{s}, o_{g\tau}^{s} \in \{0,1\} \qquad \forall g \in G, \forall t \in T, \forall \tau \in \bar{T}, \forall c \in C, \forall c' \in C', \forall (i,j) \in E, \forall s \in S; \tag{4.36}$$

$$x_{ij\tau}^{s}, \eta_{ij}^{s}, \zeta_t^{s}, \varpi_i^{s}, a_\tau^{s}, u_t^{s} \geq 0 \qquad \forall i,j \in N, \forall (i,j) \in E, \forall t \in T, \forall \tau \in \bar{T}, \forall s \in S; \tag{4.37}$$

$$y_{ij}^{s}, n^{s} \geq 0 \text{ and integer} \qquad \forall i \in L \cup T, \forall j \in C \cup C', \forall s \in S. \tag{4.38}$$

Constraint (4.15) affirms that the difference between the total outflow and total inflow in each scenario equals twice the amount of generated waste at this specific node. The equity between the total outflow of the copy transfer stations and the residual capacity of vehicles in each scenario is guaranteed in (4.16). Constraint (4.17) ensures that the total entering flow for the copy of a temporary transfer station in each scenario equals the total collected waste from all generation nodes allocated to the

same transfer facility. Constraint (4.18) guarantees that the total inflow of the copy of a temporary transfer station does not violate the specified total vehicle capacities in each scenario. Constraint (4.19) makes sure, provided that edge (i, j) is included in a tour, the summation of the forward and backward flows on that edge is equal to the capacity of the vehicle. In other words, this constraint ensures that both x^s_{ijm} and x^s_{jim} take feasible values. Constraint (4.20) enforces the model not to assign any load on the vehicle which has just left a temporary transfer station. Constraint (4.21) states that each small generation node has two incident edges. Constraints (4.22) and (4.23) force the tour to end at the corresponding copy of a temporary transfer station from which the vehicle had started its route. This is achieved by forbidding the treatment centers from participating in other copies' tours and preventing movements between copies of transfer stations. Constraint (4.24) states that a tour from temporary storage can be initiated provided that the facility is opened. Constraint (4.25) guarantees that each small generation node should only be served in one tour. The flow balances among the three tiers are ensured in Eqs. (4.26)-(4.30). Eq. (4.26) equals the temporary transfer station and its copy. Eq. (4.27) totals the waste amount of small generation nodes to the waste collection amount for temporary transfer stations. Eqs. (4.28)-(4.30) respectively balance the temporary transfer stations and treatment centers, the large generation nodes and treatment centers, as well as the shipping and storage amounts of the treatment centers. The establishment of capacity constraints in transfer stations and treatment centers is handled in (4.31) to (4.33). Constraint sets (4.34) and (4.35) are the logic constraints of decision variables. In this regard, Constraint (4.34) determines the number of times that the vehicle should travel in the direct routes based on vehicle capacity and the amount of

waste to be transferred between the second and third tiers. Also, Constraint (4.35) allows waste transportation between second and third tiers when the treatment centers are opened or activated. Finally, Constraint sets (4.36)-(4.38) determine the nature of the decision variables in the problem.

4.4 Solution method

The difficulty of solving the above model lies in two aspects. First, the bi-objective structure requires a technology that can effectively and efficiently generate the Pareto optimal set. An augmented ε-constraint method is applied here. Secondly, Samanlioglu (2013) and Yu and Solvang (2016) showed that a single objective location routing problem is NP-hard. Given the additional objective and uncertain features, our model is clearly NP-hard. Thus a branch-and-price algorithm is proposed to solve the model to optimality.

4.4.1 Augmented ε-constraint method

We use the augmented ε-constraint method, proposed by Mavrotas and Florios (2013), to deal with the bi-objective nature of the presented model. Belonging to the category of generation methods for multiple objective problems, the ε-constraint method outshines the most commonly applied weighting approach (Mavrotas, 2009) in the following aspects, 1) capability of producing non-extreme efficient solutions and hence providing a richer representation of the solution set, 2) being able to handle integer and mixed-integer models, 3) indifference in the scale of multiple objectives, and 4) the easiness in adjusting the number of solutions. In addition to the benefits of

the standard ε-constraint method, the augmented ε-constraint method is further enhanced by incorporating acceleration issues to ensure the solution efficiency while keeping reasonable solution times.

In this exact method, one of the objectives stays in the objective function, while the rest are treated as constraints according to some limitations and values determined by the decision-maker. Defining $f_1(x)$ as the primary objective function and transferring $f_2(x)$ into the problem constraints section as a new constraint with an enforcing upper bound results in the following terms:

$$\min\ f_1(x) - eps \times ({}^{\delta}/_{\Delta})$$

s.t.

$$f_2(x) + \delta = \varepsilon,$$

$$B(x, b) = 0,$$

$$\delta \geq 0.$$

Herein, ε and δ represent the upper bound of the second objective and the corresponding slack variable for the constraint, respectively. Parameter Δ is applied to prevent scaling issues concerning the range of the second objective function, and *eps* is a small number taking a value in the interval $[10^{-6}, 10^{-3}]$ (Mavrotas and Florios, 2013).

Setting the cost function as the primary objective, the model can be written as:

$$\min \quad Z_{Cost} - eps \times ({}^{\delta}/_{\Delta}) \tag{4.39}$$

s.t. (4.1)-(4.38), and

$$Z_{Risk} + \delta = \varepsilon, \tag{4.40}$$

$$\delta \geq 0. \tag{4.41}$$

4.4.2 Branch and price algorithm

The ε-constraint model given in the previous section can be solved by CPLEX directly. However, as the scale of the problem grows, the required computational time increases exponentially. In the literature, only limited solution methods have been developed for location-routing problems with uncertainties. Examples include the parallelized adaptive large neighbourhood search (Schiffer and Walther, 2018), the Progressive Hedging algorithm (Bashiri et al., 2021), and the imperialist competition algorithm (Tayebi Araghi et al., 2021), among others. However, the majority of them are either not exact algorithms, or not suitable for the multi-level structure of our problem. To facilitate the solution procedure, especially for large-scale instances, we apply a branch-and-price (B&P) algorithm that is inspired by the work of Wang et al. (2020). By applying Dantzig-Wolfe decomposition, the mathematical model can be decomposed to a master problem following the set partitioning formulation (Subsection 4.4.2.1) and the pricing subproblem concerning the collection tours with negative reduced costs (Subsection 4.4.2.2).

Algorithm 1 summarizes the procedure of this solution approach. First, a restricted master problem (RMP) is developed for the branching nodes. By solving its linear relaxed form (RRMP) through duality, a set of new columns is added using the column generation (CG) method (subsection 4.4.2.4) built upon a pulse algorithm (subsection 4.4.2.3). If the optimal solution set of the linear master problem contains fractional values, then two new complementary subproblems are generated

using the branching rules given in subsection 4.4.2.5. Conducting the same procedure on the child nodes, the solution algorithm continues until any termination condition is reached or a final solution is obtained.

4.4.2.1 Master problem based on the set partitioning formulation

In this section, we present the set partitioning-based formulation of the model. Without loss of generality, we assume $V_2 = L \cup T$, $V_3 = C \cup C'$, and remove the scenario index from the symbols. To deal with scenarios, the master problem is further divided into a set of smaller problems, each corresponding to an individual scenario. The algorithm then begins with solving the model for the worst-case scenario, defining the system structure to handle all the possible scenarios. All required facilities are determined in this step. Benefiting from the resulting reduced number of facilities, the algorithm subsequently addresses the remaining scenarios. Each tour $r \in R_t$ starts from an open transfer station t and ends up at its corresponding copy. Therefore, we have $\sum_{t \in T} R_t = R$ as the set of feasible tours that satisfy Constraints (4.15)-(4.25). Let α_{gr} be a binary variable indicating whether a small generation node g has been visited in route r or not. Also, the cost of each tour is shown by $Cost_r$, which comprises the vehicle's traveling expenses, waste processing charges at the transfer stations, and the fixed cost of utilizing vehicles. Similarly, $Risk_r$ stands for the associated en-route risk of tours and direct routes. The accumulated demand in a tour by visiting small generation nodes is defined as $AD_r = \sum_{g \in G} \alpha_{gr} \omega_g$, where ω_g is the related waste of node g. Finally, the existence of route r in the solution is presented using the binary variable e_r. The two-commodity-based formulation can be represented holding the

Algorithm 1: B&P algorithm

Let Ω be the list of all active nodes in the B&P tree;
Let ϱ_r be the relaxed solution of node ϱ;
Let V_{ts} and V_{tc} be the potential transfer station and treatment center nodes, respectively;
Let V'_{ts} and V'_{ts} be the set of potential facilities obtained after branching on the facility locations;
$Best \leftarrow$ The intuitive initial solution;
Initialize RMP at root node $\bar{\varrho}$ using routes in $Best$ and compute $\bar{\varrho}_r$ using CG, $\Omega \leftarrow \{\bar{\varrho}\}$;
while $\Omega \neq \emptyset$ **do**
    $\varrho \leftarrow$ The node with the minimum LB, $\Omega \leftarrow \Omega \setminus \varrho$;
    if ϱ_r *is better than* $Best$ **then**
        if ϱ_r *is feasible* **then**
            $Best \leftarrow \varrho_r$;
        else
            Start branching on ϱ;
            if *branching on location variables* **then**
                Modify the locations;
                V_{ts} becomes V'_{ts} according to branching results;
                Generate new columns using the pulse algorithm for each of the transfer stations $t \in V'_{ts}$;
                Add the new columns to the associated RLMP for feasibility assurance and adapt V'_{tc} accordingly;
            if *location variables and direct-route variables are feasible* **then**
                Calculate the aggregated-based bound LB_{ag};
                if *node cost of* $\varrho_r < LB_{ag}$ **then**
                    Construct ϱ^1 and ϱ^2 achieved from branching on ϱ;
                    compute ϱ^1_r and ϱ^2_r using CG;
                    $\Omega \leftarrow \Omega \cup \{\varrho^1, \varrho^2\}$;
            else
                Construct ϱ^1 and ϱ^2 achieved from branching on ϱ;
                compute ϱ^1_r and ϱ^2_r using CG;
                $\Omega \leftarrow \Omega \cup \{\varrho^1, \varrho^2\}$;

following Master problem in the set partitioning format:

$$\min \quad CF + \sum_{i \in V_2} \sum_{j \in V_3} y_{ij} d_{ij} TCD + \sum_{c \in C} \varpi_c VCC_c + \sum_{c' \in C'} \varpi_{c'} VCC_{c'} + \sum_{r \in R} Cost_r e_r \quad (4.42)$$

s.t. (4.26)-(4.35), and

$$RF + \sum_{r \in R} Risk_r e_r + \delta = \varepsilon \quad (4.43)$$

$$\sum_{r \in R} \alpha_{gr} e_r = 1 \qquad \forall g \in G; \quad (4.44)$$

$$\sum_{r \in R} e_r AD_r \leq nVCT; \quad (4.45)$$

$$\sum_{r \in R} e_r AD_r = \sum_{j \in V_3} \eta_{gj} \qquad \forall g \in G; \quad (4.46)$$

$$e_r \in \{0, 1\} \qquad \forall r \in R. \quad (4.47)$$

Objective (4.42) includes all elements of the original cost objective; however, it has been presented in a suitable form to fit in the Dantzig-Wolfe decomposition approach. The associated risk, based on the ϵ-constraint method, is computed in (4.43). Constraint (4.44) confirms that each small generation node is visited only once using just one route. Constraint (4.45) assures that the amount of collected waste through different routes does not violate the total available capacity of the trucks in tours. Finally, (4.46) establishes the balance between the amount of collected waste in tours and the amount of waste transferred to the treatment centers.

This model can be strengthened using the following valid inequalities where t_r and LTW respectively are the accumulated time in route r and the length of the required time window:

$$n \geq \left\lceil \sum_{r \in R} e_r t_r / LTW \right\rceil, \quad (4.48)$$

$$n \geq \left\lceil \sum_{r \in R} e_r AD_r / VCT \right\rceil. \tag{4.49}$$

Constraint (4.48) addresses the minimum number of required vehicles based on the accumulated time of all routes divided by the available time windows, and Constraint (4.49) is based on satisfying the demands according to the vehicle capacities. Next, by relaxing to a linear format, i.e., RRMP, the master problem can be easily solved through duality.

4.4.2.2 Pricing subproblem

The pricing subproblem in this paper contributes to constructing the tours using the minimum reduced cost as the objective function. The reduced cost of the subproblem is built using the dual values of the restricted MP (RMP). Let v, ψ, and ϕ be the dual values of Constraints (4.44)-(4.46). We can obtain the reduced cost of decision variable e_r as:

$$\overline{Cost_r} = Cost_r - Risk_r - \sum_{g \in G} \alpha_{gr} \left[v_g + \omega_g (\psi + \phi_g) \right]. \tag{4.50}$$

Based on the above formulation, the optimality condition for the feasible routes is:

$$Cost_r - Risk_r - \sum_{g \in G} \alpha_{gr} (v_g + \omega_g (\psi + \phi_g)) \leq 0, \tag{4.51}$$

where $Cost_r$ and $Risk_r$ are computed by the following equations:

$$Cost_r = nVFC + \sum_{t \in T} \zeta_t VCT_t + \sum_{i,j \in G \cup T \cup T'} \sum_{\tau \in \bar{T}} \frac{r_{ij\tau} d_{ij} TCT}{2}. \tag{4.52}$$

$$Risk_r = \sum_{i,j \in G \cup T \cup T'} \sum_{\tau \in \bar{T}} \frac{r_{ij\tau} R_{ij}}{2}. \tag{4.53}$$

Replacing α_{gr} with $\sum_{\substack{j \in G \cup T \cup \bar{T} \\ j \neq g}} r_{gj\tau}$, the subproblem can be written as:

$$\min \quad Cost_r - \sum_{g\in G} \sum_{\substack{j\in G\cup T\cup \bar{T} \\ j\neq g}} r_{gj\tau} \left[v_g + \omega_g(\psi + \phi_g)\right]$$

s.t.

$$\sum_{j\in G\cup T\cup \bar{T}, j\neq i} (x_{ij\tau} - x_{ji\tau}) = 2w_i o_{i\tau} \qquad \forall i \in G\cup T, \forall \tau \in \bar{T}; \tag{4.54}$$

$$\sum_{g\in G}\sum_{\tau\in\bar{T}} x_{\tau g\tau} = nVCT - \sum_{g\in G} w_g o_{g\tau}; \tag{4.55}$$

$$\sum_{g\in G} x_{g\tau\tau} = \sum_{g\in G} w_g o_{g\tau} \qquad \forall \tau \in \bar{T}; \tag{4.56}$$

$$\sum_{g\in G}\sum_{m\in\bar{T}}\sum_{\tau\in\bar{T}} x_{gm\tau} \leq nVCT; \tag{4.57}$$

$$x_{ij\tau} + x_{ji\tau} = VCTr_{ij\tau} \qquad \forall i,j \in G\cup T\cup\bar{T}, i\neq j, \forall \tau\in\bar{T}; \tag{4.58}$$

$$\sum_{g\in G} x_{tg\tau} = 0 \qquad \forall t\in T, \forall\tau\in\bar{T}, \tau - t = |T|\,; \tag{4.59}$$

$$\sum_{i\in G\cup T\cup\bar{T}, i\neq g} (r_{gi\tau} + r_{ig\tau}) = 2o_{g\tau} \qquad \forall g\in G, \forall\tau\in\bar{T}; \tag{4.60}$$

$$\sum_{i\in G\cup T\cup\bar{T}, i\neq\tau} (r_{ti\tau} + r_{it\tau}) = 0 \qquad \forall t\in T, \forall\tau\in\bar{T}, \tau - t \neq |T|\,; \tag{4.61}$$

$$\sum_{j\in G\cup T\cup\bar{T}, j\neq\tau} (r_{mj\tau} + r_{jm\tau}) = 0 \qquad \forall m,\tau\in\bar{T}, m\neq\tau; \tag{4.62}$$

$$r_{tg\tau} \leq \lambda_t \qquad \forall g\in G, \forall t\in T, \forall\tau\in\bar{T}, \tau - t = |T|\,; \tag{4.63}$$

$$\sum_{\tau\in\bar{T}} o_{g\tau} \leq 1 \qquad \forall g\in G; \tag{4.64}$$

$$tt_t = \sum_{i,j\in G\cup T\cup\bar{T}} \frac{r_{ij\tau}t_{ij}}{2} + \sum_{g\in G} st_g o_{g\tau} \qquad \forall t\in T, \forall\tau\in\bar{T}, \tau - t = |T|\,; \tag{4.65}$$

$$a_\tau + M(1-\lambda_t) \geq u_t + tt_t \qquad \forall t\in T, \forall\tau\in\bar{T}, \tau - t = |T|\,; \tag{4.66}$$

$$ot_t \leq u_t \qquad \forall t\in T; \tag{4.67}$$

$$a_\tau \leq ct_t \qquad \forall t \in T, \forall \tau \in \bar{T}, \tau - t = |T|\,; \tag{4.68}$$

$$\lambda_t, r_{ij\tau}, r_{ji\tau}, o_{g\tau} \in \{0,1\} \qquad \forall g \in G, \forall (i,j) \in E, \forall t \in T, \forall \tau \in \bar{T}; \tag{4.69}$$

$$x_{ij\tau}, x_{ji\tau}, \zeta_t, a_\tau, u_t \geq 0 \qquad \forall (i,j) \in E, \forall t \in T, \forall \tau \in \bar{T}; \tag{4.70}$$

$$n \geq 0, \text{integer}. \tag{4.71}$$

Constraints (4.54) to (4.59) establish the load related requirements. Constraints (4.60) to (4.64) are regarding the flow conditions in tours. The time window specifications are applied in (4.65)-(4.68). Finally, Constraints (4.69)-(4.71) determine the domain of decision variables.

4.4.2.3 Pulse algorithm

In the pricing subproblem, load capacity and the time window constraints are the primary resource constraints. To solve the subproblems effectively, the pulse algorithm (PA) from Wang et al. (2020) is adapted and tailored accordingly. To start with, we create a label with four main elements: PP_l as the partial path, RC_l as the cumulative reduced cost, AD_l as the cumulative load capacity, and TS_l standing for the cumulative spent time in the route. Hence, the label can be stated as $L = (RC_l, PP_l, LC_l, TS_l)$. The process is summarized in Algorithm 2, and the details are elaborated next.

Infeasibility strategy The idea behind the infeasibility strategy is to prevent the pulse from propagating as soon as it is known that the traveling pulse does not reach the final destination without violating the resource constraints. For this purpose, the minimum resource consumption is calculated from any node $g \in G$ to the final

Algorithm 2: Pulse (i, L)

Assume A^1 as all the available small generation nodes;

$\Gamma^+(i) = \{j \in G \cup \bar{T} | (i, j) \in A^1\}$ as the set of next reachable nodes from small generation node i;

Reduced cost contribution as $rc_{ij} = r_{ij\tau}(v_i + \omega_i(\psi + \phi_i))$;

Time window consumption as $tw_{ij} = st_i + r_{ij\tau}t_{ij}$;

if *Feasible*(i, L) *is true* **then**

  if *checkBounds(i,L) is false* **then**

    if *rollback(i,L) is false* **then**

      $PP_l \leftarrow PP_l \cup i$;

      $AD_l \leftarrow AD_l + \omega_i$;

      for $j \in \Gamma^+(i)$ **do**

        $RC_l \leftarrow RC_l + rc_{ij}$;

        $TS_l \leftarrow TS_l + tw_{ij}$;

        pulse (j, L);

      end

    end

  end

end

node $\tau \in \bar{T}$. This process is performed by reversing the network and assuming the ending node τ as the new starting point. Then, the shortest path from τ to all of the nodes in the reverse network can be found, which is equal to the shortest path from the small generation nodes to the copy of the associated transfer station. Therefore, the minimum resource consumption ($\underline{Res_{g\tau}}$) from each node to the ending node (i.e., the copy) is computed. Having calculated the minimum resource consumption, the maximum resource consumption ($\overline{Res_{max}}$) to each small generation node equals the difference between the maximum resource available (Res_{max}) and its minimum computed value, i.e.,

$$\underline{Res_{g\tau}} = Res_{max} - \overline{Res_{max}}. \tag{4.72}$$

Now, for a partial tour to node g, if the amount of consumed resource exceeds this maximum value, this path is assumed to be infeasible.

Bounding strategy The bounding concept is similar to the infeasibility strategy discussed above. The main difference is that, instead of focusing on resource consumption, bounding addresses the cost objective. Every time the pulse finishes its journey by reaching a copy of a transfer station, a feasible tour is created. Accordingly, the best-known objective can be updated, and if any other path exceeds this bound, it will be pruned.

Rollback strategy In the rollback strategy, the two most recently visited nodes (i and j) and the succeeding node (k) are the inputs. If developing the tour directly from i to k results in a lower reduced cost compared to the situation where j is the intermediate between these two nodes, the path can be pruned safely.

Tour completion strategy When the algorithm reaches an intermediate node while developing a partial tour, it explores the pruning possibility by applying different strategies. If pruning is not an option, the tour completion strategy is employed to add the minimum cost path or the tour with the minimum resource consumption. For more clarification, assume a partial tour arrives node i during the pulse propagation. The tour completion strategy seeks the succeeding node, j, with the minimum cost to be added to the current partial tour. Provided that $P(j)$ is feasible and the cost of $P(j)$ is less than the best objective found so far, the incumbent solution can be updated. The side benefit for this process is that the incoming pulse $P(i)$ can be pruned as we already know that $P(j)$ is a better option. Moreover, the minimum resource consumption approach is conducted when the partial tour cannot be extended using the minimum path procedure. Moving from node i to the next node j, if the partial path for j, $P(j)$, is feasible and $P(j)$ leads to a better-associated cost compared to the best objective found so far, the incumbent solution is updated. In this case, the associated pulse for $P(i)$ is not pruned as there may still be paths with lower costs from i to j.

4.4.2.4 Column generation

The column generation approach is built upon PA in providing a new column with negative reduced costs for RRMP. PA is based on a depth-first approach investigating the feasible region. This feature makes PA a suitable match for the column generation scheme. By applying PA, all pulses recursively create tours, each with a reduced cost and a cumulative demand. This is accomplished by adding the nodes one by one in a sequence, and all tours are enumerated so that no restrictions stop pulses from

spreading through the network.

Then in CG, we decompose the pricing subproblem into two phases. The first phase handles the customer assignment based on the dual variables obtained from RRMP. After deciding which small generation nodes are assigned to a tour originating from a transfer station, the second phase is about building feasible columns using the pulse algorithm. The procedure continues iteratively until no column is found to satisfy the optimality condition.

For achieving an appropriate lower bound for CG, we take advantage of an aggregate-based lower bound, LB_{ag}. A simple set-partitioning problem is solved to find the optimal solution of serving a small-generation node in a tour starting from the transfer facility t. Also, the capacity limitations for the facility are neglected. Therefore, the associated set-partitioning problem can be defined as (SP_t) below:

$$\min \sum_{r \in R_t} Cost_r e_r \tag{4.73}$$

$$s.t.$$

$$\sum_{r \in R_t} \alpha_{gr} e_r = 1 \qquad \forall g \in G; \tag{4.74}$$

$$e_r \in \{0,1\} \qquad \forall r \in R_t. \tag{4.75}$$

To insert feasible columns to SP_t, we use PA to solve the LP-relaxed form of SP_t. As described in Wang et al. (2020), and by assuming $\Lambda_{g\tau}$ as the dual value of the second constraint in SP_t, the LB_{ag} can be found as:

$$LB_{ag} = CF + \sum_{i \in V_2} \sum_{j \in V_3} y_{ij}^s d_{ij} TCD + \sum_{c \in C} \varpi_c^s VCC_c + \sum_{c' \in C'} \varpi_{c'}^s VCC_{c'} + \sum_{g \in G} \min_{t \in \bar{T}} \{\Lambda_{g\tau}\}. \tag{4.76}$$

4.4.2.5 Branching rules

The primary branching is performed on the locations of the transfer stations and the treatment centers. As mentioned in Wang et al. (2020), branching on the location variables leads to better improvements in the lower bound. Apart from the location branches, several additional branching rules are applied in the procedure.

Branching on the location of temporary transfer stations If the location variable of temporary transfer station λ_t is fractional, two child nodes can be generated as $\lambda_t = 0$ and $\lambda_t = 1$. Assigning the zero value for this variable, a direct route between this t and the treatment centers no longer exists. It is noteworthy to mention that the associated subproblem of the branch with $\lambda_t = 0$, can no longer be solved as it is eliminated now.

Branching on the number of direct routes and tours The transfer stations are the intermediate facilities between the small generation nodes and the treatment centers. When the number of required vehicles in tours and direct routes is fractional, branching can be applied using the smallest greater and greatest smaller integer values of the obtained fractional value.

Branching on the assignment of customers to open transfer stations If the solution provides a fractional value for e_r, it means that there exist other routes sharing at least one common small generation node with column r. Now, if we define L_{gt} as all the columns originating from t and visiting node g, we can branch on $\sum_{r \in L_{gt}} e_r = 0$ and $\sum_{r \in L_{g\tau}} e_r = 1$. As a result, the condition of this node is stabilized

regarding temporary transfer station t.

4.4.3 Algorithm tests

In this section, we check the validity and stability of the proposed mathematical model and examine the performance of the B&P algorithm. All computational tests (including the case experiments in Section 4.5) are performed on a computer equipped with a 2.2 GHz Intel processor and 2 GB RAM using Java 11 and CPLEX 12.8.0.

Ten random problem instances with different sizes are generated and tested. The size of each instance is described by the numbers of small generation nodes (i.e., $|G|$), large generation nodes ($|L|$), temporary transfer stations ($|T|$), temporary treatment centers ($|C|$), and existing treatment centers ($|C'|$). The amount of generated waste for the small generation nodes follows a uniform distribution as $U \sim [0.5, 3]$, $U \sim [50, 200]$, and $U \sim [300, 1000]$ for scenarios 1 to 3. Similarly, the large generation nodes obtain a random number from $U \sim [4, 8]$, $U \sim [300, 600]$, and $U \sim [2000, 3000]$ for the associated scenarios. The capacity values are set to ensure feasible solutions.

Table 4.3 displays the comparison between CPLEX and B&P algorithm. Column "Best Cost" is the optimal solution or the best result obtained within 10,800 seconds (i.e., 3 hours). Columns "Gap(%)" and "Time" respectively present the optimality gap and computational time for each instance. As we can see, the presented branch-and-bound algorithm outperforms CPLEX in all instances. The proposed B&P is able to solve most of the cases to the optimality by reducing a significant amount of time. For small instances where both approaches can achieve optimality, the computational times of B&P improve more than 83% than CPLEX. Three medium instances can

only be solved to optimality by B&P within 3 hours. When the network is rather large and an optimal solution cannot be reached in both cases, B&P can improve the gap by at least 70%. Also note that developing effective cuts for this algorithm can further enhance the algorithm's performance and reduce the computation time, which is a potential pathway for future work.

Table 4.3: Random instances

#	$\|G\|$	$\|L\|$	$\|T\|$	$\|C\|$	$\|C'\|$	CPLEX			B&P			Improvement	
						Best Cost	Gap (%)	Time (s)	Best Cost	Gap (%)	Time (s)	Gap (%)	Time (%)
1	10	5	4	3	2	2.8012	0.00	915	2.8012	0.00	132	-	85.57
2	20	10	6	4	2	20.0939	0.00	3,487	20.0939	0.00	415	-	88.10
3	25	10	8	4	2	22.1733	0.00	4,274	22.1733	0.00	608	-	85.68
4	25	15	8	6	2	31.0169	0.00	5,423	31.0169	0.00	639	-	88.22
5	30	15	8	6	2	32.6125	0.00	6,791	32.6125	0.00	1,116	-	83.57
6	40	20	8	8	2	50.4507	6.47	10,800	47.1865	0.00	5,681	100	47.40
7	45	20	10	8	3	60.6884	11.33	10,800	53.8124	0.00	8,904	100	17.56
8	50	20	10	8	3	67.5755	18.48	10,800	55.0875	0.00	10,092	100	6.56
9	55	25	10	10	3	83.7921	21.79	10,800	67.0607	2.33	10,800	89.3	-
10	60	30	12	10	4	101.0870	27.32	10,800	79.3843	8.05	10,800	70.5	-
Average						-	8.539	7489	-	1.038	4918.7	45.98	50.26

4.5 Case Study

In this section, a case study based on the situation in Wuhan during the initial outbreak of the COVID-19 pandemic is applied to assess the validity and applicability of the proposed model. The related data are adopted from the study of Zhao et al. (2021). Herein, according to the official authority for Hubei medical waste man-

agement (Medical Waste Management in Hubei, 2020), 30 hospitals and clinics are considered as infectious waste generation locations. The infectious waste generation nodes are differentiated based on the available sickbeds: those with fewer than 500 sickbeds are categorized as small nodes, leaving the other nodes in the class of large infectious waste generation nodes. As shown in Fig. 4.4, this network contains twenty small and ten large generation nodes being distributed in different city regions. Eight regular transfer stations are considered candidate locations to be converted to temporary transfer stations for infectious waste. Four temporary treatment centers and two existing ones in the system are used as integrated facilities.

4.5.1 Relevant data

Scenarios and amount of generated waste Addressing different phases of the COVID-19 outbreak, three scenarios are defined. Scenario 1 represents a minor virus outbreak with a low amount of associated generated waste. In Scenario 2, the city experiences a serious epidemic. The worst-case pandemic situation, with overwhelmed medical centers, is reflected in Scenario 3. In scenarios 1 and 2, the occupancy rates of sickbeds for both small and large generation nodes were assumed to be random within ranges of [0, 1%] and [15%, 20%], respectively. In the third scenario, we assume that the hospitals are operating with their maximum capacity where all the sickbeds are occupied. The amount of infectious generated waste for each COVID-19 patient is estimated based on a report prepared by the Institute for Global Environmental Strategies (2020), as a random value between 2.2 kg/day and 2.8 kg/day. The corresponding probabilities of the scenarios are respectively set as 0.25, 0.5, and

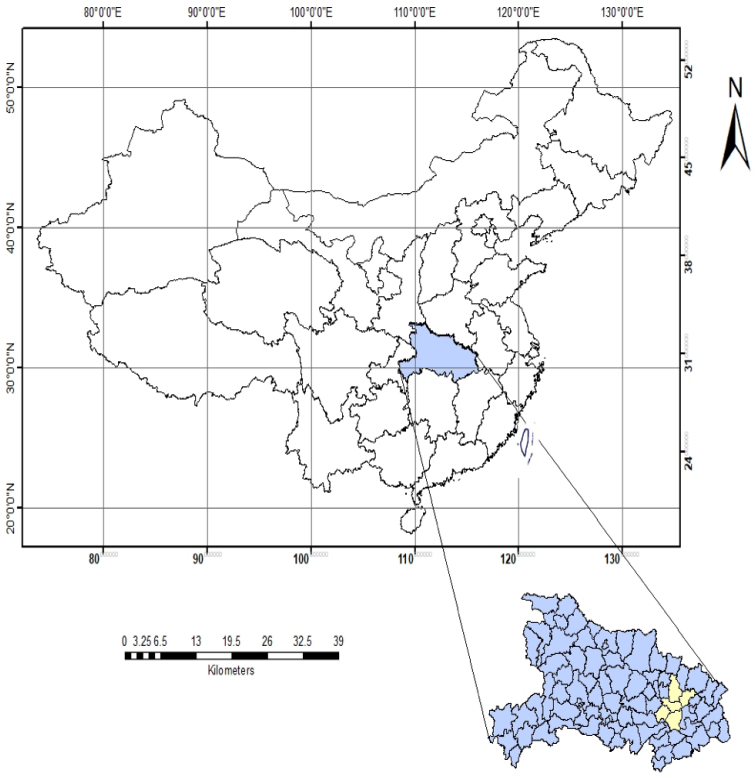

(a) Map showing the location of Wuhan city

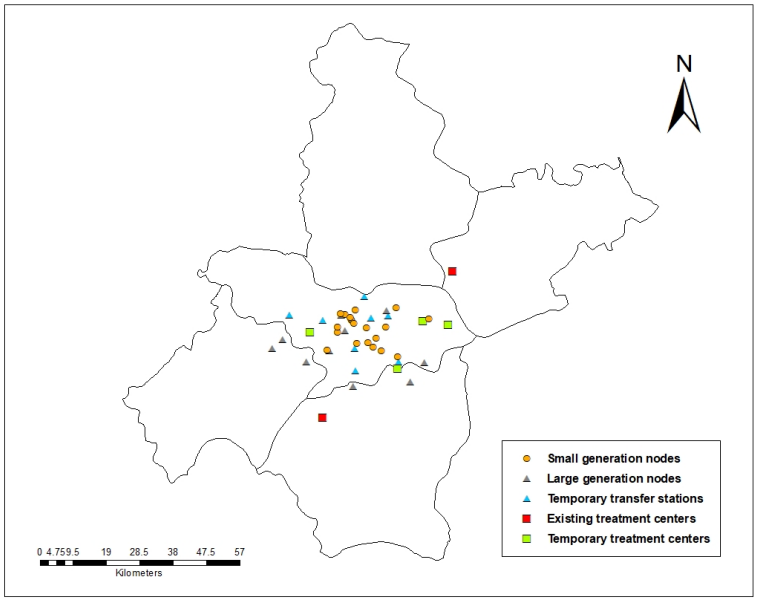

(b) Map showing the candidate facilities in the city of Wuhan

Figure 4.4: The medical waste management network in Wuhan, China

0.25. Based on this information, Table 4.4 summarizes the estimated infectious waste amount at all generation nodes in the three scenarios.

Capacities and costs The capacity of the candidate transfer station is 3 tonnes. Each temporary treatment center can process 5 tonnes of infectious waste per day; and each existing treatment facility works with a capacity of 10 tonnes/day. Two types of vehicles are considered in this paper. Having a capacity of 1.5 tonnes, the first vehicle type is responsible for collecting the infectious waste from the small generation nodes and conveying them to the transfer stations in a tour. Each vehicle that serves in tours costs 160 thousand dollars, with the unit transportation cost of waste collection equal to \$200/km. The second vehicle type, which is used in direct routes between the transfer stations and the treatment centers, takes advantage of a 3-tonne container. The unit cost of carrying waste in the direct routes is \$ 100/km. Other facility operational costs are given in Table 4.5.

Risk We approximate the number of exposed populations within the radius of 800 meters from the facilities (Alumur and Kara, 2007). The number of exposed individuals around each facility is shown in Table 4.5. All population data are acquired from the GIS database. To obtain the exposed population across each edge, we calculate the average of the people residing in the two associated nodes.

Time considerations A four-hour interval is considered as the time window at transfer stations for each tour. The effect of this duration restriction is studied in Subsection 4.5.6. First, we use a 99.9% confidence level for the chance-constrained method, and then we discuss varying this value in Subsection 4.5.4. The service

time of processing infectious waste at each station is directly related to the amount of waste at that location. We adapt the multiple regression resulting from Giel and Dabrowska (2021) to estimate the average time spent at a waste collection point. The standard deviation of the service time is assumed to be 60 seconds. The impact of the variation of the standard deviation is further examined in Subsection 4.5.7.

4.5.2 Extreme Pareto solutions

We first minimize the two objectives individually for the two extreme Pareto solutions of the case study. The results are presented in Table 4.6.

The first extreme point focuses on the minimization of cost. The total cost is \$25.1978 million, from which \$24.52 million is the fixed cost of the system, and \$0.6778 belongs to the variable cost component of the network regarding all three scenarios. Due to the 4-hour time window limitation, at least two tours are required. In this regard, both tours originate from temporary transfer station 37 in the first two scenarios. The optimal tours in both scenarios are 37-19-17-16-2-5-14-4-1-12-20-13-18-3-37 with a duration of 3.83 hours and 37-10-8-9-6-7-15-11-37 lasting 2.47 hours. Temporary treatment center 41 is the main destination for conveying the generated waste from temporary storage facilities and large generation nodes. It is noteworthy to mention that the capacity of the vehicles is not violated as the total generated wastes in Scenarios 1 and 2 equal 0.03106 and 2.2206 tonnes, respectively. These values are split due to the time window constraint. However, in Scenario 3, the situation is different as we are dealing with 12.654 tonnes of infectious waste in the first level of the network. Therefore, not only are the tours affected by the time windows, but

Table 4.4: Data for small and large generation nodes

Node type	#	Node name	Amount of waste generation (kg/day)		
			Scenario 1	Scenario 2	Scenario 3
Small generation node	1	Wuhan Red Cross Hospital	2.3	164	934.8
	2	The Sixth Hospital of Wuhan	2.18	1566	889.2
	3	The Third Hospital of Wuhan	2.09	149.5	852.15
	4	Wuhan Hankou Hospital	1.97	141	803.7
	5	Wuhan Children's Hospital	1.8	128.5	732.45
	6	Hubei Six Seven Two Integrated Traditional Chinese and Western Medicine Orthopaedics Hospital	1.75	125	712.5
	7	Hubei Hospital of traditional Chinese Medicine (Guanggu branch)	1.74	124.5	709.65
	8	The Seventh Hospital of Wuhan	1.57	112	638.4
	9	General Hospital of the Central People's Liberation Army	1.57	112	638.4
	10	Zhongnan Hospital of Wuhan University	1.56	111.5	635.55
	11	Huarun Wisco General Hospital	1.53	109.5	624.15
	12	Wuhan Youfu Hospital	1.46	104.5	595.65
	13	The Third People's Hospital of Hubei Province	1.3	93	530.1
	14	General Hospital of The Yangtze River Shipping	1.26	90	513
	15	The second Hospital of WISCO	1.08	77	438.9
	16	The Eighth Hospital of Wuhan	0.97	69.5	396.15
	17	Wuhan Zijing Hospital	0.97	69	393.3
	18	Wuhan Traditional Chinese Medicine Hospital (Hanyang branch)	2.35	168	957.6
	19	Liyuan hospital	0.83	59.5	339.15
	20	Wuhan Lung Branch Hospital	0.78	56	319.2
Large generation node	21	Wuhan Leishenshan Hospital	7.29	521	2969.7
	22	Taikang Tongji (Wuhan) Hospital	7.19	513.5	2926.95
	23	Wuhan NO.1 Hospital	7.14	510	2907
	24	Wuhan Huoshenshan Hospital	6.75	482	2747.4
	25	Tongji Hospital (Sino-French Eco-City Branch)	6.56	468.5	2670.45
	26	Wuhan Union Cancer Hospital	5.7	407	2319.9
	27	Tongji Hospital (Guanggu branch)	5.26	376	2143.2
	28	Whan Union Hospital West Campus	5	357	2034.9
	29	The Ninth Hospital of Wuhan	4.84	345.5	1969.35
	30	Renmin Hospital of Wuhan University (Eastern Hospital)	4.68	334.5	1906.65

Table 4.5: Data for facilitates

Node type	**#**	**Node name**	**Fixed cost** ($\times 10^3\$$)	**Unit variable cost** ($\$/tonne$)	**Exposed pop.** ($\times 10^3$)
Temporary transfer station	31	Ziyang Garbage Transfer Station	650	1950	37.46
	32	Hanjiadun Garbage Transfer Station	600	1950	33.97
	33	Zhangjiawan Garbage Transfer Station	500	1950	3.68
	34	Baibuting Garbage Transfer Station	550	1950	9.34
	35	Changqing Street Urban Management Sanitation Station Garbage Transfer Station	450	1950	3.66
	36	Yangyuan Domestic Waste Transfer Station	630	1950	40.94
	37	Jianshe One Road Garbage Transfer Station	540	1950	24.05
	38	Halecheng Garbage Transfer Station	500	1950	13.83
Temporary integrated treatment facility	39	Tuanchengshan Economic Development Zone	5200	2600	1.37
	40	Optical Valley Exhibition Center of East Lake High-tech Zone	5300	2600	13.38
	41	Wuhan Hanshi Medical Waste Incineration and Disposal Center	5200	2600	5.18
	42	Wuhan North Lake Yunfeng Environmental Protection Technology Company	5500	2600	1.67
Existing integrated treatment facility	43	The Changshankou landfill	390	1560	0.44
	44	Chenjiachong sanitary landfil	390	1560	1.53

Table 4.6: Extreme Pareto solutions

Extreme Pareto points	Z_{Cost}: **Cost** ($\times 10^6 dollars$)	Z_{Risk}: **Risk** ($\times 10^3 persons$)			**Scenario 1**	**Scenario 2**	**Scenario 3**
Z_1^*	Total=25.1978	Total=1116.60	Transfer station		33,34,35,37,38	33,34,35,37,38	33,34,35,37,38
Min	CF=24.52	RF=78.11	Treatment	Temporary	39,40,41,42	39,40,41,42	39,40,41,42
Cost	μ_{Cost}=0.6778	μ_{Risk}=1038.49	center	Existing	43,44	43,44	43,44
			Number of vehicles		2	2	9
			Tour		37-19-17-16-2-5-14-4-1-12-20-13-18-3-37; 37-10-8-9-6-7-15-11-37	37-19-17-16-2-5-14-4-1-12-20-13-18-3-37 37-10-8-9-6-7-15-11-37	33-3-8-33;33-18-16-33; 34-12-2-34; 34-4-14-34; 35-13-1-35; 37-19-5-37; 37-11-15-17-37; 38-7-6-38; 38-9-10-38
			Tour time		tt_1=3.83, tt_2=2.47	tt_1=3.83, tt_2=2.47	tt_1=1.70, tt_2=1.93, tt_3=1.68, tt_4=1.44, tt_5=2.00, tt_6=2.04, tt_7=1.63, tt_8=1.45, tt_9=1.53
			Direct Route	Station-Treatment	37-39	37-39	33-40; 34-44; 35-43; 37-44; 38-42
				Large generation-Treatment	21-43; 22-41; 23-41; 24-41; 25-41; 26-41; 27-40; 28-41; 29-39; 30-40	21-43; 22-41; 23-41; 24-41; 25-41; 26-41; 27-40; 28-41; 29-39; 30-40	21-43; 22-41; 23-39; 24-43; 25-43; 26-44; 27-42; 28-41; 29-44; 30-40
Z_2^*	Total=25.212	Total=1012.24	Transfer station		33,34,35,37,38	33,34,35,37,38	33,34,35,37,38
Min	CF=24.52	RF=78.11	Treatment	Temporary	39,40,41,42	39,40,41,42	39,40,41,42
Cost	μ_{Cost}=0.6928	μ_{Risk}=934.13	center	Existing	43,44	43,44	43,44
			Number of vehicles		2	2	9
			Tour		35-18-13-20-12-1-4-14-5-2-16-17-3-35; 35-8-9-10-6-7-19-11-15-35	35-18-13-20-12-1-4-14-5-2-16-17-3-35; 35-8-9-10-6-7-19-11-15-35	33-3-8-33; 33-18-13-33; 34-14-1-34; 34-2-12-34; 35-4-9-35; 37-19-17-16-20-37; 37-11-15-37; 38-7-6-38; 38-10-5-38
			Tour time		tt_1=3.90, tt_2=3.88	tt_1=3.90, tt_2=3.88	tt_1=1.89, tt_2=1.70, tt_3=1.58, tt_4=1.68, tt_5=1.46, tt_6=1.90, tt_7=1.97, tt_8=1.99, tt_9=1.45
			Direct Route	Station-Treatment	35-43	35-43	33-43; 34-44; 35-44; 37-44; 38-39
				Large generation-Treatment	21-43; 22-43; 23-43; 24-43; 25-43; 26-43; 27-44; 28-43; 29-44; 30-43	21-43; 22-43; 23-43; 24-43; 25-43; 26-43; 27-44; 28-43; 29-44; 30-43	21-43;22-42;23-44;24-40;25-41; 26-41;27-39;28-43;29-40;30-43

also the vehicle capacity imposes another burden on the system. To satisfy these two requirements, nine vehicles are utilized in tours to serve all the medical centers. For this purpose, five storage facilities are chosen as 33, 34, 35, 37, and 38. The corresponding risk objective function has a value of 1116.60 thousand persons, from which 78.11 thousand is the fixed component of risk and 1038.49 thousand stands for the variable element of it. The corresponding tours of each scenario are depicted in Fig. 4.5.

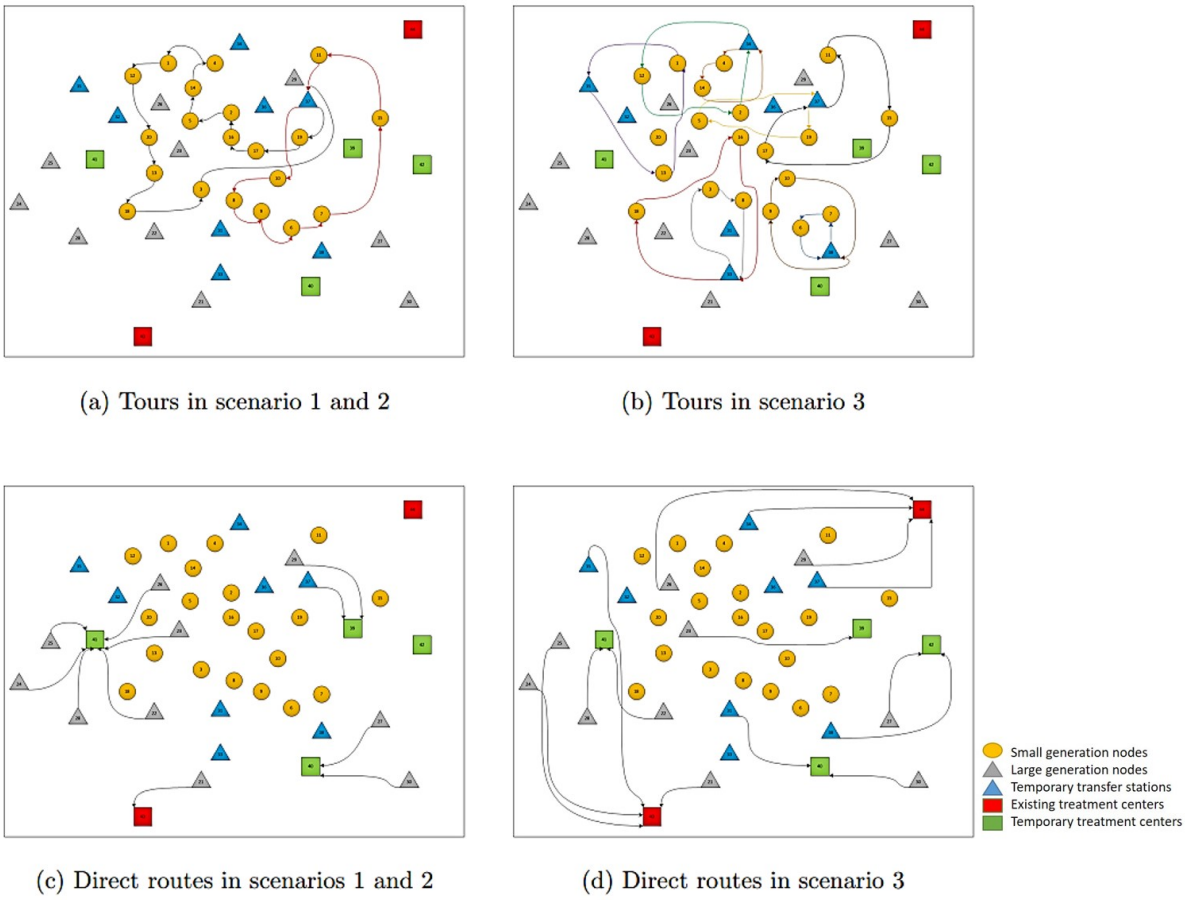

(a) Tours in scenario 1 and 2

(b) Tours in scenario 3

(c) Direct routes in scenarios 1 and 2

(d) Direct routes in scenario 3

Figure 4.5: Recommended plan for the minimum cost extreme point

In the second case, the model seeks a solution with the least possible risk. To cope with this requirement, only station 35 is picked for the first two scenarios. As a result, 35-18-13-20-12-1-4-14-5-2-16-17-3-35 with 3.90 hours of tour time and 35-8-9-10-6-7-19-11-15-35 with a total tour time of 3.88 are adopted for the waste collection in the first level of the network. Shifting the focus from the cost objective to the risk objective has led to longer traveling times, growing around 23.5% in the first two scenarios and a slight increase of approximately 1.42% in the third scenario. Moreover, both cost and risk extreme points experience a significant surge in total required tour times by 145% and 98.23%, respectively, moving from scenarios 1 and 2 to scenario 3. Another notable matter in the solution is the trivial difference between the total risk and total cost extreme points. With only accepting around 0.06% of the extra total cost, the decision-maker will be able to lower the daily risk by almost 9.35%. Focusing only on the transportation risk and cost, a more risk-efficient network will be achieved by providing an extra 2.21% of financial support. The point is that the main portion of the cost belongs to the fixed cost of the system as the high amount of infectious waste in scenario 3 necessitates the facilities to work with their full capacities.

4.5.3 Tradeoff analysis

Based on the two extreme solutions, we apply the augmented ε-constraint method to assess the risk-cost trade-off analysis in the network. Fig. 4.6 depicts the plot of the proposed Pareto frontier, which is comprised of 11 non-dominated solutions, including nine intermediate points plus the two extreme ones. A significant portion of

both cost and risk objectives in all of the cases is related to their fixed elements. For example, in the cost extreme point, the pertinent fixed cost of the network constitutes around 97% of the total cost. Considering the one-day planning focus of the study, these portions are not unreasonable. Overall, a reduction of risk by almost 9.35% requires growth of around 0.06% in the cost objective. Several considerable gaps are observable in these figures. Starting from the minimum cost solution, as the first iteration, the largest gap regarding the cost belongs to the movement from iterations 1 to 2 and 9 to 10. The sharpest risk change occurs while moving from iteration 8 toward 9 with a 1.78% decline in the value.

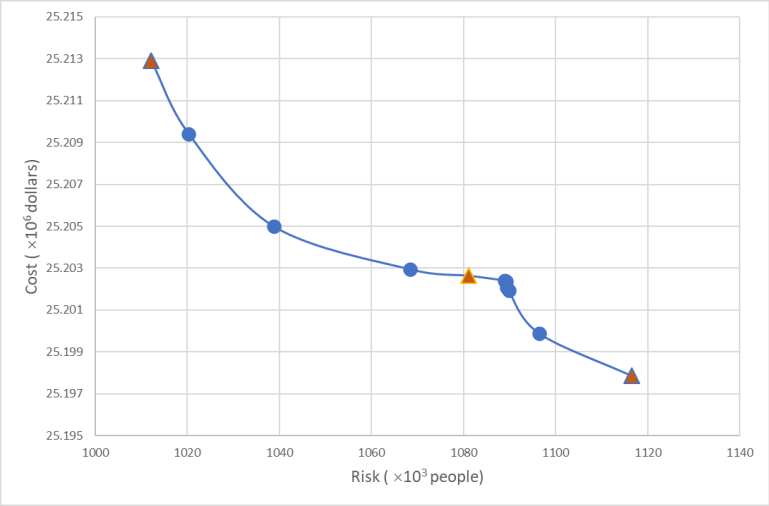

Figure 4.6: Pareto frontier

For more explanations about the existing tradeoffs, we explore the intermediate point in iteration 7 (Table 4.7). The tours in the first and second scenarios of the solution belong to temporary facilities 35 and 38. On the one hand, having tour times of 3.90 and 2.99 respectively for 38-7-15-11-19-10-6-9-8-3-17-16-38 and

35-18-13-20-12-1-4-14-5-2-35, we notice a reduction by 0.02% and an enhancement by 2.5% in the associated cost and risk, respectively, when compared to the minimum cost extreme point. On the other hand, when moving from the intermediate point 7 toward the minimum risk extreme point, a 7% reduction in risk with a 0.04% rise in cost objective is observed.

4.5.4 Sensitivity analysis on the confidence level

In this section, we review the impact of using different confidence levels in the CCP. For this purpose, considering the cost as the primary objective, we have applied seven different values for the confidence level, ranging from 70% to 99.9%. As shown in Fig. 4.7, higher degrees of confidence for adhering to the time windows limitations necessitates higher expenses. However, lower confidence level options provide the system with more flexibility in choosing the more cost-effective tours. Therefore, a confidence level equal to 70% has the most economical objective function value, while the case with 100% confidence level imposes the highest charges for the network. However, the associate risk values do not follow a particular pattern. The confidence level values equal to 80% and 95% are the most and the least risky networks, respectively.

In summary, the total cost rises along with the increase of confidence level. That means more resources are needed to avoid time window violations in tours brought by the random fluctuation of service times in small generation nodes. In other words, a more robust system entails a high confidence level at the cost of increased expenses. Also, it is more difficult to improve system cost when the confidence level is at higher levels, i.e., more than 95%.

Table 4.7: Intermediate Solution

		Scenario 1	**Scenario 2**	**Scenario 3**
Transfer Station		33,34,35,37,38	33,34,35,37,38	33,34,35,37,38
Treatment center	Temporary	39,40,41,42	39,40,41,42	39,40,41,42
	Existing	43,44	43,44	43,44
Number of vehicles		2	2	9
Tour		35-18-13-20-12-1-4-14-5-2-35; 38-7-15-11-19-10-6-9-8-3-17-16-38	35-18-13-20-12-1-4-14-5-2-35; 38-7-15-11-19-10-6-9-8-3-17-16-38	33-3-8-33; 33-18-13-33; 34-14-1-34; 34-2-12-34; 35-4-10-35; 37-11-15-37; 37-19-17-16-20-37; 38-7-6-38;38-9-5-38
Route	Station-Treatment	35-43; 38-40	35-43; 38-40	33-40; 34-44; 35-43; 37-44; 38-42
	Large generation-Treatment	21-43; 22-43; 23-43; 24-41; 25-41; 26-41; 27-40; 28-41; 29-39; 30-40	21-43; 22-43; 23-43; 24-41; 25-41; 26-41; 27-40; 28-41; 29-39; 30-40	21-43; 22-41; 23-39; 24-43; 25-43; 26-44; 27-42; 28-41; 29-44; 30-40

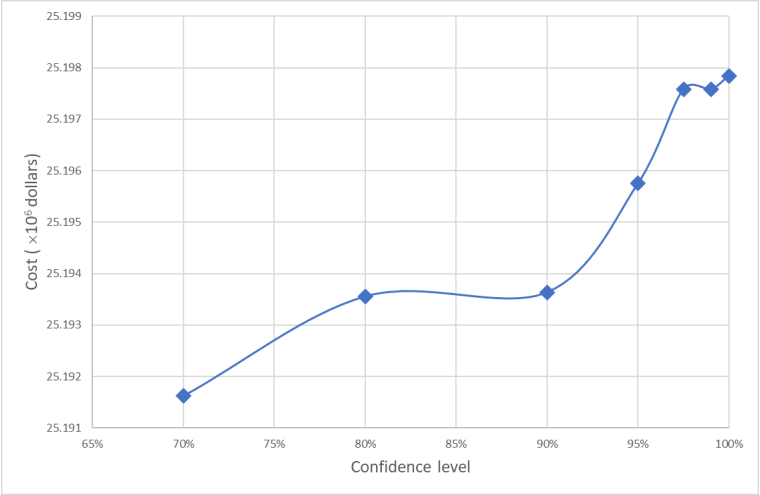

Figure 4.7: Objective function variations with regard to different confidence levels

4.5.5 Sensitivity analysis on tour vehicle capacity

We have considered four different vehicle capacities for the waste collection of the first tier of the network and compared the results in Table 4.8. The vehicle capacity alteration mainly affects the results of the last scenario, as we are still limited with the time windows of the temporary facilities. This issue highlights the importance and impacts of both the time windows and the vehicle capacity. The major effect of considering a higher capacity for the trucks is reducing the number of required trucks for the waste collection, which in turn leads to more savings in transportation costs. Compared to the original case, the number of required vehicles has decreased by one and four respectively by assuming 0.5 and 1.5 tonnes of extra capacity.

4.5.6 Sensitivity analysis on the duration of time window

In this section, we evaluate the impact of manipulating the time windows duration in the network. While minimizing cost is the primary objective for the system. Four

Table 4.8: Sensitivity analysis on tour vehicle capacity

Vehicle Capacity (tonnes)	Number of vehicles[a]	Total Cost ($\times 10^6 dollars$)	μ_{Cost}	Total Risk	μ_{Risk}
1	(2,3,16)	25.4830	0.9630	1123.11	1044.99
1.5	(2,2,9)	25.1978	0.6778	1116.60	1038.49
2	(2,2,8)	25.1030	0.5829	1104.10	1025.98
3	(2,2,5)	25.0343	0.5143	1094.92	1016.81

[a] (Scenario 1, Scenario 2, Scenario 3)

different cases have been considered ranging from 3 to 6, and the results are displayed in Table 4.9. Our previous analyses are performed assuming a four-hour time window condition. Reducing this period by one hour forces the model to utilize three vehicles in scenarios 1 and 2, where scenario 3 remains untouched. In scenario 3, the high amount of generated waste and vehicle capacity limitations make the model insensitive to the time window alteration. Not only in this case but also in all the applied changes, the time window variations do not affect the last scenario, as the maximum required tour time of it according to Table 4.6 equals 2.04. Starting from the lowest employed duration, the cost objective enhances, and a 6-hour duration, which acts like a no time window case, has the best cost objective. However, no specific pattern is observable in the associated total risk value.

4.5.7 Sensitivity analysis on the degree of uncertainty in the service time

The degree of uncertainty in the service time can be evaluated by the standard deviation. Apart from the original value of 60 seconds for the standard deviation in

Table 4.9: Sensitivity analysis of time windows

Time windows duration (hours)	Number of vehicles[a]	Total Cost ($\times 10^6 dollars$)	μ_{Cost}	Total Risk	μ_{Risk}
3	(3,3,9)	25.3158	0.9630	1111.10	1032.99
4	(2,2,9)	25.1978	0.6778	1116.60	1038.49
5	(2,2,9)	25.1830	0.6630	1034.26	956.15
6	(1,1,9)	25.0915	0.5715	1075.12	997.01

[a] (Scenario 1, Scenario 2, Scenario 3)

the CCP approach, we consider three other values of 30, 90, and 120 seconds for this parameter and compare the results. A comparison between the associated cost objective using different values for standard deviation is displayed in Fig. 4.8. As shown in this figure, higher values of this parameter lead to higher required expenses. It means that the system has to assign more resources to compensate for the increases in the service times in tours.

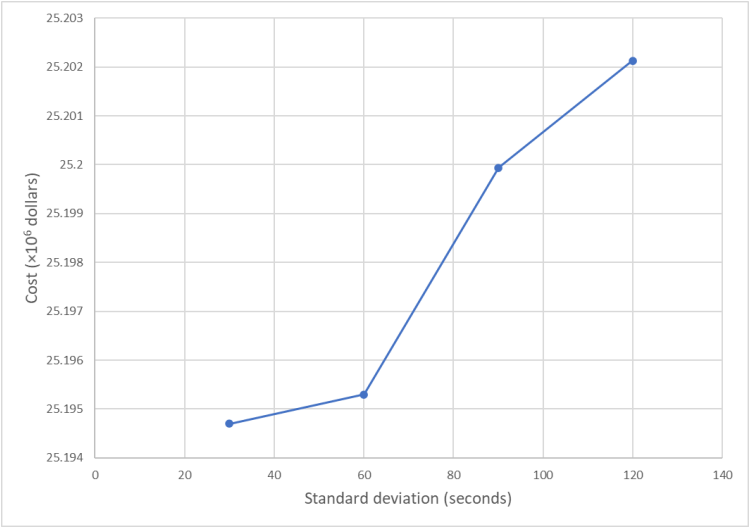

Figure 4.8: Sensitivity analysis on the standard deviation of the service time with a 95% confidence level

4.5.8 A comparison of different systems

Herein, we further study the benefit of considering uncertainties at the system design stage through a comparison of the performances of different systems. To be particular, the stochastic system obtained from our previous analysis is evaluated and compared with two other systems described as follows. All systems are based on the cost minimization solution.

Current system The system is used currently (with no pandemic consideration). That is to say, no temporary facilities exist; the treatment center is determined by the normal waste amount; and only direct routes are used for waste collections.

Deterministic system The system is constructed in view of only the most likely pandemic scenario (i.e., Scenario 2). That being the case, the temporary transfer station at node 35 is chosen as the only transfer station with the associated tours of 35-18-13-2-12-1-4-14-5-2-16-17-3-35 and 35-8-9-10-6-7-19-11-15-35. Also, due to the lower opening and processing cost of the existing treatment centers than the temporary ones, only treatment 43 operates in this model type.

Stochastic system The system is planned by using the 3-scenario model and algorithm proposed in this research.

Five testing scenarios are employed to mimic the real-world situations that may occur. Besides the three pandemic scenarios used in this case study: optimistic ($s1$), most likely ($s2$), and pessimistic ($s3$), two additional scenarios are also considered. A normal scenario (sn) reflects the normal situation without any disease outbreak. The

waste amounts are estimated according to the 2019 Wuhan data of medical waste. An extreme pandemic scenario (se) assumes that the capacity of each generation node is exceeded by randomly 40% to 60%. Table 4.10 lists the comparison based on three major criteria.

Table 4.10: Comparison of other criteria in the models

	Demand fulfillment (%)				
System	sn	$s1$	$s2$	$s3$	se
Current system	100	100	100	26.84	13.42
Deterministic system	100	100	100	26.84	13.42
Stochastic system	100	100	100	100	53.52
	Facility utilization (%)				
System	sn	$s1$	$s2$	$s3$	se
Current system	0.21	0.91	65.35	100	100
Deterministic system	0.21	0.91	65.35	100	100
Stochastic system	0.05	0.23	16.34	93.12	100
	Number of vehicles				
System	sn	$s1$	$s2$	$s3$	se
Current system	20	20	20	2	2
Deterministic system	2	2	2	2	2
Stochastic system	2	2	2	9	16

It is clear that the recommended stochastic system outperforms the other two in all testing scenarios in terms of all criteria. All waste demand can be fully handled for planned scenarios. In an acute situation ($s3$), this system can still maintain certain redundancy (almost 8% still available) which can be useful if the case becomes worse. When the pandemic is extremely severe (se), with fully occupied facilities, the system can process more than 53% of the generated waste, which is nearly four times the amount that other systems can manage. Looking into the current and determinis-

tic systems, both have massive difficulties when facing serious pandemic situations. Almost three quarters of the demand cannot be processed, and the system capacity needs to be increased by at least 3.7 and 7.4 times to satisfy the requirements respectively in $s3$ and se. Further comparing the current and deterministic systems, although the facility utilization and demand fulfillment are the same, the number of vehicles in the latter is much less (more than 72% less on average) and the resulting average transportation cost is lower by approximately 69%. Such a cost advantage can also be observed in the stochastic system. In summary, by taking into account the uncertain pandemic scenarios, our proposed stochastic model can design a waste management system that can timely and properly adjust to various pandemic situations at a rather low cost, while, at the same time, is also capable of efficiently dealing with the situations with no outbreak.

4.6 Managerial insights

The ongoing COVID-19 crisis has been putting enormous pressure on all aspects and levels of society financially and mentally. In this circumstance, enhancing the performance of different organizations and presenting more affordable and less risky approaches is crucial. This section highlights the managerial insights derived from our experiments and discussions to help the carriers and relevant authorities in waste management construct an effective and reliable network.

First, although health centers act as the first defense line against pandemics, the companies and carriers responsible for collecting and treating the related infectious waste from these centers play a significant role in controlling the situation. Inappro-

priate management of infectious waste exposes health and waste workers to irreparable infection consequences. In this regard, developing redundant medical-waste management systems to prevail and control the pandemics should be a priority. Note that it may seem costly to keep the redundancy when building up the network, but there will undoubtedly be benefits during pandemics.

Secondly, embedding temporary facilities during a pandemic facilitates modifying the existing waste network to cope with the unexpected generated medical waste and its associated viral spread effects. Also, the temporary locations help the system to work with its maximum capacity and deal with the peaks and hot spots as quickly as possible. The other aspect of this redundant network is the application of tours instead of only direct routes. The savings resulting from the tour collection approach, through reducing the number of vehicles, also can be significant.

Thirdly, improving the geographical distribution of both transfer stations and treatment centers may contribute to cost reduction and risk mitigation. When the facilities are spread relatively evenly in the network, both en-route and on-site risks can be more equitably distributed. Therefore, the proposed network can facilitate practical strategy development for the authorities in designing flexible and redundant waste management systems with the ability to react appropriately during unanticipated and severe pandemics.

Fourthly, the scenario-based stochastic model presented in this research can be implemented as a helpful tool to derive practical solutions. When the records and statistics regarding the situations are sufficient enough at the moment, the scenarios can be generated based on a detailed investigation of historical situations for accurate estimations. In any other cases when data are unavailable or insufficient, the deci-

sion maker's risk perspective can be examined and quantified. Moreover, providing different non-dominant alternatives using the augmented ε-constraint method creates extra flexibilities in the authorities' decision-making process.

Fifthly, it is shown that using different confidence levels in CCP affects the optimal solution. Higher degrees of confidence necessitate higher expenses. In other words, a more robust system entails a high confidence level at the cost of increased expenses. The government and healthcare managers can define the confidence level based on an integrative consideration of the pandemic status, public concerns, and any other relevant factors. The time window at temporary faculties can also be adjusted accordingly.

Finally, entering the third year of the COVID-19 pandemic, although hospitalizations and other pandemic markers continuously shrink or level off, many experts still have concerns over the potential of other variants. The pressure on the waste management system is not eased but alters to a new state with lessened tension at large healthcare centers yet higher-than-normal demand at small clinics, medical offices, and residential areas. These changes make the use of temporary transfer stations more appealing than ever. As living with COVID becomes a new normal, some of these temporary stations may be upgraded with larger capacities and better compatibility following higher containment standards. Additional clinical necessities include: creating benchmarks or guidelines for safety and infection control in medical waste management, training and protection of front-line workers handling infectious waste, and adjusting collection routes adaptively driven by real-time data, to name a few.

4.7 Conclusion

In this research, we investigate the infectious waste management problem with different waste generation scenarios and time window assumptions. Temporary transfer stations act as storage for the accumulated waste from small generation nodes via tours. Then, existing and temporary treatment centers receive the infectious waste from these stations and large generation nodes. Planning the numbers and locations of temporary facilities assuming possible high-demand conditions caused by a future pandemic is integral for this study. The proposed bi-objective stochastic model addresses the location-routing problem of infectious wastes with demand and service time uncertainties. Another realistic consideration is utilizing tours for the waste collection process instead of direct routes. A vehicle routing problem using a two-commodity formulation is embedded into the scenario-based optimization to handle complicated situations with both uncertainties and time constraints. Then, the model is solved by adopting an ϵ-constrained approach accompanied by a branch-and-price algorithm. To demonstrate our model's practicality and validity, we applied the proposed model to a real-world case study based on the COVID-19 outbreak in Wuhan, China. Numerical experiments are conducted to examine the tradeoff between the two objectives, and to study the sensitivity of the model to several key parameters, such as vehicle capacity, confidence level, and the uncertainty degree of the service time. Managerial insights are derived and explained from which the government and other stakeholders can benefit.

For future research, other realistic considerations in making delivery plans such as the time-dependent issues through varying traffic density and speed over different

times of the day can be included in the model. The time-dependent parameters will result in divergent transportation risks and costs associated with various departure times of the vehicle. Considering a bi-level model incorporating the government or healthcare system and the carrier's benefits will make the proposed model more realistic. For this purpose, policies on planning and controlling the waste management infrastructure and environmental-related concerns in treating infectious waste can be on the upper level, while optimizing the collection process adhering to these policies can be the focus of the lower level. Another research avenue is to introduce proper cuts for the developed branch-and-price algorithm and apply the proposed B&P algorithm in other uncertain environments such as robust optimization techniques. A comparison of the result with our present work would provide additional interesting and informative insights for the authorities.

Chapter 5

A multi-stage decision framework for managing hazardous waste logistics with random release dates

Abstract This research develops a multi-stage decision framework for a three-echelon collection network for hazardous waste considering random release dates. Applying a cost-based clustering approach, the first stage decisions involve locating the transfer stations and allocating generation nodes to the chosen facilities. The corresponding results, along with a subjective risk-aversion notion and estimated release dates, are utilized to generate an a priori collection plan, which can be further revised once the actual release dates are realized. We performed sensitivity analysis on important model elements, including the subjective risk-aversion parameter and vehicle capacity for collection tours. Our findings indicate that depending on the subjective perspective of the collector, deviations from the original scheduled plan can happen to be a positive or negative phenomenon. For an optimistic decision-maker, adaption to the realized deviations necessitates accepting additional total risk. On the other hand, a pessimistic decision-maker is more likely to benefit from deviations. The findings can facilitate relevant authorities with practical and realistic strategic and operational decisions.

Keyword Multi-stage Decision-making, Hazardous Waste, Location-Routing-Inventory Problem, Random Release Date, Risk-aversion

5.1 Introduction

Hazardous waste management consists of handling wastes that are harmful to human health and the environment (Zhao and Ke, 2019). Hazardous waste (HW) includes waste that has been contaminated by chemicals, bacteria, viruses, and other harmful agents and can have serious adverse effects on human health if it is not dealt with properly and safely. Handling HW involves procedures and policies regarding the collection, storage, transportation, and treatment of waste safely and economically (Samanlioglu, 2013). Each of these processes is entwined with complex decisions that can impose an immediate or long-term risk to the surrounding environment and population (Zhao et al., 2016). As a result, improper storing or processing of HW is deemed as a menace to the exposed population near locations where associated activities take place.

In 2009, the US healthcare sector accounted for 17.9% of GDP, with an annual production of 5.9 million tonnes of waste and 8% of total carbon dioxide emissions in the US (Voudrias, 2018). As mentioned by Eurostat (2018), of the total waste generated in 2016 in the European Union, 4% of the total generated waste (100.7 million tonnes) belonged to the hazardous type. This significant amount of waste originated from different sources such as industrial and manufacturing processes, hospitals, and e-wastes. The statistics regarding the situation in developing countries are worrying. For example, the WHO mentioned environmental risk factors to account for one-third

of the burden of disease, where hazardous waste was stated to be among the first three main factors (McCormack and Schüz, 2012).

Hazardous wastes can take the form of solids, liquids, sludge, or contained gases, and they are generated primarily by chemical production, medical centers, manufacturing, and other industrial activities. Among these, medical waste is becoming a growing concern as it generates high levels of hazardous and infectious materials. Hazardous medical waste (HMW) comprises biohazardous waste from blood samples, fluids, and tissues. Also, it involves all the sharp items and personal protective equipment such as masks and gloves utilized in the hospitals. Especially after the recent pandemic, the necessity of establishing an effective medical waste management system was highlighted more than ever. The pandemic unveiled the existing weakness of the available waste handling network and attracted the attention of researchers from different fields to enhance the current system structure and associated processes. Apart from COVID-19, there are many sources of severe illnesses in the medical waste that can result in the spread of infectious diseases with their relevant exponential rises of medical waste amounts such as HIV, hepatitis, and typhoid (Eren and Tuzkaya, 2021). To better understand the significant impact of the outbreak, a comparison between the amount of generated waste before and after the pandemic is helpful. For example, in Wuhan, China, an average of 45 tonnes of medical waste was generated each day before December 19, when the first known case of COVID-19 was identified (Yu et al., 2020c). However, in a couple of months, the amount of generated medical waste rose by almost 150% and surged to nearly 247 tonnes/day by March 15, during peaks (Singh et al., 2020). This was not the end, as the growth in infected cases and social sensitivity toward this issue led to substantial boosts in personal

protective equipment (PPE) demand, such as masks and gloves. Based on a report by (Ma et al., 2020), the national medical waste disposal level in China increased by almost 420% from January 20, 2020, to March 21, 2020. As a result, the necessity of developing robust and redundant waste management systems for HMW is a pressing matter.

There are guidelines developed in consultation with experts in the field to enable the authorities to handle the waste safely and effectively. For example, the European Commission issued special guidelines regarding waste management during the coronavirus crisis. These guidelines mainly address three issues, including preventing distortions in the waste management system, ensuring the health and safety of citizens, and maintaining a high standard of environmental security (European Commission, 2020). It should be mentioned that such a pandemic setting is not limited to COVID-19, and governments have always been dealing with different types of infectious diseases. Some recent examples during the latest two decades are the severe acute respiratory syndrome (SARS) in 2003, the Marburg hemorrhagic fever in 2007, and the Ebola virus in 2014 (Yu et al., 2020c). Therefore, the findings of this research are applicable to any similar situation.

Like many other real-life activities, there are many uncertainties associated with the waste collection process. These uncertainties can significantly impact the quality of service provided by municipalities and collector companies. In fact, medical waste collection and disposal have been viewed as a vital stage in managing the source of infection as well as strict establishment and standardization of the waste management (Peng et al., 2020; Tirkolaee et al., 2021). Apart from general sources of uncertainties such as weather conditions and disruptions in transportation networks,

decision-makers confront other uncertainties like uncertain demand/waste availability, travel time, and service time (Tasouji Hassanpour et al., 2021). Inspired by the studies in distribution planning problems, where the delivery of a product is dependent on the availability of sufficient product with known and determinist rate (Coelho et al., 2014; Díaz-Madroñero et al., 2015), we consider the waste availability concept. Considering stochastic waste generation speed in medical centers, a signal is sent to the collector company indicating the availability of the hazardous waste to be picked up. However, there is an important factor the collector company should consider as the maximum permissible time that the hazardous waste can be stored while waiting for collection. For example, the Ministry of Ecology and Environment of the People's Republic of China published the "Management and Technical Guidelines for Emergency Disposal of Medical Waste in the Pneumonia Pandemic of COVID-19," limiting the temporary storage time of COVID-related waste to 24 hours. In separate work, a similar period was also suggested by Peng et al. (2020). Another criterion that should not be ignored is that the collection process for the hazardous waste should be handled in limited hours of a day, as the regular daily waste should be managed as well.

Medical waste logistics focuses mainly on collecting, transporting, storing, and disposing of medical wastes. The task should be performed by reducing the associated cost and risk of the network without jeopardizing humans and the environment. The work involved in safely storing the relevant waste can be very time-consuming and expensive. In order to minimize the hazardous material's exposure to the staff, patients, and even the animals which may come into contact with the contaminated material, suitable safeguards must be taken at every stage of its management, from

the generation to disposal.

In summary, the contribution of this paper is fourfold. *First*, for the first time, we develop a multi-stage location-routing-inventory model for hazardous waste management, considering uncertainties through waste generation speed and release time as well as deviations from the original plan. More specifically, the application of temporary waste storage facilities is proposed to establish a well-organized and efficient method to handle the corresponding hazardous waste separately and safely. The cost considerations are involved in the designed network through a cost-clustering algorithm that tackles the locations of temporary storage centers and allocation of medical centers to the selected facilities. The risk mitigation and inventory considerations are handled in the second stage to prepare the a priori plan. Finally, deviations in the pre-specified plan are addressed using recourse actions in the last stage of the solution procedure. The deviations are described by three scenarios, reflecting different severity levels as minor, normal, and major deviations from the a priori plan. *Second*, we apply a subjective risk-aversion parameter to incorporate the decision-maker mentality in the model and convert the stochastic model into a deterministic one. *Third*, we incorporate waste inventory management with location-allocation-routing decisions to derive more realistic solutions. Moreover, we take advantage of collection tours instead of direct routes between generation nodes and treatment centers. *Fourth*, a case study of Kunming in China during the coronavirus outbreak is explored, from which we provide practical indications and managerial insights for authorities when dealing with real-world hazardous waste management, especially under unexpected circumstances like a pandemic.

The rest of this paper is structured as follows. Section 5.2 reviews related literature

on the management of medical waste. The details about the network and model formulation are presented in section 5.3. Then, the proposed model is applied to a case study in section 5.4 to be validated and assessed. Practical managerial insights are derived from numerical experiments and explained in section 5.5. Finally, section 5.6 concludes this work and suggests future research directions.

5.2 Related Work

The most related works to this research mainly address two areas in hazardous waste management: (1) uncertainty issues, and (2) vehicle routing problem (VRP) with release dates. When talking about uncertainty applications, we explore investigations with uncertain parameters, not methods like fuzzy MCDM which do not apply the uncertainty in the inputs of the mathematical model. Also, as a new concept in the literature in the VRPs with a release date, a release date is associated with each customer, which can be defined as a lower bound on the time a vehicle can start its route to visit that customer (Mor and Speranza, 2022). In this section, we will review the available literature on both the pathways mentioned above. A summary of the relevant studies is provded in Table 5.1.

5.2.1 Hazardous waste management with uncertainty

Reflecting the real-life circumstances into mathematical models usually involves many uncertainties regarding the input information. As a result, including uncertainties, especially in sensitive and health-threatening operations like hazardous waste management, is vital. However, most of the proposed networks for hazardous waste man-

Table 5.1: A comparison of relevant literature

Reference	**Decision**			**Uncertainty**	**Uncertain Parameter**	**Risk Aversion**	**Multi-period**
	L	R	I				
Berglund and Kwon (2014)	✓	✓		Robust	Demand, Risk		
Ardjmand et al. (2016)	✓	✓		Stochastic	TC		
Rabbani et al. (2019a)	✓	✓	✓	Stochastic	GW, EP		✓
Delfani et al. (2020)	✓	✓		Stochastic, Fuzzy	TC, Risk, MC, MW		
Homayouni and Pishvaee (2020)	✓			Robust	GW		
Saeidi-Mobarakeh et al. (2020)	✓	✓		Robust	GWR		
Tirkolaee et al. (2020)	✓	✓		Fuzzy, CCP	Demand		✓
Yu et al. (2020b)	✓	✓		Stochastic	Cost, Demand, EP		
Negarandeh and Tajdin (2021)	✓	✓		Robust fuzzy	GW, TC		
Zhao et al. (2021)	✓	✓	✓	Robust	GW		
Raeisi and Jafarzadeh Ghoushchi (2022)	✓	✓		Robust fuzzy	GW, TC		
This study	✓	✓	✓	Stochastic	Release Date, Deviations	✓	✓

L: Facility Location, R: Routing Plan, I: Inventory Considerations, TC: Transportation Cost, GW: Amount of Generated Waste, GWR: Generated Waste Rate, EP: Exposed Population, MC: Maximum Capacity, MW: Minimum Required Waste to Open a Facility

agement were formulated under a deterministic setting. To the best of our knowledge, only a few studies apply uncertain settings in their mathematical models in this scope.

Stochastic In Ardjmand et al. (2016) the transportation cost was regarded as a source of uncertainty in developing a stochastic model for the locating-allocation-routing problem of hazardous waste. They also embedded the environmental risk and profitability in their model and applied a genetic algorithm to derive desirable solutions. Rabbani et al. (2019a) formulated a multi-period multi-objective location-routing-inventory problem (LRI) of hazardous waste management. The uncertainty in their stochastic model originated from the amount of generated waste and the exposed population. They suggested a simheuristic approach by combining a Monte Carlo and NSGA-II simulation. Yu et al. (2020b) employed two-stage stochastic programming to formulate the hazardous waste location-routing problem. Assuming the cost, demand, and affected population as stochastic parameters, they considered a bi-objective MILP model with minimizing total cost and population exposure of the network. A sample average approximation-based goal programming approach was utilized to solve the mathematical model.

Robust A bi-level robust model was developed by Berglund and Kwon (2014) for the location-routing problem of handling hazardous waste. The facility location decisions were determined at the upper level while leaving the routing decisions to be made at the lower level by third-party logistics providers. The randomness in their model originated from demand and risk uncertainty. The authors converted the bi-level model into a single-level problem by replacing the inner maximization

problem with its dual. Finally, a genetic algorithm was proposed for large-scale instances. A scenario-based LRP was developed by Saeidi-Mobarakeh et al. (2020) to address hazardous waste management through a bi-level optimization model. Their upper level consisted of the strategic reverse network design problem, while waste collection decisions were determined in the lower level. A robust optimization approach was developed to incorporate the uncertain waste generation rates in the model, which was solved using a multi-part solution methodology. Delfani et al. (2020) studied the multi-objective hazardous waste LRP minimizing total costs as well as both risks of transportation and population. They developed a basic possibilistic chance-constrained programming and a robust possibilistic programming model of the proposed problem for handling the uncertainties. Homayouni and Pishvaee (2020) applied a robust optimization method to introduce a bi-objective hospital waste collection and disposal network design problem with an uncertain amount of generated waste. The implemented augmented ε-constraint method to solve the proposed model and obtain efficient Pareto solutions. Negarandeh and Tajdin (2021) designed a sustainable hospital waste management network incorporating resiliency and profitability concepts into the model. The proposed model dealt with uncertainty using a robust fuzzy programming approach with an uncertain amount of waste generated and transportation costs. Two solution methods were implemented: the improved goal programming technique and the Lp-metric method. In a more recent study, Raeisi and Jafarzadeh Ghoushchi (2022) explored the multi-objective LRP for hazardous wastes with uncertain transportation costs and waste generation amounts. For handling the uncertainty, a robust fuzzy optimization approach was employed. Also, two types of wastes, including industrial and hospital wastes, were involved in

developing the proposed mathematical model. Finally, the model was solved using several metaheuristic methods.

Pandemic setting An investigation of the infectious waste management during the COVID-19 pandemic was presented in Tirkolaee et al. (2020). The authors studied the fuzzy multi-trip LRP for medical waste management. The fuzzy chance-constrained programming technique was applied to address the uncertain demands. In this research, the model was solved using the weighted goal programming method. Another article concentrating on COVID-related infectious waste management was Zhao et al. (2021). In this study, a scenario-based bi-objective robust approach was developed with random waste generation and temporary facility applications during a pandemic. Three different solution methods were adapted and compared, including the ε-constraint solution technique, goal programming method, and a lexicographic weighted Tchebycheff approach.

5.2.2 Vehicle routing problem with release dates

The classical vehicle routing problem assumes that the shipments to be delivered to customers or collected from them are ready to be handled at the beginning of the planning period. However, due to the available uncertainties in real-life conditions, this is not always true, and there are deviations available in the specified time that products are ready to be picked up or delivered. To cover this context, recently, the VRP with release dates (VRPRD) has been introduced in the relevant literature. To the best of our knowledge, Cattaruzza et al. (2016) made the first attempt to incorporate the release dates of customers in the decisions. They explored the multi-

Trip VRP with customer time windows and merchandise release dates. They defined the release date as the moment that the merchandise becomes available at the depot for final delivery. Their model was solved using a hybrid genetic algorithm applying a route decomposition technique for chromosome decoding and a local search.

Following the work of Cattaruzza et al. (2016), several works have included release dates in their studies. Reyes et al. (2018) explore the complexity of the single depot dispatching problems with release dates. In their paper, each order has a release date indicating when the order can be shipped and a service guarantee acting as a deadline. Their findings show that single and multiple vehicle variants with customers located on a half-line can be solved to optimality in polynomial time. A formulation for the Traveling Salesman Problem (TSP) with release date and completion time minimization was proposed in Archetti et al. (2018). The authors introduced some properties and proposed an iteration-based local search approach with two variants. Pina-Pardo et al. (2021) investigated the TSP with release dates and drone resupply. Considering that each order's release date was known during delivery planning, their focus was on defining a minimum time route for a single truck that can receive newly available orders en-route using drones. For this purpose, they developed a Mixed-Integer Linear Program (MILP) and a decomposition-based solution approach.

Shelbourne et al. (2017) assumed release and due dates for each customer and incorporated machine scheduling into VRP. Their work includes a convex combination of operational costs and customer service level, which is solved using a path-relinking algorithm with neighborhood search. Soman and Patil (2020) studied a heterogeneous VRP with release and due dates. Their model encompassed several properties such as order consolidation, finite warehousing capacities, and lateness-dependent

tardiness costs. They proposed a scatter search technique with strategic oscillation capable of solving large-size instances. Focusing on the container drayage problem, Bruglieri et al. (2021) formulated a multi-trip multiperiod with release and due dates model. Each truck was likely to perform more than one trip in their model, respecting customers' associated release and due dates. They proposed both an Arc-based ILP formulation and a Trip-based ILP formulation and designed six Combinatorial Benders' Cuts to solve this problem efficiently. Assuming stochastic release dates and dynamic customer order arrivals, Darvish et al. (2020) explored the multi-period VRP. The deliveries in their model could happen between release and due dates, where the customer specified the due date of order with penalties for deviations from delivery dates. An exact solution for solving VRP with release and due dates was proposed by Yang et al. (2021), where each vehicle leaves the depot after the release dates of the customers. The authors developed an exact branch-price-and-cut algorithm based on the self-partitioning formulation. Their objective comprised of minimizing the total routing and weighted tardiness costs of a vehicle routing problem.

Applications of release dates in the e-commerce industry were investigated by Liu et al. (2017). They assumed that order availability time is specified by the precedent order picking and packing stage in the warehouse of the online grocer and modeled it using a capacitated vehicle routing problem. Also, a granular tabu search, as well as a Lagrangian relaxation algorithm, were developed to obtain solutions. Inspired by the last-mile delivery concept in e-commerce, Li et al. (2020) studied a multi-trip VRP with order release time. Their model requires the starting time of any trip to be not earlier than the release time of every onboard order in the trip. The relatively short delivery distance in this type of problem necessitates multiple trips of vehicles.

A combination of an adaptive large neighborhood search algorithm with a labeling method was presented as a solution procedure.

Time considerations through customer time windows and package release dates were involved in Zhen et al. (2020) in a multi-depot multi-trip VRP. The proposed MILP model was solved using a hybrid particle swarm optimization algorithm and a hybrid genetic algorithm. Sun et al. (2021) focused on providing a vehicle routing problem with flexible time windows and order release for the fresh food industry. Introducing several valid inequalities, they solved the model using a branch-and-cut algorithm. Simultaneous consideration of product and service delivery, time windows, and the explicit reflection of order release dates were embedded in the VRP model introduced by Li et al. (2021a). They assumed that any vehicle could not start earlier than the largest order release date associated with orders assigned to it. Moreover, an adaptive large neighborhood search algorithm with three new customized removal operators was suggested as the solution procedure.

5.2.3 Research gaps

Despite the efforts mentioned above, the hazardous waste literature with uncertain data is still in its infancy. Except for Rabbani et al. (2019a) and Zhao et al. (2021), no publications focused on embedding inventory considerations in the model and jointly exploring the location, routing, and inventory decisions of HMW. Multi-period planning is an essential tool in managing hazardous medical waste programs. It is used to identify and anticipate future needs and determine appropriate courses of action to meet those needs. Taking into account the potential consequences of various

actions over time allows for more accurate decision-making and better stewardship of resources to appropriately manage and dispose of medical waste. In this regard, only two articles involved multi-period programs in their research (Rabbani et al., 2019a; Tirkolaee et al., 2020).

Decision-makers have a unique perspective on their decisions, as they see them through the lens of their own experience, mentality, and knowledge. However, this perspective is often not incorporated into models and solutions in the literature. This can lead to suboptimal decision-making because the mathematical model fails to reflect the unique viewpoint of individual stakeholders. Risk-averse decision-makers tend to be more conservative and often avoid taking risks, while risk-taking decision-makers are more inclined to take on risks. Such assumption in the relevant studies of medical waste has not been employed so far, and we try to fill this gap by applying the subjective risk-aversion parameter. Finally, this is the first study to explore a multi-stage decision framework with a priori plans, recourse actions, and uncertain release dates. Other random parameters such as the amount of generated waste or transportation cost have been investigated frequently, and no research has handled stochastic release dates.

5.3 Model

In this model, we deal with a multi-period 3-tier hazardous waste collection network, as illustrated in Figure 5.1. The first tier includes generation nodes or clients spread over the network. The second tier consists of temporary storage or repository where each truck starts its collection route and returns to the same facility after visiting

at least one client. Finally, there are integrated treatment and disposal centers as the final destination for the accumulated waste at the storage facilities. The routing process starts by picking up the generated waste from clients and delivering it to the candidate transfer stations. Then, the accumulated waste is transferred from repositories to treatment centers via direct routes.

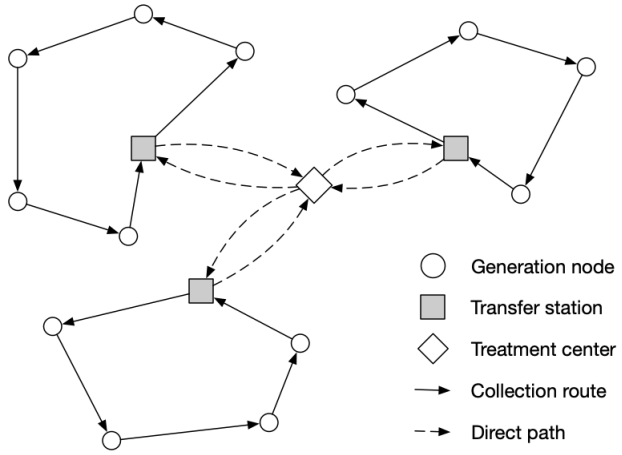

Figure 5.1: Network for the hazardous waste management

This research develops a multi-stage decision framework for managing hazardous waste logistics with random release dates. The waste generation speed is subject to uncertainty leading to stochastic release dates of waste. As a result, the pickup signals arrive dynamically over the planning horizon from generation nodes. Applying a cost-based clustering approach, the first stage of the decision framework involves locating the transfer stations and allocating generation nodes to the chosen facilities. Then, the information obtained from the first stage, along with a subjective risk aversion notion and estimated release dates, are utilized to generate *a priori* plans in the second stage. Finally, adaptive *recourse actions* are taken in the third stage to revise

the decisions for the remaining periods once the actual release dates are realized. The first decision-making stage is built upon cost and capacity considerations. Risk reductions are imposed on the model through the second stage, and the third stage focuses on deviation management.

In summary, the decisions that need to be made for this waste system include location decisions focused on temporary transfer stations, routing decisions for the collection tours from client nodes to transfer stations, inventory management for the waste along the planning horizon, and adapting the model when deviations occur.

5.3.1 Assumptions and notation

In this model, we assume that the collector is responsible for picking up the waste loads over a finite planning horizon of T days. The speed of waste generated at each client is assumed to have an uncertain nature. Therefore, the loads are expected to become ready for pickup at generation nodes on a given date. Inspired by the work of Darvish et al. (2020), we name these dates as release dates. We consider a discrete probability distribution for the availability of loads. The clients request waste collection on different days of the planning horizon. Waste pickup for each client must be handled within a time interval, starting with the order date (signal date) and ending at the due date. On the signal day, a signal is sent from the generation node to the collector regarding the availability of the load. As we are dealing with hazardous waste, the due date for managing the load cannot exceed a specific limit. This limit is known in advance, making the due date depending on the signal date. It should be highlighted that stocking the shipments in the transfer

stations or generation nodes imposes an additional risk to the system. Moreover, all the waste generated during the planning horizon must be transferred to the available treatment center at the end of the planning horizon. Considering that each transfer station has only one vehicle to handle the waste in each period, the overtime option will be applied only in the last period of the planning horizon, if required, to ensure that waste management is performed entirely. However, the associated cost for the overtime is assumed large enough to enforce the model to avoid it unless necessary.

Based on estimations of signal dates, the decision-maker develops an initial schedule, a priori plan, at the beginning of the planning horizon. A recourse action is taken when the realized information does not match the estimated values. Such incompatibility might stem from two matters. First, the realized time of waste availability is sooner than the anticipated period. In this case, the a priori plan is disrupted because of the existing new node in the current period, which must be handled within a permissible time interval. The collector should adapt to the realized situation and might be willing to alter the collection schedule by accepting a bumping penalty. The second case happens when the collector does not receive any signals on the expected date leading to postponing waste-handling of the associated client. This issue bumps some generation nodes from their initial schedule route by bearing bumping penalties. Moreover, having some loads unavailable on their estimated availability date leaves extra vehicle space for the collector. Due to the uncertainties, more pickup signals might be received in the same period. These data mismatches require rescheduling the a priori plans by accepting bumping penalties.

As our model is built upon an existing system, we assume that all the vehicles have already been purchased. Therefore, vehicle acquisition is not discussed in the model.

It is also assumed that all facilities and vehicles satisfy the mandated security and safety measures for handling hazardous waste. Table lists the notation used in this work, based on which a detailed discussion of the mathematical model is presented next.

5.3.2 Decision Framework

The decision framework for this research is built upon three main stages, including location and allocation, a priori routing plan, and recourse routing decision, as illustrated in Figure 5.2. Each stage is described comprehensively in continue.

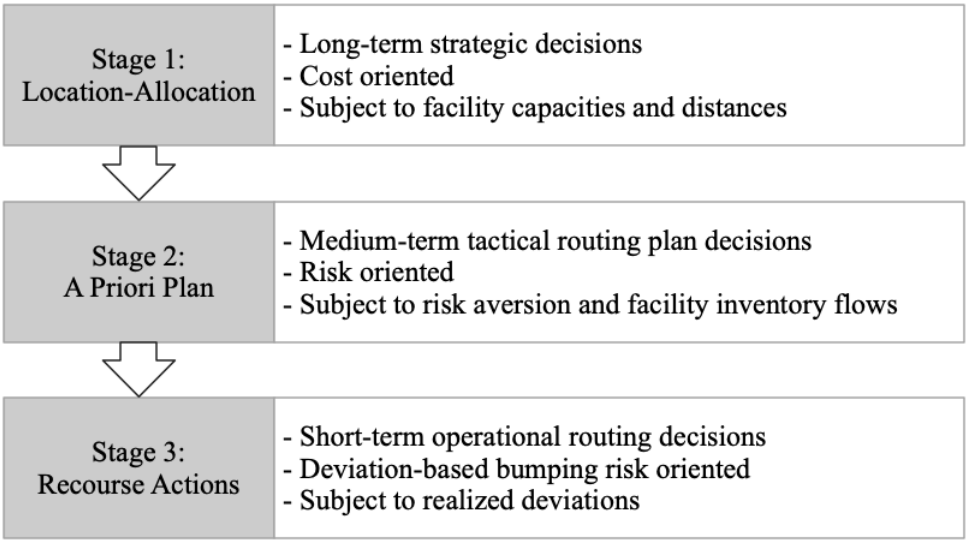

Figure 5.2: Multi-stage decision framework for the proposed collection network

5.3.2.1 Stage 1: Location and allocation

The first stage of this framework determines the locations of transfer stations and the assignment of available generation nodes to the established facilities. For this

Table 5.2: Notation

Sets	
$\mathcal{N}$	Set of nodes, indexed by i and j. $\mathcal{N} = \mathcal{G} \cup \mathcal{C} \cup \mathcal{T}$
$\mathcal{E}$	Set of edges, indexed by (i, j)
$\mathcal{G}$	Set of generation nodes, indexed by g
$\mathcal{S}$	Set of transfer stations, indexed by s
$\mathcal{C}$	Set of treatment centers, indexed by c
$\mathcal{T}$	Set of periods, indexed by t, $t = 1, 2, ..., T$
Parameters	
W_g^t	Amount of waste generated at node $g \in \mathcal{G}$ in period t
CS_s	Capacity of temporary transfer station s
CV	Vehicle capacity for collection tours
C'	Bumping penalty
R_{ij}	Risk of traveling from node i to j
R_s	Risk around treatment center s
L_g^t	Maximum permissible lateness for generation node g in period t
ρ_g^t	Probability of waste being available at generation node g in period t
P_g^t	Cumulative probability of waste being available at generation node g in period t
λ_g^t	Subjective estimate of the collector on the availability of the waste at node g in period t
θ	Risk aversion level of the collector
δ_g^s	1 if the waste at generation node g is ready to pickup in period t; 0 otherwise
M	A large number
Decision variables	
$x_{ij\bar{s}}^t$	1 if node j is visited just after node i in a tour ending at $\bar{s}$ in period t; 0 otherwise
y_{gs}^t	1 if the generation node g, allocated to transfer station s, is visited on the day t; 0 otherwise
$p_{gs}^{tt'}$	1 if the waste available to be collected on the day t is handled on day t', where $t' \geq t$; 0 otherwise
α_g^t	1 if bumping happens in period t for the planned pickup of waste at node g; 0 otherwise
γ_g^t	1 a pickup is planned for node g in period t; 0 otherwise

Table 5.2 (continue) : Notation

η_{sc}^t	Amount of hazardous waste transported to treatment centers c from transfer station s in period t
ζ_s^t	Amount of hazardous waste collected at transfer station s in period t
b_s^t	Beginning inventory at transfer station s in period t
e_s^t	Ending inventory at transfer station s in period t
u_g^t	A positive variable used for subtour elimination

purpose, a cost-based clustering approach is utilized by involving the fixed opening cost of candidate transfer stations, the fixed cost of activating available treatment centers, and transportation cost for both direct path and collection routes. Assuming a single period, the model is solved by considering the worst-case scenario for the generated waste at each node, which is the highest possible demand over T periods. The steps for handling the location and allocation are as follows:

1. *Initialization:* Let $\mathcal{A}_s$ and $\hat{\mathcal{A}}_s$ be the set of generation nodes assigned to transfer station s and the nodes in the waiting list of this station, respectively. Similarly, $\mathcal{B}$ represents the set of transfer stations that are located and allocated, while $\hat{\mathcal{B}}$ is the set of transfer stations in the waiting list. In this step, it is assumed that all these sets are empty, meaning that $\mathcal{A}_s = \emptyset$, $\hat{\mathcal{A}}_s = \emptyset$, $\mathcal{B} = \emptyset$, and $\hat{\mathcal{B}} = \emptyset$.

2. *Cost-based clustering:* In this step, determining the locations of transfer stations, allocating generation nodes to the chosen stations, and matching the opened transfer stations to treatment centers is conducted. All the located stations are added to $\hat{B}$, and all generation nodes are moved to corresponding $\mathcal{A}_s$.

3. *Break allocation:* The process starts with finding the station with the lowest opening cost. Then, the capacity constraint is checked to ensure the station's capacity is not violated. For example, assuming $s1$ as the station with the least establishing cost, the following steps are checked:

   - If the total waste amount exceed the station's capacity, the farthest generation node is identified, removed from the associated list $\mathcal{A}_{s1}$, and be added to $\hat{\mathcal{A}}$. This process is repeated until the capacity constraint is satisfied. Being satisfied, $s1$ is moved to $\mathcal{B}$.
   - If the transfer station's capacity constraint is not violated but any additional pickup results in breaking the constraint, $s1$ is added to $\mathcal{B}$.
   - $s1$ is kept in $\hat{\mathcal{B}}$ if the station has extra capacity.

4. *Termination:* The process is stopped if $\hat{\mathcal{A}} = \emptyset$. If $\hat{\mathcal{A}} \neq \emptyset$, reassignment will be performed.

5. *Reassignment:* For each node in $i \in \hat{\mathcal{A}}$ the nearest station in $\hat{\mathcal{B}}$ is identified and added to the associated set. For example, considering $s2$ as the nearest station for i, it will be moved to $\mathcal{A}_{s2}$. If no more node can be assigned to $s2$ without violating its capacity, $s2$ is added to $\mathcal{B}$. If there are no transfer stations in the waiting list, $\hat{\mathcal{B}} = \emptyset$, the process is continued starting from cost-based clustering with nodes in $\hat{\mathcal{A}}$ and candidate station locations in $\mathcal{S} \setminus \hat{\mathcal{B}}$.

5.3.2.2 Stage 2: A priori routing plan

In this stage, a deterministic plan is developed based on the obtained $\mathcal{B}$ and $\mathcal{A}_s$ ($s \in \mathcal{B}$) from the location-allocation phase. Consider an undirected graph $\mathcal{G} = (\mathcal{N}, \mathcal{E})$

with $\mathcal{N}$ nodes and $\mathcal{E}$ edges. There are four types of nodes in the network, namely generation nodes ($\mathcal{G}$), candidate transfer stations ($\mathcal{S}$), copies of transfer stations ($\bar{\mathcal{S}}$), and treatment centers ($\mathcal{C}$). Moreover, the edge set is $\mathcal{E} = \{(i,j) : i,j \in \mathcal{N}, i \neq j\}$ with an associated risk and cost. The risk consideration is through the exposed population along the edges, meaning that the more populated an area is, the more risk would be involved in the process. Both the vehicles and transfer facilities have capacity limitations. A finite planning horizon of $\mathcal{T} = \{1, ..., T\}$ is defined for the model. It is noteworthy to mention that an infinite horizon can be assigned a rolling-horizon mechanism where the problem is solved each day iteratively for $\{t, t+1, ..., t+T-1\}$.

In this stage, it is assumed that the amount of the generated waste on the day t for each node (W_g^t) is known and deterministic. A maximum permissible lateness (L_g^t) limits the collection process by imposing a collection due date for the system. Here, same-day pickup is represented by maximum permissible lateness equal to zero. It is assumed that the speed of waste generation is stochastic leading to uncertainty in the release date for collection at each node. However, once the waste is released on the day t, it remains available until the end of the planning horizon. Moreover, the probability of waste being available on the day t (ρ_g^t) is known before its scheduled collection on the day t. Therefore, the associated cumulative availability probability of waste at each node on different days (P_g^t) is known beforehand. As a result, if the amount of generated waste on the day t at node g is positive ($W_g^t > 0$), the cumulative probability of the waste being available in its due date must equal to one ($P_g^{t'} = 1$, where $t' = t + L_g^t$). Also, the signal is only sent to the transfer station for collection when the amount reaches a pre-determined threshold. Consequently, if the waste is available for collection at period t ($W_g^t > 0$), the collection action can occur

any period on and after that period.

We adopt the subjective estimate of the collector on the availability of the waste on the day t at node g, denoted by λ_g^t, from Darvish et al. (2020). This binary parameter is utilized to incorporate the risk aversion level of the collector ($\theta \in [0, 1]$) and the cumulative waste availability probabilities as follows:

$$\lambda_g^t = \begin{cases} 1, & \text{if } P_g^t \geq \theta \\ 0, & \text{otherwise} \end{cases} \tag{5.1}$$

A risk-averse decision-maker (pessimistic point of view) proceeds by assuming that the generated waste will only be available on the last possible day. Higher values of θ indicate this personality type where $\theta = 1$ is the most risk-averse level. On the other hand, an optimistic decision-maker builds the model considering the earliest possible availability of waste. Lower values of θ represent a risk-taking decision-maker with $\theta = 0$ standing for the most optimistic collector. Apart from these extreme values, intermediate values can be applied to define more precise risk aversion levels of the collector. The challenge in developing the routing plans is that the collector should be notified of the availability of the waste through a signal from the generation nodes, where the exact time of this signal is uncertain. The λ_g^t contributes to developing a deterministic-equivalent form for the stochastic model.

After determining the locations of transfer stations and allocating the generation nodes to the chosen facilities, the decision-maker establishes an a priori plan by applying the estimated release dates. However, the a priori plan might require modifications when the actual release dates are realized. In this case, a recourse action is activated to revise the pre-specified schedules. When applying a recourse plan, a

bumping penalty (C') is imposed on the model if collection rescheduling occurs for a node.

The cost reduction considerations were embedded in the model during the location-allocation stage. In this stage, the focus is on mitigating the total risk of the network. The risk can be originated from the following sources:

- inventory risk at the transfer station, which is calculated based on the amount of waste
- transportation risk representing the risk of conveying the hazardous waste on the edges
- penalty risk in generation nodes caused by delays in pickup
- overtime operation risks in transfer stations

It is noteworthy to mention that the penalty risk is imposed on the system due to capacity reasons, where a pickup is postponed to another day. Due to its hazardous nature, the remaining inventory in the facility burdens the station with additional inventory risk.

In this model, a time-based risk evaluation is employed. Let BI_s^t and EI_s^t be the beginning and ending inventory in period t, respectively. Assuming ζ_s^t as the total amount of collection sent to facility s in period t, we can define the following relations:

$$EI_s^0 = 0 \qquad \forall s \in \mathcal{S} \tag{5.2}$$

$$BI_s^{t+1} = EI_s^t \qquad \forall s \in \mathcal{S}, \forall t \in \mathcal{T} \setminus \{T\} \tag{5.3}$$

$$BI_s^t + \zeta_s^t = EI_s^t \qquad \forall s \in \mathcal{S}, \forall t \in \mathcal{T} \tag{5.4}$$

Equation (5.2) sets the beginning inventory for the planning horizon. Equations (5.3) and (5.4) together ensure the inventory balance over each period. In the last period T, all waste inventory, E_s^T, is shipped to existing treatment centers.

The value of ending inventory is used to obtain the total risk of transfer station s. Considering POP_s as the exposed population around s, and R_s as the total risk around s, the site risk component of the objective function can be established:

$$R_s = \sum_{s \in \mathcal{B}} \sum_{t \in \mathcal{T}} POP_s EI_s^t \tag{5.5}$$

The penalty risk amount for the generation nodes, assuming POP_g as the exposed population around g, can be defined as:

$$R'_g = \sum_{g \in \mathcal{A}_s} \sum_{s \in \mathcal{B}} \sum_{t' \in \mathcal{T}} \sum_{t \in \mathcal{T}, t \leq t'} p_{gs}^{tt'}(t' - t) POP_g W_g^t \tag{5.6}$$

To reflect the waste collection deferments in the model, a binary variable, $p_{gs}^{tt'}$, is defined. We have $p_{gs}^{tt'} = 1$ if and only if the waste available to be collected on the day t is handled on day t', where $t' \geq t$. Therefore, based on (5.6), postponing the generated waste pickup at node g imposes an additional risk to the system each day.

Let $x_{ij\bar{s}}^t$ be a binary variable indicating whether the truck traverses from node i to j in a tour ending in the copy of transfer station s at the day t. Also, $y_{gs}^t = 1$ if and only if the generation node g, allocated to station s, is visited by the truck on the day t. Assuming $\mathcal{B}'$ as the copies of transfer stations in $\mathcal{B}$, the transportation risk (R_t) and overtime risk (R_o) components of the a priori objective function is developed as follows:

$$R_t \;=\; \sum_{t} \sum_{i \in \mathcal{A}_s} \sum_{j \in \mathcal{A}_s} \sum_{s' \in \mathcal{B}'} x_{ijs'}^t R_{ij} \tag{5.7}$$

$$R_o = \sum_{s\in\mathcal{B}}(EI_s^T - CV)\varepsilon_s^T POP_s \tag{5.8}$$

We assume that waiting for the overtime pickups imposes extra on-site risk and utilize it as the overtime penalty. Here, ε_s^T is a binary parameter indicating if the amount of accumulated waste at the last period T is more than the vehicle capacity. However, we need to linearize the this element, assuming $\psi_s^T = EI_s^T\varepsilon_s^T$ as follows:

$$\psi_s^T = EI_s^T\varepsilon_s^T \tag{5.9}$$

$$\psi_s^T \leq EI_s^T \tag{5.10}$$

$$\psi_s^T \leq M\varepsilon_s^T \tag{5.11}$$

$$\psi_s^T \geq EI_s^T - M(1-\varepsilon_s^T) \tag{5.12}$$

$$\psi_s^T \geq 0 \tag{5.13}$$

Therefore, the overtime objective component can be rewritten as:

$$R_o = \sum_{s\in\mathcal{B}} POP_s(\psi_s^T - CV\varepsilon_s^T) \tag{5.14}$$

Now, based on the introduced variables and assumptions, we can develop the a priori model as follows:

$$\min R_s + R_g + R_t + R_o$$

$$x_{ijs'}^t \leq y_{js}^t \qquad \forall i \in \mathcal{A}_s \cup \{s\}, \forall j \in \mathcal{A}_s, \forall s \in \mathcal{B}, \forall s' \in \mathcal{B}', s' - s = |\mathcal{B}|, \forall t \in \mathcal{T} \tag{5.15}$$

$$\sum_{j\in\mathcal{A}_s} x_{sjs'}^t \geq y_{is}^t \qquad \forall i \in \mathcal{A}_s, \forall s \in \mathcal{B}, \forall s' \in \mathcal{B}', s' - s = |\mathcal{B}|, \forall t \in \mathcal{T} \tag{5.16}$$

$$\sum_{j\in\mathcal{A}_s\cup\{s'\},i\neq j} x^t_{ijs'} + \sum_{j\in\mathcal{A}_s\cup\{s\},i\neq j} x^t_{jis'} = 2y^t_{is} \quad \forall i\in\mathcal{A}_s, \forall s\in\mathcal{B}, \forall s'\in\mathcal{B}', s'-s=|\mathcal{B}|, \forall t\in\mathcal{T} \tag{5.17}$$

$$\sum_{j\in\mathcal{A}_s} x^t_{sjs'} - \sum_{j\in\mathcal{A}_s} x^t_{js's'} = 0 \quad \forall s\in\mathcal{B}, \forall s'\in\mathcal{B}', s'-s=|\mathcal{B}|, \forall t\in\mathcal{T} \tag{5.18}$$

$$\sum_t y^t_{is} = 1 \quad \forall i\in\mathcal{A}_s, \forall s\in\mathcal{B} \tag{5.19}$$

$$u^t_j \geq u^t_i + x^t_{ijs'} - |\mathcal{A}_s|(1-x^t_{ijs'}) \quad \forall i\in\mathcal{A}_s\cup\{s\}, \forall j\in\mathcal{A}_s\cup\{s'\}, \forall s'\in\mathcal{B}', \forall t\in\mathcal{T} \tag{5.20}$$

$$p^{tt'}_{is} \leq y^t_{is} + M\delta^t_i \quad \forall i\in\mathcal{A}_s, \forall s\in\mathcal{B}, \forall t\in\mathcal{T}, \forall t'\in\mathcal{T} \tag{5.21}$$

$$\sum_{t,t\leq t'} p^{tt'}_{is}\delta^t_i \leq My^{t'}_{is} \quad \forall i\in\mathcal{A}_s, \forall s\in\mathcal{B}, \forall t'\in\mathcal{T} \tag{5.22}$$

$$\sum_{t,t\leq t'} p^{tt'}_{is}\delta^t_i \geq y^{t'}_{is} \quad \forall i\in\mathcal{A}_s, \forall s\in\mathcal{B}, \forall t'\in\mathcal{T} \tag{5.23}$$

$$\sum_{i\in\mathcal{A}_s}\sum_{t\in\mathcal{T},t\leq t'} p^{tt'}_{is}W^t_i \leq CV \quad \forall s\in\mathcal{B}, \forall t'\in\mathcal{T} \tag{5.24}$$

$$\sum_{t'\in\mathcal{T},t\leq t'\leq t+L^t_i} p^{tt'}_{is} \leq M\delta^s_i \quad \forall i\in\mathcal{A}_s, \forall s\in\mathcal{B}, \forall t\in\mathcal{T} \tag{5.25}$$

$$\sum_{t'\in\mathcal{T},t\leq t'\leq t+L^t_i} p^{tt'}_{is} \geq 1-M(1-\delta^t_i) \quad \forall i\in\mathcal{A}_s, \forall s\in\mathcal{B}, \forall t\in\mathcal{T} \tag{5.26}$$

$$p^{tt'}_{is} \leq \lambda^{t'}_{is} + M(1-\delta^t_i) \quad \forall i\in\mathcal{A}_s, \forall s\in\mathcal{B}, \forall t\in\mathcal{T}, \forall t'\in\mathcal{T}, t\leq t'\leq t+L^t_i \tag{5.27}$$

$$\sum_{i\in\mathcal{A}_s}\sum_{t,t\leq t'} p^{tt'}_{is}W^t_i = \zeta^{t'}_s \quad \forall s\in\mathcal{B}, \forall t'\in\mathcal{T} \tag{5.28}$$

$$\zeta^t_s \leq CS_s \quad \forall s\in\mathcal{B}, \forall t\in\mathcal{T} \tag{5.29}$$

$$BI^1_s = 0 \quad \forall s\in\mathcal{B} \tag{5.30}$$

$$BI_s^{t+1} = EI_s^t \qquad \forall s \in \mathcal{B}, \forall t \in \mathcal{T}, t \neq \mathcal{T} \tag{5.31}$$

$$BI_s^t + \zeta_s^t = EI_s^t \qquad \forall s \in \mathcal{B}, \forall t \in \mathcal{T} \tag{5.32}$$

$$EI_s^T - CV \leq M\varepsilon_s^T \qquad \forall s \in \mathcal{B} \tag{5.33}$$

$$\psi_s^T = EI_s^T \varepsilon_s^T \qquad \forall s \in \mathcal{B} \tag{5.34}$$

$$\psi_s^T \leq EI_s^T \qquad \forall s \in \mathcal{B} \tag{5.35}$$

$$\psi_s^T \leq M\varepsilon_s^T \qquad \forall s \in \mathcal{B} \tag{5.36}$$

$$\psi_s^T \geq EI_s^T - M(1 - \varepsilon_s^T) \qquad \forall s \in \mathcal{B} \tag{5.37}$$

$$x_{ij\bar{s}}^t, y_{gs}^t, p_{gs}^{tt'}, \alpha_g^s, \gamma_g^s, \varepsilon_s^T \in \{0,1\} \qquad \forall g \in \mathcal{G}, \forall i,j \in N, \forall s \in \mathcal{S}, \forall \bar{s} \in \bar{S}, \forall t \in \mathcal{T} \tag{5.38}$$

$$\eta_{sc}^t, \zeta_s^t, BI_s^t, EI_s^t, u_g^t, \psi_s^T \geq 0 \qquad \forall g \in \mathcal{G}, \forall s \in \mathcal{S}, \forall \bar{s} \in \bar{S}, \forall c \in C, \forall t \in \mathcal{T} \tag{5.39}$$

The objective function of the model is presented in (5.15). The risk mitigation is built upon three elements: fixed risk of established transfer stations, transportation risk, and the penalty risk of postponing waste collection. The connection between the routing variables and allocation variables are shown in (5.15)-(5.17). Constraint (5.18) ensures if any route starts from station s on the day t, it will end up at the associated copy of s. Constraint (5.19) guarantees that all the generation nodes are visited over the planning horizon. The sub-tour elimination is handled by (5.20). The connection between $p_{is}^{tt'}$ and y_{is}^t variables is reflected through (5.21) to (5.23) in the model. In inequality (5.21) $\delta_i^t = 1$ if the load is available to pickup at client i in period t. Constraint (5.24) deters violating the vehicle capacity in each period. Constraint (5.25) and (5.26) enforce the model to assign a pickup date for the load which is available in period t in the permissible collection interval. Constraint (5.27)

makes sure that handling the waste for a client is done after it becomes available. Equation (5.28) calculates the amount of waste accumulated at transfer station s in each period. Constraint (5.29) ensures that the transfer station's capacity is not violated. The waste inventory management is handled by (5.30)-(5.32). Overtime considerations are embedded in the model using (5.33)-(5.37). If the accumulated waste in the last period exceeds the vehicle capacity, the overtime penalty will be included in the model. Finally, constraint sets (5.38)-(5.39) determine the nature of the decision variables in the problem.

5.3.2.3 Recourse model

The solutions obtained from a priori plan are based on the decision-maker estimations regarding the release dates of the waste. However, in reality, the release dates might not adhere to this plan, demanding re-optimizing the model based on the realized data. Therefore, this research attempts to develop an adaptive sequential decision problem capable of adjusting the solutions when the uncertainties are realized. As mentioned earlier, the uncertainties lie in the speed of waste generation and, as a result, in the release dates of waste for pickups.

Recourse plans are employed to address the model dynamism by iteratively solving the model. A decision has to be made at the beginning of each period t based on the realization of data. If the estimations are correct, then λ_g^t is correct, and no adjusting is necessary. However, two types of estimation errors can occur regarding the release dates. First, the waste signal that was supposed to be sent on the day t from node g occurs earlier. In this case, as we have an unexpected amount of waste in the current day, modifications for the current day or the subsequent periods might be required.

Second, the amount of waste considered to be ready in period t is not available on that day leading to postponing (bumping) at least one pickup to a day after t.

Let $\bar{x}^t_{ij\bar{s}}$ and $\bar{p}^{tt'}_{ij}$ be the optimal solution of the a priori plan. In continue, we will apply an adaptive approach inspired by Darvish et al. (2020). If the waste becomes available based on the anticipation, $\lambda^s_g = 1$, no recomputation of λ^s_g is involved in the process. Maintaining the same risk estimate as before, the values of λ^s_g demands modifications considering the remaining probabilities P^t_g and the risk aversion level parameter (θ). Assuming the period t for decision-making, this parameter can be calculated as follows in the recourse plan:

$$\lambda^t_g = \begin{cases} 1, & \text{if } P^t_g - P^{t-1}_g \geq \theta \\ 0, & \text{otherwise} \end{cases} \tag{5.40}$$

Provided that any deviations from the pre-defined release dates happen on the day t, the collector company has to apply the recourse model to achieve the optimal solution for the remaining decisions. The recourse actions are performed considering the same risk aversion level for the decision-maker as the a priori model. A new binary variable is defined as α^t_g to reflect the deviations of release dates. $\alpha^t_g = 1$ if and only if bumping happens on the day t for the planned pickup of waste at node g. To connect the a priori model with the recourse plan, we define the parameter β^t_g and the variable γ^t_g. The former is utilized to demonstrate whether the collection was scheduled for node g in period t, while the latter indicates whether a pickup is

planned for node g on the day t. Parameter β_g^t is defined as follows:

$$\beta_g^{t'} = \begin{cases} 1, & \text{if } \sum_{t \le t'} \bar{p}_{ij}^{tt'} \ge 1 \\ 0, & \text{otherwise} \end{cases} \tag{5.41}$$

There is an additional part for the objective function in the recourse action as the bumping penalty. We can simply define it using equation (5.42).

$$R_b = \sum_{t' \in \mathcal{T}} \sum_{i \in \mathcal{A}_s} C' \alpha_i^{t'} \tag{5.42}$$

Now, the recourse model can be developed as follows:

$$\min R_s + R_g + R_t + R_o + R_b \tag{5.43}$$

$$\gamma_i^{t'} \le \sum_{t \le t'} p_{is}^{tt'} \qquad \forall i \in \mathcal{A}_s, \forall t' \in \mathcal{T} \tag{5.44}$$

$$\sum_{t \le t'} W_i^t \gamma_i^{t'} \ge \sum_{t \le t'} p_{is}^{tt'} \qquad \forall i \in \mathcal{A}_s, \forall t' \in \mathcal{T} \tag{5.45}$$

$$\alpha_i^{t'} \ge \beta_i^{t'} - \gamma_i^{t'} \qquad \forall i \in \mathcal{A}_s, \forall t' \in \mathcal{T} \tag{5.46}$$

$$\alpha_i^{t'} \ge \gamma_i^{t'} - \beta_i^{t'} \qquad \forall i \in \mathcal{A}_s, \forall t' \in \mathcal{T} \tag{5.47}$$

$$\beta_i^t, \gamma_i^t \in \{0, 1\} \qquad \forall i \in \mathcal{A}_s, \forall t' \in \mathcal{T} \tag{5.48}$$

The objective function (5.43) is developed by incorporating the bumping penalties into (5.15). Constraint (5.44) ensures that if a pickup is scheduled for a client in a period, there exists a load to be collected on that period. The waste quantities to be handled are guaranteed by (5.45). Bumping penalties are imposed to the model based on constraints (5.46) and (5.47). In these inequalities, having a conflict between a new optimized plan and the previously planned schedule results in a bumping penalty as the associated variable $\alpha_i^t = 1$.

The values of $p_{is}^{tt'}$ are stored in $\bar{p}_{ij}^{tt'}$ for any $t \geq 2$. After stabilizng the past decisions, the recourse model is re-optimized by applying the following constraint:

$$p_{is}^{\tilde{t}t'} = \bar{p}_{is}^{\tilde{t}t'} \qquad \tilde{t} \in \{1, ..., t\} \tag{5.49}$$

5.3.3 Sample tests

In this section, we check the validity and performance of the proposed mathematical model using several randomly generated sample instances. All computational tests (including the case experiments in section 5.4 are performed on a computer equipped with a 2.2 GHz Intel processor and 2 GB RAM using Java 11 and CPLEX 12.8.0.

Totally, 28 random problem instances with different sizes and different values for θ are generated and tested. Four different values for θ are considered, including 0.1, 0.4, 0.7, and 0.9, to test how various risk-aversion viewpoints can affect the model. Also, the size of each instance is described by the number of generation nodes (i.e., $|\mathcal{G}|$) and candidate temporary transfer stations ($|\mathcal{T}|$). We assume there is only one existing treatment center capable of handling all the system waste in all of these instances. The medical centers can be small facilities like laboratories and clinics or large centers like large-sized hospitals. As a result, the generated waste for these generation nodes follows a uniform distribution as $U \sim [300, 2500]$ with regard to medical center size and assuming a worst-case scenario. The capacity values are set to ensure feasible solutions.

Table 5.3 displays the obtained results for the available test instances. We consider a computation time of 18000 seconds (i.e., 5 hours). Column "Best Obj" is the optimal solution or the best result obtained within 18000 seconds. Columns "Gap(%)" and

"Time" respectively present the optimality gap and computational time for each instance.

As we can observe in Table 5.3, the more optimistic the decision-maker, the more complex the problem would be. Therefore, lower values of θ result in more computation time and gaps. For example, the average computation time and gap for $\theta = 0.1$ are respectively 230% and 73% higher than of $\theta = 0.9$. The reason behind this boost lies in the existence of more flexible plans in a more optimistic setting. On the other hand, when dealing with a more pessimistic situation with higher values of θ, the routing decisions are postponed to the ending periods leaving fewer possibilities for generating the a priori plan. In other words, less flexibility in the model leads to a more constrained setting with fewer pickup options for the collector.

In general, the risk objective worsens when we increase the values of θ. For example, in a problem setting with 20 generation nodes, a growth of almost 50% is observable when moving from $\theta = 0.1$ to $\theta = 0.9$. This means that a more pessimistic collector should expect a higher system risk. It is noteworthy to mention that in higher values of θ overtime option is more likely to be activated as the system faces a less flexible setting where all the waste should be handled by the end of the planning horizon.

In all values of θ and for problems with less than or equal to 40 generation nodes, the model is solved to optimality within 18000 seconds. For larger instances, we obtain the final result with a small gap. Also, in $\theta = 0.9$, due to less complexity, we achieve the optimal value for the sample test with 50 generation nodes as well.

Table 5.3: Random instances

#	θ	$\lvert\mathcal{G}\rvert$	$\lvert\mathcal{S}\rvert$	**Best Obj**	**Gap (%)**	**Time (s)**
1		10	3	210768.58	0.00	23
2		20	4	284822.40	0.00	103
3		30	6	319001.09	0.00	1553
4	0.1	40	8	357281.22	0.00	6448
5		50	10	428737.46	1.63	14164
6		60	12	488760.71	1.94	18000
7		80	16	586512.85	2.30	18000
Average				-	0.84	8327.29
8		10	3	221139.51	0.00	18
9		20	4	335059.86	0.00	76
10		30	6	371916.44	0.00	1271
11	0.4	40	8	423984.75	0.00	5187
12		50	10	500302.00	1.01	11614
13		60	12	580350.32	1.24	13140
14		80	16	679009.88	1.86	14454
Average				-	0.59	6537.14
15		10	3	337476.90	0.00	18
16		20	4	489096.95	0.00	73
17		30	6	538006.65	0.00	1080
18	0.7	40	8	594497.34	0.00	4824
19		50	10	677726.97	0.93	9407
20		60	12	759054.21	1.11	10643
21		80	16	857731.25	1.35	13442
Average				-	0.48	5641.17
22		10	3	422814.21	0.00	14
23		20	4	595512.97	0.00	67
24		30	6	643154.01	0.00	972
25	0.9	40	8	701037.87	0.00	4438
26		50	10	785162.41	0.00	8843
27		60	12	863678.65	0.86	8621
28		80	16	993230.45	0.92	11023
Average				-	0.25	4854.02

5.4 Case Study

In this section, a case study based on the situation in Kunming, a city in China, is applied to assess the validity and applicability of the proposed model. As shown in Fig. 5.3, there are 25 nodes, including 20 generation nodes ($G1$-$G20$), four storage center candidates ($S1$-$S4$), and one existing treatment center ($T1$). We assume one general type of hazardous waste is involved in this case. The amount of generated waste for the hazardous waste produced at generation nodes and the nodes' associated surrounding population has been provided in Table 5.4. Also, the relevant data for transfer and treatment centers are presented in Table 5.5.

5.4.1 Relevant data

Capacities and costs Each storage center candidate has a capacity of 10 tonnes for storing the hazardous waste, and the corresponding variable cost of storing is 120 dollars/tonne. No capacity consideration has been applied to the treatment center. It is assumed that the treatment center is capable of processing all the generated waste during the planning horizon. The unit cost of processing the waste is 110 dollars/tonne in the treatment center. First, we assume that the vehicle capacity for tours is 10 tonnes, and then we discuss varying this value in section 5.4.4. Moreover, we consider that the unit cost of transportation in the tours and direct routes are 100 and 6 dollars, respectively. Other facility operational costs are given in Table 5.5.

Risk The number of exposed populations is estimated within the radius of 800 meters from the facilities (Alumur and Kara, 2007). The associated number of exposed

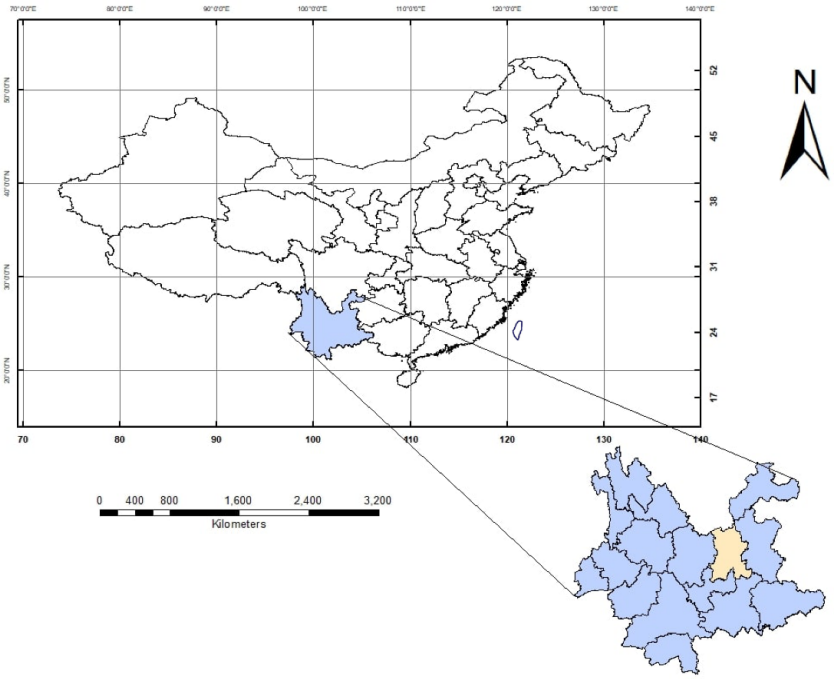

(a) Map showing the location of Kunming city

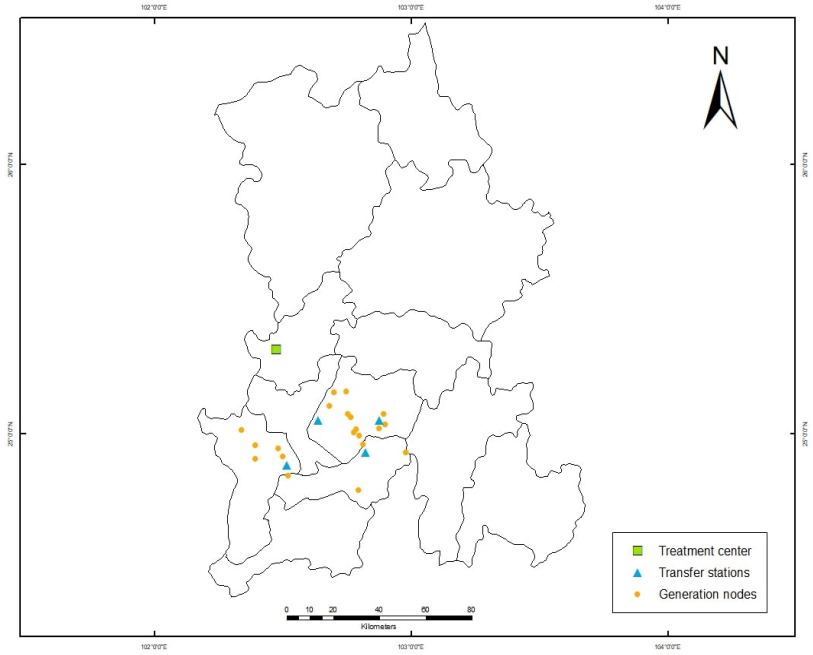

(b) Map showing the candidate facilities in the city of Kunming

Figure 5.3: The medical waste management network in Kunming, China

individuals around each facility is shown in Table 5.5. Also, the exposed population around each generation node can be found in Table 5.4. All population data are obtained from the GIS database. The average number of people residing in the two associated nodes presents the exposed population across each edge.

Time considerations A five-day planning time horizon is considered in this case, where each day stands for a period in the model. When dealing with COVID-19 hazardous waste, it is vital to avoid storing it for more than one day in the storage centers. In this regard, the Ministry of Ecology and Environment of the People's Republic of China implied in the "Management and Technical Guidelines for Emergency Disposal of Medical Waste in the Pneumonia Pandemic of COVID-19" that COVID-related waste should be processed separately from any other types of waste, with a maximum of a 24-hour storing period in the temporary facilities. A study by Shammi et al. (2021) also highlighted that we should anticipate higher risks of COVID-19 transmission for longer storage time for biomedical medical waste. As a result, the maximum permissible lateness for the generation nodes is regarded one day.

Deviations For the recourse plan, we assume that the model is exposed to three different deviation scenarios, including minor, normal, and major cases. The minor deviation case represents a minor divergence from the a priori plan by only considering changes in the availability of waste in $G1$ and $G6$. The availability for $G1$ is shifted from day 1 to day 2 ($t1 \rightarrow t2$), and for $G6$ from day 3 to day 2 ($t3 \rightarrow t2$). In the normal deviation scenario, the model experiences more deviations compared to the minor

circumstance. Four changes are embedded in the model as $G1(t1 \rightarrow t2)$, $G2(t3 \rightarrow t2)$, $G6(t3 \rightarrow t2)$, and $G19(t4 \rightarrow t5)$. Finally, the major deviation situation, with six deviations from the original plan, is evaluated in the recourse plan. The changes include $G1(t1 \rightarrow t2)$, $G2(t3 \rightarrow t2)$, $G6(t3 \rightarrow t2)$, $G11(t3 \rightarrow t2)$, $G19(t4 \rightarrow t5)$, and $G20(t1 \rightarrow t2)$.

Risk-aversion parameter To cover different levels of the risk-aversion characteristic of the decision-maker, we apply four different values for θ, including 0.1, 0.4, 0.7, and 0.9. The more this value is, the more pessimistic the collector becomes. Therefore, in the higher values of θ, the collector tries to postpone the collection process as much as possible, while lower values of θ oblige the model to handle the waste as soon as possible.

Probabilities We assume random values for the probabilities of generated waste availability in the model. The generated values do not follow particular trends like low/high starting point with gradual/abrupt changes. This is done to apply more generalized information in the model. Evaluating different trends can be a potential pathway for future studies. The relevant data for the probabilities are shown in Table 5.6.

5.4.2 Location-allocation solution

By considering the cost objective in the first stage, the location-allocation model is solved using the clustering approach described earlier. Based on the results, two candidate transfer stations are chosen, including $S2$ and $S3$. The lower opening

Table 5.4: Data for generation nodes

Node type	#	**Amount of waste generation** (tonnes/planning horizon)	**Population**
Small generation node	G1	5.48	280.82
	G2	1.37	347.78
	G3	4.93	202.62
	G4	3.95	34468.26
	G5	3.5	280.82
	G6	2.58	3269.80
	G7	1.46	162.65
	G8	5.12	410.50
	G9	1.73	650.06
	G10	1.64	413.48
	G11	1.32	2143.01
	G12	1.51	2221.40
	G13	2.05	11089.38
	G14	4.44	347.78
	G15	2.33	900.82
	G16	2.96	4880.35
	G17	3.29	1558.59
	G18	0.41	529.40
	G19	2.74	12347.27
	G20	0.82	3343.80

Table 5.5: Data for facilitates

Node type	#	**Fixed cost** ($\times 10^3$\$)	**Unit variable cost** (\$/*tonne*)	**Exposed pop.**
Storage centers	S1	331	120	1054.00
	S2	327	120	2150.32
	S3	321	120	6079.15
	S4	338	120	347.78
Treatment center	T1	-	110	1322.65

Table 5.6: Associated probabilities for the generated waste availability

	Probabilities for each period				
Node	$t1$	$t2$	$t3$	$t4$	$t5$
G1	0.43	0.21	0.17	0.13	0.06
G2	0.13	0.19	0.32	0.2	0.16
G3	0.06	0.09	0.26	0.35	0.24
G4	0.1	0.14	0.2	0.38	0.18
G5	0.03	0.08	0.11	0.31	0.47
G6	0.11	0.19	0.33	0.24	0.13
G7	0.39	0.2	0.15	0.14	0.12
G8	0.23	0.36	0.21	0.12	0.08
G9	0.4	0.2	0.16	0.12	0.12
G10	0.21	0.32	0.18	0.16	0.13
G11	0.08	0.21	0.43	0.18	0.1
G12	0.05	0.12	0.2	0.22	0.41
G13	0.16	0.42	0.16	0.13	0.13
G14	0.44	0.22	0.17	0.13	0.04
G15	0.2	0.44	0.19	0.1	0.07
G16	0.1	0.22	0.34	0.25	0.09
G17	0.04	0.17	0.19	0.21	0.39
G18	0.12	0.14	0.19	0.32	0.23
G19	0.11	0.16	0.21	0.37	0.15
G20	0.33	0.23	0.18	0.14	0.12

cost of these two facilities plays a significant role in appearing in the final solution. Based on the capacity limitations, each of these facilities is assigned ten generation nodes. The obtained location-allocation solution is then stored in sets $\mathcal{B}$ and $\mathcal{A}_s$. Therefore, $\mathcal{B} = \{S2, S3\}$, $\mathcal{A}_{s2} = \{G1, G2, G5, G7, G9, G10, G11, G14, G15, G18\}$, and $\mathcal{A}_{s3} = \{G3, G4, G6, G8, G12, G13, G16, G17, G19, G20\}$. It is noteworthy to mention that the computation time for this stage of the problem is less than two minutes for the applied problem set. The a priori model and the recourse plan will be optimized by employing the obtained $\mathcal{B}$ and $\mathcal{A}_s$ sets in this stage.

5.4.3 A priori stage

In this section, we will discuss the results obtained in the a priori phase of the model. This stage is built upon assuming that the decision-maker can determine the most probable release dates for the generated waste at each node based on the available data. For example, according to Table 5.6, the signal from node $G3$ is most likely to be sent at the fourth period.

Table 5.7 includes different elements of the objective function for the a priori plan for the assumed values of the risk parameter. In this table, site risk stands for the risk around the transfer stations due to the accumulated waste during the planning horizon. Overtime risk is the risk of the network for handling the waste when the capacity limitations force the model to activate the overtime option. Node risk is the associated risk value of the exposed population around the generation nodes. The en-route risk of waste collection is reflected in the transportation risk. Finally, the total risk encompasses all the mentioned risk elements for the network.

Similar to the discussion in section 5.3.3, it is evident that with more values of θ, one can anticipate that more risk is imposed on the system. A nearly 123% growth of total risk in the pessimistic case with $\theta = 0.9$ compared to the optimistic condition with $\theta = 0.1$ verifies this claim. The site risk demonstrates a declining trend moving toward higher values of θ. With a pessimistic collector, the first periods of the planning horizon are less likely to be assigned with waste collection tours. As a result, the transfer stations will not store the hazardous waste and jeopardize the surrounding population. Using similar logic, more values of θ increase the chances of activating the overtime option. The behavior of the node risk is the opposite of the site risk. When a collector follows a pessimistic point of view, the hazardous waste at the generation nodes might remain uncollected for several periods. Postponing the pickup time endangers the surrounding residents and imposes more risk on the system. Finally, the lowest variations are noticeable in the transportation risk, where the vehicle's capacity plays a major role. A detailed sensitivity analysis of the vehicle capacity is performed in section 5.4.4.

Table 5.8 summarizes the routing decisions for each transfer station in each period for different risk-averse levels. The overtime operations is shown by ot in this table. In the lower values of θ, the burden of waste collection is distributed in all periods. However, higher values of θ enforce the model to delay the pickup to the ending periods. For example, in $\theta = 0.1$, all the periods have been used considering both transfer stations. No pickup is performed for transfer station $S2$ on $t3$, while operations begin from $t2$ in facility $S3$. On the other hand, a pessimistic collector with a risk-averse level equal to 0.9 starts the collection from $t4$ for both stations. This leads to overtime activities in the system with additional associated risks.

Table 5.7: Results for the a priori stage

	Theta			
	0.1	0.4	0.7	0.9
Site Risk	232,990.12	232,990.12	208,977.48	148,775.37
Overtime Risk	0.00	0.00	36,018.96	126,322.13
Nodes Risk	8,590.21	8,827.67	214,65293	319,775.33
Transportation Risk	43,242.07	43,242.07	41,453.91	42,747.51
Total	284,822.40	285,059.86	501,103.27	637,620.34

5.4.4 Sensitivity analysis

By altering the vehicle capacity for the tour collection, we explore the obtained risk elements and compare the results in this section. For this purpose, we used four different values for the vehicle capacity, including 8, 10, 12, and 15 tonnes per tour. A summary of the obtained results has been provided in Table 5.9. As expected, more savings in the total risk can be achieved with a more spacious truck. This is because higher capacities are able to collect more waste and consequently avoid unnecessary overtime activities. For example, the average total risk for a truck with 8 tonnes capacity is more than 37% higher than that of a vehicle with 15 tonnes of space for the waste pickup.

There are several interesting points in Table 5.9. First, for each risk-averse level, increasing the vehicle capacity results in more risk savings for the model. The change is more tangible when moving from 8 tonnes to 10 tonnes, whereas the impact gets slighter for values more than 10 tonnes. Also, it seems that a more pessimistic perspective does not go through sharp increases or decreases by manipulating the vehicle capacity. However, a drop of 55% and 31% happens for $\theta = 0.1$ and $\theta = 0.4$, assuming an additional space of 2 tonnes for a vehicle capacity of 8 tonnes. In other

Table 5.8: A priori plan

θ	**Transfer station**	**Period**	**Route**
0.1	**S2**	$t1$	$S2 \rightarrow G1 \rightarrow G7 \rightarrow G9 \rightarrow S2$
		$t2$	$S2 \rightarrow G15 \rightarrow G10 \rightarrow G14 \rightarrow S2$
		$t3$	-
		$t4$	$S2 \rightarrow G11 \rightarrow G2 \rightarrow G18 \rightarrow S2$
		$t5$	$S2 \rightarrow G5 \rightarrow S2$
	S3	$t1$	-
		$t2$	$S3 \rightarrow G8 \rightarrow G13 \rightarrow G20 \rightarrow S3$
		$t3$	$S3 \rightarrow G6 \rightarrow G16 \rightarrow S3$
		$t4$	$S3 \rightarrow G4 \rightarrow G19 \rightarrow S3$
		$t5$	$S3 \rightarrow G3 \rightarrow G17 \rightarrow G12 \rightarrow S3$
0.4	**S2**	$t1$	$S2 \rightarrow G1 \rightarrow G9 \rightarrow S2$
		$t2$	$S2 \rightarrow G7 \rightarrow G15 \rightarrow G10 \rightarrow G14 \rightarrow S2$
		$t3$	-
		$t4$	$S2 \rightarrow G11 \rightarrow G2 \rightarrow G18 \rightarrow S2$
		$t5$	$S2 \rightarrow G5 \rightarrow S2$
	S3	$t1$	-
		$t2$	$S3 \rightarrow G8 \rightarrow G13 \rightarrow G20 \rightarrow S3$
		$t3$	$S3 \rightarrow G6 \rightarrow G16 \rightarrow S3$
		$t4$	$S3 \rightarrow G4 \rightarrow G19 \rightarrow S3$
		$t5$	$S3 \rightarrow G3 \rightarrow G17 \rightarrow G12 \rightarrow S3$
0.7	**S2**	$t1$	-
		$t2$	-
		$t3$	$S2 \rightarrow G7 \rightarrow G14 \rightarrow G15 \rightarrow G9 \rightarrow S2$
		$t4$	$S2 \rightarrow G1 \rightarrow G2 \rightarrow G10 \rightarrow G11 \rightarrow S2$
		$t5$	$S2 \rightarrow G5 \rightarrow G18 \rightarrow S2$
	S3	$t1$	-
		$t2$	-
		$t3$	$S3 \rightarrow G8 \rightarrow G13 \rightarrow G20 \rightarrow S3$
		$t4$	$S3 \rightarrow G19 \rightarrow G6 \rightarrow G16 \rightarrow S3$
		$t5$	$S3 \rightarrow G3 \rightarrow G12 \rightarrow G17 \rightarrow S3$
		ot	$S3 \rightarrow G4 \rightarrow S3$

Table 5.8 (continue) : A priori plan

θ	**Transfer station**	**Period**	**Route**
0.9	**S2**	$t1$	-
		$t2$	-
		$t3$	-
		$t4$	$S2 \rightarrow G7 \rightarrow G11 \rightarrow G1 \rightarrow G9 \rightarrow S2$
		$t5$	$S2 \rightarrow G2 \rightarrow G10 \rightarrow G14 \rightarrow G15 \rightarrow S2$
		ot	$S2 \rightarrow G5 \rightarrow G18 \rightarrow S2$
	S3	$t1$	-
		$t2$	-
		$t3$	-
		$t4$	$S3 \rightarrow G8 \rightarrow G16 \rightarrow S3$
		$t5$	$S3 \rightarrow G13 \rightarrow G20 \rightarrow G6 \rightarrow G4 \rightarrow S3$
		ot	$S3 \rightarrow G19 \rightarrow G3 \rightarrow G17 \rightarrow G12 \rightarrow S3$

words, a pessimistic collector demonstrates a more stable behavior toward the vehicle capacity alteration. Another point is that in all capacity values except for the $CV = 8$, there is an increasing trend when the value of θ rises. It seems that being unable to handle the waste for the starting period due to the lack of space surges the node risk for waiting for waste collection more than anticipated. The overtime risk for this vehicle capacity amount shows similar behavior to the total risk. For $CV \in \{10, 12, 15\}$, we observe an increasing trend for overtime risk, node risk, and total risk when being more pessimistic. There is no special trend for the transportation risk, and it mainly fluctuates slightly by varying the risk-averse level. Finally, the site risk for all the capacity amounts has a higher value for optimistic decision-makers. This is because lower values of θ are more capable of dealing with waste during ordinary working time with fewer chances of requiring overtime activities.

Table 5.9: Sensitivity analysis for vehicle capacity

Vehicle capacity	Risk component	**Theta**			
		0.1	0.4	0.7	0.9
8	Site Risk	148,775.37	223,810.60	192,958.76	108,947.15
	Overtime Risk	126,322.13	8,288.51	104,219.06	186,064.45
	Nodes Risk	312,878.12	142,989.12	222,125.37	329,415.87
	Transportation Risk	42,747.51	39,619.16	32,914.66	24,041.60
	Total	630,723.13	414,707.39	522,769.84	648,469.08
10	Site Risk	232,990.12	232,990.12	208,977.48	148,775.37
	Overtime Risk	0.00	0.00	36,018.96	126,322.13
	Nodes Risk	8,590.21	8,827.67	214,65293	319,775.33
	Transportation Risk	43,242.07	43,242.07	41,453.91	42,747.51
	Total	284,822.40	285,059.86	501,103.27	637,620.34
12	Site Risk	232,990.12	232,990.12	232,990.12	192,841.80
	Overtime Risk	0.00	0.00	0.00	60,222.48
	Nodes Risk	6,284.62	6,284.62	191,168.78	312,696.04
	Transportation Risk	43,487.47	43,487.47	43,757.26	43,160.76
	Total	282,762.21	282,762.21	467,916.15	608,921.08
15	Site Risk	232,990.12	232,990.12	232,990.12	194,653.33
	Overtime Risk	0.00	0.00	0.00	57,505.19
	Nodes Risk	6,016.80	6,227.34	179,995.19	302,461.43
	Transportation Risk	42,260.71	42,260.71	43,100.62	44,519.18
	Total	281,267.63	281,478.17	456,085.93	599,139.12

5.4.5 Recourse action

In this section, we explore the results of the recourse model as a result of available deviations. As mentioned earlier, we assume three different deviation scenarios for the recourse plan: 1) the minor deviation case including a minor divergence from the a priori plan by only considering changes in the availability of waste in $G1(t3 \rightarrow t2)$ and $G6(t3 \rightarrow t2)$ 2) the normal deviation scenario with four changes as $G1(t1 \rightarrow t2)$, $G2(t3 \rightarrow t2)$, $G6(t3 \rightarrow t2)$, and $G19(t4 \rightarrow t5)$ 3) the major deviation scenario with six deviations as $G1(t1 \rightarrow t2)$, $G2(t3 \rightarrow t2)$, $G6(t3 \rightarrow t2)$, $G11(t3 \rightarrow t2)$, $G19(t4 \rightarrow t5)$, and $G20(t1 \rightarrow t2)$.

The total risk comparison between a priori plan and different disrupted situations has been provided in Figure 5.4. Except for the optimistic case, where the average risk is slightly higher than the non-disrupted condition, in the other deviation scenarios, the average network risk is lower compared to the case without deviations, i.e., the a priori plan. We can observe an average risk variation of 0.53%, -1.90%, and -3.45% in minor, normal, and major deviation situations, respectively, compared to the original plan. The site and overtime risks do not get impacted in the disrupted condition for lower values of θ. This is because the system still depends on all the available periods for each transfer station and handles all the generated waste during the ordinary working time. As a result, still system can process the waste without the necessity for an overtime operation. However, the pessimistic perspective experiences variations in the site and overtime risk. A higher value of θ puts more pressure on the ending periods, and with deviation occurring, it is more likely for the system to require overtime activities to cope with the changes.

The exciting matter regarding the recourse plan is the impact of the risk-averse parameter on the final risk value after adapting to the realized situation. As shown in Table 5.10, an optimistic collector ($\theta \in \{0.1, 0.4\}$) adapts to the deviations by accepting additional risk for the whole system. As a result, considering $\theta = 0.1$, a rise of about 3.71%, 5.48%, and 5.59% occurred, respectively, in minor, normal, and major deviation scenarios compared to the original plan. Similarly, there is an extra risk burden of 4.32%, 5.90%, and 6.29% for $\theta = 0.4$. On the other hand, a pessimistic point of view seems to benefit from deviations. In fact, the more significant a deviation is, the more reductions in total risk can be derived. As discussed earlier, a pessimistic decision-maker postpones the pickup to the ending days, and deviations happening during the planning horizon enforce the collector to start the process earlier than what was scheduled in the a priori model. This issue leads to less overtime and hectic pickups in the ending periods with fewer overtime activities. In this regard, for $\theta = 0.7$, the total risk declines by 1.38%. 4.46%, and 6.31% in minor, normal, and major deviation cases. Besides, the recourse model cuts off 1.08%, 6.67%, and 9.60% of the total risk in the associated scenarios. Also, it is evident that the recourse model goes through more bumping penalties with more disrupted conditions.

In summary, we can conclude that, depending on the subjective perspective of the collector, deviations can happen to be a positive or negative phenomenon. For an optimistic decision-maker managing the hazardous waste from the generation nodes as soon as possible, the realization of different data than the a priori plan is not pleasant. Adaption to this matter necessitates accepting extra total risk. On the other hand, a pessimistic decision-maker benefits from deviations. Higher values of θ postpone waste handling to the ending days. However, with variations in the original plan, the

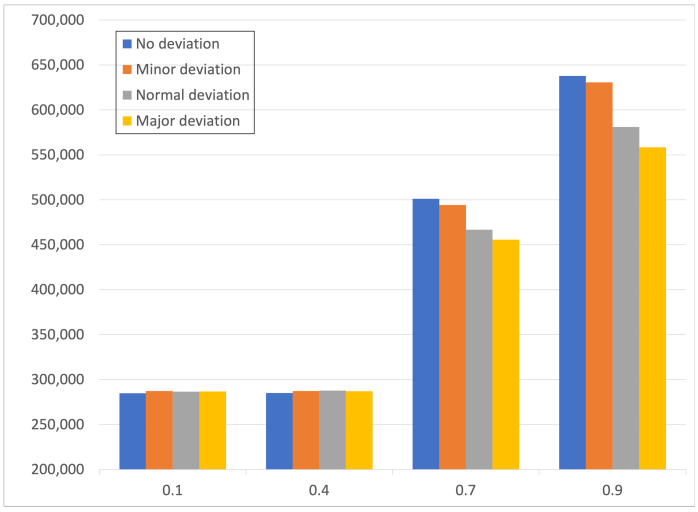

Figure 5.4: Total risk comparison between different scenarios

collector is forced to start the pickup process earlier, which in return, cuts off the overtime actions and reduces the total risk. It can be seen that the overtime amount declines when we move from minor deviation toward major deviation scenarios.

5.5 Managerial insights

Hazardous waste management is a complicated and sensitive matter requiring a reasonable plan to handle the waste effectively and safely while still meeting all legal requirements. When developing a hazardous waste management plan, there are several factors to consider, such as the type and number of facilities where the hazardous material will be stored or processed and the amount and risk of hazards posed by the material. Also, it should be noted that, as discussed in this research, the attribute of a decision-maker can directly impact the derived decisions regarding the associated network. Proper management can lead to many benefits, including reduced risk of potential incidents and reduced costs associated with waste management.

Table 5.10: Results for the recourse stage

Minor deviation				
Cost component	θ			
	0.1	0.4	0.7	0.9
Site Risk	232,990.12	232,990.12	208,977.48	148,775.37
Overtime Risk	0.00	0.00	36,018.96	126,322.13
Nodes Risk	15,482.14	14,170.28	207,755.71	312,878.12
Transportation Risk	42,905.78	40,223.92	41,453.91	42,747.51
Bumping Penalty	4,000.00	10,000.00	0.00	0.00
Total	295,378.03	297,384.33	494,206.06	630,723.13
Normal deviation				
Cost component	θ			
	0.1	0.4	0.7	0.9
Site Risk	232,990.12	232,990.12	208,977.48	172,320.20
Overtime Risk	0.00	0.00	36,018.96	91,004.88
Nodes Risk	11,871.51	13,171.38	179,276.41	271,196.09
Transportation Risk	41,571.88	41,706.20	42,469.49	46,558.52
Bumping Penalty	14,000.00	14,000.00	12,000.00	14,000.00
Total	300,433.51	301,867.70	478,742.34	595,079.69
Major deviation				
Cost component	θ			
	0.1	0.4	0.7	0.9
Site Risk	232,990.12	232,990.12	218,333.25	172,320.20
Overtime Risk	0.00	0.00	24,985.31	91,004.88
Nodes Risk	10,752.05	10,989.52	175,868.60	248,753.24
Transportation Risk	43,012.50	43,012.50	36,318.64	46,298.60
Bumping Penalty	14,000.00	16,000.00	14,000.00	18,000.00
Total	300,754.67	302,992.13	469,505.79	576,376.91

The COVID-19 crisis has exposed the vulnerabilities of various public and private sectors and organizations regarding their preparedness, response, coordination, and communication. As a result, all aspects and levels of society have undergone immersing pressure both financially and mentally. In light of coping with similar pandemics, it is worth examining strategies for presenting more affordable and less risky approaches when dealing with hazardous wastes and infectious diseases. This section underlines the managerial insights derived from our experiments and discussions. We highlight several points to support the carriers and relevant authorities in establishing practical and reliable networks.

The improper management of hazardous waste exposes health and waste workers to irreparable infections. Many relevant organizations have highlighted the need for appropriate waste management, such as the World Health Organization, a leading authority in public health. Therefore, carrier companies are a central part of the system responsible for collecting and processing waste. The decisions made by the collector are vital in establishing a redundant medical-waste management system capable of controlling the pandemics. Of course, there are investments required for maintaining such a redundant network. However, in the long run, the advantages of the applied redundancy will prevail over the initial expenses by mitigating the associated risks and costs in different circumstances.

The majority of studies do not take into account the decision-maker's point of view in their models. We filled this gap and overcame this limitation using a risk-averse parameter. Introducing the risk-averse function to the model allows users to observe how their decisions lead to significant variations in the derived solutions. This parameter can be utilized to determine if managers' risk-taking or risk-aversing

attitude is suitable for different settings.

An effective waste collection system should be able to benefit from its assets, properties, capacities, and composing elements as much as possible. Especially during unexpected circumstances such as an outbreak, the ability to adapt to the situation quickly and with utmost capacity is a must. Application of temporary facilities is one of the methods to adapt quickly to the realized conditions with less risky and cost-efficient solutions. As a result, incorporating temporary facilities in the network simplifies adjusting the existing waste network to deal with the unplanned generated medical waste and control the associated viral spread. Living with COVID has become a new normal these days. In the upcoming years, we might face other infectious diseases, where upgrading these temporary stations with larger capacities and more satisfactory compatibility will help authorities handle unpleasant situations skillfully.

Serving multiple customers in a single tour imposes less risk and cost on the system by avoiding unnecessary trips compared to the straight-to-and-back mode. Furthermore, basic environmental principles encourage a shorter time for collecting and disposing of waste. As a result, by applying tours instead of direct routes, the collector benefits from reduced waste management process time and consequently reduced associated costs as well as population exposure by omitting the unnecessary commuting between transfer stations and medical centers.

The model suggested in this study entails a comprehensive point of view. Not only does it incorporate the subjectivity of decision-making, but also it considers both risk and cost minimization. The multi-stage decision framework provided in this research allows the collector to plan and schedule the entire planning horizon once in

the beginning. Then, it deals with deviations once they occur and proposes modified plans. Three types of deviation are reflected in the model to evaluate different possible scenarios, including minor, normal, and major deviations from the original plan. Therefore, this research can be implemented as a helpful tool to derive practical solutions for real-life applications where the decision maker's risk perspective can be examined and quantified.

5.6 Conclusions

In this research, we proposed a multi-stage decision framework for the hazardous waste management location-routing-inventory problem. The first stage of the problem determines the locations of candidate storage centers using a cost-based clustering algorithm. Focusing on mitigating different sources of risk, we prepare the a priori plan where estimations for release dates are applied. Finally, our model is modified once disruptions happen. We consider several important assumptions. Firstly, random release dates and waste generation speeds in medical centers. Secondly, temporary transfer stations act as storage for the accumulated waste from medical centers via tours. Finally, the decision maker's risk perspective is applied and quantified using a subjective risk-aversion parameter. The concept of this parameter helps convert the stochastic model into a deterministic one. To demonstrate our model's practicality and validity, we applied the proposed model to a real-world case study of hazardous waste management in Kunming, China. Numerical experiments are conducted to examine different stages of the solution and explore the model's sensitivity to several key parameters, such as vehicle capacity and the subjective risk-aversion parame-

ter. Besides, we examined three different disruption scenarios as minor, normal, and major deviations. In the end, we derive and explain several managerial insights to underline beneficial points for the government and other stakeholders.

There are several potential pathways for future research. Investigating multiple hazardous waste types or simultaneously handling both hazardous and non-hazardous waste is one research avenue to help provide a more generalized model. Future studies can incorporate more realistic considerations in making collection plans, such as the time-dependent parameters. Also, apart from the location, routing, and inventory decisions, scheduling considerations will be a suitable research contribution for deriving a more practical solution. Considering more complicated exact solution methods such as the branch-and-price technique, hoping to achieve better computation time, especially in the larger instances, would be another potential contribution. Finally, one can incorporate different stakeholders such as the government or healthcare system and the carrier through a bi-level model. The upper level provides the associated policies, and the lower level optimizes the waste management process by adhering to these policies.

Chapter 6

Conclusions and Future Research

6.1 Conclusions

In contrast to many other application domains, there is a limited number of articles focusing on applications of optimization with uncertain data in the location-routing problem of hazmat transportation. In this dissertation, we proposed a set of three compatible approaches respectively in hazmat, infectious waste, and hazardous waste management and transportation areas.

Chapter 3 presented a new hazmat model by assuming edge unavailability scenarios to develop a scenario-based robust program. Time considerations were addressed in this research through customer time windows and time-dependent parameters. The former reflected the period that the corresponding customer plans to receive the delivery. It was assumed that the population exposures alter in various time horizons during the day leading to variations in the corresponding hazmat transportation risks at different times of the day. Also, time-dependent vehicle average traveling speeds

were considered on different paths leading to time-variant travel times between nodes. Then, the ε-constraint method was implemented to handle the model's bi-objective nature and provide trade-offs between risk and cost. In this chapter, we defined two indicators, including Cost Increment Rate (CIR) and Risk Improvement Rate (RIR), to obtain more insight into the relationship between risk and cost objective functions, respectively showing the incremental changes of the cost and risk. We guaranteed covering all disastrous scenarios within an acceptable range in the optimal solution by keeping variability functions within a threshold. Finally, we conducted a sensitivity analysis on weights of variability and the warehouse capacity and derived several managerial insights.

Our results showed that the cost variability is more sensitive in low-risk situations, demanding larger weights to be maintained under a satisfaction level of 10%. On the other hand, the risk variability is more sensitive in the medium-risk situation. It was deducted that reducing the warehouse capacity may burden the system with more transportation costs and risks. Moreover, we compared our model with a disruption-free model. The result revealed that disruptions in location routing decisions create both higher cost and risk, respectively 14% and 5% on average. However, the design variables derived from a no-disruption system led to more costly decisions for the carrier if there was a possibility of edge unavailability. In this case, involving a scenario-based robust optimization model conveyed the best possible solutions to the proposed location-routing problem.

Chapter 4 investigated infectious waste management in a 3-tier network during a pandemic. The generated infectious waste from clinics and laboratories (first tier) piled up in a temporary storage location suing tours. Then, the accumulated waste

was shipped from the storage stations and the large medical centers (second tier) to the available integrated treatment centers (third tier) via direct routes. The optimal solution included locations of temporary storage and treatment facilities, determining the best routing decision according to the trade-off between risk and cost objectives, and acquiring the optimum vehicle acquisition. We applied a two-commodity flow formulation with time windows for tour planning. The uncertainty was involved in the network through the amount of generated waste. For this purpose, three scenarios were defined addressing different severity levels of a pandemic. Another source of uncertainty was the service time in small generation nodes, which was incorporated in the chance constraint to guarantee that the pre-defined time windows of temporary establishments can be satisfied at a specific confidence level. For the solution part, we integrated the augmented ε-constraint technique and a branch-and-price algorithm. The branch-and-price algorithm took advantage of a pulse algorithm for column generation purposes. Finally, we studied a case study of Wuhan in China during the coronavirus pandemic and provided several practical indications and managerial insights.

We compared our proposed solution method with CPLEX for several random instances, from small-scale tests to large-scale ones. The test results showed a superiority of the B&P algorithm over CPLEX by saving more than 83% of required computation time in small-sized problem instances and lowering the gaps by at least 70% in large-scale ones. We also compared our scenario-based stochastic model with the current and deterministic systems. The results indicated that our proposed system could timely adjust itself to fulfill almost four times the demand of other systems in the worst-case pandemic scenario while maintaining a cost-efficient operation with

no outbreak. The sensitivity analysis on the confidence levels of the chance constraint approach revealed that higher confidence level values necessitate higher total cost for the system to avoid time window violations in tours brought by the random fluctuation of service times in small generation nodes. Also, we investigated the impact of manipulating vehicle capacities in tours and found that more savings are expected with higher capacities of utilized trucks. Finally, it was demonstrated that higher values of degree of uncertainty in the service time result in more expensive decisions due to assigning more resources to compensate for the increases in the service times in tours.

In chapter 5, considering stochastic waste release dates, we incorporated the ICT developments in the hazardous waste management network. This was performed through signals sent from generation nodes to the logistic company responsible for waste collection actions. Using a mathematical modeling approach, we considered a three-stage decision framework to reflect the network: Location-allocation decisions at the first stage using a cost-clustering algorithm, 2) risk-based a priori routing decisions at the second stage, and 3) solution adaption to deviations from a priori plan using recourse actions at the third stage. The decision-maker risk aversion perspective was involved in the model using a parameter built upon the cumulative waste availability probabilities. The recourse actions were made according to three deviation scenarios reflecting minor, normal, and major variations from the original plan. Finally, we conducted a sensitivity analysis on important model components: the subjective risk-aversion parameter and vehicle capacity for collection tours.

We concluded that in the a priori plan assuming a higher risk aversion level of the collector, more risk is imposed on the system. In this regard, $\theta = 0.9$ achieved the

optimal solution with a nearly 123% growth of total risk compared to the optimistic condition with $\theta = 0.1$. Also, with higher values of θ, there was a higher chance of activating the overtime option. Finally, the lowest variations were detectable in the transportation risk, with the vehicle's capacity playing a significant role. Our findings pointed out that deviations from the original scheduled plan can have positive or negative impacts depending on the subjective perspective of the collector. An optimistic point of view should expect additional costs to adapt to the realized deviations, while a pessimistic decision-maker is more likely to find deviations pleasant. Also, it was shown that the recourse model goes through more bumping penalties with more disrupted conditions.

6.2 Future Research

Specific extensions associated with the three research pieces were elaborated in the respective chapters, i.e., chapters 2-4. In the following, we elaborate on some of the previously mentioned research pathways or point out other directions for future research.

Intelligent systems With the exponential urban sprawl, we observe an increase in population in big cities, putting pressure on the amenities, current infrastructure, and public services. One of the state-of-art methods to overcome this problem is converting to smart cities by applying information and communication technologies (ICT). With the improvement of ICT tools and protocols and the enhancement of various routing protocols, IoT devices, and applications of sensor networks, we can

build intelligent systems to keep up with the fast-changing conditions. In chapter 5, we discussed signals being sent from medical centers to the collector to indicate the availability of waste for collection. This is an example of applying ICT in the hazmat or reverse logistics area. Considering more communications between different system components, such as treatment centers and storage stations, can be a potential research avenue. The other potential direction is embedding smart bins capable of classifying ordinary waste from hazardous waste at facilities, such as medical centers, based on their nature. The application of ICT in hazmat transportation is still in its infancy, and more research is required to employ the application of IoT and wireless sensor networks to design cost-effective routing algorithms. Recent improvements in technologies such as IoT, machine learning, and cloud computing have encouraged researchers to develop computerized vehicle routing programs for collecting and treating waste within a city.

Using real-time data in logistics is crucial in coping with the growing digital world and generating a vehicle routing that ameliorates adverse consequences such as congestion, unsatisfactory safety, and environmental damage. Therefore, apart from transporting regular materials, there is a necessity for mindful planning and scheduling of hazmat transportation from origin to destination using big data. Intelligent transport refers to the visualization and analysis of real-time usage of the transport network. In this regard, future studies can focus on applications of data-driven and real-time and implement appropriate methods to embed these concepts in the associated models. Given data availability, effectively employing various structured and unstructured forms of real-time data to develop sustainable hazmat vehicle routing analytics almost remains an open research question. There is a vast potential research

gap in generating models and algorithms employing data availability to support policymakers in developing new regulations to mitigate congestion and improve network safety.

Data-driven approaches In recent years, data-driven operations research (DDOR) has emerged as a promising tool for addressing problems in logistics and transportation problems. DDOR is a powerful approach that can be used to help optimize the flow of goods and resources within complex systems. A combination of opportunities can be provided using Big Data to develop intelligent transportation and logistics industries. The complex real-life problems can be handled more efficiently by embedding the tremendous trove of data and data analytics into operations research techniques. As mentioned in Teoh et al. (2018), data generated through sensors challenge the logistics industry on how to use these real-time data to develop intelligent and safer transportation. The enormous accumulated data provides a huge potential for researchers in the hazmat logistics area to yield safer and cost-efficient models.

Hence, presenting a data-driven multi-objective HLRP is another contribution to enhancing the discussed models in this thesis. This model can be further extended by assuming a bi-level model. The non-convex nature of the bi-level program can be handled by a data-driven bundle method as it can stabilize the model solutions and reduce relative gaps between iterations (Chiou, 2020). There are articles applying data-driven methods in the network design of hazmat (Chiou, 2020) or signal design for traffic networks Chiou (2019). However, the location-routing problem of hazardous materials lacks efficient algorithms built upon data-driven procedures. Moreover, developing practical solution algorithms by utilizing data availability is another research

avenue in the hazmat scope that has not achieved sufficient attention so far.

Risk assessment A concept that is ignored in the majority of articles is equity. The importance of equity is generally twofold. First, public opposition will arise with neglecting equity in the designing routes for hazmat-carrying vehicles. Second, the risk inequity perception through overloading specific road segments with hazmat flows is more likely to result in higher incident probabilities and probably more severe consequences (Erkut et al., 2007). Therefore, a potential direction for future studies is embedding risk equity assumptions in the model. The concept of equality has always been one of the most important concerns of human beings throughout history, and in this regard, many definitions have been provided for its applications. For example, experts have defined different interpretations of the concept of equality in the health system. According to health experts, we face inequality or injustice in the health system whenever there is a difference in health outcomes due to irreversible imbalances in the distribution of facilities and access to different social groups or communities. Similar to the health system example, equity concerns in hazmat transportation, apart from the public risk perceptions, double the public sensitivity toward this issue. Unequal distribution of risk among the population, especially among different layers of society, based on their income, will impose pressure on the authorities. One of the most famous indicators by which the distribution of resources and the economic inequality in different societies is measured is the Gini coefficient. Focusing on the unequal distribution of income and opportunities between different groups in society, this coefficient is defined by a ratio that has a value between zero and one. A lower Gini coefficient shows greater equality in the distribution of income or wealth, while

a higher Gini coefficient indicates an unequal distribution. Zero means that everyone has the same income and wealth (absolute equality), and number one means absolute inequality.

As mentioned in Cordeiro et al. (2016), one of the fundamental elements in defining the risk in hazmat transportation is the type and nature of the material being shipped, which is scarcely explored in the literature. Distinguishing among different hazmat types is a realistic assumption because different limitations will be imposed on the system based on different substances, such as vehicle speed and consequences, directly affecting the network risk evaluation. Last but not least, as mentioned by Ditta et al. (2019), network design and facility location decisions might be affected by the hazmat type. For instance, while establishing a network based on the fuel as the hazmat product, one should expect a less rigorous transportation scheme compared to explosives.

In the literature, risk measurement has been mainly handled through minimizing population exposure (human fatalities and injuries) or property damage. However, proposing sustainable models with three associated pillars of sustainability as economic, environmental, and social considerations still requires attention. With the vulnerability of ecosystems and societies and considering the potential negative impacts of hazmat releases, it is essential to build up sustainable networks by mitigating environmental and social consequences, among the other aspects of risk assessment.

Value at Risk (VaR) was originally designed in finance as a measure to determine the amount of potential loss that could occur over a specified period. The main criticism for VaR is ignoring what is happening in the tail of a distribution. Because hazmat accidents are low-probability, high-consequence events, applying VaR as a

risk measure may lead the model to ignore such road segments from computations. Conditional Value at Risk (CVaR) is an extension of VaR. Unlike VaR, CVaR is a computationally tractable and coherent risk measure that mainly concentrates on the long tail of the risk distribution to avoid extreme events. This measure calculates the average losses that occur beyond the VaR breakpoint in a distribution. CVaR can be taken into account as the risk-averse factor for routing and scheduling Hazmat trucks to protect against high levels of loss in the underlying risk, which will support robustness as well as determining safe transport routes for hazardous materials. Moreover, CVaR can quantify some factors such as population exposure that may be encountered in the tail of distribution to avoid extreme events. As Hosseini and Verma (2018) was the first article addressing the application of CVaR for rail Hazmat transportation, this approach, or a developed version of it, or a worst-case CVaR, can be applied in intermodal problems such as RMIT.

Network A sensitive matter that has been neglected in the literature is the availability of vulnerable spots such as gas stations or hazmat depots along the routes where the dangerous cargo is being transported. Incorporating the impacts of these location types in the incident consequences is another pathway worthy of consideration. Talking about consequences, generally, a fixed value for the radius or bandwidth is assumed to obtain the exposed population or evaluate the link consequences. However, in reality, the severity of incident consequence is higher when getting closer to the accident origin and diminishes when getting far from it. Applying this concept in the model would lead to more practical solutions for decision-makers.

Incorporating variations and network dynamics into the model seems to be a

suitable research direction. Although many aspects of transportation networks are dynamic, the hazmat transportation with uncertain data field still suffers from the lack of model embedding network dynamics, such as time-dependent traffic congestion, weather impacts, and dynamic population along routes. Therefore, assuming a static value for such elements is not practical, and more flexible procedures are required that can integrate such variations.

The social pillar has been neglected in the majority of the works, where mostly, potential damages to human health are taken into account as a social factor. Although minimizing the associated risk of the network is an essential element for establishing sustainable networks; still, other criteria such as jobs opportunities created, the total number of days to be lost due to accidents at work, equitable routes, employment stability, and maximizing the distance between the disposal and treatment locations that lead to social satisfaction.

Solution algorithm As mentioned in Alumur and Kara (2007), the LRP of hazmat is NP-hard since it can be reduced to an uncapacitated facility location problem which is itself an NP-hard problem. Therefore, a challenge for the researcher is dealing with the exponential required computational time to find the exact solution, especially when solving large-scale instances. For exact algorithms, set partitioning-based formulations are the most effective methods for solving VRP variants where the variables embrace the feasible routes in this type of formulation (Pecin et al., 2017). However, since numerous feasible routes exist, the intention to generate all feasible paths for application in the set partitioning formulation is an unwise and unrealistic action. Therefore, the column generation technique, which has demonstrated its

suitability for the VRPTW variant, usually accompanies such problems for facilitating the process. Moreover, the integration of the column generation technique with a branch-and-bound tree is known as the branch-and-price method, which is usually implemented for generating a subset of the non-dominated extreme points. In chapter 4, we introduced a new branch-and-price algorithm for managing infectious waste. However, this algorithm still faces challenges in achieving optimal solutions with more than 100 nodes, including all the medical centers and facilities. Further studies can present more efficient algorithms, such as applying new cuts when developing a branch-and-price-and-cut method. Considering that a few studies are applying such effective techniques, the necessity for introducing more intelligent approaches is highlighted for future studies.

References

Amin Aalaei and Hamid Davoudpour. A robust optimization model for cellular manufacturing system into supply chain management. *International Journal of Production Economics*, 183:667–679, 2017.

A Aboutahoun. Combined distance-reliability model for hazardous waste transportation and disposal. *Life Sciences Journal*, 9(2):1286–1295, 2012.

HA Abu-Qdais, MA Al-Ghazo, and EM Al-Ghazo. Statistical analysis and characteristics of hospital medical waste under novel coronavirus outbreak. *Global Journal of Environmental Science and Management*, 6(4):1–10, 2020.

Z Akca, RT Berger, and TK Ralphs. A branch-and-price algorithm for combined location and routing problems under capacity restrictions. In *Operations Research and Cyber-infrastructure*, pages 309–330. Springer, 2009.

Abdulaziz S Alidi. An integer goal programming model for hazardous waste treatment and disposal. *Applied Mathematical Modelling*, 16(12):645–651, 1992.

Ertugrul Alp. Risk-based transportation planning practice: Overall methodology and a case example. *INFOR: Information Systems and Operational Research*, 33 (1):4–19, 1995.

Hussam Alshraideh and Hani Abu Qdais. Stochastic modeling and optimization of medical waste collection in northern jordan. *Journal of Material Cycles and Waste Management*, 19(2):743–753, 2017.

Sibel Alumur and Bahar Y Kara. A new model for the hazardous waste location-routing problem. *Computers & Operations Research*, 34(5):1406–1423, 2007.

Jose A Lopez Alvarez, Paul Buijs, Rogier Deluster, Leandro C Coelho, and Evrim Ursavas. Strategic and operational decision-making in expanding supply chains for lng as a fuel. *Omega*, 97:102093, 2020.

Henrik Andersson, Arild Hoff, Marielle Christiansen, Geir Hasle, and Arne Løkketangen. Industrial aspects and literature survey: Combined inventory management and routing. *Computers & Operations Research*, 37(9):1515–1536, 2010.

Konstantinos N Androutsopoulos and Konstantinos G Zografos. A bi-objective time-dependent vehicle routing and scheduling problem for hazardous materials distribution. *EURO Journal on Transportation and Logistics*, 1(1-2):157–183, 2012.

Claudia Archetti, Dominique Feillet, Andrea Mor, and M Grazia Speranza. An iterated local search for the traveling salesman problem with release dates and completion time minimization. *Computers & Operations Research*, 98:24–37, 2018.

Ehsan Ardjmand, Gary Weckman, Namkyu Park, Pooya Taherkhani, and Manjeet Singh. Applying genetic algorithm to a new location and routing model of hazardous materials. *International Journal of Production Research*, 53(3):916–928, 2015.

Ehsan Ardjmand, William A Young II, Gary R Weckman, Omid Sanei Bajgiran, Bizhan Aminipour, and Namkyu Park. Applying genetic algorithm to a new bi-objective stochastic model for transportation, location, and allocation of hazardous materials. *Expert Systems with Applications*, 51:49–58, 2016.

Hossein Asefi, Samsung Lim, Mojtaba Maghrebi, and Shahrooz Shahparvari. Mathematical modelling and heuristic approaches to the location-routing problem of a cost-effective integrated solid waste management. *Annals of Operations Research*, 273(1):75–110, 2019.

Nasrin Asgari, Mohsen Rajabi, Masoumeh Jamshidi, Maryam Khatami, and Reza Zanjirani Farahani. A memetic algorithm for a multi-objective obnoxious waste location-routing problem: a case study. *Annals of Operations Research*, 250 (2):279–308, 2017.

Ayyuce Aydemir-Karadag. A profit-oriented mathematical model for hazardous waste locating-routing problem. *Journal of Cleaner Production*, 202:213–225, 2018.

A Azadeh, N Atrchin, V Salehi, and H Shojaei. Modelling and improvement of supply chain with imprecise transportation delays and resilience factors. *International Journal of Logistics Research and Applications*, 17(4):269–282, 2014.

Samira Bairamzadeh, Mohammad Saidi-Mehrabad, and Mir Saman Pishvaee. Modelling different types of uncertainty in biofuel supply network design and planning: A robust optimization approach. *Renewable energy*, 116:500–517, 2018.

Roberto Baldacci, Eleni Hadjiconstantinou, and Aristide Mingozzi. An exact al-

gorithm for the capacitated vehicle routing problem based on a two-commodity network flow formulation. *Operations research*, 52(5):723–738, 2004.

Mahdi Bashiri, Erfaneh Nikzad, Andrew Eberhard, John Hearne, and Fabricio Oliveira. A two stage stochastic programming for asset protection routing and a solution algorithm based on the progressive hedging algorithm. *Omega*, 104: 102480, 2021. ISSN 0305-0483. https://doi.org/10.1016/j.omega.2021.102480.

R. Batta and S.S. Chiu. Optimal obnoxious paths on a network: transportation of hazardous materials. 36(1):84–92, 1988.

BBC News. Ibeirut explosion: Lebanon's government 'to resign' as death toll rises, 2020. URL `https://www.bbc.com/news/world-middle-east-53720383`. Retrieved on: October 28, 2020.

José-Manuel Belenguer, Enrique Benavent, Christian Prins, Caroline Prodhon, and Roberto Wolfler Calvo. A branch-and-cut method for the capacitated location-routing problem. *Computers & Operations Research*, 38(6):931–941, 2011.

Edward J Beltrami and Lawrence D Bodin. Networks and vehicle routing for municipal waste collection. *Networks*, 4(1):65–94, 1974.

Aharon Ben-Tal, Laurent El Ghaoui, and Arkadi Nemirovski. *Robust Optimization,*, volume 28. Princeton University Press, 2009.

Rosemary T Berger, Collette R Coullard, and Mark S Daskin. Location-routing problems with distance constraints. *Transportation Science*, 41(1):29–43, 2007.

Paul G Berglund and Changhyun Kwon. Robust facility location problem for hazardous waste transportation. *Networks and Spatial Economics*, 14(1):91–116, 2014.

Lucio Bianco, Massimiliano Caramia, and Stefano Giordani. A bilevel flow model for hazmat transportation network design. *Transportation Research Part C: Emerging Technologies*, 17(2):175 – 196, 2009. ISSN 0968-090X. https://doi.org/10.1016/j.trc.2008.10.001. Selected papers from the Sixth Triennial Symposium on Transportation Analysis (TRISTAN VI).

Lucio Bianco, Massimiliano Caramia, Stefano Giordani, and Veronica Piccialli. Operations research models for global route planning in hazardous material transportation. In *Handbook of OR/MS models in Hazardous Materials Transportation*, pages 49–101. Springer, 2013.

John R Birge. State-of-the-art-survey—stochastic programming: Computation and applications. *INFORMS journal on computing*, 9(2):111–133, 1997.

Omid Boyer, Tang Sai Hong, Ali Pedram, Rosnah Bt Mohd Yusuff, and Norzima Zulkifli. A mathematical model for the industrial hazardous waste location-routing problem. *Journal of Applied Mathematics*, 2013, 2013.

Maurizio Bruglieri, Simona Mancini, Roberto Peruzzini, and Ornella Pisacane. The multi-period multi-trip container drayage problem with release and due dates. *Computers & Operations Research*, 125:105102, 2021.

Aysenur Budak and Alp Ustundag. Reverse logistics optimisation for waste collection and disposal in health institutions: the case of turkey. *International Journal of Logistics Research and Applications*, 20(4):322–341, 2017.

Bureau of Transportation Statistics. Freight facts & figures 2017: Freight moved in domestic and international trade, 2017. URL https://www.bts.gov/product/freight-facts-and-figures. Retrieved on: October 28, 2020.

Bureau of Transportation Statistics. January 2020 north american transborder freight numbers, 2020. URL https://www.bts.gov/newsroom/january-2020-north-american-transborder-freight-numbers. Retrieved on: May 28, 2020.

Calma, Justine. The covid-19 pandemic is generating tons of medical waste, 2020. URL https://www.theverge.com/2020/3/26/21194647/the-covid-19-pandemic-is-generating-tons-of-medical-waste.

Canadian Transport Emergency Center. Transportation of dangerous goods newsletter: 2021 edition, 2021. URL https://tc.canada.ca/en/dangerous-goods/newsletter/transportation-dangerous-goods-newsletter-2021-edition#_CANUTEC_-_Dangerous.

Paola Cappanera, Giorgio Gallo, and Francesco Maffioli. Discrete facility location and routing of obnoxious activities. *Discrete Applied Mathematics*, 133(1-3):3–28, 2003.

George Casella and Roger L. Berger. *Statistical Inference*. Duxbury, 2nd edition, 2001.

Diego Cattaruzza, Nabil Absi, and Dominique Feillet. The multi-trip vehicle routing problem with time windows and release dates. *Transportation Science*, 50(2):676–693, 2016.

CDC. The continuum of pandemic phases. https://www.cdc.gov/flu/pandemic-resources/planning-preparedness/global-planning-508.html, 2016. accessed: 2022-01-18.

Abraham Charnes and William W Cooper. Chance-constrained programming. *Management Science*, 6(1):73–79, 1959.

Chang Chen, Jiaao Chen, Ran Fang, Fan Ye, Zhenglun Yang, Zhen Wang, Feng Shi, and Wenfeng Tan. What medical waste management system may cope with covid-19 pandemic: Lessons from wuhan. *Resources, Conservation and Recycling*, 170: 105600, 2021. ISSN 0921-3449. https://doi.org/10.1016/j.resconrec.2021.105600.

Suh-Wen Chiou. An efficient bundle-like algorithm for data-driven multi-objective bi-level signal design for traffic networks with hazardous material transportation. In *Data Science and Digital Business*, pages 191–220. Springer, 2019.

Suh-Wen Chiou. Data-driven stochastic optimization for transportation road network design under uncertainty. In *Handbook of Research on Big Data Clustering and Machine Learning*, pages 231–278. IGI Global, 2020.

Robert Chira. The role of transport activities in logistics chain. *Knowledge Horizons. Economics*, 6(3):17, 2014.

Geoff Clarke and John W Wright. Scheduling of vehicles from a central depot to a number of delivery points. *Operations Research*, 12(4):568–581, 1964.

Leandro C Coelho, Jean-François Cordeau, and Gilbert Laporte. Thirty years of inventory routing. *Transportation Science*, 48(1):1–19, 2014.

Claudio Contardo, Jean-François Cordeau, and Bernard Gendron. A computational comparison of flow formulations for the capacitated location-routing problem. *Discrete Optimization*, 10(4):263–295, 2013.

Claudio Contardo, Jean-François Cordeau, and Bernard Gendron. An exact algorithm based on cut-and-column generation for the capacitated location-routing problem. *INFORMS Journal on Computing*, 26(1):88–102, 2014.

Francyelly Giovany Cordeiro, Barbara Stolte Bezerra, Anna Silvia Palcheco Peixoto, and Rui António Rodrigues Ramos. Methodological aspects for modeling the environmental risk of transporting hazardous materials by road. *Transportation Research Part D: Transport and Environment*, 44:105–121, 2016.

John Current and Samuel Ratick. A model to assess risk, equity and efficiency in facility location and transportation of hazardous materials. *Location Science*, 3(3): 187–201, 1995.

George B Dantzig and John H Ramser. The truck dispatching problem. *Management Science*, 6(1):80–91, 1959.

Maryam Darvish, Leandro C Coelho, and Gilbert Laporte. *The Dynamic Routing Problem with Due Dates and Stochastic Release Dates*. Faculté des sciences de l'administration, 2020.

Atanu Kumar Das, Nazrul Islam, Morsaline Billah, and Asim Sarker. Covid-19 pandemic and healthcare solid waste management strategy–a mini-review. *Science of the Total Environment*, page 146220, 2021.

Giuseppe De Sensi, Francesco Longo, and Giovanni Mirabelli. Inventory policies analysis under demand patterns and lead times constraints in a real supply chain. *International Journal of Production Research*, 46(24):6997–7016, 2008.

Fatemeh Delfani, Abolfazl Kazemi, Seyed Mohammad SeyedHosseini, and Seyed Taghi Akhavan Niaki. A novel robust possibilistic programming approach for the hazardous waste location-routing problem considering the risks of transportation and population. *International Journal of Systems Science: Operations & Logistics*, pages 1–13, 2020.

Francesco Di Maria, Eleonora Beccaloni, Lucia Bonadonna, Carla Cini, Elisabetta Confalonieri, Giuseppina La Rosa, Maria Rosaria Milana, Emanuela Testai, and Federica Scaini. Minimization of spreading of sars-cov-2 via household waste produced by subjects affected by covid-19 or in quarantine. *Science of the Total Environment*, 743:140803, 2020.

Manuel Díaz-Madroñero, David Peidro, and Josefa Mula. A review of tactical optimization models for integrated production and transport routing planning decisions. *Computers & Industrial Engineering*, 88:518–535, 2015.

Ziyi Ding, Huashan Chen, Jingyong Liu, Haiming Cai, Fatih Evrendilek, and Musa Buyukada. Pyrolysis dynamics of two medical plastic wastes: Drivers, behaviors, evolved gases, reaction mechanisms, and pathways. *Journal of Hazardous Materials*, 402:123472, 2021.

A Ditta, O Figueroa, G Galindo, and R Yie-Pinedo. A review on research in trans-

portation of hazardous materials. *Socio-Economic Planning Sciences*, 68:100665, 2019.

Burak Eksioglu, Arif Volkan Vural, and Arnold Reisman. The vehicle routing problem: A taxonomic review. *Computers & Industrial Engineering*, 57(4):1472–1483, 2009.

Evren Emek and Bahar Y Kara. Hazardous waste management problem: The case for incineration. *Computers & Operations Research*, 34(5):1424–1441, 2007.

Emre Eren and Umut Rıfat Tuzkaya. Safe distance-based vehicle routing problem: Medical waste collection case study in covid-19 pandemic. *Computers & Industrial Engineering*, 157:107328, 2021.

Erhan Erkut, Stevanus A Tjandra, and Vedat Verter. Hazardous materials transportation. *Handbooks in Operations Research and Management Science*, 14:539–621, 2007.

Tolou Esfandeh, Rajan Batta, and Changhyun Kwon. Time-dependent hazardous-materials network design problem. *Transportation Science*, 52(2):454–473, 2018. 10.1287/trsc.2016.0698.

European Commission. Waste managment in the context of the coronairus crisis, 2020. URL `https://ec.europa.eu/info/sites/default/files/waste_management_guidance_dg-env.pdf`.

Statistics Explained Eurostat. Waste statistics, 2018.

Jie Fan, Lean Yu, Xiang Li, Changjing Shang, and Minghu Ha. Reliable location allocation for hazardous materials. *Information Sciences*, 501:688–707, 2019.

Tijun Fan, Wen-Chyuan Chiang, and Robert Russell. Modeling urban hazmat transportation with road closure consideration. *Transportation Research Part D: Transport and Environment*, 35:104 – 115, 2015. https://doi.org/10.1016/j.trd.2014.11.009.

Hamed Farrokhi-Asl, Reza Tavakkoli-Moghaddam, Bahare Asgarian, and Esmat Sangari. Metaheuristics for a bi-objective location-routing-problem in waste collection management. *Journal of Industrial and Production Engineering*, 34(4):239–252, 2017.

Hamed Farrokhi-Asl, Ahmad Makui, Armin Jabbarzadeh, and Farnaz Barzinpour. Solving a multi-objective sustainable waste collection problem considering a new collection network. *Operational Research*, pages 1–39, 2018.

William C. Frank, Jean-Claude Thill, and Rajan Batta. Spatial decision support system for hazardous material truck routing. *Transportation Research Part C: Emerging Technologies*, 8(1):337 – 359, 2000.

Jay Galbraith. Designing complex organizations. *Reading, Mass*, 1973.

Yuan Gao, Marie Schmidt, Lixing Yang, and Ziyou Gao. A branch-and-price approach for trip sequence planning of high-speed train units. *Omega*, 92:102150, 2020.

Zeynep Gergin, Nükhet Tunçbilek, and Şakir Esnaf. Clustering approach using artificial bee colony algorithm for healthcare waste disposal facility location problem. *International Journal of Operations Research and Information Systems (IJORIS)*, 10(1):56–75, 2019.

Abdolsalam Ghaderi and Robert L Burdett. An integrated location and routing approach for transporting hazardous materials in a bi-modal transportation network. *Transportation Research Part E: Logistics and Transportation Review*, 127:49–65, 2019.

VR Ghezavati and M Beigi. Solving a bi-objective mathematical model for location-routing problem with time windows in multi-echelon reverse logistics using meta-heuristic procedure. *Journal of Industrial Engineering International*, 12(4):469–483, 2016.

Ioannis Giannikos. A multiobjective programming model for locating treatment sites and routing hazardous wastes. *European Journal of Operational Research*, 104(2): 333–342, 1998.

Robert Giel and Alicja Dabrowska. Estimating time spent at the waste collection point by a garbage truck with a multiple regression model. *Sustainability*, 13(8): 4272, 2021.

Kannan Govindan, Arash Khalili Nasr, Parisa Mostafazadeh, and Hassan Mina. Medical waste management during coronavirus disease 2019 (covid-19) outbreak: A mathematical programming model. *Computers & Industrial Engineering*, 162: 107668, 2021.

Guanghua Han, Xujin Pu, Zhou He, and Cong Liu. Integrated planning and allocation: A stochastic dynamic programming approach in container transportation. *Chaos, Solitons & Fractals*, 114:264–274, 2018.

Md Sazzadul Haque, Shariar Uddin, Sayed Md Sayem, and Kazi Mushfique Mohib. Coronavirus disease 2019 (covid-19) induced waste scenario: A short overview. *Journal of Environmental Chemical Engineering*, page 104660, 2020.

Nikolai Holeczek. Hazardous materials truck transportation problems: A classification and state of the art literature review. *Transportation Research Part D: Transport and Environment*, 69:305–328, 2019.

Zahra Homayouni and Mir Saman Pishvaee. A bi-objective robust optimization model for hazardous hospital waste collection and disposal network design problem. *Journal of Material Cycles and Waste Management*, 22(6):1965–1984, 2020.

S Davod Hosseini and Manish Verma. Conditional value-at-risk (cvar) methodology to optimal train configuration and routing of rail hazmat shipments. *Transportation Research Part B: Methodological*, 110:79–103, 2018.

Hao Hu, Sini Guo, Hongguang Ma, Jian Li, and Xiang Li. A credibilistic mixed integer programming model for time-dependent hazardous materials vehicle routing problem. *Journal of Uncertain Systems*, 11(3):163–175, 2017.

Hao Hu, Xiang Li, Yuanyuan Zhang, Changjing Shang, and Sicheng Zhang. Multi-objective location-routing model for hazardous material logistics with traffic restriction constraint in inter-city roads. *Computers & Industrial Engineering*, 128: 861–876, 2019.

UM Ikeagwuani and GA John. Safety in maritime oil sector: Content analysis of machinery space fire hazards. *Safety Science*, 51(1):347–353, 2013.

Institute for Global Environmental Strategies. Waste management during the covid-19 pandemic: From response to recovery., 2020.

Armin Jabbarzadeh, Nader Azad, and Manish Verma. An optimization approach to planning rail hazmat shipments in the presence of random disruptions. *Omega*, 96: 102078, 2020.

Timothy L Jacobs and John M Warmerdam. Simultaneous routing and siting for hazardous-waste operations. *Journal of urban planning and development*, 120(3): 115–131, 1994.

Benoît Julien. An extension to possibilistic linear programming. *Fuzzy Sets and Systems*, 64(2):195–206, 1994.

Ismail Karaoglan, Fulya Altiparmak, Imdat Kara, and Berna Dengiz. A branch and cut algorithm for the location-routing problem with simultaneous pickup and delivery. *European Journal of Operational Research*, 211(2):318–332, 2011.

Saeed Kargar, Mohammad Pourmehdi, and Mohammad Mahdi Paydar. Reverse logistics network design for medical waste management in the epidemic outbreak of the novel coronavirus (covid-19). *Science of the Total Environment*, 746:141183, 2020.

Ginger Y Ke. Managing rail-truck intermodal transportation for hazardous materials with random yard disruptions. *Annals of Operations Research*, S.I.: Data-Driven OR in Transportation and Logistics, 2020a. https://doi.org/10.1007/s10479-020-03699-1.

Ginger Y Ke. Managing rail-truck intermodal transportation for hazardous materials with random yard disruptions. *Annals of Operations Research*, pages 1–27, 2020b.

Ginger Y Ke, Huiwen Zhang, and James H Bookbinder. A dual toll policy for maintaining risk equity in hazardous materials transportation with fuzzy incident rate. *International Journal of Production Economics*, 227:107650, 2020.

Jiří Jaromír Klemeš, Yee Van Fan, Raymond R Tan, and Peng Jiang. Minimising the present and future plastic waste, energy and environmental footprints related to covid-19. *Renewable and Sustainable Energy Reviews*, 127:109883, 2020.

Walid Klibi and Alain Martel. Scenario-based supply chain network risk modeling. *European Journal of Operational Research*, 223(3):644–658, 2012.

Bhargavi N Kulkarni and V Anantharama. Repercussions of covid-19 pandemic on municipal solid waste management: Challenges and opportunities. *Science of the Total Environment*, 743:140693, 2020.

Ernesto Alonso Lagarda-Leyva, Luis Fernando Morales-Mendoza, Nidia Josefina Ríos-Vázquez, Alicia Ayala-Espinoza, and Claudia Karina Nieblas-Armenta. Managing plastic waste from agriculture through reverse logistics and dynamic modeling. *Clean Technologies and Environmental Policy*, 21(7):1415–1432, 2019.

Gilbert Laporte and Yves Nobert. An exact algorithm for minimizing routing and operating costs in depot location. *European Journal of Operational Research*, 6(2): 224–226, 1981.

Gilbert Laporte, Francois Louveaux, and Hélène Mercure. Models and exact solutions

for a class of stochastic location-routing problems. *European Journal of Operational Research*, 39(1):71–78, 1989.

Jan Karel Lenstra and AHG Rinnooy Kan. Complexity of vehicle routing and scheduling problems. *Networks*, 11(2):221–227, 1981.

Wenli Li, Yong Wu, PN Ram Kumar, and Kunpeng Li. Multi-trip vehicle routing problem with order release time. *Engineering Optimization*, 52(8):1279–1294, 2020.

Wenli Li, Kunpeng Li, PN Ram Kumar, and Qiannan Tian. Simultaneous product and service delivery vehicle routing problem with time windows and order release dates. *Applied Mathematical Modelling*, 89:669–687, 2021a.

Xiangyong Li, YP Aneja, and Jiazhen Huo. Using branch-and-price approach to solve the directed network design problem with relays. *Omega*, 40(5):672–679, 2012.

Xiangyong Li, Kai Wei, Zhaoxia Guo, Wei Wang, and YP Aneja. An exact approach for the service network design problem with heterogeneous resource constraints. *Omega*, 102:102376, 2021b.

George List and Pitu Mirchandani. An integrated network/planar multiobjective model for routing and siting for hazardous materials and wastes. *Transportation Science*, 25(2):146–156, 1991.

Ling Liu, Kunpeng Li, and Zhixue Liu. A capacitated vehicle routing problem with order available time in e-commerce industry. *Engineering Optimization*, 49(3):449–465, 2017.

Sen Liu, Jinxin Zhang, Ben Niu, Ling Liu, and Xiaojun He. A novel hybrid multi-criteria group decision-making approach with intuitionistic fuzzy sets to design reverse supply chains for covid-19 medical waste recycling channels. *Computers & Industrial Engineering*, page 108228, 2022.

Xufei Liu and Changhyun Kwon. Exact robust solutions for the combined facility location and network design problem in hazardous materials transportation. *IISE Transactions*, pages 1–17, 2020.

Hong Ma, Brenda Cheang, Andrew Lim, Lei Zhang, and Yi Zhu. An investigation into the vehicle routing problem with time windows and link capacity constraints. *Omega*, 40(3):336–347, 2012.

Yufeng Ma, Xiaoqing Lin, Angjian Wu, Qunxing Huang, Xiaodong Li, and Jianhua Yan. Suggested guidelines for emergency treatment of medical waste during covid-19: Chinese experience. *Waste Disposal & Sustainable Energy*, 2(2):81–84, 2020.

Gerasimos Mantzaras and Evangelos A Voudrias. An optimization model for collection, haul, transfer, treatment and disposal of infectious medical waste: Application to a greek region. *Waste Management*, 69:518–534, 2017.

Iliya Markov, Michel Bierlaire, Jean-François Cordeau, Yousef Maknoon, and Sacha Varone. Waste collection inventory routing with non-stationary stochastic demands. *Computers & Operations Research*, 113:104798, 2020. https://doi.org/10.1016/j.cor.2019.104798.

George Mavrotas. Effective implementation of the ε-constraint method in multi-

objective mathematical programming problems. *Applied Mathematics and Computation*, 213(2):455–465, 2009.

George Mavrotas and Kostas Florios. An improved version of the augmented ε-constraint method (augmecon2) for finding the exact pareto set in multi-objective integer programming problems. *Applied Mathematics and Computation*, 219(18): 9652–9669, 2013.

Valerie A McCormack and Joachim Schüz. Africa's growing cancer burden: environmental and occupational contributions. *Cancer Epidemiology*, 36(1):1–7, 2012.

Medical Waste Management in Hubei. Wuhan municipal health commission, 2020. URL `http://wjw.wuhan.gov.cn/ztzl_28/fk/tzgg/202004/t20200430_1197173.shtml`.

Wei Meiyi, Li Xiang, and Yu Lean. Time-dependent fuzzy random location-scheduling programming for hazardous materials transportation. *Transportation Research Part C: Emerging Technologies*, 57:146–165, 2015.

Bruce L Miller and Harvey M Wagner. Chance constrained programming with joint constraints. *Operations Research*, 13(6):930–945, 1965.

Mehrdad Mohammadi, Payman Jula, and Reza Tavakkoli-Moghaddam. Design of a reliable multi-modal multi-commodity model for hazardous materials transportation under uncertainty. *European Journal of Operational Research*, 257(3):792–809, 2017.

Seyed Sina Mohri, Mehrdad Mohammadi, Michel Gendreau, Amir Pirayesh, Ali

Ghasemaghaei, and Vahid Salehi. Hazardous material transportation problems: A comprehensive overview of models and solution approaches. *European Journal of Operational Research*, 2021.

Andrea Mor and Maria Grazia Speranza. Vehicle routing problems over time: a survey. *Annals of Operations Research*, pages 1–21, 2022.

Josefa Mula, Raul Poler, and José Pedro Garcia-Sabater. Material requirement planning with fuzzy constraints and fuzzy coefficients. *Fuzzy Sets and Systems*, 158(7): 783–793, 2007.

John M Mulvey, Robert J Vanderbei, and Stavros A Zenios. Robust optimization of large-scale systems. *Operations Research*, 43(2):264–281, 1995.

Rana Negarandeh and Ali Tajdin. A robust fuzzy multi-objective programming model to design a sustainable hospital waste management network considering resiliency and uncertainty: A case study. *Waste Management & Research*, page 0734242X211038134, 2021.

AK Nema and SK Gupta. Multiobjective risk analysis and optimization of regional hazardous waste management system. *Practice Periodical of Hazardous, Toxic, and Radioactive Waste Management*, 7(2):69–77, 2003.

Arvind K Nema and SK Gupta. Optimization of regional hazardous waste management systems: an improved formulation. *Waste Management*, 19(7-8):441–451, 1999.

Long D Nghiem, Branwen Morgan, Erica Donner, and Michael D Short. The covid-

19 pandemic: considerations for the waste and wastewater services sector. *Case Studies in Chemical and Environmental Engineering*, 1:100006, 2020.

Pamela C Nolz, Nabil Absi, and Dominique Feillet. A stochastic inventory routing problem for infectious medical waste collection. *Networks*, 63(1):82–95, 2014.

Piotr Nowakowski, Sandra Kuśnierz, Patrycja Sosna, Jakub Mauer, and Dawid Maj. Disposal of personal protective equipment during the covid-19 pandemic is a challenge for waste collection companies and society: A case study in poland. *Resources*, 9(10):116, 2020.

Eneko Osaba, Xin-She Yang, Iztok Fister Jr, Javier Del Ser, Pedro Lopez-Garcia, and Alejo J Vazquez-Pardavila. A discrete and improved bat algorithm for solving a medical goods distribution problem with pharmacological waste collection. *Swarm and Evolutionary Computation*, 44:273–286, 2019.

Alexander Pavlov, Dmitry Ivanov, Frank Werner, Alexandre Dolgui, and Boris Sokolov. Integrated detection of disruption scenarios, the ripple effect dispersal and recovery paths in supply chains. *Annals of Operations Research*, pages 1–23, 2019.

Jie Peng, Xunlian Wu, Rongli Wang, Cui Li, Qing Zhang, and Daiqing Wei. Medical waste management practice during the 2019-2020 novel coronavirus pandemic: Experience in a general hospital. *American journal of infection control*, 48(8):918–921, 2020.

PHMSA. Annual update hazardous material/class 1 transportation incident

rates, 2015. URL https://www.ime.org/content/phmsa_hazardous_materials_incident_data. Retrieved on: October 28, 2020.

PHMSA. 10 year incident summary reports, 2019. URL https://www.phmsa.dot.gov/hazmat-program-management-data-and-statistics/data-operations/incident-statistics. Retrieved on: October 28, 2020.

Maja I Piecyk and Alan C McKinnon. Forecasting the carbon footprint of road freight transport in 2020. *International Journal of Production Economics*, 128(1):31–42, 2010.

Juan C Pina-Pardo, Daniel F Silva, and Alice E Smith. The traveling salesman problem with release dates and drone resupply. *Computers & Operations Research*, 129:105170, 2021.

Sattrawut Ponboon, Ali Gul Qureshi, and Eiichi Taniguchi. Branch-and-price algorithm for the location-routing problem with time windows. *Transportation Research Part E: Logistics and Transportation Review*, 86:1–19, 2016.

Rojee Pradhananga, Eiichi Taniguchi, Tadashi Yamada, and Ali Gul Qureshi. Bi-objective decision support system for routing and scheduling of hazardous materials. *Socio-Economic Planning Sciences*, 48(2):135–148, 2014.

Rojee Pradhananga, Eiichi Taniguchi, Tadashi Yamada, and Ali Gul Qureshi. Risk of traffic incident delay in routing and scheduling of hazardous materials. *International Journal of Intelligent Transportation Systems Research*, 14(1):50–63, 2016.

Joana C Prata, Ana LP Silva, Tony R Walker, Armando C Duarte, and Teresa Rocha-

Santos. Covid-19 pandemic repercussions on the use and management of plastics. *Environmental Science & Technology*, 54(13):7760–7765, 2020.

Yuzhuo Qiu, Jun Qiao, and Panos M Pardalos. A branch-and-price algorithm for production routing problems with carbon cap-and-trade. *Omega*, 68:49–61, 2017.

Masoud Rabbani, Razieh Heidari, Hamed Farrokhi-Asl, and Navid Rahimi. Using metaheuristic algorithms to solve a multi-objective industrial hazardous waste location-routing problem considering incompatible waste types. *Journal of Cleaner Production*, 170:227–241, 2018.

Masoud Rabbani, Razieh Heidari, and Reza Yazdanparast. A stochastic multi-period industrial hazardous waste location-routing problem: Integrating nsga-ii and monte carlo simulation. *European Journal of Operational Research*, 272(3):945–961, 2019a.

Masoud Rabbani, Razieh Heidari, and Reza Yazdanparast. A stochastic multi-period industrial hazardous waste location-routing problem: Integrating nsga-ii and monte carlo simulation. *European Journal of Operational Research*, 272(3):945–961, 2019b.

Masoud Rabbani, Alireza Nikoubin, and Hamed Farrokhi-Asl. Using modified metaheuristic algorithms to solve a hazardous waste collection problem considering workload balancing and service time windows. *Soft Computing*, 25(3):1885–1912, 2021.

Diba Raeisi and Saeid Jafarzadeh Ghoushchi. A robust fuzzy multi-objective location-routing problem for hazardous waste under uncertain conditions. *Applied Intelligence*, pages 1–21, 2022.

Meisam Ranjbari, Zahra Shams Esfandabadi, Sneha Gautam, Alberto Ferraris,

and Simone Domenico Scagnelli. Waste management beyond the covid-19 pandemic: Bibliometric and text mining analyses. *Gondwana Research*, 2022. ISSN 1342-937X. https://doi.org/10.1016/j.gr.2021.12.015. URL `https://www.sciencedirect.com/science/article/pii/S1342937X22000272`.

Pradeep Rathore and SP Sarmah. Economic, environmental and social optimization of solid waste management in the context of circular economy. *Computers & Industrial Engineering*, 145:106510, 2020.

Charles ReVelle, Jared Cohon, and Donald Shobrys. Simultaneous siting and routing in the disposal of hazardous wastes. *Transportation Science*, 25(2):138–145, 1991.

Damián Reyes, Alan L Erera, and Martin WP Savelsbergh. Complexity of routing problems with release dates and deadlines. *European journal of operational research*, 266(1):29–34, 2018.

Zahra Saeidi-Mobarakeh, Reza Tavakkoli-Moghaddam, Mehrzad Navabakhsh, and Hossein Amoozad-Khalili. A bi-level and robust optimization-based framework for a hazardous waste management problem: A real-world application. *Journal of Cleaner Production*, 252:119830, 2020.

Funda Samanlioglu. A multi-objective mathematical model for the industrial hazardous waste location-routing problem. *European Journal of Operational Research*, 226(2):332–340, 2013.

Maximilian Schiffer and Grit Walther. Strategic planning of electric logistics fleet networks: A robust location-routing approach. *Omega*, 80:31–42, 2018. ISSN 0305-0483. https://doi.org/10.1016/j.omega.2017.09.003.

Secretariat of the Basel Convention. Technical guidelines on the environmentally sound management of biomedical and healthcare wastes, 2003. URL http://synergies.pops.int/Portals/4/download.aspx?d=UNEP-CHW-WAST-GUID-BiomedicalHealthcareWastes.English.pdf.

Mashura Shammi, Arvind Behal, and Shafi M Tareq. The escalating biomedical waste management to control the environmental transmission of covid-19 pandemic: A perspective from two south asian countries. *Environmental science & technology*, 55(7):4087–4093, 2021.

Benjamin C Shelbourne, Maria Battarra, and Chris N Potts. The vehicle routing problem with release and due dates. *INFORMS Journal on Computing*, 29(4): 705–723, 2017.

Li-Hsing Shih and Yung-Teh Lin. Multicriteria optimization for infectious medical waste collection system planning. *Practice Periodical of Hazardous, Toxic, and Radioactive Waste Management*, 7(2):78–85, 2003.

Bin Shuai and Jiahong Zhao. Multi-objective 0-1 linear programming model for combined location-routing problem in hazardous waste logistics system. *Journal of Southwest Jiaotong University*, 46(2):326–332, 2011.

Narendra Singh, Yuanyuan Tang, and Oladele A Ogunseitan. Environmentally sustainable management of used personal protective equipment. *Environmental Science & Technology*, 54(14):8500–8502, 2020.

Lawrence V. Snyder and Mark S. Daskin. *Models for Reliable Supply Chain Network*

Design, pages 257–289. Springer Berlin Heidelberg, Berlin, Heidelberg, 2007. 10 .1007/978-3-540-68056-7_13.

Jaikishan T Soman and Rahul J Patil. A scatter search method for heterogeneous fleet vehicle routing problem with release dates under lateness dependent tardiness costs. *Expert Systems with Applications*, 150:113302, 2020.

Rajesh Srivastava. Alternate solution procedures for the location-routing problem. *Omega*, 21(4):497–506, 1993.

Curtis L Stowers and Udatta S Palekar. Location models with routing considerations for a single obnoxious facility. *Transportation Science*, 27(4):350–362, 1993.

Xinrui Sun, Kunpeng Li, and Wenli Li. The vehicle routing problem with release dates and flexible time windows. *Engineering Optimization*, pages 1–17, 2021.

Christos D Tarantilis and Chris T Kiranoudis. Using the vehicle routing problem for the transportation of hazardous materials. *Operational Research*, 1(1):67, 2001.

Masoumeh Taslimi, Rajan Batta, and Changhyun Kwon. Medical waste collection considering transportation and storage risk. *Computers & Operations Research*, 120:104966, 2020. https://doi.org/10.1016/j.cor.2020.104966.

Saeed Tasouji Hassanpour, Ginger Y. Ke, and David M. Tulett. A time-dependent location-routing problem of hazardous material transportation with edge unavailability and time window. *Journal of Cleaner Production*, 322:128951, 2021. ISSN 0959-6526. https://doi.org/10.1016/j.jclepro.2021.128951. URL `https://www.sciencedirect.com/science/article/pii/S0959652621031437`.

Saeed Tasouji Hassanpour, Ginger Y Ke, and David M Tulett. A time-dependent location-routing problem of hazardous material transportation with edge unavailability and time window. *Journal of Cleaner Production*, 322:128951, 2021.

Mohammad Ebrahim Tayebi Araghi, Reza Tavakkoli-Moghaddam, Fariborz Jolai, and Seyyed Mohammad Hadji Molana. A green multi-facilities open location-routing problem with planar facility locations and uncertain customer. *Journal of Cleaner Production*, 282:124343, 2021. ISSN 0959-6526. https://doi.org/10.1016/j.jclepro.2020.124343.

Boon Ean Teoh, SG Ponnambalam, and Nachiappan Subramanian. Data driven safe vehicle routing analytics: a differential evolution algorithm to reduce co2 emissions and hazardous risks. *Annals of Operations Research*, 270(1):515–538, 2018.

Erfan Babaee Tirkolaee, Parvin Abbasian, and Gerhard-Wilhelm Weber. Sustainable fuzzy multi-trip location-routing problem for the epidemic outbreak of the novel coronavirus (covid-19). *Science of The Total Environment*, page 143607, 2020.

Erfan Babaee Tirkolaee, Parvin Abbasian, and Gerhard-Wilhelm Weber. Sustainable fuzzy multi-trip location-routing problem for medical waste management during the covid-19 outbreak. *Science of the Total Environment*, 756:143607, 2021.

Iakovos Toumazis and Changhyun Kwon. Routing hazardous materials on time-dependent networks using conditional value-at-risk. *Transportation Research Part C: Emerging Technologies*, 37:73 – 92, 2013.

Renan Tunalıoğlu, Çağrı Koç, and Tolga Bektaş. A multiperiod location-routing prob-

lem arising in the collection of olive oil mill wastewater. *Journal of the Operational Research Society*, 67(7):1012–1024, 2016.

U.S. Department of Energy. U.S.department of energy (2019) Energy Information Administration, Movements between PAD Districts, 2019. URL `http://www.eia.gov/petroleum/data.php`. Retrieved on: October 28, 2020.

Manish Verma and Vedat Verter. Railroad transportation of dangerous goods: Population exposure to airborne toxins. *Computers & Operations Research*, 34(5): 1287–1303, 2007.

Thibaut Vidal, Gilbert Laporte, and Piotr Matl. A concise guide to existing and emerging vehicle routing problem variants. *European Journal of Operational Research*, 286(2):401–416, 2020.

Evangelos A Voudrias. Healthcare waste management from the point of view of circular economy, 2018.

Juyoung Wang, Mucahit Cevik, Saman Hassanzadeh Amin, and Amir Ali Parsaee. Mixed-integer linear programming models for the paint waste management problem. *Transportation Research Part E: Logistics and Transportation Review*, 151: 102343, 2021.

Mentong Wang, Michael GH Bell, and Lixin Miao. A branch-and-price algorithm for a green two-echelon capacitated location routing problem. 2020.

John M Warmerdam and Timothy L Jacobs. Fuzzy set approach to routing and siting hazardous waste operations. *Information Sciences-Applications*, 2(1):1–14, 1994.

Meiyi Wei, Lean Yu, and Xiang Li. Credibilistic location-routing model for hazardous materials transportation. *International Journal of Intelligent Systems*, 30(1):23–39, 2015.

WHO. *Management of Solid Health-Care Waste at Primary Health Care Centres: A Decision-Making Guide*. Produced by the WHO Department of Water, Sanitation and Health Series. World Health Organization, 2005. ISBN 9789241592741. URL `https://apps.who.int/iris/bitstream/handle/10665/43123/9241592745.pdf`. Department of Immunization, Vaccines and Biologicals (IVB), Protection of the Human Environment, Department of Water, Sanitation and Health (WSH).

WHO. Who's dashboard. `https://covid19.who.int/table/`, 2021.

WHO. About pandemic phases. `https://www.euro.who.int/en/health-topics/communicable-diseases/influenza/data-and-statistics/pandemic-influenza/about-pandemic-phases`, 2022. accessed: 2022-01-18.

Max M Wyman and Michael Kuby. Proactive optimization of toxic waste transportation, location and technology. *Location Science*, 3(3):167–185, 1995.

Weijun Xie, Yanfeng Ouyang, and Sze Chun Wong. Reliable location-routing design under probabilistic facility disruptions. *Transportation Science*, 50(3):1128–1138, 2016.

Li Xue, Zhixing Luo, and Andrew Lim. Exact approaches for the pickup and delivery problem with loading cost. *Omega*, 59:131–145, 2016.

Mohd Najib Yacob and Mimi Haryani Hassim. Comprehensive review on risk assessment methodologies for hazmat transportation between 1995-2015. *Journal of Advanced Review on Scientific Research*, 30(1):12–59, 2017.

Weibo Yang, Liangjun Ke, David ZW Wang, and Jasmine Siu Lee Lam. A branch-price-and-cut algorithm for the vehicle routing problem with release and due dates. *Transportation Research Part E: Logistics and Transportation Review*, 145:102167, 2021.

Liming Yao, Zhongwen Xu, and Ziqiang Zeng. A soft-path solution to risk reduction by modeling medical waste disposal center location-allocation optimization. *Risk Analysis*, 40(9):1863–1886, 2020.

Morteza Yazdani, Madjid Tavana, Dragan Pamučar, and Prasenjit Chatterjee. A rough based multi-criteria evaluation method for healthcare waste disposal location decisions. *Computers & Industrial Engineering*, 143:106394, 2020.

İlker Yılmaz. Emissions from passenger aircraft at kayseri airport, turkey. *Journal of Air Transport Management*, 58:176–182, 2017.

Chian-Son Yu and Han-Lin Li. A robust optimization model for stochastic logistic problems. *International Journal of Production Economics*, 64(1-3):385–397, 2000.

Hao Yu and Wei Deng Solvang. An improved multi-objective programming with augmented ε-constraint method for hazardous waste location-routing problems. *International Journal of Environmental Research and Public Health*, 13(6):548, 2016.

Hao Yu, Xu Sun, Wei Deng Solvang, Gilbert Laporte, and Carman Ka Man Lee. A

stochastic network design problem for hazardous waste management. *Journal of Cleaner Production*, 277:123566, 2020a.

Hao Yu, Xu Sun, Wei Deng Solvang, Gilbert Laporte, and Carman Ka Man Lee. A stochastic network design problem for hazardous waste management. *Journal of Cleaner Production*, 277:123566, 2020b.

Hao Yu, Xu Sun, Wei Deng Solvang, and Xu Zhao. Reverse logistics network design for effective management of medical waste in epidemic outbreaks: insights from the coronavirus disease 2019 (covid-19) outbreak in wuhan (china). *International journal of environmental research and public health*, 17(5):1770, 2020c.

Yang Yu, Sihan Wang, Junwei Wang, and Min Huang. A branch-and-price algorithm for the heterogeneous fleet green vehicle routing problem with time windows. *Transportation Research Part B: Methodological*, 122:511–527, 2019.

L Zhang, Songshan Guo, Yunsong Zhu, and Andrew Lim. A tabu search algorithm for the safe transportation of hazardous materials. In *Proceedings of the 2005 ACM symposium on Applied computing*, pages 940–946, 2005a.

Min Zhang, Yunfeng Ma, and Kerui Weng. Location-routing model of hazardous materials distribution system based on risk bottleneck. In *Proceedings of IC-SSSM'05. 2005 International Conference on Services Systems and Services Management, 2005.*, volume 1, pages 362–368. IEEE, 2005b.

Jiahong Zhao and Ginger Y. Ke. Incorporating inventory risks in location-routing models for explosive waste management. *International Journal of Production Economics*, 193:123 – 136, 2017. https://doi.org/10.1016/j.ijpe.2017.07.001.

Jiahong Zhao and Ginger Y Ke. Optimizing emergency logistics for the offsite hazardous waste management. *Journal of Systems Science and Systems Engineering*, 28(6):747–765, 2019.

Jiahong Zhao and Vedat Verter. A bi-objective model for the used oil location-routing problem. *Computers & Operations Research*, 62:157–168, 2015.

Jiahong Zhao and Jun Zhao. Model and algorithm for hazardous waste location-routing problem. In *ICLEM 2010: Logistics For Sustained Economic Development: Infrastructure, Information, Integration*, pages 2843–2849. 2010.

Jiahong Zhao and Fumin Zhu. A multi-depot vehicle-routing model for the explosive waste recycling. *International Journal of Production Research*, 54(2):550–563, 2016.

Jiahong Zhao, Biaohua Wu, and Ginger Y Ke. A bi-objective robust optimization approach for the management of infectious wastes with demand uncertainty during a pandemic. *Journal of Cleaner Production*, page 127922, 2021.

Jun Zhao, Lixia Huang, Der-Horng Lee, and Qiyuan Peng. Improved approaches to the network design problem in regional hazardous waste management systems. *Transportation Research Part E: Logistics and Transportation Review*, 88:52–75, 2016.

Lu Zhen, Chengle Ma, Kai Wang, Liyang Xiao, and Wei Zhang. Multi-depot multi-trip vehicle routing problem with time windows and release dates. *Transportation Research Part E: Logistics and Transportation Review*, 135:101866, 2020.

Zhen Zhou, Ada Che, Feng Chu, and Chengbin Chu. Model and method for multiob-

jective time-dependent hazardous material transportation. *Mathematical Problems in Engineering*, 2014, 2014.

Enrico Zio and Nicola Pedroni. *Possibilistic methods for uncertainty treatment: An application to maintenance modelling*. FonCSI, 2014.

Konstantinos G Zografos and Konstantinos N Androutsopoulos. A heuristic algorithm for solving hazardous materials distribution problems. *European Journal of Operational Research*, 152(2):507–519, 2004.

Kostas G Zografros and Saadedeen Samara. Combined location-routing model for hazardous waste transportation and disposal. *Transportation Research Record*, 1245: 52–59, 1989.

Emir Zunic, Dzenana DJonko, and Emir Buza. An adaptive data-driven approach to solve real-world vehicle routing problems in logistics. *Complexity*, 2020, 2020.